ENGINEERED T CELLS FOR MULTIPLE MYELOMA

DEVELOPMENT OF BCMA-SPECIFIC ENGINEERED T CELLS TARGETING MULTIPLE MYELOMA

By KSENIA BEZVERBNAYA, B.Sc.

A Thesis Submitted to the School of Graduate Studies in Partial Fulfillment of the Requirements for the Degree Doctor of Philosophy

McMaster University DOCTOR OF PHILOSOPHY (2021) Hamilton, Ontario (Medical Sciences)

TITLE: Development of BCMA-Specific Engineered T Cells Targeting Multiple Myeloma

AUTHOR: Ksenia Bezverbnaya, B.Sc. (University of Toronto)

SUPERVISOR: Dr. Jonathan L. Bramson

PAGES: xxv, 223

Lay Abstract

Multiple myeloma is an incurable blood cancer that has a remarkable ability to develop resistance to different types of chemotherapy. In recent years, treatments redirecting immune cells against tumors have shown impressive clinical responses against different types of chemotherapy-resistant blood cancers, including multiple myeloma. Our lab has developed a new technology for redirecting T cells against tumors, called T cell antigen coupler (TAC) receptor. This thesis describes optimization of a fully human TAC receptor specific for a target on the surface of myeloma cells, known as BCMA. Durable remissions induced by TAC-engineered T cells in a preclinical mouse model of myeloma in the absence of toxicity warrant further testing of this therapeutic in a clinical trial.

Abstract

Multiple myeloma is a plasma cell cancer that progressively evolves to an aggressive, multi-drug resistant disease, which presents an unmet clinical need. In clinical trials, myeloma shows susceptibility to novel immunotherapeutic agents, particularly those targeting B-cell maturation antigen (BCMA). Among different classes of immunotherapies, T cell-based approaches have progressed the most due to their ability to induce durable responses in patients with advanced drug-resistant blood cancers. Most T cell engineering strategies rely on the use of chimeric antigen receptors (CARs), which although effective, can cause serious life-threatening toxicities. We created a new synthetic receptor, T cell antigen coupler (TAC), which recruits the endogenous T cell receptor and allows T cells to autoregulate their activity. Our experience in solid tumor models has shown that TAC-T cells are similarly efficacious and significantly less toxic than CAR-T cells. This thesis describes our optimization of BCMA-specific TAC-T cells and analysis of different anti-BCMA antigen-binding domains.

TAC receptor functions by engaging endogenous TCR-CD3 complex and redirecting it to the target of interest. In Chapter 3, we characterize optimization and humanization of the CD3-recruitment domain in the TAC scaffold and provide evidence that TAC-T cells are effective against multiple myeloma, irrespective of receptor surface levels. In Chapter 4, we describe selection of the human BCMA-binding domain and the creation of a fully humanized TAC receptor against

BCMA. Chapters 5 and 6 describe how a BCMA-targeting antigen-binding domain that cross-reacts with an unknown antigen in mice augments *in vivo* efficacy of TAC- and CAR-T cells, respectively.

The work described in Chapters 3 and 4 presents an optimized, fully human BCMA-TAC that is being moved into clinical testing. The work in Chapters 5 and 6 improves our understanding of how antigen-targeting domains in synthetic receptors influence the functionality of engineered T cells.

Acknowledgements

As much as I have been fortunate to work on an interesting and impactful project and watch the field of cancer immunotherapy grow and save patients' lives, I have been even luckier with the people in my life who made this journey possible.

To my supervisor, Jonathan – thank you for all the fantastic opportunities you have given me to grow as a scientist, for believing in me, encouraging me to challenge myself, and for being a supportive mentor along the way. Thank you for nurturing our lab family, creating an intellectually stimulating and safe environment for pursuing new scientific ideas, and for showing us how to build collaborative relationships that turn these ideas into reality. You put your heart and soul into our lab, and we are lucky to have you as a supervisor. Thank you for being an incredible scientist, a dedicated mentor, and a great leader.

I am also grateful for the guidance I received from my supervisory committee members, Dr. Carl Richards and Dr. Ronan Foley. Thank you for challenging me to be a better scientist and for encouraging me to always keep the big picture in mind and ensure that my approach stays clinically relevant.

The Bramson lab has become my family during my studies, and I am thankful for the impact you have all had on my development as a scientist and as a person. To the technicians and scientists in the lab, Joni, SeungMi, Duane, Galina, Chris H., Chris B., Derek, Bonnie, Craig, Danielle, Limin, Bella, Daniela, and Carole – thank you for the wealth of expert advice and unwavering support

throughout the years. To the HITS team, Robin, Alina, Ying, Meg, Jess, Jamie, Tanya, and Preethi – your knowledge of flow cytometry, sample processing, and data analysis have really helped my project move forward. To Jonathan's assistant, Jenn – thank you for helping me navigate the administrative part of graduate school and for being the support system for the entire Bramson lab. To the students of the lab, Arya, Ken, Rebecca B., Rebecca T., Kaylyn, Sarah, Phil, Nick, Ally, Chris S., Lisa, Michael, Tianning, Ben, Adam, Anumita, Ashish, Jerry, Jessie, Ritchie, Heather, and Vivian – this journey would not have been possible without you. Thank you for sharing the joys and disappointments of science and for making my graduate school experience fun and unforgettable. I look forward to seeing the amazing things you will do with your careers!

McMaster Immunology Research Centre has been a truly wonderful place to work at. The faculty, trainees, and technicians have created a very collaborative, inspiring, and welcoming environment. I am also grateful for the support of the technicians and staff in the core histology, flow cytometry, and animal facilities. Additionally, I would like to thank all my friends and colleagues at the Stem Cell and Cancer Research Institute and the students and faculty I met through teaching the HTH SCI 3I03 Introductory Immunology course and volunteering with the McMaster Children and Youth University, Let's Talk Science, Graduate Management Consulting Association, and University Consulting Group.

The scientific progress of this project would not have been possible without the generosity of the multiple myeloma patients at the Juravinski Cancer Centre.

We are forever grateful for your participation in our research and for your help in driving the innovation forward. I am also deeply thankful for the Ontario Graduate Scholarship, BioCanRx, and Triumvira Immunologics for funding the work in this thesis. A special thank you to the Samuel Family Foundation who have been a generous and supportive donor for the entire duration of my project from the very first day I joined the lab. Without your help, my work would not have been possible.

I am already tearing up writing this section, but this last paragraph is definitely the hardest. Thank you, Mom and Dad, for quitting your careers in academia 12 years ago and immigrating to Canada to allow my brother and I to pursue our dreams. Thank you for enduring night shifts at factories, going back to school, starting your careers from scratch, and working your way up in a new country. I hope I can make it worth it to you one day. To my brother, Denis – thank you for teaching me strength and perseverance and for inspiring me every day. To my partner, Rolan – thank you for being a remarkably loving, supportive, and caring human being. I don't know what lucky stars aligned for us to meet, but I am grateful every day. I love you and can't wait to see what the future holds for us.

Table of Contents

List of Figures

Chapter 1: Introduction

Chapter 3: Optimization of the CD3-binding domain and the TAC receptor surface expression

List of Tables

List of Abbreviations

ADC – antibody-drug conjugate

ADCC – antibody-dependent cellular cytotoxicity

ADCP – antibody-dependent cellular phagocytosis

ANOVA – analysis of variance

AP-1 – activator protein 1

APC – allophycocyanin

APRIL – a proliferation-inducing ligand

ASCT – autologous stem cell transplant

BAFF – B-cell activating factor

Bcl-# – B-cell lymphoma/leukemia #

Bcl-X_L – B-cell lymphoma-extra large

BCMA – B-cell maturation antigen

BIM – Bcl-2-like protein 11

BiTE – bi-specific T-cell engager

Blimp-1 – B lymphocyte-induced maturation protein 1

BRAF – V-Raf murine sarcoma viral oncogene homolog

BSA – bovine serum albumin

BTLA – B- and T-lymphocyte attenuator

BV# – Brilliant Violet #

CAIX – carbonic anhydrase IX

CAR – chimeric antigen receptor

CAR-T – chimeric antigen receptor-engineered T cell

CCAB – Centre for the Commercialization of Antibodies and Biologics

CCL# – C-C motif chemokine ligand #

CD# – cluster of differentiation #

CDC – complement-dependent cytotoxicity

cDNA – complementary DNA

CR – complete response

CRAB criteria – calcium, renal impairment, anemia, bone involvement

cSMAC – central supramolecular activation cluster

CTA – cancer-testis antigen

CTLA-4 – cytotoxic T lymphocyte-associated antigen 4

CXCL# – C-X-C motif ligand #

CXCR# – C-X-C motif receptor #

DGS-NTA(Ni) - 1,2-dioleoyl-sn-glycero-3-[(N-(5-amino-1-carboxypentyl) iminodiacetic acid) succinyl]

DMEM – Dulbecco's Modified Eagle Medium

DMSO – dimethyl sulfoxide

DNA – deoxyribonucleic acid

DOPC – 1,2-dioleoyl-sn-glycero-3-phosphocholine

dSMAC – distal supramolecular activation cluster

ECM – extracellular matrix

effLuc – enhanced firefly luciferase

eGFP – enhanced green fluorescent protein

EMM – extramedullary multiple myeloma

ER – endoplasmic reticulum

ERK – extracellular signal-regulated kinase

F(ab) – fragment, antigen-binding

Fas-L – Fas ligand

FBS – fetal bovine serum

FcRH5 – Fc receptor-homolog 5

FcγR – Fc gamma receptor

FDA – Food and Drug Administration

FGFR3 – fibroblast growth factor receptor 3

FITC – fluorescein isothiocyanate

FN-1 – fibronectin 1

G4S – GGGGS linker

G-CSF – granulocyte colony-stimulating factor

GFP – green fluorescent protein

GITR – glucocorticoid-induced TNFR-related protein

GM-CSF – granulocyte-macrophage colony-stimulating factor

gp100 – glycoprotein 100

GpNLuc – eGFP-NanoLuc chimeric protein

GPRC5D – G protein-coupled receptor class C group 5 member D

GVHD – graft versus host disease

HEK293T – human embryonic kidney 293 cells, transduced

HEPES – 4-(2-hydroxyethyl)-1-piperazineethanesulfonic acid

HER2 – human epidermal growth factor receptor 2

HLA – human leukocyte antigen

HSA – human serum albumin

i.p. – intraperitoneal

i.v. – intravenous

ICAM-1 – intercellular adhesion molecule-1

ICANS – immune effector cell-associated neurotoxicity syndrome

ICOS – inducible T cell co-stimulator

IFN-γ – interferon gamma

IGF-1R – insulin-like growth factor 1 receptor

IgG – immunoglobulin G

IgK – immunoglobulin kappa

IHC – immunohistochemistry

IL-# – interleukin #

IMiD – immunomodulatory imide drug

IP_3 – inositol trisphosphate

IPTG – isopropyl β-d-1-thiogalactopyranoside

IRF4 – interferon regulatory factor 4

IS – immunological synapse

ISH – *in situ* hybridization

ITAM – immunoreceptor tyrosine-based activation motif

KRAS – Kirsten rat sarcoma viral oncogene homolog

LAG-3 – lymphocyte-activation gene 3

LAGE-1 – L antigen family member 1

LAT – linker for activation of T cells

LB – Luria-Bertani broth

Lck – lymphocyte-specific protein tyrosine kinase

LFA-1 – lymphocyte function-associated antigen 1

LIGHT – herpesvirus entry mediator

LLPC – long-lived plasma cell

LSP-1 – lymphocyte-specific protein 1

MAGE-A3 – melanoma-associated antigen A3

MAPK – mitogen-activated protein kinase

MART-1 – melanoma-associated antigen recognized by T cells 1

MCL-1 – myeloid cell leukemia 1 protein

MCP-1 – monocyte chemoattractant protein 1

MEM – Minimal Essential Media

MFI – median fluorescence intensity

MGUS – monoclonal gammopathy of undetermined significance

MIL – marrow-infiltrating lymphocyte

MM – multiple myeloma

MOI – multiplicity of infection

MSC – mesenchymal stromal cell

mTOR – mammalian target of rapamycin

NAD – nicotinamide adenine dinucleotide

NCI – National Cancer Institute

NF-κB – nuclear factor kappa B

NGFR – nerve growth factor receptor

NK – natural killer cell

NKG2D – natural killer group 2D

NRG – NOD.Cg-Rag1tm1MomIl2rgtm1Wjl/SzJ mouse

NY-ESO-1 – New York esophageal squamous cell carcinoma

OD_{600} – optical density measured at a wavelength of 600 nm

ORR – overall response rate

OS – overall survival

PBMC – peripheral blood mononuclear cells

PBS – phosphate-buffered saline

PCL – plasma cell leukemia

PCR – polymerase chain reaction

PD-1 – programmed cell death protein 1

PD-L1 – programmed death-ligand 1

PE – phycoerythrin

PerCP-Cy5.5 – peridinin chlorophyll protein-cyanine 5.5

PFS – progression-free survival

PI – proteasome inhibitor

PI3K – phophoinositide 3-kinase

PLC-γ – phospholipase C gamma

pSMAC – peripheral supramolecular activation cluster

RANKL – receptor activator of nuclear factor kappa B ligand

RB1 – retinoblastoma protein 1

rhIL-# – recombinant human IL-#

RNA – ribonucleic acid

RPMI – Roswell Park Memorial Institute medium

scFv – single-chain variable fragment

SD – standard deviation

SDF-1 – stromal cell-derived factor 1

SDS-PAGE – sodium dodecyl-sulfate polyacrylamide gel electrophoresis

SEER – Surveillance, Epidemiology, and End Results program

SLAMF7 – self-ligand receptor of the signaling lymphocytic activation molecule family member 7

SLP76 – SH2-domain-containing leukocyte protein of 76 kDa

SMM – smoldering multiple myeloma

SOCS1 – suppressor of cytokine signaling 1

TAC – T cell antigen coupler

TACI – transmembrane activator and CAML interactor

TAC-T – T cell antigen coupler receptor-engineered T cells

TCR – T-cell receptor

TIL – tumor-infiltrating lymphocyte

TIM-3 – T cell immunoglobulin and mucin domain-containing protein 3

TIRF – total internal reflection fluorescence

TNFR – tumor necrosis factor receptor

TNF-α – tumor necrosis factor alpha

TP53 – tumor protein 53

TRAF-# – TNF receptor-associated factor #

TRAIL – TNF-related apoptosis-inducing ligand

T_{reg} – regulatory T cell

T_{scm} – stem cell memory T cell

t-SNE – t-distributed stochastic neighbor embedding

UPR – unfolded protein response

VCN – vector copy number

VEGF – vascular endothelial growth factor

V_H – heavy chain variable fragment

V_L – light chain variable fragment

ZAP-70 – zeta-chain-associated protein kinase 70

Declaration of Academic Achievement

The studies described in this thesis were conceptualized and analyzed by Ksenia Bezverbnaya in collaboration with Dr. Jonathan Bramson. Ksenia Bezverbnaya was the primary researcher for all experiments, with assistance from colleagues outlined below:

- Dr. Ronan Foley provided patient samples used in Chapter 3.
- Rebecca C. Turner helped purify UCHT1, huUCHT1, and huUCHT1(YT) proteins used for assays in Figure 3.1C and generated bio-layer interferometry data in Figure 3.1E.
- Dr. Galina F. Denisova performed analysis of specific contacts formed between different UCHT1 variants and CD3ε presented in Figure 3.1D and designed the cloning strategy for the J22.9-xi scFv.
- Carole C. Evelegh generated effLuc-expressing KMS-11 cell line.
- Dr. Duane Moogk generated and analyzed TAC-T cell binding and immunological synapse data in Figures 3.5C and 3.6.
- Derek Cummings generated vector copy number data in Table 1, cloned the J22.9-xi scFv, and assisted with production of all lentiviruses used in Chapters 3-6.
- Jamie D. McNicol used the data generated by Ksenia Bezverbnaya to conduct flowSOM analysis and produced t-SNE plots in Figure 3.8.

- Michael Sun helped manufacture T cells used in experiments in Figure 3.9A,B.
- Dr. Christopher W. Helsen conceptualized the framework for the UCHT1, huUCHT1, and huUCHT1(YT) backbones, designed the humanized BCMA-TAC variants described in Table 3, and generated the data in Figures 4.1 and 4.2.
- Dr. Bonnie Bojovic cloned the fully humanized BCMA-TAC constructs used in Figures 4.1-4.3, manufactured most of the lentiviruses used in Chapter 4, and generated GpNLuc-expressing KMS-11 cell line.
- Limin Liu cloned the fully humanized BCMA-TAC constructs used in Figures 4.4-4.6.
- Dr. Joanne A. Hammill designed the cloning strategy for constructs cloned by Limin Liu and analyzed serum cytokine data in Figure 4.7. The cells used for the analysis in Figure 4.7 were manufactured by Triumvira Immunologics.
- Christopher L. Baker and Craig Aarts performed *in vivo* tumor and T cell injections and monitoring for the studies described in Figures 3.3C, 3.13, 3.14, 3.15, 4.3, 4.6, 5.3, 5.4C, 5.5, 5.6, 6.5, 6.6, and 6.7. Christopher L. Baker also helped Ksenia Bezverbnaya process the tissue samples for analysis in Figure 6.8A.
- Spencer Revill performed HALO analysis of tissue sections for Figure 5.5A,B.

- McMaster Immunology Research Centre Core Histology facility prepared tissue sections and immunohistochemistry staining for samples in Figure 5.5.
- Dr. Jacek Kwiecien provided a blinded opinion on the pathology of tissue samples in Figure 5.5.
- Ying Wu generated proliferation data in Figure 6.8B.

Chapter 1

Introduction

1. Multiple Myeloma

1.1 Biology of long-lived plasma cells

Plasma cells are an integral component of our immune system, responsible for antibody-mediated defense from pathogens. Following antigen exposure in the periphery, some plasma cells home to the bone marrow or gut-associated lymphoid tissue and become long-lived plasma cells (LLPC), which continuously secrete antibodies and provide lasting immune protection[1]. The length of LLPC survival varies and is typically measured indirectly through antibody titers in blood, which can persist for months and even years post-infection[2-4], independent of the antigen[5]. In a healthy person, this long-term antibody production by LLPCs is key to durable vaccine efficacy.

The bone marrow niche is crucial for supporting LLPC longevity, as evidenced by the inability of murine[6] and human[7] plasma cells isolated from the bone marrow to survive in *in vitro* culture in the absence of bone marrow stromal cells. Mesenchymal stromal cells (MSC) in the bone marrow produce chemokine CXCL12, or SDF-1, which binds CXCR4 on plasma cells and guides them to the bone marrow niche[8]. Once in that niche, integrin-mediated direct cell-cell contacts between plasma cells and MSCs activate phosphoinositide 3-kinase (PI3K) signaling in plasma cells and suppress activation of caspases 3 and 7, thus inhibiting apoptosis[9]. MSCs also secrete fibronectin-1 (FN-1), which serves as an important component of the extracellular matrix (ECM) in the bone marrow niche. FN-1

supports survival of LLPCs likely by anchoring them via binding to CD138 and enhancing autophagy via downregulation of mammalian target of rapamycin (mTOR) signaling[7]. Finally, MSCs together with dendritic cells, megakaryocytes, and eosinophils secrete an abundance of IL-6 cytokine, which further promotes LLPC survival[10] and immunoglobulin secretion by activating the STAT3 signaling pathway[11].

IL-6 synergizes with another soluble factor, a proliferation-inducing ligand (APRIL) in sustaining LLPCs in the bone marrow niche[10]. APRIL is secreted by hematopoietic cells such as myeloid precursors[12], macrophages[13], and eosinophils[14], and binds B cell maturation antigen (BCMA) on plasma cells. BCMA knockout in mice leaves peripheral T cell-dependent B cell responses intact, but dramatically lowers the numbers of LLPCs in the bone marrow, underscoring the crucial role of BCMA in LLPC survival[15]. Stimulation of the BCMA receptor increases transcription of the anti-apoptotic protein Mcl-1[16] and hinders activation of caspase 12 via the nuclear factor κB (NF-κB) pathway[9]. Besides APRIL, BCMA can also bind B-cell activating factor (BAFF), but affinity between BCMA and APRIL is stronger than affinity between BCMA and BAFF[17]. Additionally, a close relative of BCMA, transmembrane activator, calcium modulator and cyclophilin ligand interactor (TACI), is also expressed on plasma cells and binds both APRIL and BAFF. TACI promotes plasma cell differentiation by driving expression of the transcription factor Blimp-1 and augments plasma cell survival by downregulating pro-apoptotic protein BIM[18].

Besides megakaryocytes, dendritic cells, and myeloid cells, T regulatory (T_{reg}) cells are another type of hematopoietic cells that participate in shaping the LLPC bone marrow niche. Intravital imaging, transcriptomic analysis, systemic infection, and cell depletion mouse models suggest that T_{regs} mediate homeostasis of the LLPC niche by mitigating loss of plasma cells from the LLPC niche during systemic infection and limiting the number of plasma cells in the niche in the absence of infection[19].

A multitude of complementary factors supports survival of healthy LLPCs in the bone marrow niche. As multiple myeloma (MM) cancer cells arise from healthy LLPCs, they further exploit natural survival factors by remodeling their microenvironment to maximize the space and nourishment for the growing tumor masses.

1.2 Pathogenesis of multiple myeloma

The plasma cell origin of MM was first described in 1900 by James H. Wright[20], but despite decades of research, we are still uncovering the process by which MM evolves from LLPCs. We do know that MM is preceded by a pre-cancerous condition called monoclonal gammopathy of undetermined significance (MGUS)[21], which is distinguished from MM by lower percentage of clonal plasma cell infiltration in the bone marrow and the absence of end-organ damage[22]. A subset of patients present with smoldering multiple myeloma (SMM), which is an intermediate state between MGUS and MM and is characterized by over 10% bone

marrow infiltration with clonal plasma cells and serum monoclonal protein levels over 30 g/L, but no end-organ damage[23].

The current paradigm of myelomagenesis centers around sequential acquisition of genetic abnormalities by plasma cell clones that lead to enhanced proliferative capacity[24]. The two main early pre-malignant events supporting the emergence of MGUS are hyperdiploidy and translocations involving the immunoglobulin heavy chain gene[25, 26]. A common downstream effect of these genetic abnormalities is dysregulation of cell cycle, primarily through overexpression of cyclin D[27], which facilitates transition from the G1 to the S stage of the cell cycle[28]. Secondary genetic events facilitating MM emergence include mutations, and copy number changes that affect a multitude of genes regulating proliferation and apoptosis, e.g. TP53, BRAF, MCL1, MYC, KRAS, and RB1[29]. The phenotype of MM cells is also affected by epigenetic events, as evidenced by widespread DNA hypomethylation in MM, compared to MGUS and SMM[30, 31]. Notably, the broad DNA hypomethylation in MM is accompanied by select hypermethylation of B cell-specific enhancer regions, facilitating maintenance of a less-differentiated state by the MM cells[32].

In addition to the aberrations acquired by the MM cells, transformations in the bone marrow niche further support development of the myeloma disease. Comparative genetic analysis of endothelial cells in MGUS and MM revealed 22 differentiating genes involved in cell adhesion, regulation of apoptosis, chemotaxis, and angiogenesis[33]. Progressive angiogenesis along the spectrum of healthy

controls – MGUS – SMM – MM has been further confirmed by immunohistochemical analysis of microvessel density in the patient bone marrow samples[34]. Additional evidence of niche remodeling comes from proteomic analysis of the ECM components, highlighting the presence of matrisome-associated proteins annexin A2 and galectin-1 in the ECM of MM patients, but not in the ECM of MGUS patients or healthy donors[35]. Expression of each of these proteins on myeloma cells was associated with decreased overall survival, and the authors proposed that these proteins promoted niche remodeling by enhancing angiogenesis and bone resorption, in addition to supporting MM growth and resistance to apoptosis[35].

The crosstalk between MM cells and other cells in their microenvironment occurs though multiple routes. The cell-cell contacts and soluble factors that normal LLPCs use to send and receive signals (reviewed in the previous section) are used by the MM cells as well. Recently, a lot of attention has been drawn to the exosome-based signaling in the tumor microenvironment. For example, the contents of the exosomes released by bone marrow MSCs from healthy individuals and MM patients are substantially different. Exosomes from normal MSCs contain more tumor suppressive miR-15a, whereas exosomes from MM MSCs have more CCL2, IL-6, fibronectin, and junction plakoglobin[36]. MM cells, on their part, secrete exosomes carrying micro-RNA miR-146a, which they can transfer to MSCs. When miR-146a is elevated in healthy MSCs, they increase expression of IL-6, CXCL1, CXCL10, and CCL5, which facilitate MM cell migration and survival[37]. Other

micro-RNAs detected in MM endosomes are miR-21, let-7b, and miR-18a, which further support bone marrow niche remodeling[38].

Clinical presentation of MM is characterized by the presence of end-organ damage through CRAB criteria: hypercalcemia, renal failure, anemia, and bone lesions[39]. These symptoms are a consequence of the biological activity of MM cells. For instance, MM cells retain the main function of LLPCs and secrete immunoglobulins, which put a strain on patients' kidney function, as the disease burden increases[40]. The monoclonal immunoglobulins, or M protein, are routinely measured in blood of MM patients and serve as an indicator of disease progression or response to treatment[41]. Although the secretory ability typically remains intact, the quality control of the antibody synthesis can be poor, with most MM patients showing incomplete immunoglobulins in the serum and 15% of patients presenting with light chain-only MM[42].

The majority of MM patients experience anemia, which stems from the hematopoietic niche invasion by MM cells, inadequate erythropoietin production by failing kidneys[43], and upregulation of death receptor ligands Fas-L and TRAIL on the MM cells, leading to apoptosis of erythroblasts[44]. Besides overtaking the space available for hematopoiesis, MM cells suppress osteoblasts and stimulate osteoclastogenesis to remodel the bones, generating lytic bone lesions and hypercalcemia[45]. Adipocytes, another common cell type present in the bone marrow, also participate in MM niche remodeling by secreting SDF-1α and MCP-

1 chemokines that attract MM cells, leptin adipokine that induces autophagy in MM cells, and CXCL1 and CXCL2 chemokines that promote osteoclastogenesis[46].

Taken together, intrinsic genetic and epigenetic abnormalities driving proliferation and resistance to apoptosis in MM cells synergize with extrinsic signals from other cells in the MM niche to support survival and growth of the MM lesions in the bones.

In some cases, MM patients develop extramedullary MM (EMM), meaning their tumors grow independently from the bone marrow microenvironment either adjacent to the bone, in a completely different organ, or freely in the blood stream[47]. The most aggressive variant of EMM is plasma cell leukemia (PCL), characterized by more complex cytogenetics and alteration of expression of cell adhesion molecules, chemokine receptors, and mediators of apoptosis, when compared to conventional MM[48]. EMM is notoriously difficult to treat and carries a very poor prognosis of only a few months even in the cases of treatments that work well for the bone marrow-restricted MM[47]. As a primary event at diagnosis, EMM occurs in 7-17% of patients, and as a secondary event during disease relapse/resistance, it develops in 6-20% of patients[49]. Although currently infrequent, EMM patients may become a larger group of treatment-resistant cases in the future, as novel therapeutics get progressively better at eliminating conventional MM.

1.3 Epidemiology of MM

Since individuals with MGUS and SMM represent a pool of prospective MM patients, the epidemiology of these conditions is relevant to the overall understanding of MM prevalence. MGUS has an estimated serologic prevalence of 3.2 - 5.8% in people over the age of 50[50, 51], and long-term follow-up of MGUS patients indicates a 1% yearly risk of progression to MM[52]. SMM is less frequent, but carries a higher risk of progression to MM, compared to MGUS. Estimated prevalence of SMM is 0.4-0.9 cases per 100,000 people[53, 54]. In the first 5 years post-diagnosis, the annual risk of SMM transformation to MM is 10%, but it drops to 3% in the following 5 years, and to 1% after year 10[23].

The International Agency for Research on Cancer estimates MM world-wide incidence as 2.3 cases per 100,000 people, which translates to 176,404 new diagnoses of MM in 2020[55]. In the U.S., the average incidence of MM is 9 cases per 100,000 people in males and 5.9 cases per 100,000 people in females, based on the cumulative 2012-2016 data from the Surveillance, Epidemiology and End Results (SEER) Program[56]. The average annual growth of MM incidence in the U.S. was 3.9% in 2007-2010 and 1.2% in 2010-2017[57]. In general, MM occurs in older people, with an average age at diagnosis of 66-70, and tends to affect males more than females as well as people of African American descent more than those of Caucasian descent[58].

According to the Canadian Cancer Statistics, over 3,400 new MM cases are estimated in Canada in 2020, with 2,000 cases in males and 1,450 cases in females[59]. 1,600 Canadians are expected to die from MM in 2020, with 56% of deaths occurring in males[59]. Compared to the 2019 report, the incidence of MM in Canada has increased by approximately 3% and, on average, has been increasing by 2.6% annually since 2007[60]. This steady growth in MM cases in Canada could be a reflection of the progressively aging population and the advances in the diagnostic methods. The Statistics Canada projects the proportion of people aged 65 or older to rise from 17.2% in 2018 to 21.4-23.4% by 2030, to 21.4-29.5% by 2068[61]. Given these projections, it is fair to expect further increase in MM incidence in Canada and a growing need for new therapeutics to support this group of cancer patients.

2. Conventional therapeutic landscape for MM

2.1 Early therapies

For the first 100 years since MM was first described in 1844, the treatment options were highly primitive and included rhubarb pills, orange peel infusion, leeches, steel, and quinine[62]. In 1940s and 50s, urethane was used as the first anti-myeloma drug, but it proved to be highly toxic and carcinogenic, and actually showed reduced overall survival when compared to placebo in a randomized controlled trial[63]. Although several additional drugs were tested against MM in mid-1900s, responses were very poor and patient survival remained under the 6-month

mark until the introduction of melphalan in 1960s, which produced 49% response rate and elevated survival to 34 months post-diagnosis[64]. Melphalan is an alkylating agent, which interferes with replication and transcription, and to this day remains a prominent component of MM treatment plans, particularly during the pre-transplant high-dose induction therapy[65]. In the late 1960s, after the introduction of melphalan, a corticosteroid, prednisone, was added to the MM treatment palette, and provided additional 6 months of survival benefit, when compared to melphalan alone[66]. Following the promising effects of the melphalan-prednisone combination, several other alkylating agents were tried in anti-MM combination regimens, but did not provide substantial survival benefit beyond what melphalan and prednisone had already accomplished[62].

2.2 Hematopoietic stem cell transplantation

In the 1980s, clinicians observed dose-dependent efficacy of melphalan, with the high dose of 140 mg/m^2 able to induce complete remissions, although at the cost of profound myelosuppression[63]. A therapeutic approach based on high-dose chemotherapy and stem cell collection, followed by an autologous stem cell transplant (ASCT), resolved the cytopenias and allowed patients to capitalize on the remission induced by chemotherapy. Randomized trials comparing chemotherapy alone to chemotherapy followed by ASCT demonstrated over 4-fold improvement in complete responses and median survival increase to 5 years[67, 68]. At present, transplant eligibility remains one of the key considerations in the treatment plan for MM patients and shapes the choice of drug regimens.

In some cases, MM patients receive an allogeneic graft during transplantation. Here, lymphocytes in the graft mount an anti-tumor activity called graft-versus-myeloma response, which reduces the incidence of myeloma relapse, but introduces the risk of toxicities due to the graft-versus-host disease (GVHD)[69]. In recent years, support has emerged for the graft-versus-tumor effect in the autologous transplant setting. Quicker absolute lymphocyte count (particularly NK cell count[70]) recovery within the first two weeks post-transplant correlates with better progression-free survival (PFS) and better overall survival (OS)[71]. MM patients whose autografts have higher lymphocyte content have faster absolute lymphocyte count recovery and better therapeutic outcomes[72, 73]. Specifically, CD4 T cell concentration of at least 0.45 x 10^9 cells/kg in MM autografts is associated with 80% 2-year PFS, compared to 40% 2-year PFS in patients with lower CD4 T cell content in the autografts[74]. The choice of stem cell mobilization regimen can influence autograft lymphocyte count and, thus, affect downstream clinical outcomes. When cyclophosphamide is added to the standard mobilization reagent granulocyte colony stimulating factor (G-CSF), lymphocyte mobilization is reduced[75]. On the other hand, when G-CSF is combined with a CXCR4 antagonist, Plerixafor, lymphocyte mobilization is enhanced[76]. Vuckovic and colleagues recently provided a mechanistic insight into the T cell-mediated MM tumor control in a preclinical murine transplantation model. In this set of experiments, antigen-experienced CD8 T cells in the bone marrow grafts mounted IFN-γ-mediated anti-

MM response in recipient mice, which was augmented by the addition of a PD-1 blockade or a 4-1BB agonist[77].

The studies described in this section position hematopoietic stem cell transplant as the first immunotherapeutic approach in MM treatment. Section 3 further highlights a multitude of more recent strategies for harnessing immune responses and redirecting them against MM tumor.

2.3 Thalidomide and immunomodulatory drugs

Thalidomide was first marketed in the 1950s as a drug against morning sickness, but was found to cause severe fetal abnormalities due to its teratogenic properties. In the decades following, several groups investigated its mechanism of teratogenesis and explored potential use of thalidomide as a cancer treatment for a variety of tumors. Studies in a rabbit corneal neovascularization model aimed at elucidating the basis of thalidomide-induced teratogenesis revealed potent anti-angiogenic activity of orally administered thalidomide[78]. Since angiogenesis had been implicated in MM tumor growth, Barlogie and colleagues conducted a single-agent trial of thalidomide in chemotherapy-refractory MM patients and observed an overall response rate (ORR) of 32%[79]. In subsequent trials, thalidomide combined with steroids or steroids and cyclophosphamide further improved ORR in refractory and newly-diagnosed MM[80].

Lenalidomide (Revlimid), a thalidomide analogue developed to reduce toxicity, falls in the category of immunomodulatory drugs (IMiDs) due to its effects

on multiple immunologic pathways. Clinically, lenalidomide alone or in combination with other drugs has demonstrated potent anti-MM activity in relapsed refractory, newly diagnosed, and maintenance treatment settings[81]. Mechanistically, lenalidomide binds to cereblon in the E3 ubiquitin ligase complex and induces degradation of transcription factors Ikaros and Aiolos[82]. Degradation of these proteins inhibits IRF4-dependant survival pathways in MM cells and increases IL-2 production in NK and T cells, thus harming tumor cells directly and facilitating anti-tumor immune activity[82]. Other immunomodulatory properties of lenalidomide include enhancement of the CD28-dependent NFκB activation in T cells[83] and SOCS1 downmodulation in immune effector cells, leading to improved IFN-γ production[84].

The newest thalidomide derivative to achieve regulatory approval for MM treatment is pomalidomide. The multifaceted activity of pomalidomide includes downmodulation of IL-6 and IL-1β in the MM microenvironment, inhibition of IRF4 in MM cells leading to reduced survival and proliferation, enhancement of T cell co-stimulation and cytokine production, and reduction in the activity of T_{regs} and osteoclasts[85]. Pomalidomide has been tested alone or in combination with other drugs and showed clinical efficacy against lenalidomide-refractory MM[85].

2.4 Proteasome inhibitors

Since MM cells continue to produce immunoglobulins, they are under the risk of endoplasmic reticulum stress and rely on the unfolded protein response

(UPR) mechanisms to avoid cell death. Thus, therapeutic approaches targeting UPR in MM cells have been an active area of investigation. The ubiquitin-proteasome pathway of protein degradation plays an important role in UPR, and the first proteasome inhibitor (PI), bortezomib, has been used for MM treatment since the early 2000s[86]. Bortezomib is used in a variety of chemotherapeutic regimens for newly diagnosed and relapsed refractory MM, but as MM becomes progressively resistant to available drug combinations, new PIs are still actively investigated. Carfilzomib and ixazomib have already received regulatory approval after demonstrating efficacy in patients previously treated with bortezomib-containing regimens, and several other PIs are currently making their ways through the clinical trials[87].

2.5 Other chemotherapeutic agents

As MM keeps acquiring resistance to approved chemotherapeutic drugs, including PIs and IMiDs, the arsenal of additional therapeutics keeps growing continuously. Newer drugs coming down the pharmaceutical pipelines include inhibitors of heat shock proteins[88] and histone deacetylases[89], antiapoptotic protein Bcl-2[90], and selective inhibitors of nuclear export[91]. Although these agents have shown responses in early-stage clinical trials, their transient efficacy and associated toxicities leave an unmet clinical need for specifically targeted approaches that can lead to deep, lasting remissions and reduce the number of lines of therapy the patients go through. Following on the transplantation and IMiD-based regimens that engage patients' immune system in anti-MM battle, there is now a range of

novel immunotherapies that will be discussed below. As the new immunotherapeutics first become available to heavily pretreated patients and are tested alone or in combination with the currently used drugs, the careful layering of different treatment modalities becomes important for maximizing the functionality of the patients' immune responses.

3. Novel immunotherapies for MM

Novel immunotherapeutic approaches for MM can be broadly classified into 3 categories: 1) monoclonal antibodies and antibody-drug conjugates; 2) bi-specific T-cell engagers (BiTEs), and 3) T cell-based therapeutics. As the pool of known MM-specific markers is limited, the same molecules are often targeted by multiple types of immunotherapeutics.

3.1 Monoclonal antibodies and antibody-drug conjugates

3.1.1 Monoclonal antibodies

Non-conjugated monoclonal antibodies designed to bind MM cells exert therapeutic efficacy through blockade of vital receptor/ligand interactions, direct cytotoxicity, complement-dependent cytotoxicity (CDC), antibody-dependent cellular cytotoxicity (ADCC) and antibody-dependent cell-mediated phagocytosis (ADCP)[92]. The drug conjugates attached to the monoclonal antibodies can directly enhance toxicity to the MM cells once the antibody is internalized and the drug is released inside the cell[93]. The choice of target antigen for monoclonal antibody therapies is not limited to molecules on the surface of MM cells and can include

soluble mediators and molecules expressed on other cells in the MM microenvironment.

The most clinically advanced monoclonal antibodies for MM target myeloma cells directly. CD38 is an ectoenzyme expressed on MM cells, which catabolizes NAD^+ and facilitates extracellular adenosine (ADO) production. ADO inhibits cytotoxicity and proliferation of T cells and cytotoxicity and IFN-γ production by NK cells, thus protecting MM cells from the immune attack[94]. Not surprisingly, CD38 presents an attractive target for anti-MM therapeutics. Two monoclonal antibodies targeting CD38 have already been approved by FDA (daratumumab and isatuximab)[95, 96], and several others are being evaluated in clinical trials[97]. As a single agent, daratumumab produced 31.1% ORR in heavily pretreated MM patients, with PFS of 4 months[98]. Studies into the mechanisms of action of daratumumab reveal that it extends beyond direct cytotoxicity and Fc-mediated cytotoxic immune activity on MM cells and includes depletion of $CD38^+$ immunosuppressive cells and skewing of T-cell repertoire towards a more cytotoxic phenotype[99].

Signaling lymphocyte activation molecule family member 7 (SLAMF7) is also highly expressed on the surface of MM cells and is known to induce proliferation and autocrine cytokine secretion in B cells[100] and promote MM cell adhesion to stromal cells[101]. A monoclonal anti-SLAMF7 antibody elotuzumab that eliminates myeloma cells primarily through ADCC and direct NK cell activation has been approved by the FDA for IMiD-containing combination regimens[102].

Elotuzumab was not clinically effective as a single agent[103], but led to 82% objective response rate when combined with lenalidomide and dexamethasone[104]. Other surface molecules targeted with monoclonal antibodies that failed to produce meaningful clinical efficacy in MM patients include CD40[105, 106], ICAM-1[107], CD74[108], IGF-1R[109], and FGFR3[110].

Several monoclonal antibodies have been investigated against soluble factors in MM tumor microenvironment, with mostly underwhelming clinical results. Although MM tumor microenvironment is characterized by enhanced angiogenesis, targeting of the vascular endothelial growth factor (VEGF) or its receptors through monoclonal antibodies or drugs has failed to produce meaningful clinical responses[111-114]. Similarly, although IL-6 has been extensively characterized as an important cytokine supporting MM pathogenesis[115] and preclinical data were encouraging[116], an IL-6-targeting monoclonal antibody, siltuximab, provided only modest clinical benefit at the cost of high infection rates[117]. Finally, monoclonal antibody blockade of BAFF[118] and APRIL[119], also yielded low response rates. Denosumab, a monoclonal antibody against RANKL, does not target a soluble factor that would impact MM cells directly, but has been approved for treating MM-associated bone disease[120].

Antibodies targeting checkpoint receptors on T cells, particularly the receptor-ligand pair programmed cell death protein 1 (PD-1) and its ligand PD-L1, have received wide regulatory approval for a variety of tumors[121]. In myeloma, however, their journey has been more complicated. Two phase III trials testing the

PD-1 inhibitor, pembrolizumab, in combination with dexamethasone and either lenalidomide or pomalidomide had to be stopped due to increased pulmonary, cardiac, and intestinal toxicities[122, 123]. These observations highlight the importance of careful testing of novel immunotherapeutics, particularly when combined with IMiDs.

3.1.2 Antibody-drug conjugates

Advances in biochemical engineering technologies created an opportunity for capitalizing on the highly specific targeting provided by monoclonal antibodies and delivering cytotoxic agents directly to MM cells in the form of antibody-drug conjugates (ADC). Different cytotoxic loads and linker engineering approaches used for ADC design have been reviewed elsewhere[93]. Compared to monoclonal antibodies, ADCs are less forgiving to broad target expression patterns because delivery of the cytotoxic agent to non-MM cells can cause serious toxicities.

As discussed in section 1, BCMA is a cell-surface receptor expressed on long-lived plasma cells and involved in survival and proliferation of MM. Due to its highly restricted expression pattern[124, 125], BCMA has emerged as the leading target for MM immunotherapies. Recently, an afucosylated anti-BCMA antibody conjugated to monomethyl auristatin F (GSK2857916) has received regulatory approval. In the phase II, single-agent DREAMM-2 study, GSK2857916 demonstrated 31-34% ORR and median PFS of 2.9-4.9 months, depending on the dose group[126]. GSK2857916 is now being evaluated in combinations with standard

anti-MM drugs, and early data suggest improvements in ORR to 78% or better, although assessments of median PFS have not yet been reported[127, 128]. AMG 224 is another ADC targeting BCMA, which carries a different chemotherapeutic agent, mertansine[129]. AMG 224 tested as a single-agent in a dose-escalation study demonstrated 23% ORR with 14.7 months median duration of response and no PFS reported[129]. No further studies are currently underway for AMG 224. The latest BCMA-specific ADC that has clinical data available is MEDI2228, an antibody designed to bind cell surface-expressed BCMA preferentially over soluble BCMA and deliver pyrrolobenzodiazepine to MM cells[130]. In the dose-escalation study, MEDI228 had 16.7-61% ORR, depending on the dose level, and median duration of response had not been reached for the most effective dose at the time of reporting[130]. Two additional BCMA-specific ADCs have either entered clinical trials (CC-99712, NCT04036461 trial) or are on the way to be tested in the clinics (HDP-101), but no data are available yet.

Some monoclonal antibodies that demonstrated good tolerability but poor clinical efficacy in MM were repurposed as antibody-drug conjugates, although these modified therapeutics were still mostly ineffective. Conjugation of a CD74-targeting antibody, milatuzumab, to doxorubicin failed to provide clinical benefit to relapsed refractory MM patients, and its phase I trial NCT01101594 was terminated without publication of results. When the CD138-specific antibody, indatuximab, was conjugated to maytansinoid DM4 and evaluated in a multi-dose phase I study, the ORR was only 5.9% with median PFS of 3 months[131]. Other

ADCs that have shown minimal clinical benefit as monotherapies have targeted SLAMF7[132], FcRH5[133], and CD56[134], although CD56-targeting ADC IMGN 901 had 59% ORR when combined with lenalidomide and dexamethazone[135].

3.2 Bi-specific T-cell engagers

Bi-specific T-cell engagers (BiTEs), like monoclonal antibodies, are off-the-shelf targeted immunotherapeutics that facilitate MM tumor cell killing by engaging endogenous immune cells. BiTEs contain a CD3-specific domain for recruiting T cells and were originally created as two single-chain variable antibody fragments (scFvs) linked together, although a variety of design variants have now been described[136]. Besides the overall BiTE structural format, other design considerations include affinities of the BiTE arms for their targets, epitopes targeted, inclusion of the Fc domain, use of fully human sequences, biophysical stability, and solubility[136].

Because BiTEs are designed to trigger specific cytotoxic T cell responses, off-target reactivity can lead to devastating toxicities. Consequently, BiTEs are typically limited by the same target considerations as ADCs. Blinatumomab was the first-in-class BiTE that demonstrated durable clinical activity and ultimately received regulatory approval for the treatment of CD19-positive B-cell cancers[137].

In MM, most BiTEs that have entered clinical trials have been designed to bind BCMA due to its plasma cell-restricted expression profile. Notably, all of the anti-BCMA BiTEs with currently available in-human data have shown meaningful

clinical efficacy in heavily pretreated relapsed refractory MM patients. The first BCMA-specific BiTE to be tested in a phase I trial was AMG 420, which showed 70% ORR at the maximum tolerable dose[138]. Nevertheless, because of a short half-life of AMG 420, Amgen moved forward with AMG 701 for further clinical development due to its extended half-life stemming from the inclusion of the Fc domain[138, 139]. Interim phase I trial data for AMG 701 revealed 83% ORR and a manageable safety profile that included 61% cytokine release syndrome (CRS) (7% grade 3) and 8.5% low-grade neurotoxicity[140]. Teclistamab, a BCMA-specific BiTE from Janssen has recently demonstrated 63.8% ORR, 53% low grade-only CRS, and 5% neurotoxicity (2% grade 3 or higher) in a phase I study[141]. Regeneron's anti-BCMA BiTE, REGN5458, has shown 60% ORR at the highest dose level (35.6% ORR across all doses), 37.8% low grade-only CRS, 12% neurotoxicity (grade 3 in 1 patient), and grade 4 acute kidney injury in 1 patient[142]. Finally, TNB-383B, an anti-BCMA BiTE from AbbVie, had 80% ORR at the highest doses tested to date, 45% low grade-only CRS, 1 grade 3 confusion and no other reports of neurotoxicities to date[143].

Although ADC targeting FcRH5 has been clinically unsuccessful for MM[133], FcRH5 expression pattern limited to mature B cells and plasma cells has warranted investigations into FcRH5-specific BiTE therapy[144, 145]. A dose-escalation study of BFCR4350A, an anti-FcRH5 BiTE, has demonstrated interim ORR of up to 66.7% and 74.5% CRS (2% grade 3) with no reports of neurotoxicity[146]. Another recently emerging target for anti-MM immunotherapy is

GPRC5D, which is overexpressed in the bone marrow of MM patients and is associated with poor prognosis[147, 148]. An ongoing phase I study shows 78% ORR for intravenous (i.v.) and 67%% ORR for subcutaneous administration of the anti-GPRC5D BiTE[149]. CRS rate was 47% (<8% grade 3, all in i.v.-treated patients) and 5% of patients reported neurotoxicity (2% grade 3)[149].

3.3 T cell-based therapies

3.3.1 Rationale

To date, the only monoclonal antibodies that have shown efficacy as single agents in MM are those targeting CD38 with up to 31% ORR[98]. ADCs are potentially more efficacious as monotherapies, with reports of around 60% ORR in phase I trials[130, 150]. Different BiTEs against 3 distinct MM targets have now demonstrated 60-83% ORR as single agents (described above). Nevertheless, ADCs and BiTEs have limited serum half-life, which over time leads to insufficient therapeutic titers, so these agents need to be administered repeatedly for best therapeutic results[151, 152]. Protein-based therapeutics also rely on passive diffusion into tumors, unlike active trafficking of T cell-based therapies, and might have poor access to tumors with disrupted vasculature[153]. Moreover, monoclonal antibodies and BiTEs rely on recruitment and activation of endogenous immune effector cells at the tumor site, which might be challenging due to immune dysfunction associated with MM disease[154-156]. T cells, whether engineered or selected against tumor, are "living" drugs that once administered to patients, multiply *in vivo* and can

potentially generate memory cells to confer long-term anti-tumor protection[157, 158]. Additionally, the *ex vivo* manufacturing process offers an opportunity to expand and pharmacologically or genetically enhance the T cell product to best equip it for functioning in the harsh tumor microenvironment[159].

3.3.2 T cell activation

To understand the strategies guiding the current T cell-based therapeutic approaches, it is necessary to discuss the basic principles of T cell activation and function. Following development and maturation in the thymus, naïve T cells exit to the periphery in search for their antigen. The two signals required for full activation of naïve T cells are 1) stimulation through the T cell receptor (TCR)-CD3 complex and 2) ligand binding to co-stimulatory receptors[160] (Figure 1.1). The magnitude of the TCR-CD3 signaling and the cytokines present in the environment at the time of activation further shape the functional phenotype of the activated T cells[161].

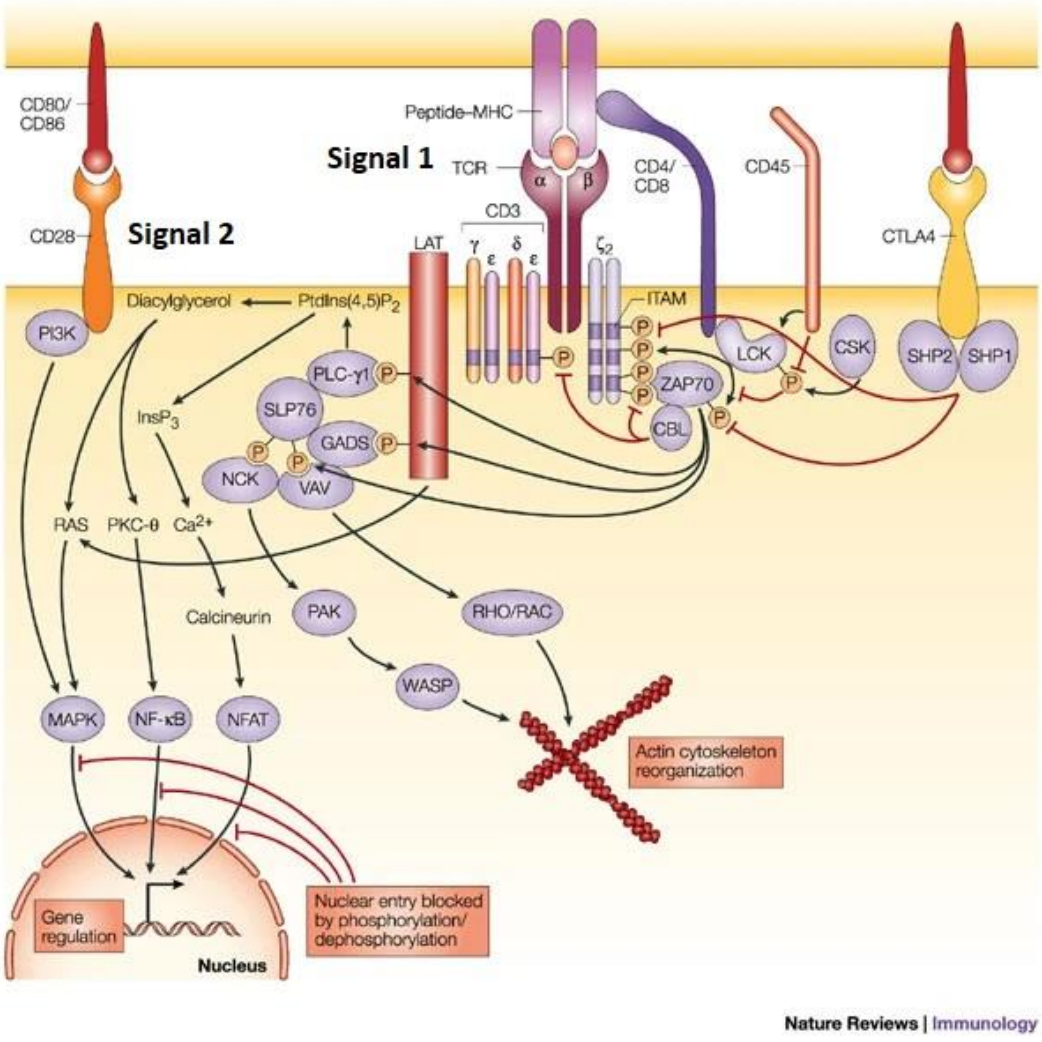

Figure 1.1. The two signals of T cell activation. Image adapted from Baniyash et al.[162]

Different models exist to describe the early events surrounding signal transduction from the point of TCR-CD3 engagement with a peptide ligand presented by the human leukocyte antigen (HLA)[163]. Several cellular components are recognized as key signal transduction players, irrespective of the model. The first such component is the cluster of immunoreceptor tyrosine-based activation motifs (ITAMs) in the cytoplasmic tails of the CD3 proteins, particularly those in

the CD3ζ chain. Phosphorylation of the CD3 ITAMs is at the top of the TCR-driven activation cascade[164] and is facilitated primarily by the Src family kinase, Lck[165]. The CD4 and CD8 co-receptors bind Lck and are generally believed to facilitate co-localization of Lck and CD3 ITAMs during T cell stimulation[166]. The activity of Lck is tightly regulated by the CD45 phosphatase to limit potential hyperactivation of T cells[167]. Phosphorylated CD3 ITAMs act as a binding site for the ZAP-70 kinase, which phosphorylates adaptor proteins LAT and SLP76 and drives the formation of a multi-protein signalosome[168-171]. This signaling complex triggers activation of the mitogen-activated protein kinase (MAPK) cascades and inositol trisphosphate (IP_3)-mediated calcium release from the endoplasmic reticulum[161]. Ultimately, the TCR-driven signaling pathways control changes in metabolism and activation of transcription factors responsible for cytokine production, cytotoxic granule release, and proliferation of activated T cells[161, 172, 173].

Structurally, antigen engagement and downstream signal transduction are a series of tightly coordinated events, which start with formation of the immunological synapse (IS)[174] (Figure 1.2). Microscopy studies have revealed that the structure of the IS resembles a bullseye with 3 distinct circular areas: central, peripheral, and distal supramolecular activation clusters (cSMAC, pSMAC, and dSMAC respectively)[175, 176]. The cSMAC area of the IS is rich in TCR microclusters, downstream signal transducers such as Lck and ZAP-70, and co-signaling molecules, such as those from the CD28 family[174]. Immediately surrounding cSMAC is the pSMAC, a ring rich in LFA-1 cell adhesion molecules,

which separates the cSMAC activation area from the negative regulators of T cell signaling (e.g. CD45) in the dSMAC[174]. This spatial segregation allows for efficient compartmentalization of proteins from the same pathways and selective targeting of secretory effector responses[176].

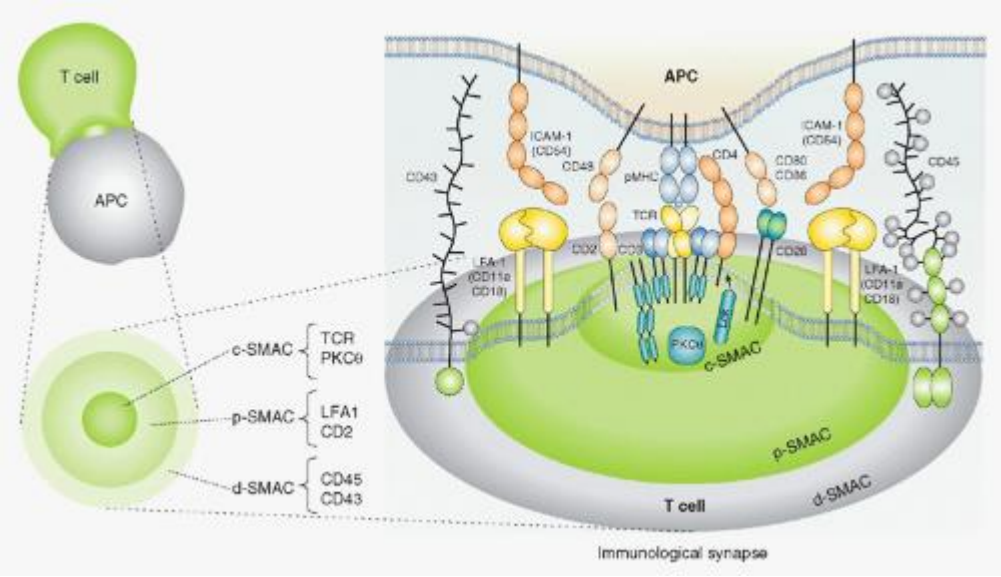

Figure 1.2. The structure of the immunological synapse. Image adapted from Oncohema Key[177].

As mentioned earlier, co-stimulatory signals are vital for effective T cell activation. The two main types of co-stimulatory receptors come from the CD28 family and the tumor necrosis factor receptor (TNFR) superfamily[178]. The ligands for the co-stimulatory receptors are expressed on antigen-presenting cells and are upregulated in response to inflammatory mediators present during infection[179]. The CD28 family of receptors includes stimulatory molecules CD28 and inducible T-cell co-stimulator (ICOS) and inhibitory molecules cytotoxic T-lymphocyte-associated protein 4 (CTLA-4), PD-1, and B- and T-lymphocyte attenuator

(BTLA)[178]. CD28 has been extensively studied as a potent co-stimulator of T cells and has been shown to trigger IL-2 secretion and upregulation of anti-apoptotic protein Bcl-X_L in activated T cells[180]. ICOS is homologous to CD28 and facilitates T cell activation by driving phosphorylation of Akt, which induces proliferation and survival signaling[181]. The TNFR superfamily receptors involved in T cell co-stimulation are 4-1BB, OX40, CD27, glucocorticoid-induced tumor necrosis factor receptor (GITR), CD30, and herpesvirus entry mediator (LIGHT)[182]. 4-1BB signals through the TNF receptor associated factor 1 (TRAF-1) and TRAF-2 adaptor proteins to activate p38 MAPK, ERK1/2, and canonical NF-κB pathway[183]. OX40 recruits TRAF-2 and -3 to induce both canonical and noncanonical NF-κB signaling[184]. CD27 also activates both types of NF-κB signaling along with c-Jun kinase via recruitment of TRAF-2 and -5 adaptor proteins[185]. Similarly to CD27, GITR also engages TRAF-2 and -5 to drive NF-κB activation[186]. CD30 is capable of recruiting TRAF-1, -2, and -5 to induce canonical NF-κB and c-Jun signaling[187]. Finally, HVEM can exert stimulatory or inhibitory functions on T cells, depending on the ligand it engages[188]. In addition to the CD28 and TNFR families of co-stimulatory molecules, integrin LFA-1, CD2, CD5, CD150, and several other receptors have been shown to augment T cell stimulation[189].

Combined together, stimulation through the TCR-CD3 complex and co-stimulatory receptors allows T cells to exert effector functions, proliferate, survive, and drive formation of T cell memory[178].

3.3.3 Early TCR-reliant approaches for T cell therapy

Early T cell-based approaches to cancer therapy did not emphasize specific signaling components of T cell activation and holistically focused on tumor-infiltrating lymphocytes (TILs) and antigen-specific T cells. The TIL strategy relied on isolation of lymphocytes from tumors, followed by *ex vivo* expansion and reinfusion, and proved particularly effective in melanoma cancer, which is characterized by high TIL infiltrates[190]. Unfortunately, the use of the TIL therapy is limited by the immunogenicity of tumors, ability to expand sufficient numbers of TILs from different patients, and the need for supplemental IL-2 administration, which can cause serious toxicities[190-192]. In MM, a similar concept of marrow-infiltrating lymphocytes (MILs) has been tested clinically. In a study where MILs were infused shortly after an ASCT, 27% of patients achieved a complete response (CR), with an ORR of 54%[193]. Notably, this was a relatively lightly pretreated patient population with 55% of study participants having received only 1 prior line of treatment. The presence of myeloma-specific T cells in the MIL product and persistence of myeloma-specific T cells in the bone marrow post-infusion correlated with better clinical outcomes[193].

As the TIL therapy started showing clinical promise, the interest of researchers turned to specific targets that the TILs were recognizing to create more focused therapeutics using transgenic TCRs. This approach highlighted the potential danger of targeting antigens expressed on normal tissues when a trial of melanoma antigen recognized by T cells (MART-1)- and glycoprotein 100 (gp100)-

specific high-affinity TCR-engineered cells used against melanoma led to eye, skin, and ear toxicities due to on-target, off-tumor reactivity of infused T cells[194]. Aspects of tumorigenesis resemble germ-cell development, and cancer-testis antigens (CTAs) have emerged as a group of germline-expressed genes that are reactivated in tumors and present a safer alternative to antigens that are only upregulated in tumors, but are still expressed at low levels on healthy tissues[195]. In MM, post-ASCT infusion of TCR-engineered T cells specific for a peptide shared by CTAs New York esophageal squamous cell carcinoma (NY-ESO-1) and L antigen family member 1 (LAGE-1) has been evaluated in a phase I/II trial[196]. This patient population was more heavily pretreated than the group in the MIL study[193], and no systemic supplemental IL-2 was administered. 80% of patients responded to the treatment with a median PFS of 19.1 months and an overall favorable safety profile, including 25% of patients showing skin or gastrointestinal graft-versus-host events that were resolved with treatment[196]. This engineered TCR approach is currently being evaluated as a monotherapy or in combination with a PI[197]. While the NY-ESO-1-specific transgenic TCR strategy has shown good clinical efficacy in MM, it is limited to patients whose MM cells express a specific HLA that the TCR is designed to recognize. Additionally, as the TCR-based therapeutics evolve to target different antigens, there remains a danger of cross-recognition of antigen-unrelated, but similar peptides presented on healthy tissues. For example, a melanoma study of T cells engineered with TCRs specific for a CTA melanoma-associated antigen 3 (MAGE-A3) led to off-target, off-tumor lethal cardiac toxicity in two patients due

to unexpected recognition of a titin-derived peptide by the MAGE-A3-targeting TCRs[198, 199].

3.3.4 Chimeric antigen receptors

Chimeric antigen receptors (CARs) were created as synthetic, HLA-independent receptors that include an antigen-binding domain of choice, followed by the hinge region, the transmembrane domain, and the intracellular signaling domain(s) that can trigger T cell activation (Figure 1.3). Since tumors commonly lose HLA expression as a way of immune evasion[200], HLA-independent targeting of CARs can provide an advantage over therapeutics with TCR-based tumor recognition.

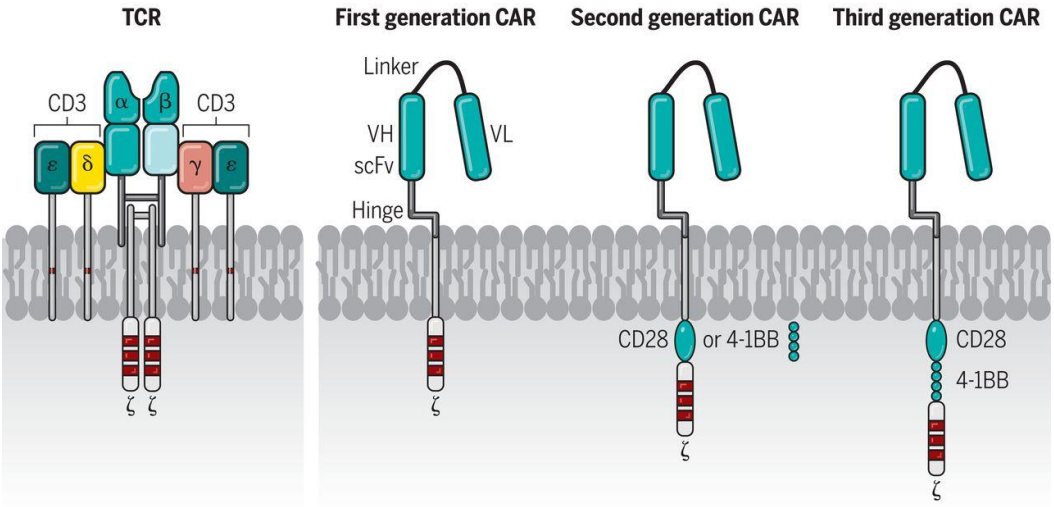

Figure 1.3. The three generations of CARs. Image adapted from June et al[201].

Most antigen-binding domains are designed using antibody fragments in the form of an scFv, but can include other synthetic or naturally occurring proteins and

even peptides. We have previously reviewed the diversity of choices for antigen-binding domains and the concepts of affinity and specificity pertaining to their selection (Appendix). The antigen-binding domain of a CAR is followed by a hinge or a spacer region that can impact the efficiency of epitope access by the antigen-binding domain and affect the overall CAR-engineered T (CAR-T) cell efficacy[202]. A longer, flexible hinge is preferred for membrane-proximal target epitopes[203], whereas a shorter hinge is more optimal for membrane-distal target epitopes[204]. A hinge region might also lead to undesirable off-target activation if it is taken from a protein domain with a ligand-binding capacity. For instance, immunoglobulin G1 (IgG1)-based hinge has been shown to retain its Fc gamma receptor (FcγR)-binding capacity and trigger CAR-T cell activation by FcγR-expressing innate immune cells[205]. Following the hinge, is the transmembrane domain that is responsible for anchoring the CAR in the plasma membrane. Transmembrane domains of CD3ζ, CD4, CD8α, CD28, and ICOS have been used in the CAR design, with some reports suggesting that certain downstream signaling domains might work better with some transmembrane domains than others[202].

Since CARs are designed to function independently from the TCR, the intracellular signaling domains of the synthetic receptor have received a lot of attention. Three generations of CAR designs have now been described in literature (Figure 1.3). First-generation CARs contained the CD3ζ ITAMs without any co-stimulatory domains and triggered cytotoxicity and cytokine production in *vitro*[206], but were inefficient at activating resting T cells[207], producing IL-2 in the absence

of co-stimulation[208], and clearing tumors *in vivo*[209]. Second-generation CAR designs incorporated intracellular domains responsible for both signals necessary for T cell activation. Out of a myriad of potential co-stimulatory domains, CD28 and 4-1BB signaling domains have been used more frequently than others[202]. CD19-specific CD28- and 4-1BB-based second-generation CAR-T cells demonstrated remarkable clinical efficacy in heavily pretreated, refractory B-cell lymphoma and leukemia patients and ultimately reached regulatory approval[210-212]. Third-generation CARs combine several co-stimulatory domains, but any additive advantage of these domains in a single receptor is still subject to debate[213]. To date, CD19-specific CAR-T cells for B cell malignancies have been leaders in the field, but second- and third-generation CAR constructs for multiple other targets and types of cancer are in various stages of clinical development and have been reviewed extensively in literature[214-216].

In MM, BCMA has been the leading candidate for CAR-T cell therapies with multiple CAR-T trials demonstrating susceptibility of MM to engineered T cell products. The first BCMA-specific CAR-T cells to reach clinical trials were from the National Cancer Institute (NCI) and had the second-generation CD28ζ scaffold. The highest dose of this product led to 81% ORR in a very heavily pretreated group of patients with a median of 9.5 lines of prior therapy[217]. Median PFS was 7 months, and at the time of reporting, 38% or patients had ongoing responses. Another product that used the same murine scFv-based antigen-binding domain on a 4-1BBζ scaffold was the bb2121 CAR that resulted in 73% of patients

responding and 33% of patients achieving a CR[218]. Median PFS was 8.8 months, and at the time of reporting, 60% of patients with an initial CR had relapsed. The same construct, but manufactured in the presence of a PI3K inhibitor to enrich for memory-like T cells (bb21217 product) has been showing 48% ORR across all dose levels in an ongoing dose escalation study[219]. A fully human BCMA-specific 4-1BBζ CAR-T cell product from the University of Pennsylvania (CART-BCMA) has demonstrated 64% ORR at the highest dose level, including 18% CR, and just over 4 months median PFS[220]. Another fully human BCMA-specific CAR-T construct JCARH125 that is manufactured with enrichment for central memory T cells has a 91% ORR (39% CR) combined across all levels[221].

Two studies have been published on the LCAR-B38M product, which uses two llama-derived antibody fragments (VHH domains) for antigen binding and a 4-1BBζ CAR scaffold. In the first trial, where T cells were administered over 3 infusions, patients experienced an 88% ORR (68% CR) and a median PFS of 15 months[222]. In the second trial, the LCAR-B38M T cell treatment was administered either as a single infusion or over 3 infusions, with a different conditioning regimen for each dosing schedule, but no difference in responses or toxicity was observed between the two schedules, so the combined ORR was 88% (76% CR) and median PFS was 12 months[223]. The same product is currently being evaluated under the name JNJ-68284528 as a single-dose administration with an interim ORR of 95% (56% CR)[224].

Several other BCMA-specific CAR-T cell products are advancing through the early-stage clinical trials. A 4-1BBζ CAR construct with a human heavy chain-only fragment in the antigen-binding domain (FHVH33) has an interim ORR of 90%[225]. CT053, another 4-1BBζ-based CAR with a human anti-BCMA scFv 25C2 in the antigen-binding domain is demonstrating 100% ORR (40% CR), based on the data from 10 evaluable patients[226]. P-BCMA-101 is a 4-1BBζ-based CAR product that contains a Centyrin in the antigen-binding domain and is manufactured with a method enriching for stem cell memory T cells[227]. To date, the ORR in the P-BCMA-101 trial is at 57% and 100% in the four patients who received lenalidomide following the CAR-T cell treatment[227]. Another BCMA-specific design with a non-antibody-based antigen-binding domain on a 4-1BBζ scaffold is CART-ddBCMA[228]. To date, report of only 4 patients treated with this construct is available with all 3 of the evaluable patients demonstrating clinical response[228]. Finally, an allogeneic BCMA-specific CAR-T cell product ALLO-715 has entered clinical testing, administered along with an anti-CD52 antibody ALLO-647 for host lymphodepletion[229]. At the highest dose administered at the data cutoff time, 60% of patients were responding to the ALLO-715 treatment without signs of GVHD[229].

Although BCMA is the most widely recognized target for anti-MM engineered T cell therapies, other proteins are being evaluated in the CAR-T cell trials. CD19 is not expressed on MM cells, but it is expressed on MGUS and is believed to be one of the markers of the myeloma-initiating cells[230]. Based on this idea, CD19-directed CAR-T cells were tested in a small-scale trial with MM

patients, but provided modest clinical benefit[231]. Other MM CAR-T cell therapy targets under early-phase clinical investigation include CD38, SLAMF7, GPRC5D, and NKG2D[232].

3.3.5 Mechanisms of non-responses/relapses

Since CD19 CAR-T cell trials in leukemia and lymphoma are several years ahead of studies with other targets/indications and have produced the first regulatory approvals in the field, most of our current understanding of resistance to CAR-T cell therapies comes from the use of these clinically approved products. 29-57% of patients relapse post-CD19-directed CAR-T cell therapy with various trials attributing 16-75% of relapses to CD19-negative disease[233]. Genetic studies have implicated mutations causing alternative splicing or loss of CD19 surface expression in the mechanisms underlying CD19-negative relapses[234]. Use of alternative targets such as CD22 has been proposed as a solution for treating CD19-negative or CD19-low disease[235]. Durability of responses following CD19 CAR-T cell therapy has also been associated with persistence of CAR-T cells[236, 237], with 4-1BB-based backbone promoting long-term CAR-T cell survival more efficiently than the CD28-based backbone in preclinical studies[238].

The clinical experience with CAR-T cell treatments in MM is still in early stages. Nevertheless, there have been a few reports of BCMA loss or downregulation in relapsing disease[217, 225, 239]. γ-Secretase is responsible for BCMA cleavage off the surface of MM cells[240], and the use of γ-secretase inhibitors

alongside BCMA-specific CAR-T cells has been proposed as a strategy to combat antigen loss/downregulation[241]. Other studies have found no correlation between BCMA levels and efficacy[222, 242] and reported BCMA expression on relapsed disease[223, 243]. Limited experience with patients who have undergone multiple types of BCMA-targeted immunotherapies[244] also suggests that antigen loss or downregulation might not be as influential in MM relapses as it is in the field of CD19-positive tumors. Observations uncoupling therapeutic efficacy from BCMA expression and post-treatment PFS data of 15 months or less argue that despite encouraging initial responses to BCMA CAR-T cell therapy, there remains a lot of room for improving engineered T cell products with the goal of deepening and prolonging responses.

3.3.6 CAR treatment toxicities

Therapeutic efficacy of CAR-T cell treatments comes at the cost of potentially severe toxicities. Similarly to the observations with TCR-engineered T cells, CAR-T cells can trigger on-target, off-tumor toxicity, if the antigen they are designed to recognize is expressed on healthy tissues. CAR-T cells specific for human epidermal growth factor receptor 2 (HER2) and carbonic anhydrase IX (CAIX) have both shown lethal toxicity due to CAR-T cell-mediated attack on lung epithelium and biliary epithelium respectively[245, 246]. Even the widely successful CD19-directed CAR-T cell treatments lead to B-cell aplasia, but the side effects of B cell loss can be managed with intravenous immunoglobulin administration[212, 247]. Strategies like modulation of CAR affinity might help CAR-T cells discriminate

between tumor cells expressing high levels and healthy cells expressing low levels of the antigen of interest[248], but the choice of the target remains incredibly important for the success of treatment.

Clinical experience with CAR-T cells highlights two types of toxicity specifically linked to this treatment. The first one is CRS, briefly mentioned in section 3.2 because of its association with the BiTE therapy. CRS is a consequence of systemic inflammatory response stemming from the activation of infused engineered T cells and, if left untreated, can escalate to widespread vascular leakage, hypotension, tachycardia, and in severe cases, multiple organ failure and death[249]. Lee and colleagues have provided a comprehensive grading summary of CRS severity that is now widely used in the field[250]. Currently published and ongoing trials with BCMA-directed CAR-T cells in MM report high rates of CRS in the range of 67-100%, with 2-41% or patients experiencing grade 3 or higher CRS[217-225, 242].

The second CAR-T-associated toxicity is immune effector cell-associated neurotoxicity syndrome (ICANS)[251]. ICANS manifestations vary in severity from milder conditions such as confusion and lethargy to life-threatening cerebral edema[251]. Severe ICANS is commonly associated with high-grade CRS, but the mechanisms underlying CAR-T-cell-induced neurotoxicity are still largely unknown[249]. In BCMA CAR-T trials, 18-42% of patients experience neurotoxicity (3-14% grade 3 or higher)[217-221, 225, 242]. The first LCAR-B38M trial seemed to have lower neurotoxicity rates with only 2% of patients experiencing low-grade

events[222], but an ongoing larger-scale study is now reporting 20.6% neurotoxicity rates (10.3% grade 3 or higher)[224], which are in line with data from other BCMA-specific CAR-T cell products. None of the 14 patients treated with the CT053 CAR-T product have shown high-grade CRS or ICANS, despite 86% and 7% of subjects reporting low-grade CRS and ICANS respectively, but the trial is still ongoing[226]. P-BCMA-101 CAR-T-treated patients have so far demonstrated a comparatively lower toxicity profile, including 17% rate of CRS (2% grade 3) and 2% low grade-only ICANS, which researchers attributed to the delayed expansion of engineered T cells, compared to other products[227]. The same trial has an interim ORR that is lower, relative to other BCMA-CAR-T cell trials, so it remains to be seen whether the lower toxicity rates are also associated with a lower percentage of responders.

3.3.7 Next-generation TCR-reliant approaches

The CAR-T cell strategy has produced impressive responses in heavily pretreated cancer patients, but high toxicity rates remain a concern and preclude frail patients from benefitting from this treatment. The synthetic design of CARs is capable of triggering T cell activation, but lacks the intricate network of signaling pathways associated with the TCR that allows T cells to autoregulate their activity. Engineering strategies that manage to engage these endogenous regulatory mechanisms could help uncouple toxicities from therapeutic efficacy.

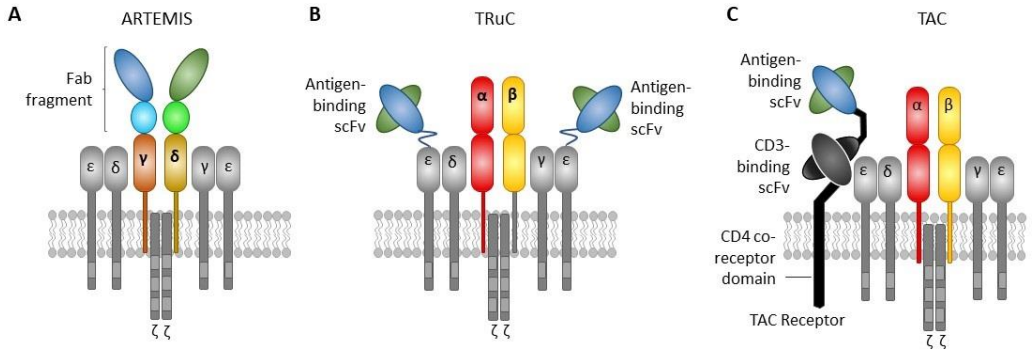

Figure 1.4. New TCR-dependent T cell engineering strategies. (A) ARTEMIS. (B) TRuC. (C) TAC. T cell receptor chains (γδ or αβ) and the antigen-binding domain(s) in each technology are shown in color. CD3 chains are shown in grey.

Several groups, including ours, have sought to merge the benefits of HLA-independent antigen recognition characteristic of CARs with TCR-driven modulation of effector responses. ARTEMIS technology (Figure 1.4A) combines Fab antibody domain with TCR γ and δ chains and has demonstrated reduced cytokine production and comparable efficacy, relative to the 28ζ and 4-1BBζ second-generation CAR constructs in preclinical studies[252]. A CD19-redirected ARTEMIS product has shown interim 78% ORR and no reported CRS of ICANS in a trial with B-cell leukemia and lymphoma patients[253]. Two more ongoing studies are evaluating alpha fetoprotein-redirected ARTEMIS cells in hepatocellular carcinoma (NCT03888859 and NCT03965546). The TRuC platform (Figure 1.4B) leaves the TCR chains intact and redirects T cells to the antigen of interest via a CD3ε chain fused to an scFv[254]. Preclinical testing revealed that TRuC-engineered T cells are more efficacious *in vivo* and less likely to produce cytokines *in vitro*, when compared to conventional second-generation CAR-T cells[254]. CD19- and

mesothelin-targeting TRuC T cells have now entered clinical trials (NCT04323657 and NCT03907852).

Our lab has developed a T cell antigen coupler (TAC) platform, centered around a synthetic receptor that binds to the CD3ε chain via an scFv and redirects TCR-CD3 complex to the target of interest (Figure 1.4C). TAC is created as a modular receptor, allowing for custom modulation of receptor properties by replacing or adding different domains. The original TAC design features an antigen-binding domain connected to a CD3-binding domain via a flexible linker, followed by transmembrane and intracellular domains of the CD4 co-receptor, which is included to anchor TAC receptor in the membrane and recruit Lck in the proximity of the TCR-CD3 complex. Preclinical studies showed no tonic activation in TAC-engineered T cells along with improved efficacy, compared to CAR-T cells, and no evidence of toxicity in a HER2-positive solid tumor model[255]. Two clinical trials have now been initiated with CD19- and HER2-targeting TAC-T cells (NCT03880279 and NCT04727151).

4. Thesis objectives

Overview

Despite the introduction of novel drugs into the MM treatment landscape, this cancer continues to show adaptation to multiple classes of therapeutics and presents a currently unmet clinical need. Engineered T cells have shown promise in hematological malignancies, including MM, and studies with different types of

immunotherapeutics have produced clinical evidence that BCMA is an excellent MM-specific target antigen. While CAR-T cell trials highlight susceptibility of MM to this type of therapy, limited durability of responses and high risk of toxicity call for further innovation of T cell-based approaches. Our lab has developed a unique TAC platform for redirecting T cells to the target of interest and activating them through the endogenous TCR-driven signaling pathways. The main goal of the work presented in this thesis was to create a fully human BCMA-specific TAC receptor for subsequent testing in MM clinical trials (objectives 1 and 2). As we compared different BCMA-specific domains, we observed that non-toxic cross-reactivity of the antigen-binding domain could support therapeutic efficacy and sought to further evaluate this phenomenon using different synthetic receptor frameworks (objectives 3 and 4).

Objective 1: Optimization of the CD3-binding domain and the TAC receptor surface expression

Objective 2: Development of a fully humanized BCMA-specific TAC

Objective 3: Comparison of two murine BCMA-specific antigen-binding domains

Objective 4: Evaluation of the effects of a cross-reactive antigen-binding domain on the efficacy of second-generation CAR-T cells

Chapter 2

Materials and Methods

Cell lines

Human myeloma cell lines KMS-11 and MM.1S (kindly provided by Dr. Kelvin Lee, Roswell Park Cancer Institute, NY) were cultured in RPMI 1640 (Gibco), supplemented with 10% FBS (Gibco), 2 mM L-glutamine (BioShop), 10 mM HEPES (Roche Diagnostics), 1mM sodium pyruvate (Sigma-Aldrich), 1 mM nonessential amino acids (Gibco), 100 U/mL penicillin (Gibco), and 100 µg/mL streptomycin (Gibco). To generate luciferase-expressing cell lines, parental KMS-11 and MM.1S cell lines were transduced with lentivirus encoding enhanced firefly luciferase (effLuc)[256] or NanoLuc-eGFP fusion protein (GpNLuc)[257] as well as puromycin N-acetyltransferase at an MOI 10 and selected in culture media supplemented with 8 µg/mL puromycin (InvivoGen). HEK293T cells were cultured in DMEM (Gibco), supplemented with 10% FBS (Gibco), 2 mM L-glutamine (BioShop), 10 mM HEPES (Roche Diagnostics), 100 U/mL penicillin (Gibco), and 100 µg/mL streptomycin (Gibco), or 0.1 mg/mL normocin (InvivoGen). All cells were cultured at 37 °C, 95% ambient air, 5% CO_2.

Receptor generation and lentivirus production

TAC receptor sequence was constructed as in[255] and UCHT1 TAC variants were generated as in patent WO2019071358[258]. Human CD8α signal peptide or murine IgK signal peptide were used with the TAC constructs. C11D5.3 scFv cDNA (sequence from patent US20150051266 A1) was synthesized at GenScript. The J22.9-xi scFv was designed by linking V_H and V_L sequences provided by the

Max-Delbruck Center for Molecular Medicine (Berlin, Germany) via a Whitlow linker[259] and synthesized at GenScript. The second-generation CAR construct backbones were constructed as in[260]. Briefly, the CD28ζ CAR construct included a CD8α signal peptide, J22.9-xi scFv, cMyc tag, CD8α hinge, transmembrane and intracellular domains of CD28, and CD3ζ intracellular domain. The 4-1BBζ CAR construct included a CD8α signal peptide, J22.9-xi scFv, cMyc tag, CD8α hinge and transmembrane domains, 4-1BB intracellular domain, and CD3ζ intracellular domain. All plasmids used for T cell engineering contained a gene for the human CD271 (NGFR) with the intracellular signaling domains removed, allowing for the use of NGFR surface expression as a transduction marker.

Lentivirus production was performed as in[261]. Briefly, 12 x 10^6 HEK293T cells plated on a 15-cm dish (NUNC) were transfected with plasmids pRSV-Rev (6.25 μg), pMD2.G (9 μg), pMDLg-pRRE (12.5 μg), and pCCL (32 μg), using Opti-MEM (Gibco) and Lipofectamine 2000 (Thermo Fisher Scientific). 12-16 hours post-transfection, media were exchanged to media supplemented with 1 mM sodium butyrate (Sigma-Aldrich). 24-36 hours later, supernatants were harvested, viral particles were concentrated by centrifugation in Amicon filter system (Millipore Sigma) and stored at -80 °C. Viral titre (TU/mL) was determined post-thaw by serial dilution, transduction of HEK293T cells, and enumeration of percent $NGFR^+$ cells by flow cytometry.

Engineering of human T cells

Peripheral blood mononuclear cells (PBMCs) were obtained from healthy donors and MM patients who provided informed written consent in accordance with the Hamilton Integrated Research Ethics Board. In some cases, PBMC were collected from commercial leukapheresis products (HemaCare and StemCell Technologies). PBMCs were isolated by Ficoll-Paque-Plus gradient centrifugation (GE Healthcare) and cryopreserved in inactivated human AB serum (Corning), containing 10% DMSO (Sigma-Aldrich) (healthy donors) or RPMI (Gibco), containing 12.5% HSA (Sigma-Aldrich), and 10% DMSO (MM donors).

PBMCs were stimulated with anti-CD3/28 Dynabeads (Gibco) at a 0.8:1 bead:cell ratio and cultured in RPMI 1640 (Gibco) containing 10% FBS (Gibco), 2 mM L-glutamine (BioShop), 10 mM HEPES (Roche Diagnostics), 1 mM sodium pyruvate (Sigma-Aldrich), 1 mM non-essential amino acids (Gibco), 55 μM β-mercaptoethanol (Gibco), 100 U/mL penicillin (Gibco), 100 μg/mL streptomycin (Gibco), 100 I.U./mL rhL-2 and 10 ng/mL rhIL-7 (PeproTech). 16-24 hours later, cells were transduced with lentivirus at an MOI 2. Dynabeads were removed on day 4 of culture. Cells were sorted with EasySep Human CD271 Positive Selection Kit (StemCell Technologies) on day 6-7 of culture and expanded for a total culture period of 14 days prior to use *in vitro* and/or *in vivo*. For *in vivo* bioluminescence tracking experiments, T cells were sorted on day 4 with EasySep Human CD271 Positive Selection Kit (StemCell Technologies) and transduced with effLuc-

encoding lentivirus at an MOI 2 on the same day. For *in vivo* experiments, T cells were cryopreserved in Cryostor CS10 (StemCell Technologies) according to manufacturer's instructions.

Vector copy number analysis

Cryopreserved engineered T cells were thawed and counted. Genomic DNA from 4 x 10^6 cells/construct was isolated with a DNeasy Blood & Tissue Kit (Cat No. 69504, Qiagen) according to the manufacturer's protocol. The DNA was quantified with NanoDrop One^C. The standard curve (0.001-10 pg range) for the targets of interest was produced with a linearized pCCL plasmid containing huUCHT1-TAC sequence. The standard curve (2.5-40 ng range) for determining the amount of genomic DNA was produced with human male DNA obtained from Applied Biosystems (Catalog No. 360486). All standard curve points were done in triplicates. The following reagents were used for the qPCR assay: TaqPath ProAmp Master Mix (Cat No. A30865, Applied Biosystems), TaqMan RNase P Assay, VIC dye/QSY probe (Cat No. A30064, Applied Biosystems), forward primer AGTGGCGGAGGAGGATCACT, reverse primer GGGCAGGACTTTGATATTGGATT, probe AGAGCGGACAGGTGC (NFQ-MGB quencher) with a FAM reporter. A total of 20 ng of genomic DNA was used per reaction. All procedures were performed according to the manufacturers' instructions. Data were recorded with the StepOnePlus Real-Time PCR System

(Applied Biosciences), using StepOne software version 2.3. The following calculations were used for determining vector copy number (VCN) per cell:

$$VCN\ per\ cell = 2\ \times \frac{target\ copy\ number}{haploid\ RNase\ P\ copy\ number}$$

$$Target\ copy\ number = \frac{amount\ of\ target\ detected}{mass\ of\ a\ single\ plasmid\ molecule}$$

$$Haploid\ RNase\ P\ copy\ number = \frac{amount\ of\ RNase\ P\ detected}{mass\ of\ haploid\ genome}$$

***In silico* modeling**

Protein docking was modeled with a web-based ClusPro 2.0 software (Boston University, USA)[262] and the models were analyzed with a web-based CSU software (Weitzmann Institute of Science, Israel)[263] for the number of contacts between proteins of interest. All predicted bonds for each amino acid were added and displayed as a total number of contacts.

Protein production and purification

UCHT1 scFv variants were cloned into pET-20b(+)to add a C-terminal His-tag and transformed into competent *E. coli* BL21(DE3) (New England BioLabs). All recombinant strains were grown at 37°C to OD_{600} ~ 0.6 in LB medium with 50 μg/mL ampicillin (Sigma-Aldrich) and protein expression was induced using 0.04 mM IPTG (Sigma-Aldrich). After a 4-hr induction at 37°C, cells were harvested by

centrifugation at 5,000 x g for 10 minutes and pellets were lysed using BugBuster MasterMix (Millipore Sigma) in the presence of cOmplete Protease Inhibitor Cocktail (Roche). Denaturing buffer (PBS, 8M urea, 500 mM NaCl) was added to the cellular debris to extract the recombinant protein from inclusion bodies. After 40-minute denaturation, samples were centrifuged and loaded onto 1 mL HiTrap chelating columns (Cytiva) charged with 100 mM nickel. Denatured protein was refolded using decreasing gradient of urea (PBS, 6 - 0 M urea, 500 mM NaCl). The proteins were eluted off the column with an increasing gradient of imidazole (PBS, 0 - 250 mM imidazole, 500 mM NaCl). SDS-PAGE gels were used to determine which fraction contained the protein. The fraction was then run through a PD-10 desalting column (Cytiva) and eluted in PBS to remove salt and imidazole ions. Purified recombinant proteins were concentrated using 10 KDa Amicon Ultra-0.5 centrifugal filter units (Millipore Sigma) and quantified using a Bradford Assay (Bio-Rad Laboratories).

Determination of the binding constant using bio-layer interferometry

Bio-Layer Interferometry assays were performed on the ForteBio Octet Red96 system (Molecular Devices). The scFv proteins were dissolved in kinetics buffer (PBS, pH 7.4, Tween-20 0.02%, 0.1% BSA) to create a dilution series (1.25 nM – 500 nM). Probes were pre-wet for 600 seconds and 100 nM of biotinylated human CD3εδ heterodimer (ACROBiosystems) was loaded for 240 seconds onto streptavidin biosensors (ForteBio) and quenched in 5% milk. Association with the

scFvs lasted 180 seconds, followed by 600-second dissociation in kinetics buffer. The data were analyzed in Prism v.8 (GraphPad) with pre-installed binding kinetics formulas for one phase exponential decay and one concentration of hot ligand, to estimate the binding constant for the scFvs.

Flow cytometry

Surface expression of TAC and CAR constructs was determined by staining with recombinant human BCMA-Fc protein (Cat No.193-BC, R&D Systems), followed by PE-conjugated goat anti-human IgG (Cat No. 109-115-098, Jackson ImmunoResearch). Other phenotypic markers were detected with Pacific Blue-conjugated mouse anti-human CD4 (Cat No. 558116, BD Pharmingen), AlexaFluor700-conjugated mouse anti-human CD8α (Cat No. 56-0086-82, eBioscience), and VioBright FITC-conjugated mouse anti-human NGFR (Cat No. 130-104-893, Miltenyi Biotec). Surface expression of BCMA on tumor cells was determined by staining with PE-conjugated recombinant human anti-human BCMA (Cat No. 130-118-970, Miltenyi Biotec).

Binding of purified His-tagged scFvs was detected by staining PBMCs with scFv, followed by mouse anti-6xHis (Cat No. 552565, BD Pharmingen), PE-conjugated goat anti-mouse IgG (Cat No. 115-116-146, Jackson ImmunoResearch), and then PerCP-Cy5.5-conjugated mouse anti-human CD8α (Cat No. 45-0088-41, eBioscience) and Alexa Fluor 700-conjugated mouse anti-human CD4 (Cat No. 56-0048-41, eBioscience). Flow cytometry data were collected with BD LSRFortessa

or BD LSRII cytometer (BD Bioscience) and analyzed using FlowJo vX software (FlowJo).

Analysis of the time course of checkpoint receptor expression

0.5 x 10^6 engineered T cells were stimulated with KMS-11 tumor targets at a 1:1 effector:target ratio at 37 °C for indicated time periods or left non-stimulated. Cells were stained with Live/Dead Fixable Near-IR stain (Invitrogen), then with BCMA-Fc protein (R&D Systems), followed by PE-conjugated goat anti-human IgG (Jackson ImmunoResearch), PerCP-Cy5.5-conjugated mouse anti-human CD8α (Cat No. 45-0088-41, eBioscience), Alexa Fluor 700-conjugated mouse anti-human CD4 (Cat No. 56-0048-41, eBioscience), VioBright FITC-conjugated mouse anti-human NGFR (Miltenyi Biotec), BV510-conjugated mouse anti-human CD138 (Cat No. 356518 BioLegend), BV650-conjugated mouse anti-human CD69 (Cat No. 563835, BD Pharmingen), BV421-conjugated mouse anti-human PD-1 (Cat No. 562516, BD Pharmingen), Alexa Fluor 647-conjugated mouse anti-human LAG-3 (Cat No. 565716, BD Pharmingen), and BV785-conjugated mouse anti-human TIM-3 (Cat No. 345032, BioLegend). Flow cytometry data acquisition was performed as indicated above and pre-processed with FlowJo vX software (FlowJo).

The flow cytometry data were quality-checked by the flowAI Bioconductor package for R[264]. Detection and removal of anomalies provided the events for further pre-processing. Pre-gated viable, single-cell, $CD138^-NGFR^+$ events were

randomly subsampled to 20,000 cells and subjected to a differential analysis pipeline scripted in R (cran.r-project.org). Unsupervised clustering analysis was performed by flowSOM[265], and differential analysis was performed by diffcyt[266]. Tests for differential abundance of cell populations, represented by flowSOM meta-clusters, were calculated using the edgeR method. Tests for differential states in the expression of TAC, CD69, PD-1, LAG-3, and TIM-3 within these cell populations were calculated using the limma method. Data were visualized using t-stochastic neighbor embedding (t-SNE)[267]. The CATALYST package[268] was instrumental in providing a framework for passing data objects from one Bioconductor package to another and doing quality checks along the pipeline.

Cytokine analysis

4 x 10^5 engineered T cells were stimulated with 2 x 10^5 KMS-11, MM.1S, or HEK293T cells for 4 hours at 37 °C in the presence of brefeldin A (BD GolgiPlug, Cat No. 555029, BD Pharmingen) and monensin (BD GolgiStop, Cat No. 554724, BD Pharmingen). Patient-derived engineered T cells were stimulated at a ratio of 10^5 engineered T cells to 10^5 target cells. Cells were stained for surface expression of CD4 (BD Pharmingen) and CD8 (eBioscience), fixed and permeabilized in Cytofix/Cytoperm buffer (Cat No. 554714, BD Pharmingen), and stained with APC-conjugated mouse anti-human IFN-γ (Cat No. 554702, BD Pharmingen), PE-conjugated rat anti-human IL-2 (Cat No. 554566, BD Pharmingen), and FITC-conjugated mouse anti-human TNF-α (Cat No. 554512,

BD Pharmingen). Flow cytometry data were acquired and analyzed as indicated above.

For multiplex secreted cytokine analysis, 5 x 10^5 engineered T cells were stimulated with 5 x 10^5 KMS-11 cells for 24 hours at 37 °C. Supernatants were spun down to remove cellular debris and analyzed in duplicates by Eve Technologies (Calgary, AB) with a 14-plex Human High Sensitivity T-Cell Discovery Array (Cat No. HDHSTC14). Data were processed with Prism v.8 (GraphPad) and paired t-tests were performed to determine significance.

***In vitro* cytotoxicity assay**

Engineered T cells were stimulated with 5 x 10^4 luciferase-expressing cells in triplicates at indicated effector:target ratios for 8 hours at 37 °C. Following stimulation, 0.15 mg/mL D-Luciferin (Cat No. 122799, Perkin Elmer) was added and luminescence was measured with an open filter using SpectraMax i3 (Molecular Devices) plate reader. Percent cytotoxicity was calculated as:

$$\%\ \text{Cytotoxicity} = \left(1 - \frac{\text{Test Sample} - \text{Media Alone}}{\text{Tumor Alone} - \text{Media Alone}}\right) \times 100\%$$

Proliferation assay

Engineered T cells were labelled with CellTrace Violet dye (Invitrogen) and stimulated with KMS-11 or MM.1S tumor targets at an effector:target ratio 2:1 or left not stimulated. For bead stimulations, protein G-coated polystyrene beads

(Spherotech) were pre-coated with different concentrations of recombinant human BCMA-Fc protein (R&D Systems) overnight at 4 °C prior to the start of the assay. T cells were stimulated with beads at a 1:1 effector:target ratio. All proliferation assay samples were incubated for 4 days at 37°C and stained with Live/Dead Fixable Near-IR stain (Invitrogen), PerCP-Cy5.5-conjugated mouse anti-human CD8α (eBioscience), Alexa Fluor 700-conjugated mouse anti-human CD4 (eBioscience), VioBright FITC-conjugated mouse anti-human NGFR (Miltenyi Biotec), and APC-conjugated mouse anti-human CD138 (Cat No. 356505, BioLegend). Flow cytometry data were acquired as indicated above. Results were analysed with FCS Express v.6 (De Novo Software) by determining the starting generation peak based on the non-stimulated sample and using the software proliferation package for fitting a proliferation model and collecting corresponding statistics, such as % divided.

Conjugation assay

Engineered T cells were pre-labelled with BV421-conjugated mouse anti-human NGFR (Cat No. 562562, BD Pharmingen), and myeloma cells were pre-labelled with APC-conjugated mouse anti-human CD138 (BioLegend). 2.5 x 10^5 T cells and 2.5 x 10^5 tumor cells were briefly spun down, incubated for 0, 10, 20, and 40 minutes at 37 °C, fixed with 2% formaldehyde, and analyzed by flow cytometry without filtering or resuspension to preserve cell-cell conjugates.

Nur77 and Caspase-3 activation assessments

5 x 10^5 engineered T cells and 5 x 10^5 tumor cells per sample were incubated for 2 and 4 hours at 37 °C. Cells were stained for surface expression of CD4 (BD Pharmingen), CD8 (eBioscience), CD138 (BioLegend), NGFR (BD Pharmingen), and CD69 (BD Pharmingen), fixed and permeabilized in Cytofix/Cytoperm buffer (BD Pharmingen), and stained with PE-conjugated mouse anti-mouse Nur77 (Cat No. 12-5965-82, eBioscience).

T cells were stimulated as in the Nur77 assay for 4, 8, 28, 52, and 124 hours, stained with Live/Dead Fixable Near-IR stain (Invitrogen), then for surface markers as in the Nur77 assay, fixed, permeabilized, and stained with PE-conjugated active caspase-3 apoptosis kit (Cat No. 550914, BD Pharmingen) according to manufacturer's instructions. Flow cytometry data were acquired and analyzed as indicated above.

Assembly of supported lipid bilayers and T cell binding

Lipid preparation and assembly of supported lipid bilayers was performed as in[269] using lipids composed of 1,2-dioleoyl-sn-glycero-3-phosphocholine (DOPC) and 1,2-dioleoyl-sn-glycero-3-[(N-(5-amino-1-carboxypentyl) iminodiacetic acid) succinyl] (DGS-NTA(Ni)) (Avanti Polar Lipids). Supported lipid bilayers were assembled in 6-lane µ-Slide VI 0.4 chambers (Ibidi) and functionalized with recombinant human BCMA and human ICAM-1 proteins, each

containing C-terminal hIgG-His-tags (Novus Biologicals), at densities of 250 molecules/μm^2 and 100 molecules/μm^2, respectively. The necessary protein concentration was determined by coating silica beads (Bangs Laboratories) with the lipids, followed by titrated His-tagged protein concentrations and labeling with Alexa Fluor 647-labeled BCMA- or ICAM1-specific antibodies (Biolegend). Silica beads were analyzed by flow cytometry concurrently with Quantum Alexa Fluor 647 MESF beads (Bangs Laboratories) and protein density on beads was determined using calibration curves created from the MESF beads and the effective F/P ratio of the Alexa Fluor 647-labeled antibodies, using Simply Cellular® anti-Mouse IgG beads (Bangs Laboratories).

2 x 10^5 T cells in 100 µl of media were pipetted in each flow chamber and incubated at 37°C for the indicated times. Cells were then immediately fixed with 100 µl of Image-iT Fixative Solution (Thermo Fisher Scientific) for 20 minutes at room temperature and unattached cells were removed by continuously flowing 3 ml of PBS through the flow chamber. Chambers were imaged on an Olympus CK40 inverted microscope and the number of attached cells was determined by manual count of an entire field of view using a A10 PL 10x/0.25 objective.

TAC-T cell immune synapse formation on supported lipid bilayers

T cells were incubated on assembled lipid bilayers for indicated times, fixed and washed as described above and permeabilized for 30 minutes at room temperature with PBS containing 5% rat serum and 0.2% Triton X-100. Cells were

washed by continuous flow of 3 ml of PBS and stained for 30 minutes at room temperature in BlockAid solution (Thermo Fisher Scientific) with Alexa Fluor Plus 405 Phalloidin (Cat No. A30104, Thermo Fisher Scientific), Alexa Fluor 488-conjugated mouse anti-human CD11a/CD18 (Cat No. 363404, BioLegend), and Alexa Fluor 647-conjugated mouse anti-Lck (Cat No. 628304, BioLegend) or Alexa Fluor 647-conjugated mouse anti-human perforin (Cat No. 308110, BioLegend). Cells were finally washed by continuous flow of 2 ml PBS, followed by addition of 200 µl of PBS containing 0.5% N-propyl gallate. Images were acquired with a LEICA DMI6000 B inverted microscope equipped with adaptive focus control, a motorized X-Y stage (MCL Micro-Drive, Mad City Labs Inc.), a LEICA 100x/1.47NA oil-immersed TIRF objective and an Andor iXon Ultra EMCCD camera. Excitation was provided by 405, 488 and 647 nm diode-pumped solid-state lasers (Spectral). Image analysis was performed using Fiji version 2.0.0-rc-69/1.53p[270]. All images were background subtracted. For Lck analysis, the area of actin exclusion central to the immune synapse was outlined manually and the integrated intensity of Lck was measured within that area. For perforin analysis, images were thresholded manually on perforin signal. Regions were created for any pixels above the threshold, transferred back to an unthresholded image, and the integrated perforin intensity within the regions was measured.

In vivo studies

All animal studies were conducted in accordance with the McMaster Animal Research Ethics Board standards. 6-12-week-old NOD.Cg-Rag1tm1MomIl2rgtm1Wjl/SzJ (NRG) mice bred in-house were injected i.v. with 10^6 KMS-11 or MM.1S luciferase-expressing cells in 200 µL PBS. Depending on the experiment, either effLuc- of GpNLuc-expressing KMS-11 tumor cells were used. Mice bearing 12-day-old tumors were treated i.v. with a single 200-µL indicated dose of cryopreserved TAC^+ T cells. Tumor burden was monitored weekly by bioluminescence. For effLuc imaging, mice were injected i.p. with 150 mg/kg D-luciferin (Perkin Elmer), incubated for 14 minutes, and imaged using IVIS Spectrum imager (Caliper Life Sciences). For GpNLuc imaging, mice were injected i.v. with 500 µg/kg furimazine (Nano-Glo Luciferase Assay substrate diluted in PBS, Promega), anaesthetised and imaged 3-4 min post-injection. Images were analyzed with Living Image Software v4.2 for MacOS X (Perkin Elmer). Tumor burden was represented as the sum of dorsal and ventral average radiance (p/s/cm²/sr) signal.

In vivo toxicity monitoring

Mice were weighed using Ohaus Scout Balance Scale (OHAUS Corporation)

$$\%\ Change\ in\ weight = \frac{Current\ weight - preACT\ weight}{preACT\ weight} \times 100\%$$

For serum cytokine analyses, retro-orbital blood samples were collected on days 3 and 7 after treatment in CAPIJECT capillary micro collection serum tubes (Terumo Medical Corporation). 15 human cytokines and chemokines were quantified by the Eve Technologies Corporation.

Histology analysis

Tissues were fixed for 24 hours with 10% formalin. After initial fixation, femurs were decalcified for 24 hours with 2 mL/femur of Immunocal (StatLab) and fixed for an additional 24 hours with 10% formalin. The immunohistochemistry was performed at the McMaster Immunology Research Centre Core Histology Facility. Paraffin sections were cut at 4 μm and stained on the BOND RX automated stainer (Leica Biosystems). All slides were pretreated with Epitope Retrieval Solution 2 (Cat. No AR9640, Leica Biosystems) on the BOND RX before staining. Anti-CD138 rabbit monoclonal antibody (Cat. No ab128936, Abcam) was diluted in the IHC/ISH Super Blocking solution (Cat. No PV6122, Leica Biosystems), followed by a polymer detection and hematoxylin counterstain as part of the BOND Polymer Refine Detection kit (Cat. No DS9800, Leica Biosystems). The CD3 and Ki-67 detection was performed as a double sequential stain on the BOND RX with rabbit monoclonal anti-CD3 antibody (Cat. No ab16669, Abcam) diluted according to the instructions in the BOND Polymer Refine Detection kit, followed by rat monoclonal anti-Ki-67 antibody (Cat. No ab156956, Abcam) and rabbit anti-rat IgG antibody (Cat. No BA-4001, Vector Labs), followed by a polymer detection and hematoxylin

counterstain as part of the BOND Polymer Refine Red Detection kit (Cat. No DS9390, Leica Biosystems). All antibodies were diluted in IHC/ISH Super Blocking solution.

Quantification of histological data

The digitized CD3/Ki-67 stained slides were imported into HALO software v3.2.1851.299 (Indica Labs). Annotations were drawn around each separate tissue present on each slide, including 3 pieces of spleen tissue, 1-2 pieces of liver tissue, and 2 pieces of femur (~7 tissues/slide). Some tissues had regions folded or blurred artifacts present from the scanning process; these regions were excluded from analysis in HALO. One cellular detection algorithm was developed for each of the three respective tissue types and used across all the slides to reduce inter-slide variability while recognizing baseline and background staining differences between tissue types. The template algorithm used was the Multiplex IHC v2.1.1 module. Each algorithm was set to detect cells using the nuclear stain included in the IHC process as the designated marker for a cell, followed by detecting the presence of CD3 in the peri-nuclear vicinity and Ki-67 within the nuclear compartment. This HALO module yielded the following results for each separate annotation on each slide (~7 results/slides): total cells, dual $CD3^{-}Ki\text{-}67^{-}$ cells, $CD3^{+}$ cells, $Ki\text{-}67^{+}$ cells, $CD3^{+}Ki\text{-}67^{-}$ cells, $CD3^{-}Ki\text{-}67^{+}$ cells and dual $CD3^{+}Ki\text{-}67^{+}$ cells. Each tissue replicate was then averaged (triplicate spleen, duplicate liver, and duplicate liver) as a single specimen and each specimen was taken as part of the group average.

Chapter 3

Optimization of the CD3-binding domain and the TAC receptor surface expression

Introduction

As discussed in Chapter 1, MM is an incurable plasma cell cancer with a poor prognosis for relapsed/refractory disease and limited treatment options. The introduction of immunomodulatory drugs into the MM treatment landscape brought major improvements to overall patient survival[271-273] and supported the use of immune-based approaches for MM. Recently, the growing number of immunotherapeutic agents entering clinical testing has expanded to cell-based therapies, monoclonal antibodies, antibody-drug conjugates, and bispecific T cell engagers (BiTEs)[274-276].

Common targets for MM immunotherapeutics include B-cell maturation antigen (BCMA), CD38, CD138, SLAMF7, and GPRC5D[277, 278]. Among these targets, BCMA stands out due to its biological role in MM cell survival and proliferation[15, 279, 280], high expression levels on malignant plasma cells, and lack of expression in non-hematopoietic tissues[124]. Several BCMA-specific products have already shown clinical efficacy in patients with relapsed/refractory MM, including antibody-drug conjugates[150], BiTEs [281], and engineered T cells[217, 220, 223, 242, 282-287], highlighting the susceptibility of previously treated MM to BCMA-targeting agents.

T cell immunotherapies for MM include (1) antigen-specific endogenous[288], (2) T cell receptor (TCR)-engineered[289, 290], and (3) chimeric antigen receptor (CAR)-engineered T cells[217, 220, 223, 242, 283-287, 291, 292]. Due to their customizable

structure, lack of dependence on HLA matching, scalable manufacturing, and clinical efficacy in other hematologic malignancies, CAR-engineered T (CAR-T) cells have been leading the development of T cell therapies for MM. Although autologous BCMA-specific second-generation CAR-T cells have shown encouraging levels of efficacy, this treatment carries a risk of substantial toxicities, and many patients eventually progress or relapse[217, 242]. However, unlike clinical experience with CD19-CAR-T cell therapy, in which relapses are characterized by antigen loss or alternative splicing[234, 293, 294], baseline BCMA expression does not seem to correlate with response[222, 242] and many relapsed MM tumors remain BCMA-positive[223, 243]. This suggests that the potency of the engineered T cell product can be improved, and alternative modes of engineering are one way to address this issue.

Our lab has taken a TCR-centric approach to T cell engineering and created a synthetic TAC receptor[255], which redirects endogenous TCRs to the target of interest and effectively combines HLA-independent antigen recognition with the canonical mechanisms of T cell activation and regulation. In our previous experience, T cells engineered with TAC receptors (TAC-T) cells showed improved tolerability and enhanced discrimination between the on-target and off-target responses, when compared to second-generation CAR-T cells[255]. Since TAC-T cells may offer advantages over CAR-T cells in the setting of human myeloma, we were keen to design a TAC receptor for human testing. This chapter describes the optimization of our TAC scaffold carrying a BCMA-binding domain that has

been proven clinically (the C11D5.3 single-chain antibody fragment (scFv)[242]). Our experience shows that BCMA-TAC-T cells derived from healthy and patient donors are efficacious against disseminated multiple myeloma xenografts. Moreover, we demonstrate that different surface expression levels of BCMA-TAC receptors do not influence *in vivo* TAC-T cell efficacy, despite differences in *in vitro* performance.

Results

Optimized CD3-binding domain improves TAC-T cell efficacy

TAC receptors lack synthetic signaling domains and activate T cells by co-opting the endogenous TCR-CD3 complex. Previously, we described comparison of several CD3ε-binding scFvs and the rationale for choosing the UCHT1 domain for the TAC receptor scaffold[255] (Figure 3.1A). Recognizing that the UCHT1 framework is of mouse origin and could give rise to human anti-mouse antibodies and potentially limit the clinical utility of TAC-T cells, we replaced UCHT1 with a humanized version (hu(UCHT1))[295, 296]. We recently identified a variant UCHT1 with a point mutation of Y→T at position 54, which improved TAC surface expression and growth of TAC-T cells[297]. Given the potential benefits of the Y54→T mutation, in parallel, we also evaluated a variant of huUCHT1 with the Y54→T mutation (huUCHT1(YT)). To focus on the scaffold optimization, we used the same C11D5.3 BCMA-specific scFv as the antigen-binding domain in all scaffolds.

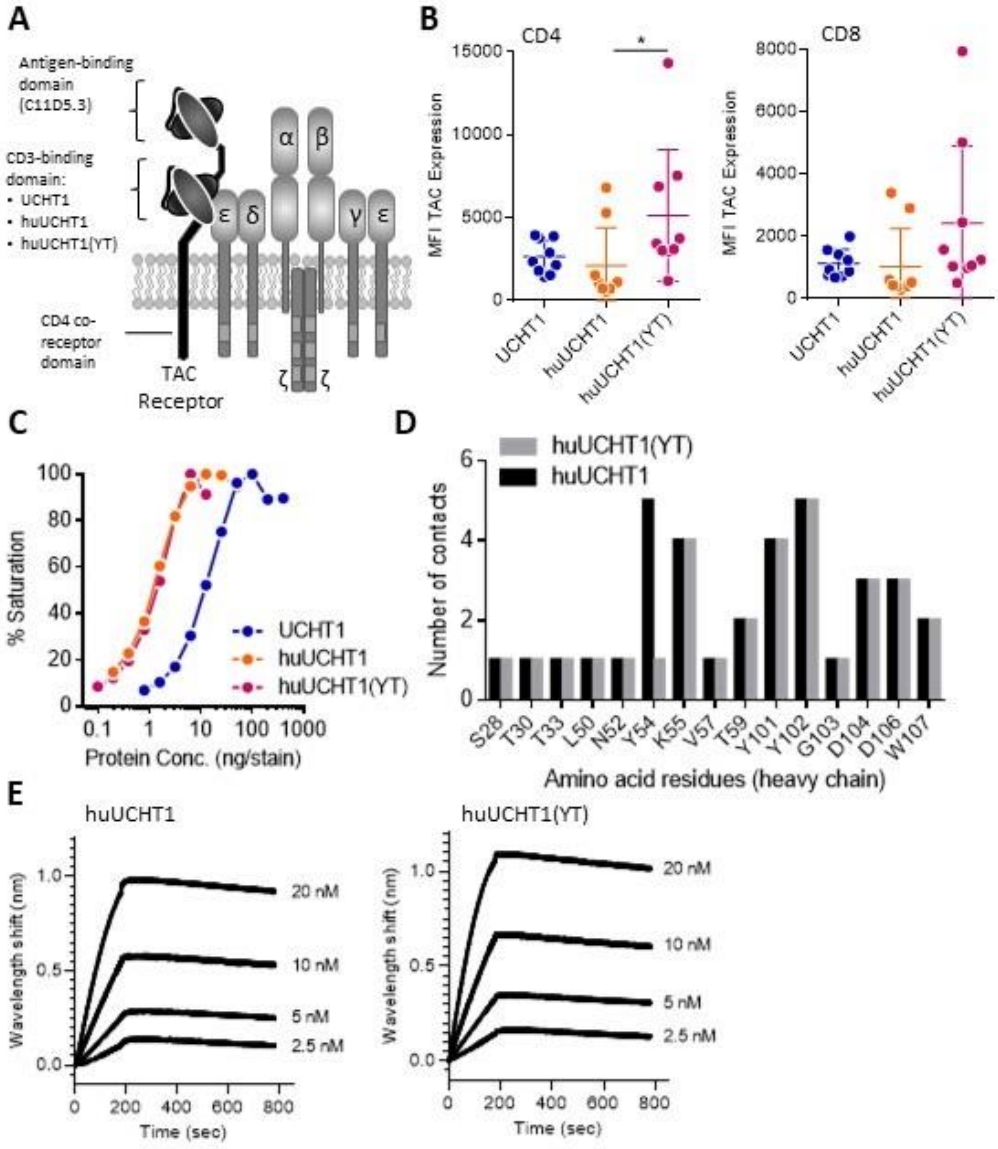

Figure 3.1. Optimized CD3-recruitment domain improves binding to CD3 and augments surface expression. (A) An illustration of the receptor design. (B) Median fluorescence intensity (MFI) of receptor surface expression on transduced cells. Cells were gated on live > singlets > CD4/CD8 > NGFR$^+$. Data are representative of 7 healthy donors. Statistical significance was determined using repeated measures ANOVA. (C) Binding of purified, His-tagged UCHT1 variants to PBMC. Flow cytometry data were gated on live > singlets > CD4$^+$/CD8$^+$. MFIs of the protein stain were recorded at each protein concentration and converted to % saturation based on the highest MFI value for each protein. (D) The impact of the Y-T mutation on the specific contacts formed between different UCHT1 variants

and CD3ε. Docking models created with ClusPro 2.0 software were analyzed for specific contacts with CSU software developed at the Weizmann Institute of Science. The total number of bonds predicted for each amino acid is shown. (E) Bio-layer interferometry comparison of humanized UCHT1 variants. Streptavidin probes were loaded with biotinylated human CD3εδ heterodimer and incubated with His-tagged purified humanized UCHT1 variants. Data were recorded with Octet BLI system and analyzed with Prism v.8.

The huUCHT1(YT) scaffold afforded higher TAC surface expression than the huUCHT1 scaffold in CD4 T cells with a similar trend for higher expression in CD8 T cells (Figure 3.1B). At the protein level, both recombinant huUCHT1 and huUCHT1(YT) bound primary human T cells equally well and markedly better than UCHT1 (Figure 3.1C). While *in silico* modeling suggested potential decrease in huUCHT1(YT) affinity for CD3 (Figure 1.1D), bio-layer interferometry studies with purified huUCHT1 and huUCHT1(YT), showed that both proteins had high affinity for CD3εδ with a K_d ~ 100 pM (Figure 3.1E).

In vitro functional assessment revealed overall comparable post-activation cytokine expression profile across all three UCHT1 variants (Figure 3.2). UCHT1-TAC showed higher variation in cytokine production, compared to TACs with humanized UCHT1 scaffolds. The only statistically significant differences were observed in CD4 T cells, where huUCHT1(YT)-TAC produced more TNF-α than huUCHT1-TAC upon KMS-11 stimulation, and UCHT1-TAC produced more TNF-α than huUCHT1-TAC upon MM.1S stimulation (Figure 3.2).

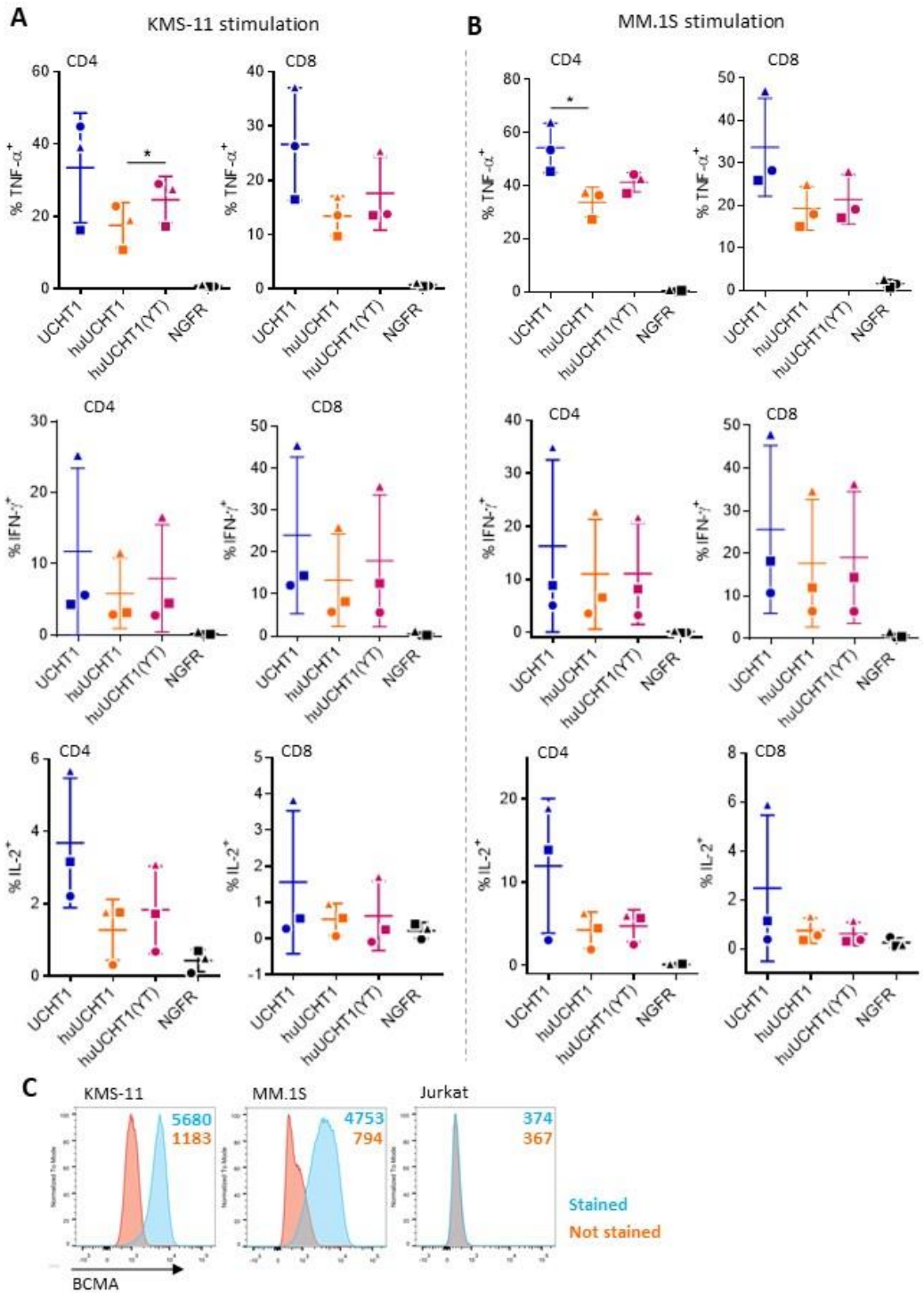

Figure 3.2. *In vitro* comparison of TAC-T cells with different CD3-binding domains. T cells were incubated with KMS-11 (A) or MM.1S (B) tumor targets for 4 hours at 37°C at a 2:1 effector:target ratio in the presence of brefeldin A and

monensin and stained for surface CD4, CD8, and intracellular IFN-γ, TNF-α, and IL-2. Plots were gated on live > singlets > CD4/CD8 > IFN-γ vs. TNF-α or IFN-γ vs. IL-2. Statistical significance was determined with repeated measures ANOVA. Data from 3 healthy donors marked by different symbols are shown. Bars represent mean and SD. (C) BCMA surface expression on target tumor cells detected by flow cytometry. Numbers represent mean fluorescence intensity values.

All three constructs were equally efficient at killing KMS-11 and MM.1S tumors *in vitro* (Figure 3.3A,B). Irrespective of comparable *in vitro* performance, huUCHT1(YT)-TAC outperformed other constructs *in vivo* (Figure 3.3C). Thus, considering favorable surface expression profile and good *in vitro* and *in vivo* efficacy, we chose to move forward with the huUCHT1(YT)-based scaffold.

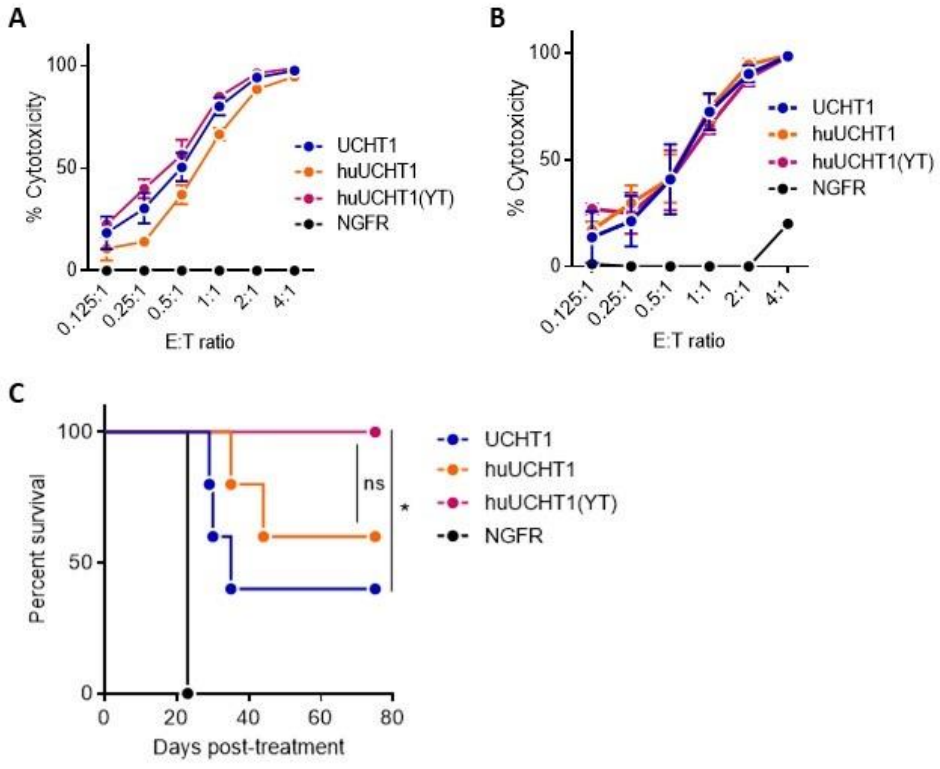

Figure 3.3. huUCHT1(YT) outperforms other UCHT1 variants *in vivo* in the KMS-11 model. (A,B) *In vitro* cytotoxicity. T cells were incubated with effLuc-expressing KMS-11 (A) or MM.1S (B) tumor targets for 8 hours at 37°C at different effector:target ratios, and all conditions were repeated in triplicates. Luminescence

was measured with an open filter upon addition of D-luciferin substrate (0.15 mg/mL). Mean and SD for each condition are displayed. Data are representative of 4 healthy donors. (C) Survival of KMS-11 tumor-bearing NRG mice treated with 3 x 10^6 cryopreserved TAC^+ T cells i.v. 12 days post-tumor injection. N = 5 mice per group. Statistical significance was determined with log-rank (Mantel-Cox) test.

Receptor surface expression differentially impacts early TAC-T cell activation

During the process of scaffold optimization, we observed that the CD8α signal peptide consistently led to more BCMA-TAC on the cell surface of T cells from healthy donors, compared to the IgK signal peptide (Figure 3.4A,B). A similar observation was made with T cells form MM patients (Figure 3.4C). The difference in surface expression was not due to a difference in vector copy number (Table 1). As receptor density can affect performance of CAR-T cells[298-300], we investigated the effect of TAC receptor density on TAC-T cell performance. At baseline, surface expression of the TACs did not influence checkpoint receptors PD-1, TIM-3, and LAG-3 (Figure 3.4D) consistent with the lack of tonic signaling produced by TAC receptors[255].

Table 1. Vector copy number (per cell) analysis of different TAC constructs generated from 3 healthy donors.

Construct	**Donor**		
	L3	**L5**	**L6**
UCHT1-TAC	1.06	1.13	1.16
huUCHT1-TAC	1.62	1.44	1.63
huUCHT1(YT)-TAC/ IgK-TAC	1.71	1.44	1.84
CD8α-TAC	1.21	1.08	1.23
cMyc-TAC	1.24	1.08	1.13
NGFR	ND	ND	ND
Non-transduced	ND	ND	ND

ND = not detected

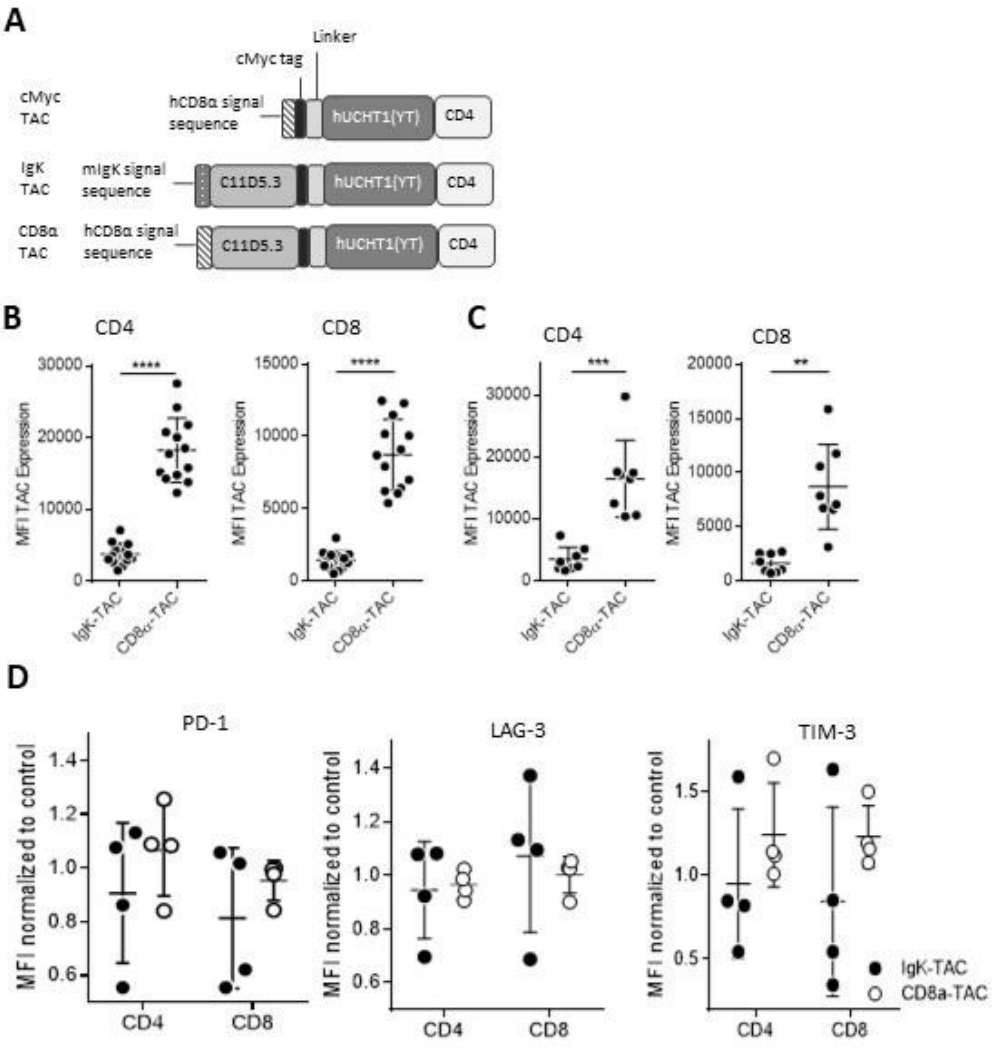

Figure 3.4. Signal peptide affects TAC surface expression. (A) Schematic of receptor design. (B, C) Median fluorescence intensity (MFI) of receptor surface expression on transduced TAC-T cells. Cells were gated on live > singlets > CD4/CD8 > NGFR$^+$. Data are representative of 5 healthy (B) and 4 patient (C) donors. Statistical significance was determined with a paired t-test. (D) T cell cultures were stained for PD-1, LAG-3, and TIM-3 surface expression at the end of 14-day culture period. Plots were gated on live > singlets > CD4/CD8 > NGFR$^+$. Median fluorescence intensities (MFI) were normalized to those of the cMyc-TAC. Statistical significance was determined with 2-way ANOVA, followed by Tukey's multiple comparisons test.

Receptor density should affect the physical interactions between the TAC-T cells and their target antigen. We compared the ability of TAC-T cells to form conjugates with BCMA-positive KMS-11 cells (Figure 3.5A). Within the first 20 minutes, CD8α- and IgK-TAC-T cells demonstrated equal ability to bind KMS-11 cells. However, by 40 minutes, TAC-T cells with lower receptor levels (IgK-TAC) started to disengage from the targets, whereas CD8α-TAC-T cells continued binding more tumor cells. When MM.1S tumor targets were used, CD8α-TAC-T cells were more efficient at binding tumor cells during earlier time points, with both types of T cells levelling off in their peak binding ability within 20 minutes (Figure 3.5B). Similarly, when TAC-T cells were exposed to a synthetic lipid bilayer functionalized with human BCMA and ICAM-1, CD8α-TAC-T cells showed greater binding than IgK-TAC-T cells (Figure 3.5C). Combined, these results indicate that higher levels of TAC receptor led to enhanced physical interaction between the TAC-T cells and antigen-containing membranes.

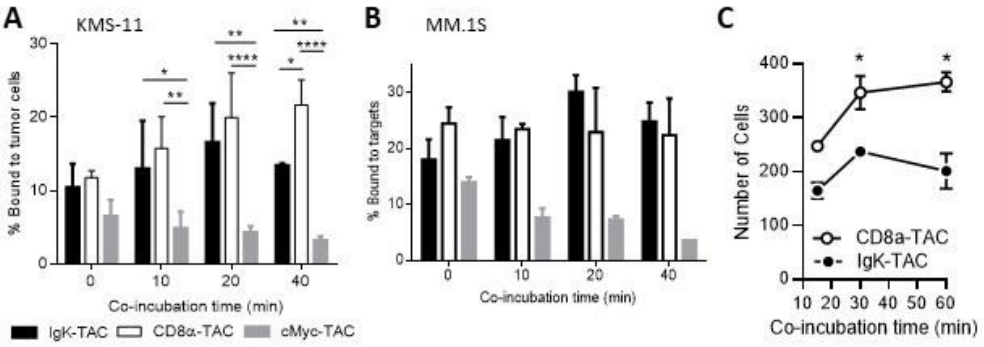

Figure 3.5. Higher TAC surface expression improves binding to antigen-positive membranes. (A,B) Conjugation assay. After pre-labelling with NGFR- and CD138-specific antibodies, T cells and KMS-11 (A) or MM.1S (B) tumor targets were incubated at a 1:1 ratio and analyzed by flow cytometry. Samples were

gated on live cells. % $NGFR^+$ cells that were also $CD138^+$ are shown. Statistical significance was determined with 2-way ANOVA, followed by Tukey's multiple comparisons test. Data are representative of 3 (A) and 2 (B) healthy donors. (C) Binding to supported lipid bilayer. 2 x 10^5 T cells were incubated in μ-Slide $VI^{0.4}$ chambers with lipid bilayer functionalized with human BCMA and ICAM-1, fixed, washed, and imaged on an Olympus CK40 inverted microscope. The number of attached cells was determined by manual count of the entire field of view using a A10 PL 10x/0.25 objective. Mean and SD for each condition are displayed. Statistical significance was determined with a t-test for each time point. Data are representative of 5 independent experiments.

We next sought to determine whether the enhanced physical associations mediated by the CD8α-TAC receptors would translate into changes in immunological synapse formation. Both CD8α- and IgK-TAC-T cells formed a classical TCR-driven synapse (Figure 3.6A,B)[301], characterized by a ring-like arrangement of F-actin and LFA-1 surrounding central supramolecular activation cluster (cSMAC)[302]. TAC-T cells with higher receptor levels on the surface (CD8α-TAC) accumulated significantly more Lck in the synapse, compared to TAC-T cells with fewer receptors (IgK-TAC) (Figure 3.6C). This translated into faster polarization of perforin to the T cell-bilayer interface in CD8α-TAC-T cells, with IgK-TAC-T cells catching up within the first hour of activation (Figure 3.6D). By 30 minutes, both CD8α- and IgK-TAC-T cell had polarized equivalent amounts of perforin (Figure 3.6E).

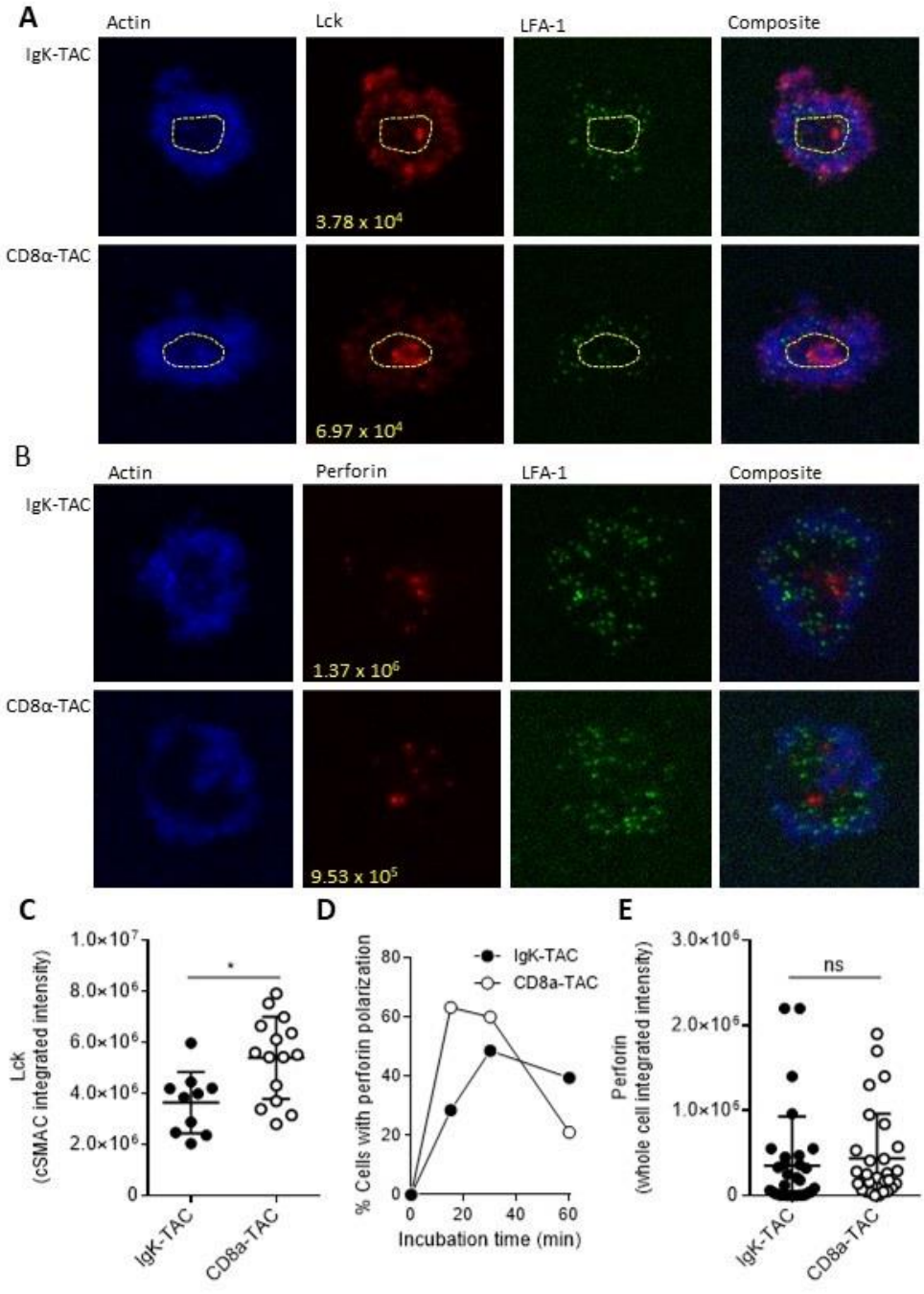

Figure 3.6. TAC receptor levels affect the strength of early signaling but not late signaling. Immune synapse formation on supported lipid bilayers. Samples were prepared as in Figure 3.5C, incubated for indicated times, fixed, permeabilized, and stained for F-actin, LFA-1, and Lck or perforin. Samples were imaged with LEICA DMI6000 B inverted microscope, a LEICA 100x/1.47NA oil-

immersed TIRF objective and an Andor iXon Ultra EMCCD camera. Excitation was provided by 405, 488 and 647 nm diode-pumped solid-state lasers, images were analyzed using Fiji version 2.0.0-rc-69/1.53p and all images were background subtracted. Representative images of Lck (A) and perforin (B) accumulation after 30-min incubation. Manually outlined immune synapses and corresponding integrated Lck intensity values within the synapse or perforin intensity values are shown. cSMAC = central supramolecular activation cluster. Comparison of integrated Lck (C) or perforin intensity values (E) after 30-min incubation. Each dot represents a cell, and lines indicate mean and SD. Statistical significance was determined with Mann-Whitney test. (D) Comparison of the fraction of cells with perforin polarization (as determined by manual threshold) at indicated incubation times. Data are representative of 4 (C) and 2 (D,E) independent experiments.

Despite differences in early activation, TAC-T cells with different receptor levels are equally efficacious in vitro

Given the more rapid maturation of the synapse in CD8α-TAC-T cells, we asked whether this would influence TCR-dependent signaling. To address this question, we measured CD69 (surrogate for T cell activation) and Nur77 (surrogate for T cell signal strength)[303] on the TAC-T cells stimulated with KMS-11 and MM.1S cells. At the 2-hour time point, there was a trend for more Nur77 activation in CD8α-TAC-T cells relative to IgK-TAC-T cells, but this was not observed in all T cell batches (Figure 3.7A-C). We questioned whether higher receptor levels could lead to overstimulation of TAC-T cells and higher levels of activation-induced cell death. Measurement of cleaved caspase-3 following stimulation of CD8α- and IgK-TAC-T cells revealed no differences in cell death post-stimulation (Figure 3.7D). Examination of the expression of the activation marker, CD69, and checkpoint receptors, PD-1, TIM3, LAG3, across a broad time frame (4h – 96h) following stimulation, also demonstrated no difference in levels or kinetics (Figure 3.8).

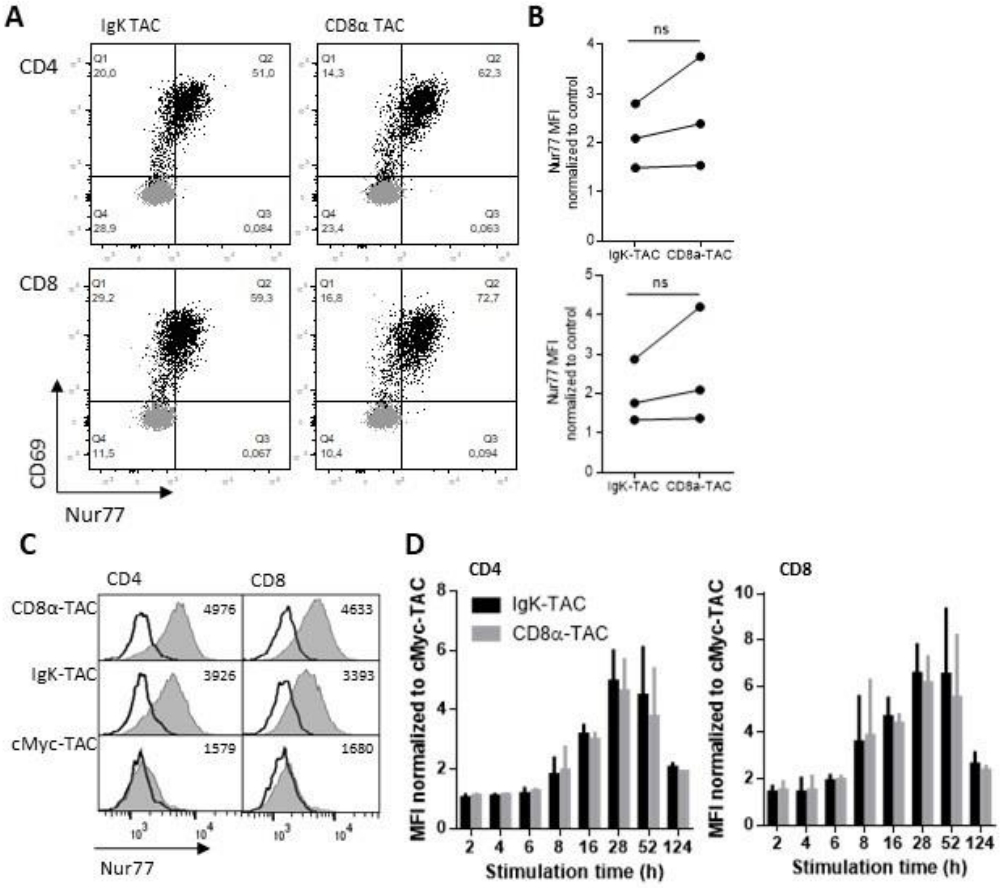

Figure 3.7. Nur77 expression and activation-induced cell death are not affected by TAC surface expression levels. T cells were incubated with KMS-11 (A,B) or MM.1S (C) cells at a 1:1 ratio for 2 hours, assayed by flow cytometry, and gated on live > singlets > $CD138^-$ > CD4/8 > $NGFR^+$ > $CD69^+$. (A) Representative plots of Nur77 an CD69 expression. (B) Median fluorescence intensities of Nur77 normalized to cMyc-TAC. Statistical significance was determined with a paired t-test. (C) Representative histograms of Nur77 expression after stimulation with MM.1S cells (grey) or media (black) for 2 h. Numbers indicate Nur77 median fluorescence intensity (MFI) of stimulated samples. (D) Caspase-3 activation. T cells were incubated with KMS-11 target cells at a 1:1 effector target ratio and assayed by flow cytometry. Samples were gated on live > singlets > $CD138^-$ > CD4/8 > $NGFR^+$ > $CD69^+$. Median fluorescence intensities (MFI) of cleaved caspase-3 normalized to cMyc-TAC are shown. Data are representative of 2 (A-C) and 3 (D) healthy donors.

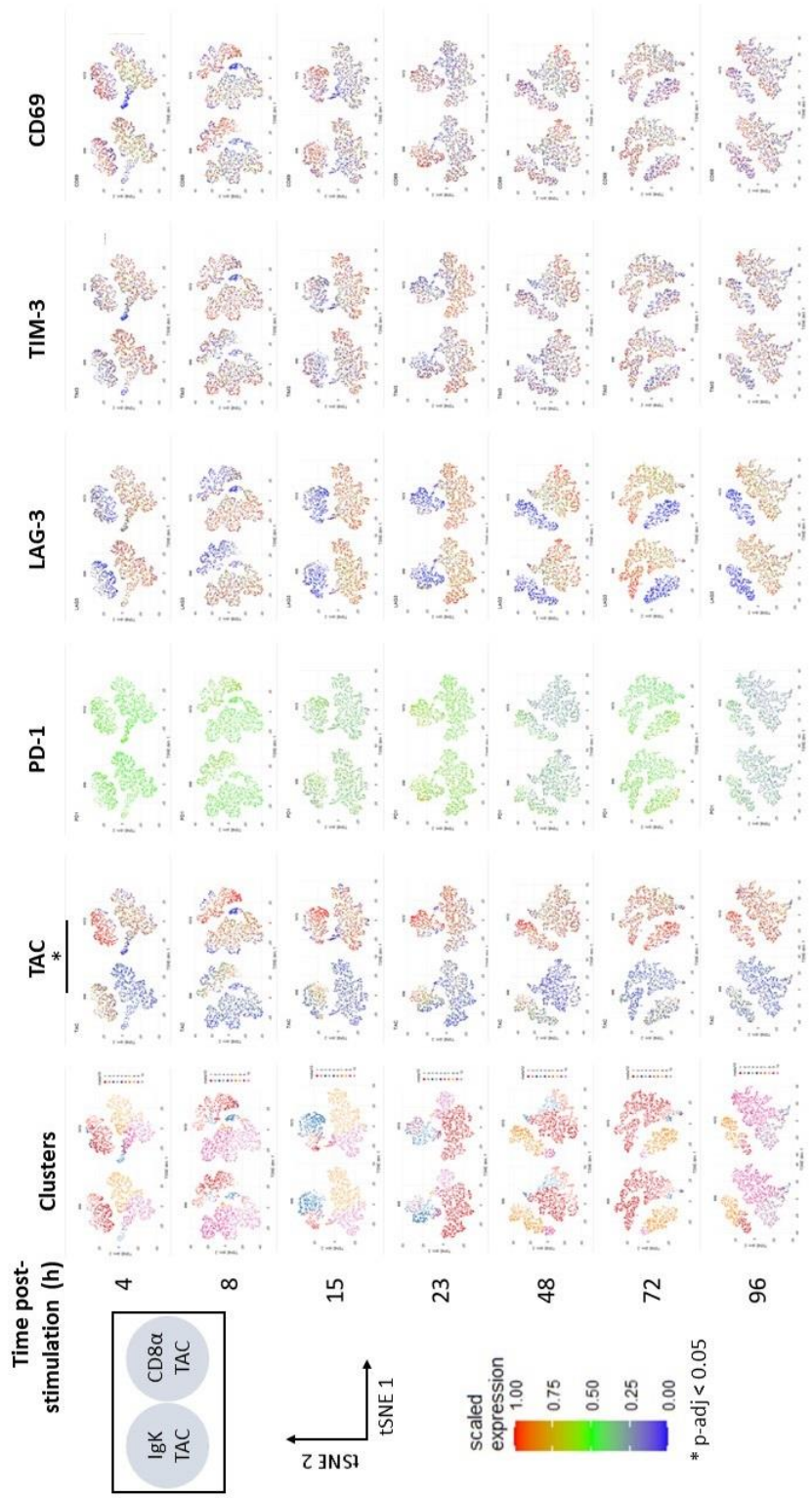
Time post-stimulation (h)
Clusters
TAC *
PD-1
LAG-3
TIM-3
CD69
4
8
15
23
48
72
96
IgK TAC
CD8α TAC
tSNE 1
tSNE 2
scaled expression
1.00
0.75
0.50
0.25
0.00
* p-adj < 0.05

Figure 3.8. Time course of checkpoint receptor expression post-activation. T cells were stimulated with KMS-11 targets at a 1:1 effector:target ratio for indicated periods of time. Samples were stained and analyzed by flow cytometry. Data are pre-gated on live > singlets > $CD138^-$ > CD4/CD8 > $NGFR^+$. 20,000 cells randomly subsampled from pre-gated $CD138^-NGFR^+$ samples were further subjected to flowSOM unsupervised clustering analysis and differential analysis with diffcyt framework. Data are representative of 3 healthy donors.

The results with Nur77 and CD69 suggested that the TAC-T cells were activated equally at both receptor densities. Using healthy donor-derived TAC-T cells, we noted that increased TAC expression had no effect on production of IFN-γ and TNF-α following stimulation with KMS-11 cells (Figure 3.9A). However, more TAC receptors on the T-cell surface led to significantly improved IL-2 production by $CD4^+$ TAC-T cells and a similar trend in $CD8^+$ T cells (Figure 3.9A). Comparable results were obtained with MM.1S targets (Figure 3.9B). Receptor density had a more striking impact on early cytokine production from TAC-T cells generated from myeloma patients. Higher receptor levels led to significantly more CD4 and CD8 TAC-T cells producing IFN-γ and TNF-α, following 4-hour stimulation with KMS-11 myeloma cells (Figure 3.9C). Similar results were obtained when MM.1S tumor targets were used for stimulation (Figure 3.9D). Nevertheless, by 24 hours of stimulation, both IgK- and CD8α-TAC T cells produced equivalent levels of cytokines, regardless of whether the T cells were obtained from healthy donors or MM patients (Figure 3.10).

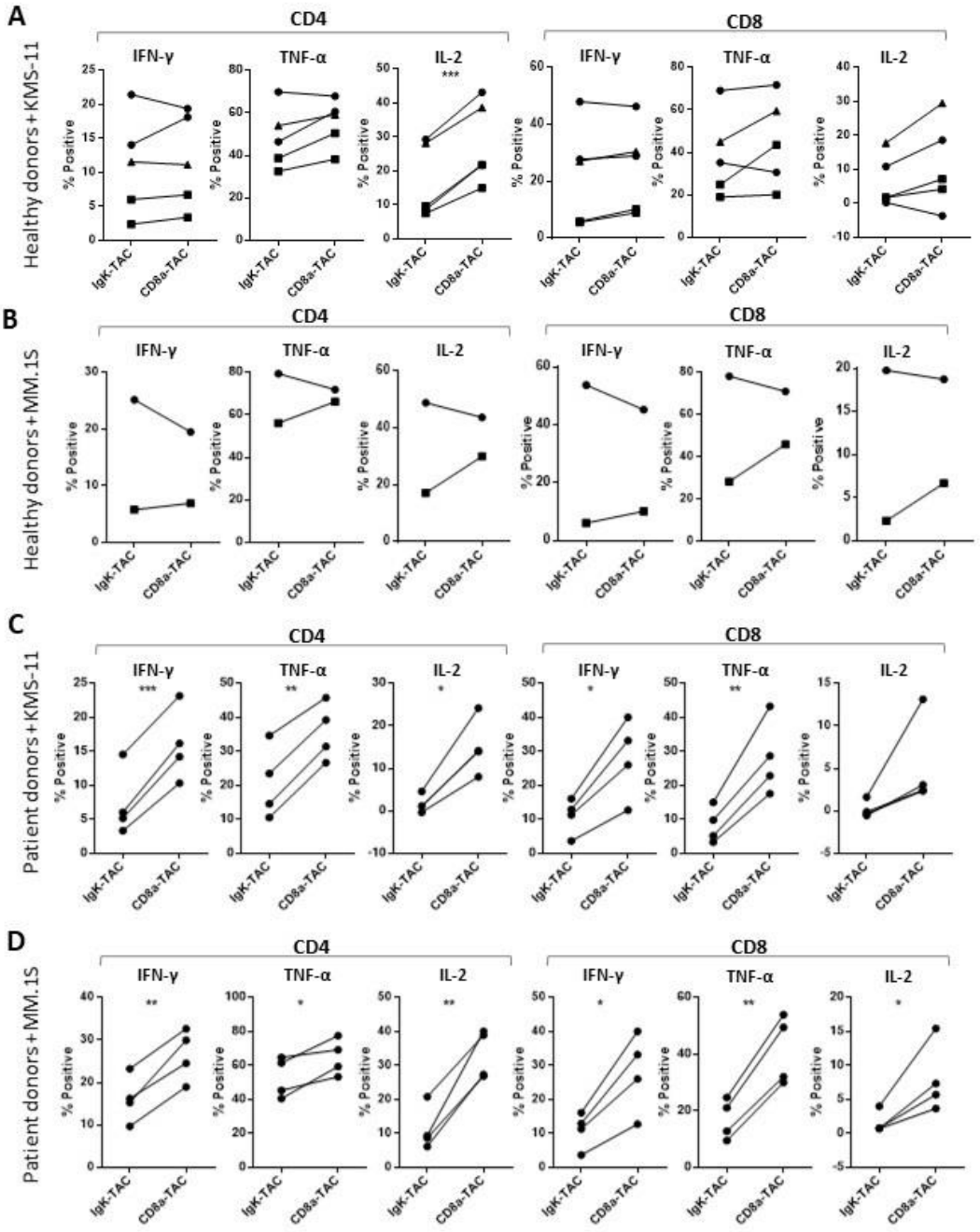

Figure 3.9. TAC receptor levels affect early cytokine production of patient-derived, but nor healthy donor-derived TAC-T cells. Intracellular cytokine expression in TAC-engineered cells from healthy (A,B) and patient (C,D) donors. T cells were incubated with KMS-11 tumor targets for 4 hours at 37°C at a 2:1 (A) or 1:1 (C) effector:target ratio or with MM.1S tumor targets for 4 hours at 37°C at a 2:1 (B) or 1:1 (D) effector:target ratio in the presence of brefeldin A and monensin

and stained for surface CD4, CD8, and intracellular IFN-γ, TNF-α, and IL-2. Plots were gated on live > singlets > CD4/CD8 > IFN-γ vs. TNF-α or IFN-γ vs. IL-2. Statistical significance was determined with a paired t-test. Data are representative of 3 (A) or 2 (B) healthy donors and 3 patient donors (C,D).

Since IL-2 was elevated in CD8α-TAC-T cells earlier than in IgK-TAC-T cells and this cytokine is known to support T cell proliferation upon activation[304], we measured proliferative capacity of the BCMA-TAC-T cells. In a reductionist system where TAC-T cells were stimulated with BCMA-Fc protein-coated polystyrene beads, TAC-T cells with higher receptor levels (CD8α-TAC) were more proliferative over the range of antigen densities tested (Figure 3.11A,B). However, when stimulated with BCMA-positive KMS-11 (Figure 3.11C) and MM.1S (Figure 3.11D) cells, both types of TAC-T cells derived from healthy donors proliferated equally well, suggesting that additional cell-cell contacts mediated by cell adhesion molecules may mitigate the effects of differential TAC receptor surface levels. Interestingly, proliferation of patient-derived CD4 TAC-T cells was reduced by high surface expression of the receptor (Figure 3.11C). Irrespective of the donor source (healthy or patient) and tumor targets (KMS-11 or MM.1S), TAC receptor density had no impact on cytotoxicity as both IgK- and CD8α-BCMA-TAC-T cells efficiently eliminated tumor cells *in vitro* (Figure 3.12).

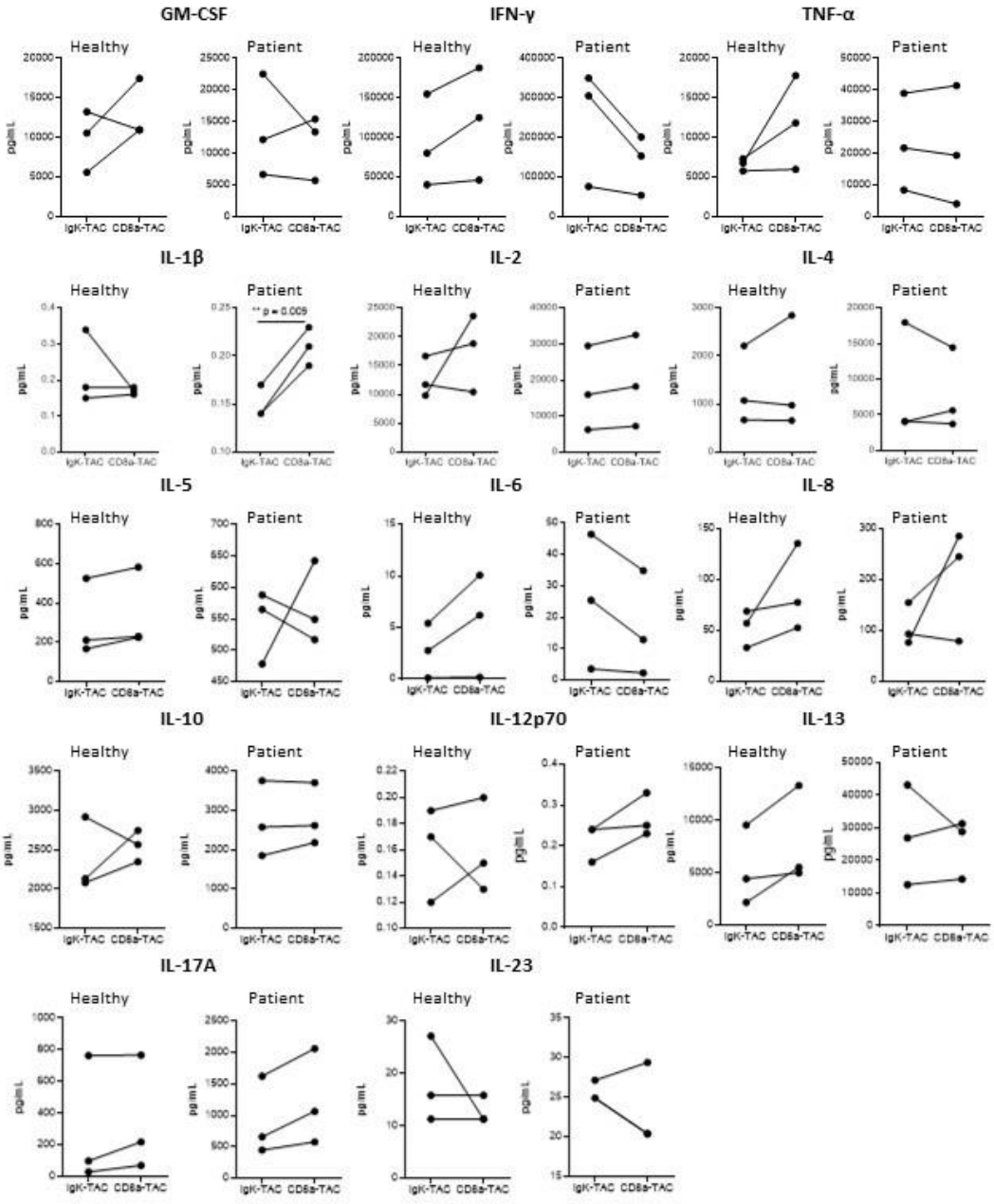

Figure 3.10. Multiplex analysis of secreted cytokines post-stimulation. T cells were stimulated with KMS-11 targets at a 1:1 effector:target ratio for 24 hours. Supernatants were collected and analyzed by Eve Technologies in duplicates. Background was subtracted from the results and statistical significance was determined using paired t-tests. Data are representative of 3 healthy and 3 patient donors.

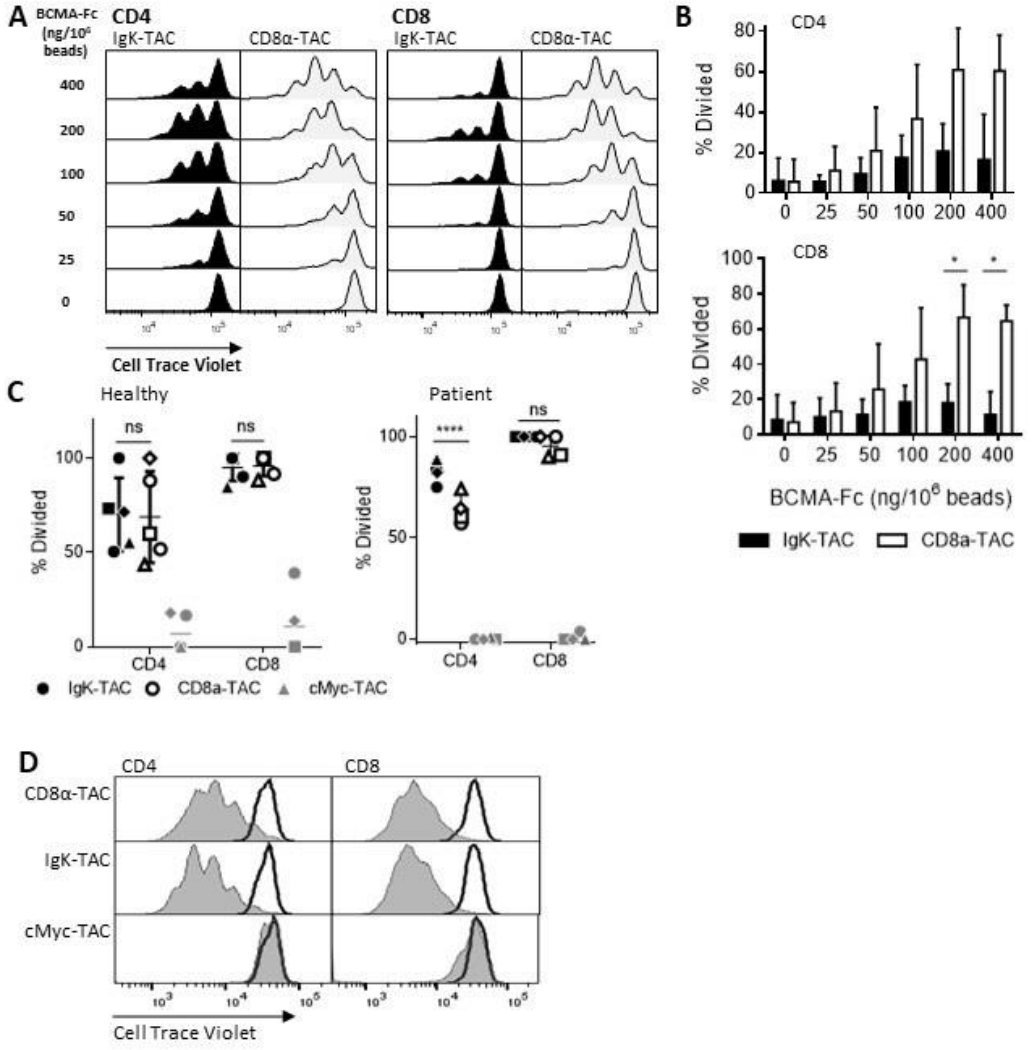

Figure 3.11. TAC-T cells with different receptor levels are equally efficacious in long-term *in vitro* proliferation assays. T cells were labelled with CellTrace Violet dye, stimulated with polystyrene protein G beads coated with indicated concentrations of BCMA-Fc (A, B) at an effector:target ratio 1:1, KMS-11 (C), or MM.1S (D) tumor targets at an effector:target ratio 2:1 for 4 days and assayed by flow cytometry. Samples were gated as singlets > live > $CD138^-$ > CD4/CD8 > $NGFR^+$. Data are representative of 4 healthy donors (A, B, C left panel), 4 patient donors (C right panel), or 2 healthy donors (D). Statistical significance was determined with 2-way ANOVA, followed by Tukey's multiple comparisons test.

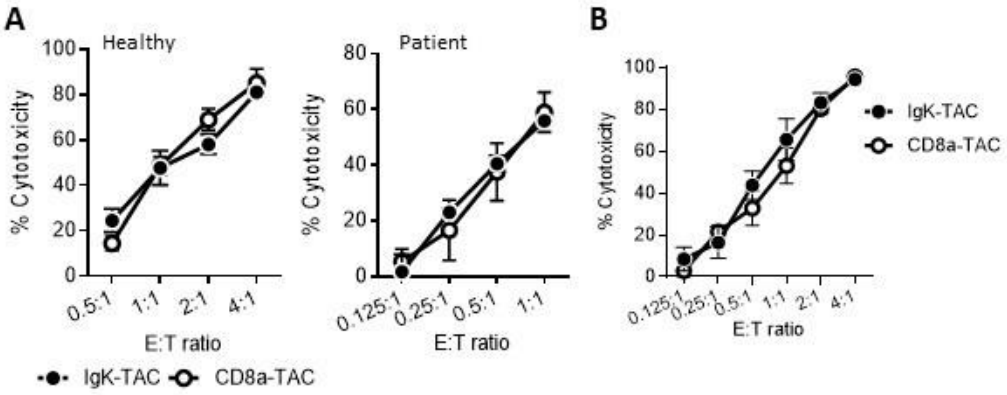

Figure 3.12. TAC-T cells are efficient at eliminating tumors *in vitro*, irrespective of receptor expression levels. T cells were incubated with effLuc-expressing KMS-11 (A) of MM.1S (B) tumor targets for 8 hours at 37°C at different effector:target ratios, and all conditions were repeated in triplicates. Luminescence was measured with an open filter upon addition of D-luciferin substrate (0.15 mg/mL). Mean and SD for each condition are displayed. Data are representative of 3 healthy (A left panel), 3 patient (A right panel), or 2 healthy (B) donors.

TAC-T cells show robust in vivo efficacy across different receptor levels

Receptor expression-dependent differences at the cell-cell binding and early signaling levels did not translate into marked functional differences *in vitro*. To assess whether therapeutic outcomes would be affected by receptor expression levels, we evaluated anti-tumor efficacy using an orthotopic, disseminated KMS-11 xenograft model. Using T cells from healthy donors, a single dose of 2 x 10^6 CD8α- or IgK-TAC-T cells per mouse was equally effective at clearing tumors and inducing sustained remissions (Figure 3.13A,B). Titrating down the dose of T cells to suboptimal therapeutic levels also did not reveal statistically significant differences between TAC-T cells with higher and lower receptor levels (Figure 3.13A,C).

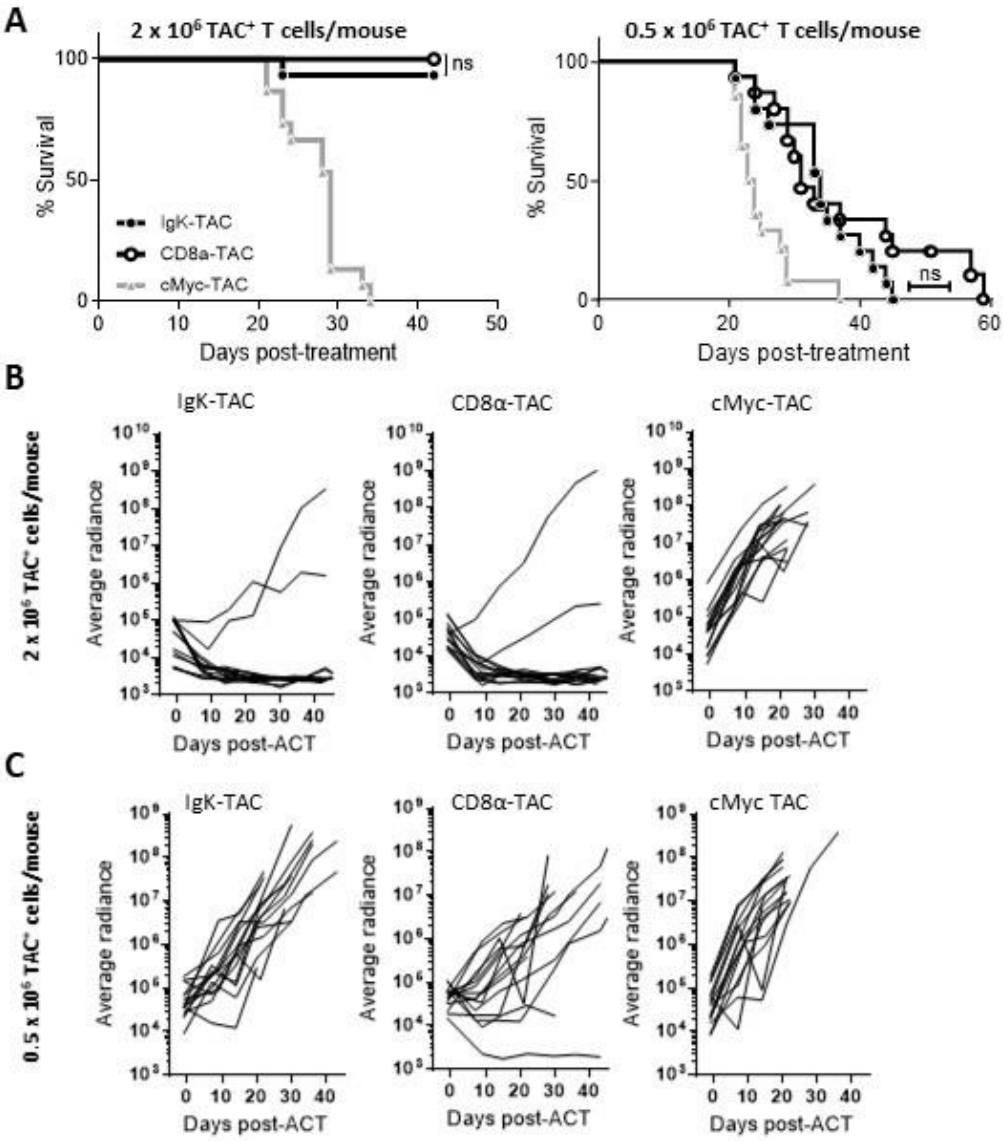

Figure 3.13. Healthy donor-derived TAC-T cells are efficacious against KMS-11 tumors *in vivo* irrespective of the receptor levels. KMS-11 tumor-bearing NRG mice were treated with 2 x 10^6 or 0.5 x 10^6 of TAC^+ cryopreserved T cells i.v. on day 12 post-tumor injection. (A) Survival data. Statistical significance was determined using log-rank (Mantel-Cox) test. (B,C) Tumor burden of firefly luciferase-expressing KMS-11 cells was tracked via bioluminescence imaging after i.p. D-luciferin injection. Data are representative of 3 healthy donors, n = 14-15 mice per group.

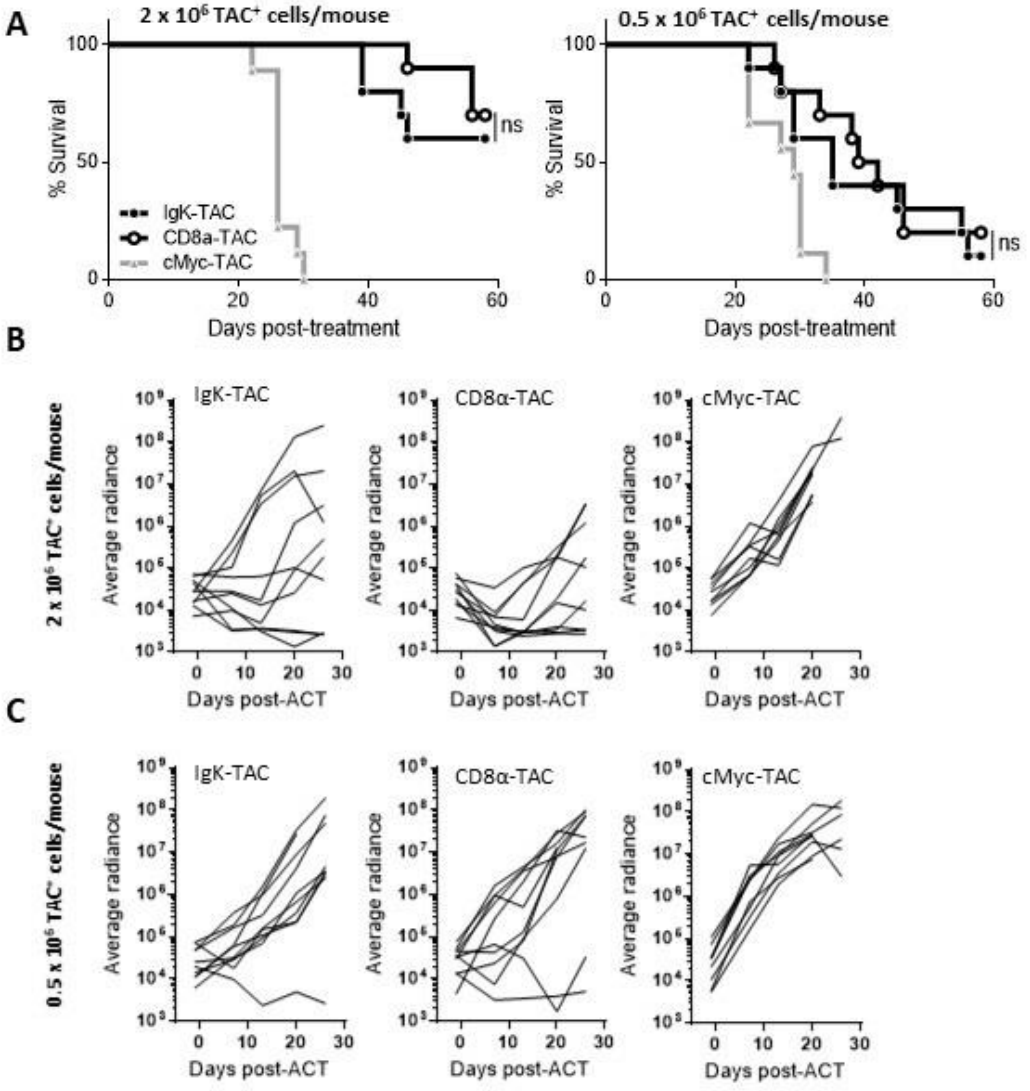

Figure 3.14. Patient donor-derived TAC-T cells are efficacious against KMS-11 tumors *in vivo* irrespective of the receptor levels. KMS-11 tumor-bearing NRG mice were treated with 2 x 10^6 or 0.5 x 10^6 of TAC^+ cryopreserved T cells i.v. on day 12 post-tumor injection. (A) Survival data. Statistical significance was determined using log-rank (Mantel-Cox) test. (B,C) Tumor burden of firefly luciferase-expressing KMS-11 cells was tracked via bioluminescence imaging after i.p. D-luciferin injection. Data are representative of 3 healthy donors, n = 9-10 mice per group.

Similarly, the therapeutic efficacy of MM patient-derived TAC-T cells was not significantly affected by the differences in TAC receptor density over a range

of TAC-T cell doses (Figure 3.14). We also tested the two TAC-T cell populations in the MM.1S model and, again, found no difference in therapeutic outcomes (Figure 3.15). Thus, despite the influence of TAC receptor density on early events following TAC engagement (cell binding, Lck recruitment, perforin polarization), receptor density did not impact therapeutic efficacy.

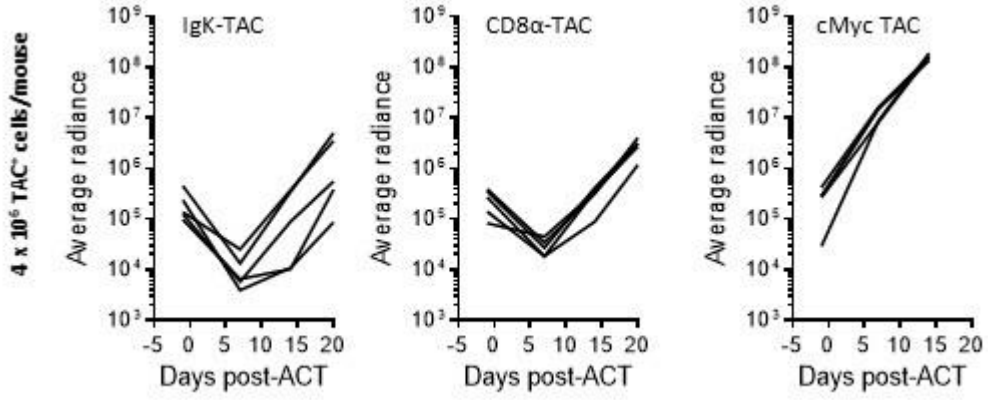

Figure 3.15. *In vivo* efficacy of healthy and patient donor-derived TAC-T cells in the MM.1S model. MM.1S tumor-bearing NRG mice were treated with 4 x 10^6 of TAC^+ cryopreserved T cells i.v. on day 15 post-tumor injection. Tumor burden of firefly luciferase-expressing MM.1S cells was tracked as in A-C; n = 5 mice per group. Data are representative of 1 healthy donor.

Discussion

The robust therapeutic activity of CAR-T cells has prompted research into other receptor designs that retain the therapeutic benefit of the current-generation CAR-T cells but diminish the unwanted toxicity profile. Recently, several alternate synthetic antigen receptors have been described that focus on co-opting natural TCR signaling, including our TAC platform[252, 254, 255]. In these studies, TCR-centric receptors were equally or more efficacious than conventional second-generation CARs and less likely to produce cytokines *in vitro* or cause *in vivo* toxicities. These observations suggest an improved ability of T cells engineered with these receptors to mediate effector responses. Unlike other TCR-centric synthetic receptors, TAC does not replace either CD3 or TCR chains. Rather, the TAC receptor redirects endogenous receptor complex through non-covalent association with the CD3ε chain. Here, we described the next generation of the TAC platform. These studies focused on the development of a BCMA-specific TAC receptor, but the optimized TAC scaffold described herein should be broadly useful against any tumor target.

For backbone optimization, we designed all receptors with the same antigen-binding domain. We selected the C11D5.3 scFv for these studies as this scFv has been clinically validated on a CAR scaffold[242]. Our *in vitro* optimization of the TAC scaffold revealed that humanization of the UCHT1 domain improved binding to CD3 on the surface of T cells. Substitution of huUCHT1 with a version carrying the Y54→T mutation (huUCHT1(YT)) further improved surface

expression and *in vivo* efficacy. In our original description of the TAC, UCHT1 emerged as the most effective CD3 binder of the five scFvs compared[255]. Here, the subtle changes to UCHT1 (humanization and single point mutation) further improved the TAC receptor performance, underscoring the importance of TAC-CD3 interaction. Despite the *in silico*-predicted reduction in the number of bonds between UCHT1 and CD3ε, the Y54→T mutation did not impact binding of recombinant scFvs to human T cells nor did it affect affinity. The improved performance of the huUCHT1(YT) variant likely reflects the subtle changes in the protein:protein interactions between UCHT1 and CD3 that are more complicated than simple binding strength and are the subject of further investigation. Based on the results described herein, we elected to move forward with huUCHT1(YT) as our optimized TAC scaffold for clinical testing.

Our observation of the signal peptide impacting receptor expression levels created an interesting system for evaluating the relationship between TAC surface levels and TAC-T cell functionality. The signal peptide targets proteins destined for secretion or surface expression to the endoplasmic reticulum (ER) and gets cleaved from the newly synthesized polypeptide chain upon translocation to the ER[305]. Length and amino acid composition of signal peptides affect kinetics and efficiency of binding to the signal recognition particle, translocation into the ER, or cleavage by the signal peptide peptidase[306]. Thus, by using different signal peptides, we likely affected one or more of these processing steps of the TAC receptor synthesis.

The CD28 co-stimulatory domain in second-generation CARs mediates tonic signaling during the manufacturing period, which can produce exhaustion of the engineered T cell product[238, 298]. Consequently, some of the strategies to reduce tonic signaling have focused on limiting CAR surface expression by optimizing promoter activity[298-300, 307] or using logic-gated receptors[308]. Here we show that TAC-T cells do not upregulate exhaustion markers, irrespective of TAC receptor expression levels. These observations support our rationale for excluding endogenous signaling domains from the TAC scaffold in favor of allowing TAC-engineered cells to auto-regulate through the endogenous TCR-dependent pathways.

Our experiments with supported lipid bilayers functionalized with BCMA antigen and ICAM-1 improved our understanding of the immunological synapse formed by TAC-T cells. The structure of TAC receptor-driven synapses was similar to the conventional bullseye structure of the TCR synapse[174], suggesting that TACs function as we intended, by redirecting endogenous TCRs to the target of interest. Higher TAC surface levels improved target binding and increased Lck accumulation at the immunological synapse. Consistent with the role of Lck in driving lytic granule polarization and degranulation[309], we observed that TAC-T cells with higher TAC receptor levels displayed more rapid perforin polarization. Nevertheless, similar levels of perforin polarization and equivalent cytotoxicity against tumor cells were ultimately achieved independent of TAC receptor expression. Given the observation that TAC receptor expression did not influence

the strength of TCR signaling (measured indirectly by Nur77 expression) and AICD, we believe that although the different levels of TAC expression may influence upstream features of T cell activation (i.e. target binding, recruitment of Lck to the immunological synapse), these events do not ultimately influence the activation threshold of the T cell or impact therapeutic efficacy.

In a reductionist bead-based activation system where only receptor-ligand interactions were present, higher TAC surface levels reduced the amount of antigen needed to trigger proliferation of TAC-T cells. These results are consistent with previous work linking proliferation with TCR surface density when antigen concentration was low[310]. In cell-based stimulation, receptor-ligand interactions were likely augmented by contacts between cell adhesion molecules. For example, integrin LFA-1 expressed on T cells, lowers the threshold for T cell activation by triggering Erk1/2 pathway and mediating AP-1 activity[311]. The additional cell:cell contact achieved through surface ligands on the tumor cells enhanced TAC-T cell proliferation, compared to antigen-coated beads, indicating that the magnitude of TAC expression is not relevant to proliferative responses when ancillary contacts are available.

We noted that T cell effector functions were differentially susceptible to TAC receptor expression levels. Our data from healthy donor-derived TAC-T cells suggest that IL-2 production is more sensitive to receptor surface expression than TNF-α or IFN-γ production. These results mirror findings from prior studies in T

cell biology. During chronic viral infection, the ability to produce IL-2 is lost before the ability to produce IFN-γ and TNF-α[312]. Coincidentally, when TCR ligand concentration is limited, IL-2 production is hindered before IFN-γ production[313]. Taken together, these data and our observations support higher activation threshold requirements for IL-2 production.

Interestingly, in patient-derived TAC-T cells, all three of the effector cytokines tested were affected by the surface levels of receptor. MM patient-derived T cells can downregulate CD28[314], PI3K, CD3ζ, and Lck[315], although reports on some of the signaling mediators are inconsistent[316]. Inadequate availability of signaling molecules downstream of TCR activation could elevate the activation threshold for patient-derived vs. healthy T cells, which offers an explanation for the increased sensitivity of cytokine secretion to TAC receptor levels when patient cells were used. The receptor expression-dependent differences in early cytokine production observed in a short-term intracellular cytokine staining assay were not detected in longer-term assays (proliferation, overnight cytotoxicity and cytokine accumulation) in healthy or MM patient-derived T cells. Thus, although the receptor expression levels may impact early events post-antigen engagement, expression levels do not impact later events, which are likely more pertinent to therapeutic efficacy.

The engineered T cell product ultimately relies on a combination of effector functions to mount an anti-tumor response *in vivo*. Thus, it was important to test

whether any of the differences we observed *in vitr*o would influence efficacy in animal models of MM, using TAC-T cells from healthy and patient donors. Equivalent efficacy *in vivo* from TAC-T cell products carrying different levels of TAC receptor highlighted robustness of the TAC platform and its stable performance irrespective of receptor expression levels. Interestingly, although the original UCHT1 and the next-generation huUCHT1(YT) scaffolds displayed similar *in vitro* functionality, huUCHT1(YT)-TAC-T cells were more efficacious *in vivo*. This observation highlights the limitation of *in vitro* systems for comparing cell-based therapies and argues for the necessity of *in viv*o testing.

In this study we described further evolution of the TAC scaffold that yields a TAC-T cell product that is efficacious against xenograft mouse models of MM. We conducted a detailed assessment of different BCMA-TAC-T cell functions and characterized how these functions were affected by changes in receptor surface expression. We have also tested this scaffold in other models of hematologic malignancy with comparable robust therapeutic outcomes. Ultimately, we established that TAC-T cells are equally efficacious across a range of receptor levels.

Chapter 4

Development of a fully humanized BCMA-specific TAC

Introduction

The antigen-binding domain is an important component of chimeric receptors responsible for the specificity of target recognition and the kinetics of T cell stimulation that affect downstream effector functions. As mentioned in Chapter 1, Section 3.3.4, scFvs are the most commonly used antigen-binding domains in the CAR constructs. ScFvs are built using variable fragments from heavy (V_H) and light (V_L) chains of an antibody connected via a linker that allows the domain to retain its affinity and specificity[317]. The variable fragments can be designed based on already known monoclonal antibodies or selected from libraries of naturally occurring and synthetic sequences and further enhanced via rational mutagenesis[318-320].

In an intact antibody, the variable fragments are stabilized by disulfide bonds and hydrophobic interactions between the constant regions of the heavy and light chains[321]. Since the constant regions are not included in the scFv, extra engineering efforts (e.g. directed evolution and rational design) are often needed to compensate for the loss of intrinsic stability[320]. In addition to modifications of the V_H and V_L fragments that increase their association with each other, the linker used to connect the V_H and V_L can facilitate scFv folding and stability and impact the resulting affinity[259, 322-324]. Aggregation of scFvs can be particularly detrimental in the context of chimeric receptors equipped with signaling domains because it can drive tonic activation of engineered T cells[213]. While TAC does not contain any signaling domains, it does include one scFv in the scaffold (the CD3-binding

domain), so we need to consider the linker between the scFv in the scaffold and the scFv used to bind the tumor targets. In concept, a flexible linker would allow for higher plasticity in accessing the antigen, but the flexibility could also increase the likelihood of interaction between the two scFvs resulting in cross-pairing or misfolding. Alternatively, a rigid linker might promote scFv segregation, but could also impede access to the target epitope.

Many of the original, and most extensively studied CARs were created with murine scFvs in the antigen-binding domains[325]. Researchers have now observed host cellular[326] and humoral[327] anti-CAR responses that can reduce persistence of engineered T cells. In extreme cases, host human anti-mouse antibodies directed at the CAR can trigger serious toxic reactions in the treatment recipient[327]. Thus, a completely humanized construct is desirable for optimal engineered T cell efficacy.

In the set of experiments described in this chapter, we sought to build on the learnings from Chapter 3 to develop a fully humanized BCMA-TAC using BCMA-specific scFvs selected from a phage display library expressing human F(ab) fragments. We compared 24 different scFv/linker combinations and narrowed down our selection to two leading candidates that are based on the V_H and V_L fragments from the scFv TRAC 3625. Subsequent *in vivo* studies revealed that the two leading candidates were equally efficacious, but one led to significantly lower levels of systemically produced cytokines than the other, suggesting lower risk of CRS toxicity. We chose the candidate with the lower *in vivo* cytokine levels as the final fully humanized BCMA-specific TAC receptor.

Results

Our collaborators from the Centre for Commercialization of Antibodies and Biologics (CCAB) at the University of Toronto, screened a phage library of human antibody sequences and selected 6 novel BCMA-specific antibodies with nanomolar affinities (Table 2).

Table 2. Affinity measurements of the BCMA-specific antibodies provided by the CCAB.

Antibody	**K_D (M)**
TRAC 3624	6.35×10^{-10}
TRAC 3625	4.97×10^{-10}
TRAC 3626	4.92×10^{-9}
TRAC 3627	1.56×10^{-9}
TRAC 3628	1.68×10^{-9}
TRAC 3630	2.14×10^{-9}

K_D = the equilibrium dissociation constant between the antibody and BCMA

The V_L-V_H or V_H-V_L orientation of fragments in the scFv can affect stability and target binding of the resultant scFv[328], so we tested both orientations. To connect the variable fragments, we chose the Whitlow linker that has been specifically designed to reduce aggregation and increase proteolytic stability of scFvs[259]. To ensure that the linker between the BCMA-specific scFv and the CD3ε-specific scFv does not undermine TAC receptor functionality, we compared a flexible glycine-serine-based linker (G4S) and a more rigid helical linker, both of which are commonly used in protein engineering[322]. Thus, for each pair of V_H and V_L, we

constructed 4 scFv variants by changing the orientation of the variable fragments relative to each other (V_L-V_H and V_H-V_L) and using either a G4S or a short helix linker between the BCMA-specific and the CD3ε-specific scFvs, leading to a total of 24 scFv + linker TAC variants (Table 3).

Table 3. Configurations of the TAC variants used in the screen.

Number in the Screen	Fragment Pair	Orientation	Linker
1	TRAC 3624	L-H	G4S
2	TRAC 3625	L-H	G4S
3	TRAC 3626	L-H	G4S
4	TRAC 3627	L-H	G4S
5	TRAC 3628	L-H	G4S
6	TRAC 3630	L-H	G4S
7	TRAC 3624	H-L	G4S
8	TRAC 3625	H-L	G4S
9	TRAC 3626	H-L	G4S
10	TRAC 3627	H-L	G4S
11	TRAC 3628	H-L	G4S
12	TRAC 3630	H-L	G4S
13	TRAC 3624	L-H	Short Helix
14	TRAC 3625	L-H	Short Helix
15	TRAC 3626	L-H	Short Helix
16	TRAC 3627	L-H	Short Helix
17	TRAC 3628	L-H	Short Helix
18	TRAC 3630	L-H	Short Helix
19	TRAC 3624	H-L	Short Helix
20	TRAC 3625	H-L	Short Helix
21	TRAC 3626	H-L	Short Helix
22	TRAC 3628	H-L	Short Helix
23	TRAC 3630	H-L	Short Helix
24	TRAC 3627	H-L	Short Helix

L = light chain; H = heavy chain

The screening candidates were expressed in primary human T cells in the original UCHT1-TAC framework and compared to the UCHT1-TAC carrying the C11D5.3 murine BCMA-specific scFv and the G4S linker in the extracellular portion (Figure 4.1A-C). Culture 24 failed to grow, so this scFv + linker variant was excluded from further assessment. All of the remaining 23 constructs transduced T cells (Figure 4.1B), but cultures 3, 9, 16, and 21 failed to express TAC on the surface of T cells or bind soluble BCMA and were eliminated from further screening. The remaining cultures were evaluated for their ability to upregulate CD69 in response to BCMA-positive KMS-11 tumor cells, as a surrogate for T cell activation[329] (Figure 4.1D). It is unclear why in this experiment, the C11D5.3-UCHT1-TAC showed little CD69 upregulation. Nevertheless, we observed a range of percentages of CD69-positive cells across the different screen candidates. The top four constructs (6, 8, 14, and 16) that showed the highest levels of activation based on CD69 expression advanced to further studies *in vitro* and *in vivo*. Notably, the two constructs with the highest activation (constructs 8 and 14; Figure 4.1D) were based on the same pair of heavy and light fragments, number TRAC 3625, although created with different orientations of V_H and V_L and with different linkers (Table 3).

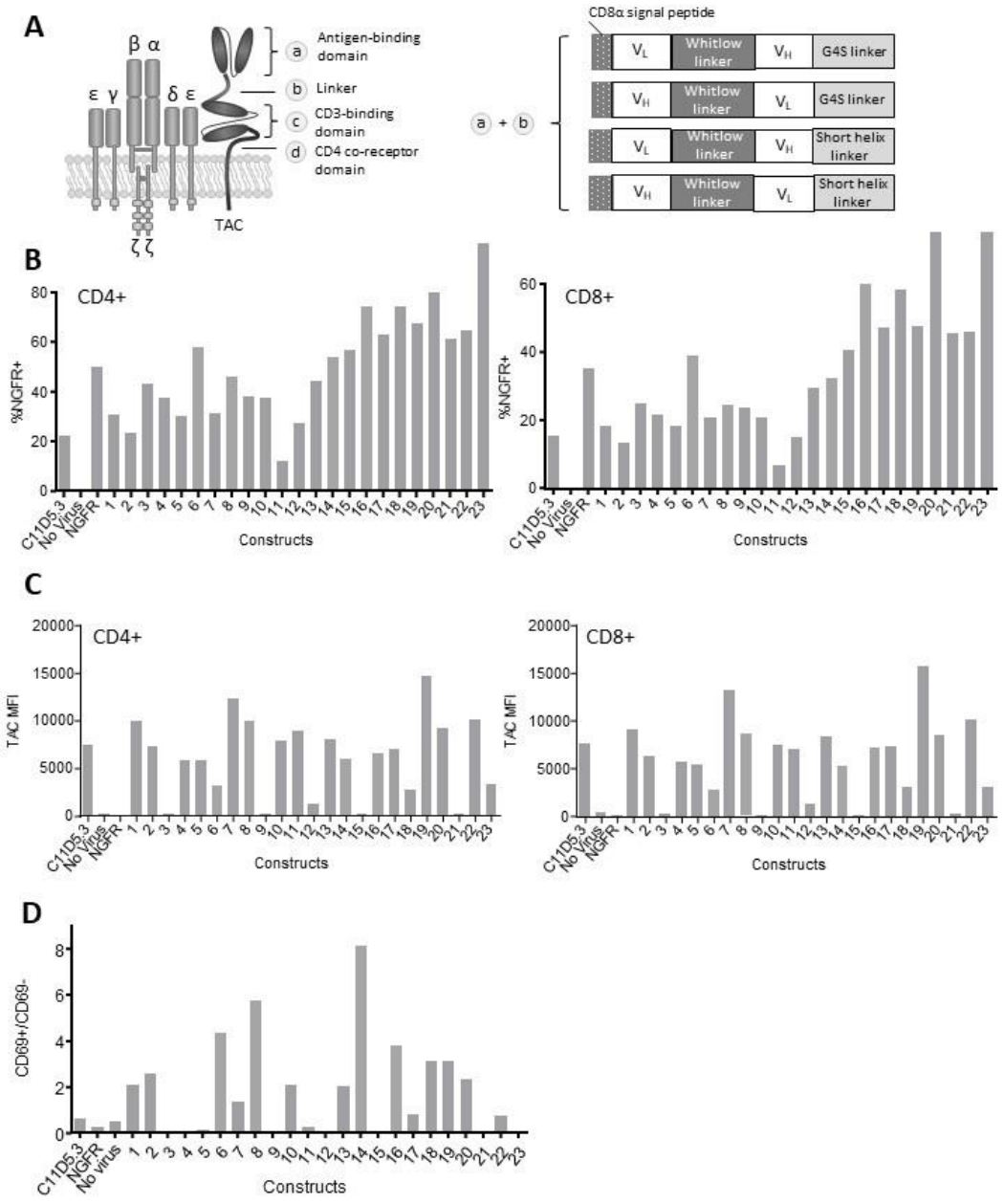

Figure 4.1. BCMA-TAC variants with novel humanized scFvs demonstrate diverse levels of expression and activation. (A) A schematic representation of the TAC receptor and the domains varied in the screen. (B) Transduction levels of different constructs. Cells were gated on live > singlets > CD4/CD8. (C) Median Fluorescence Intensity (MFI) of TAC receptors. Cells were gated on live > singlets > CD4/CD8 > $NGFR^+$. (D) Activation of different TAC cultures in response to stimulation with BCMA-positive KMS-11 tumor cells. T cells were stimulated with

KMS-11 targets at a 4:1 effector:target ratio for 4 hours and assayed by flow cytometry. Cells were gated on live > singlets > CD4/CD8 > $NGFR^+$ > $CD69^+$.

The work in this chapter was conducted in parallel with the work described in Chapter 3. When the scFv screen described in Figure 4.1 was completed, the huUCHT1-TAC framework became available. Since the end goal of this part of the project was to generate a fully human BCMA-TAC construct, the next step of comparing novel anti-BCMA scFvs was performed in the huUCHT1-TAC framework with C11D5.3- huUCHT1-TAC as a control. Phenotypically, T cells engineered with constructs 8-huUCHT1-TAC and 16-huUCHT1-TAC had stronger ability to bind BCMA, compared to T cells engineered with constructs 6-huUCHT1-TAC and 14-huUCHT1-TAC (Figure 4.2A). The 6-huUCHT1-TAC-T cells had the lowest level of binding to BCMA among the candidates tested. Constructs with scFvs number 8 and 14, which in the UCHT1-TAC framework showed the highest CD69 upregulation (Figure 4.1D), also produced more IFN-γ, TNF-α, and IL-2 upon activation, compared to constructs with scFvs number 6 and 16 (Figure 4.2B). The 6-huUCHT1-TAC showed the lowest cytokine production and may have had some tonic signaling, based on the basal IFN-γ production in CD8 T cells (Figure 4.2B). Out of the four new constructs, the 14-huUCHT1-TAC had the highest percent of cytokine-producing T cells, which was comparable to results from the original C11D5.3-huUCHT1-TAC.

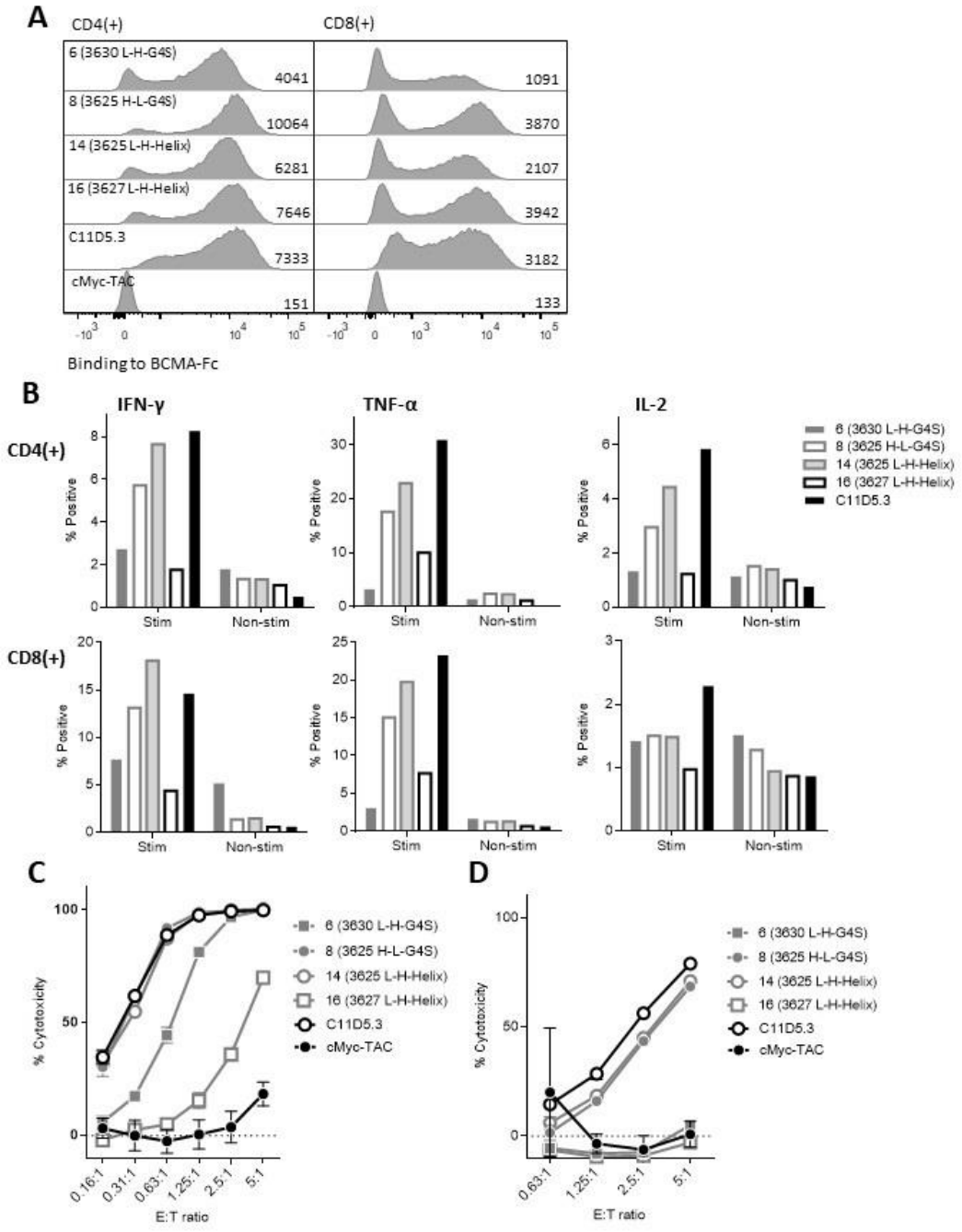

Figure 4.2. Candidates 8 and 14 outperform candidates 6 and 16 *in vitro*. (A) Representative plots of receptor surface expression tested by binding to BCMA-Fc. Cells were gated on live > singlets > CD4/CD8 > $NGFR^+$. Numbers indicate Median Fluorescence Intensity. (B) T cells were stimulated with KMS-11 targets at a 4:1 effector:target ratio for 4 hours in the presence of monensin and brefeldin A, stained for intracellular cytokine expression, and assayed by flow cytometry. Cells

were gated on live > singlets > CD4/CD8. (C,D) T cells were incubated with firefly luciferase-expressing KMS-11 (C) or Raji (D) targets for 24 hours at indicated effector:target ratios. Luminescence was read with an open filter upon addition of 0.15 mg/mL D-luciferin substrate and converted to % cytotoxicity.

The 8- and 14-huUCHT1-TAC-T cells were as efficient at killing KMS-11 and Raji tumor targets *in vitro* as the C11D5.3-G4S-huUCHT1-TAC-T cells (Figure 4.2C,D). The 6-huUCHT1-TAC-T cells had reduced killing ability, which was consistent with their low levels of cytokine production. Although the 16-huUCHT1-TAC-T cells produced more TNF-α than the 6-huUCHT1-TAC-T cells, they displayed weak cytotoxicity against KMS-11 and Raji tumors *in vitro*.

Since *in vitro* functionality does not guarantee effective *in vivo* performance, we tested the new, fully humanized BCMA-TACs in an orthotopic xenograft model of MM (Figure 4.3). Here, 14-huUCHT1-TAC-T cells had the best efficacy, with all 4 mice clearing tumors and entering long-lasting remissions. While 8- and C11D5.3-huUCHT1-TAC-T cells initially reduced tumor burden, 50% of mice in each of these two groups ultimately relapsed. 6- and 16-huUCHT1-TAC-T cells failed to provide any tumor control *in vivo*, which was consistent with their inferior performance *in vitro*, relative to the other TAC-T cells.

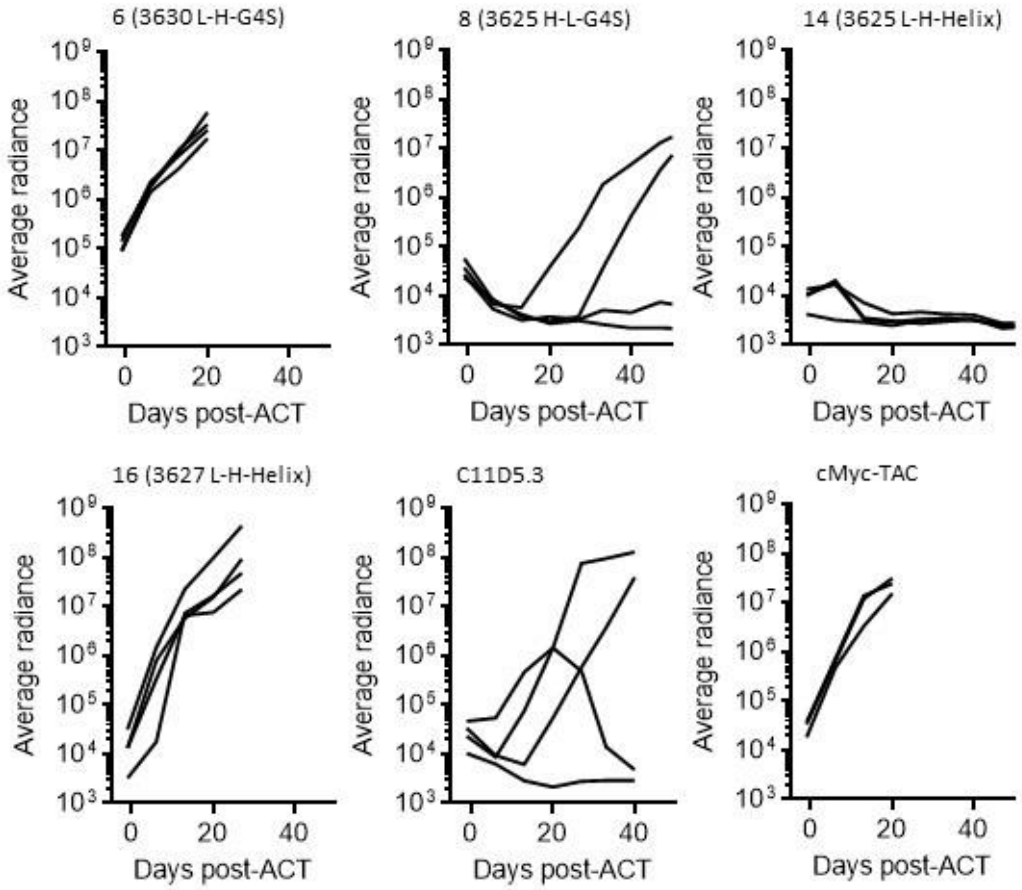

Figure 4.3. Candidates based on the scFv TRAC 3625 outperform other candidates *in vivo*. NRG mice were injected i.v. with firefly luciferase-expressing KMS-11 cells and treated i.v. with two doses of 2 x 10^6 $NGFR^+TAC^+$ cryopreserved T cells on days 11 and 14 post-tumor injection. Tumor signal was monitored by imaging mice after i.p. injection of D-luciferin, 150 mg/kg. Dorsal and ventral average (p/s/cm²/sr) signals were added for each mouse to calculate total tumor burden.

Taken together, initial *in vitro* and *in vivo* screening results favoured 8- and 14-huUCHT1-TACs, when compared with the other fully humanized TAC receptors. Both of these receptors were based on the V_L and V_H fragment pair number 3625, which supports the utility of this F(ab) for our purposes. We next elected to perform additional experiments with all configurations of the 3625 F(ab), i.e.: V_L-

V_H or V_H-V_L with a G4S linker or a short helical linker. At the same time, we had finished comparison of the huUCHT1-TAC and huUCHT1(YT)-TAC scaffolds (as described in Chapter 3) and chose to advance the huUCHT1(YT)-TAC scaffold due to its favorable surface expression and efficacy profile. Thus, our final comparisons of the 3625 scFv variants were conducted using the huUCHT1(YT)-TAC framework.

We observed that the V_L-V_H scFv configuration translated into reduced binding to BCMA-Fc for the 2-huUCHT1(YT)-TAC and 14-huUCHT1(YT)-TAC (Figure 4.4A). The difference in BCMA-Fc binding had no impact on engineered T cell growth (Figure 4.4B) or cytotoxic abilities of the culture (Figure 4.4C,D).

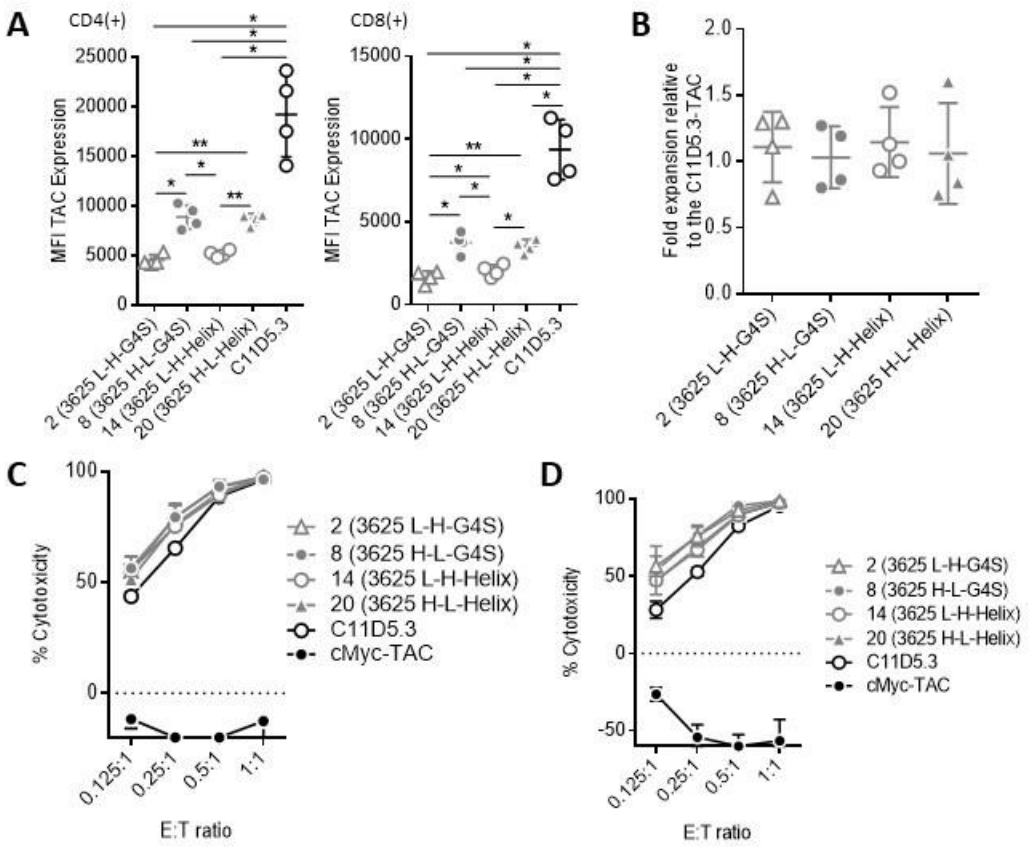

Figure 4.4. Light and heavy chain order of fragments in the 3625 scFv influences TAC surface expression. (A) Median fluorescence intensity (MFI) of receptor surface expression on transduced cells. Cells were gated on live > singlets > CD4/CD8 > NGFR$^+$. Statistical significance was determined using repeated measures ANOVA. (B) T cell fold expansion after NGFR-sorting, normalized to the expansion of the C11D5.3-TAC. (C,D) T cells were incubated with firefly luciferase-expressing KMS-11 (C) or MM.1S (D) targets for 8 hours at indicated effector:target ratios. Luminescence was read with an open filter upon addition of 0.15 mg/mL D-luciferin substrate and converted to % cytotoxicity.

The effect of the V_L/V_H chain orientation in the scFv was more pronounced in the cytokine production assay (Figure 4.5A,B). Constructs 2-huUCHT1(YT)-TAC and 14-huUCHT1(YT)-TAC produced fewer cytokines in response to BCMA-positive KMS-11 and MM.1S cells. In the cases where high donor-to-donor variability made the observations not statistically significant, the trend for the V_L-

V_H scFv constructs producing fewer cytokines was still observed. These data are in line with our observations in Chapter 3, where cytokine production was more sensitive to receptor density than cytotoxicity, underscoring different activation thresholds for these effector functions. When KMS-11 cells were used for stimulation, there was a trend towards less proliferation of the T cells expressing the V_L-V_H oriented scFv, but the results were only significant in the case of CD4 T cells, where the 8-huUCHT1(YT)-TAC-T cells displayed greater proliferation than the 2-huUCHT1(YT)-TAC-T cells (Figure 4.5C). When MM.1S cells were used for stimulation, T cells engineered with all of the TAC variants proliferated equally well (Figure 4.5D).

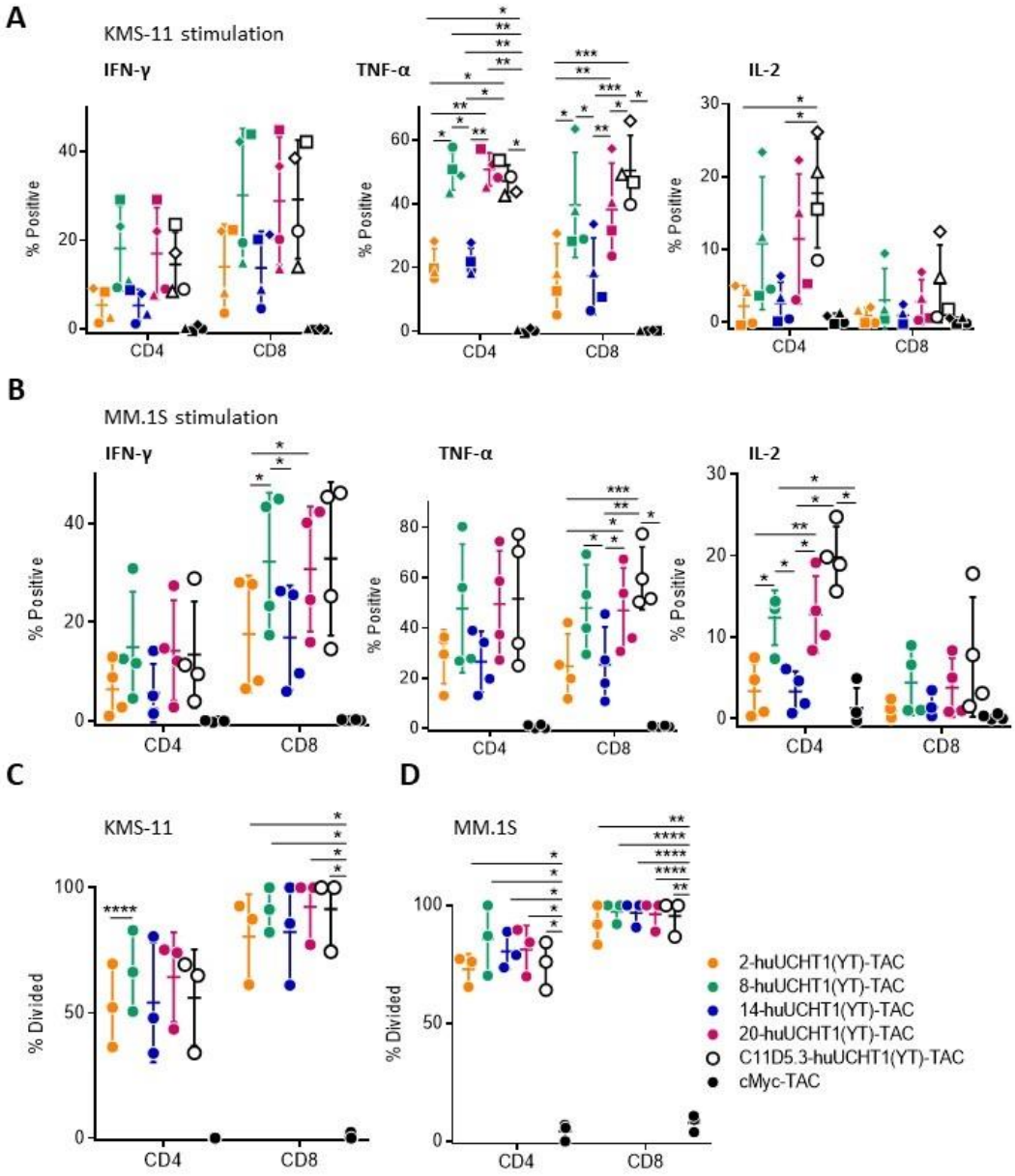

Figure 4.5. Order of heavy and light chain fragments in the 3625 scFv affects *in vitro* effector functions. (A,B) Cytokine expression. T cells were stimulated with KMS-11 (A) or MM.1S (B) targets at a 2:1 effector:target ratio for 4 hours in the presence of monensin and brefeldin A, stained for intracellular cytokine expression, and assayed by flow cytometry. Cells were gated on live > singlets > CD4/CD8. Data are representative of 4 different donors, each marked with a different symbol. (C,D) Proliferation analysis. T cells were labelled with CellTrace Violet dye, stimulated with KMS-11 (C) or MM.1S (D) tumor targets at an effector:target ratio 2:1 for 4 days and assayed by flow cytometry. Samples were

gated as singlets > live > $CD138^-$ > CD4/CD8 > $NGFR^+$. Data are representative of 3 donors. Statistical significance was determined with repeated measures ANOVA.

The surface expression and cytokine production data suggested that the V_H-V_L oriented scFvs might offer therapeutic advantage due to stronger activation of engineered T cells. Therefore, we performed *in vivo* testing of the engineered T cells using the KMS-11 xenograft model. Tumors were established and mice were treated with 3 x 10^6 or 1 x 10^6 TAC^+ T cells. The 3 x 10^6 TAC^+ T cells/mouse group showed that TAC-T cells carrying all four of the 3625 scFv variants were equally or more efficacious than the original C11D5.3-based TAC-T cells (Figure 4.6A). Data from the 1 x 10^6 TAC^+ T cells/mouse dose group suggested that the G4S linker between the 3625 scFv and huUCHT1(YT) might have an advantage over the short helical linker, as the 2-huUCHT1(YT)-TAC and the 8-huUCHT1(YT)-TAC-T cells had the best performance (Figure 4.6B). Thus, the *in vivo* efficacy studies showed that the linker between the V_H and V_L fragments of the 3625 scFv had more influence on the therapeutic efficacy than the orientation of fragments, which had a more pronounced effect on the *in vitro* TAC-T cell functions.

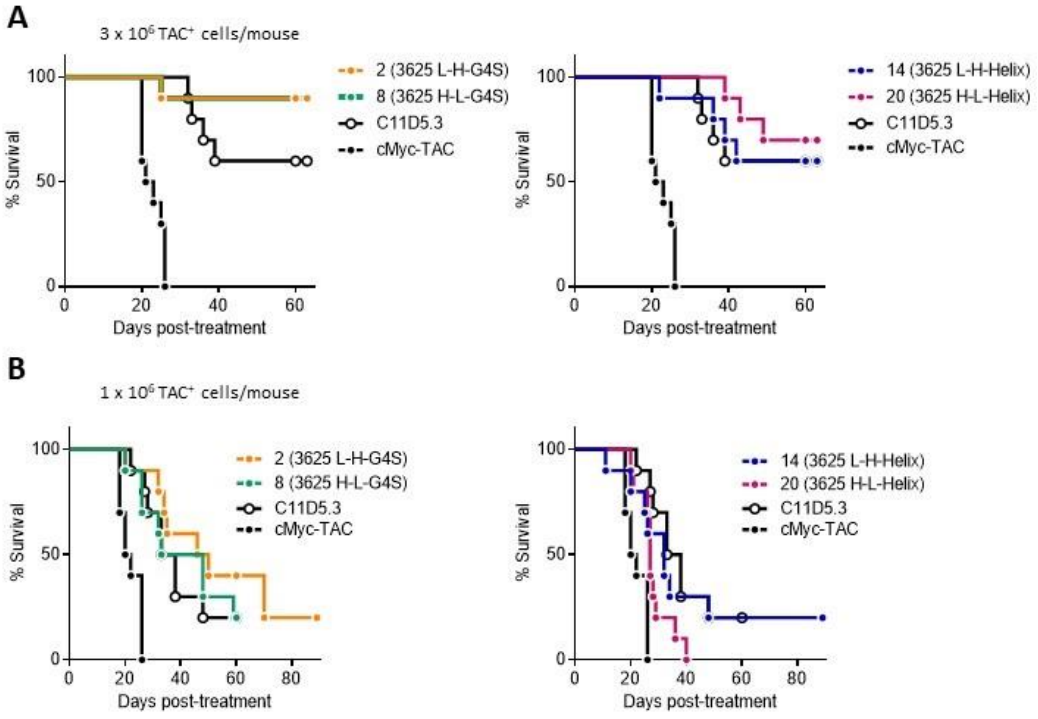

Figure 4.6. huUCHT1(YT)-TAC-T cells carrying the 3625 scFv are effective against KMS-11 tumors *in vivo*. KMS-11 tumor-bearing NRG mice were treated with 3 x 10^6 (A) or 1 x 10^6 (B) of TAC^+ cryopreserved T cells i.v. on day 12 post-tumor injection. Survival data are shown. For clear visualization, data from each dose level are presented as 2 graphs with the cMyc-TAC and the C11D5.3-TAC data included in each graph for reference. Data are representative of 2 healthy donors, n = 10 mice per group.

Since the 2-huUCHT1(YT)-TAC and the 8-huUCHT1(YT)-TAC-T cells had equivalent efficacy *in vivo*, but their *in vitro* cytokine production levels were markedly different, we wanted to perform additional *in vivo* tests to decide on which construct to move forward with. CRS is a potentially life-threatening toxicity associated with engineered T cell therapies, and a product producing more cytokines *in vivo* might carry a higher risk for causing CRS. The 8-huUCHT1(YT)-TAC-T cells produced more cytokines *in vitro* than the 2-huUCHT1(YT)-TAC-T

cells, so we wondered whether the *in vivo* cytokine levels would follow a similar trend.

Neither the 2- nor the 8-huUCHT1(YT)-TAC-T cell-treated mice exhibited overt signs of toxicity, but our model is not suitable for assessment of the clinical signs of CRS because the mice are immunodeficient and not all of the human cytokines are recognized by murine receptors. Thus, we focused on comparing the levels of serum cytokines between the two constructs. In addition to the data presented in Figure 4.7, our cytokine panel included IL-1β, IL-1Ra, IL-6, IL-8, IL-12p40, IL-12p70, and MCP-1, but the values for these markers were below detection. Overall, the 8-huUCHT1(YT)-TAC-T cells produced significantly more cytokines *in vivo*, compared to the 2- huUCHT1(YT)-TAC-T cells (Figure 4.7). The IFN-γ, IL-2, IL-4, IL-5, and IL-10 production was rapidly induced early after the activation of 8-huUCHT1(YT)-TAC-T cells and quickly declined by day 7 post-injection. The GM-CSF, IL-13, and TNF-α secretion was also rapidly triggered after activation, but the levels of these cytokines declined slower and were still significantly elevated at day 7 post-treatment. The 2-huUCHT1(YT)-TAC-T cells, in addition to secreting significantly lower levels of cytokines than the 8-huUCHT1(YT)-TAC-T cells, had different kinetics for some of the cytokines tested. Particularly, the levels of IFN-γ, IL-4, and IL-5 did not substantially differ between days 3 and 7 in the 2-huUCHT1(YT)-TAC-T cell-treated mice, while the 8-huUCHT1(YT)-TAC-T cell-treated mice had a noticeable expansion and contraction in the secretion of the same cytokines in the first week post-treatment.

Finally, we also detected an increase in IL-10 in the serum of non-treated mice by day 7 of analysis, but this cytokine was likely coming from growing KMS-11 tumors which had been shown to secrete IL-10 *in vitro*[330].

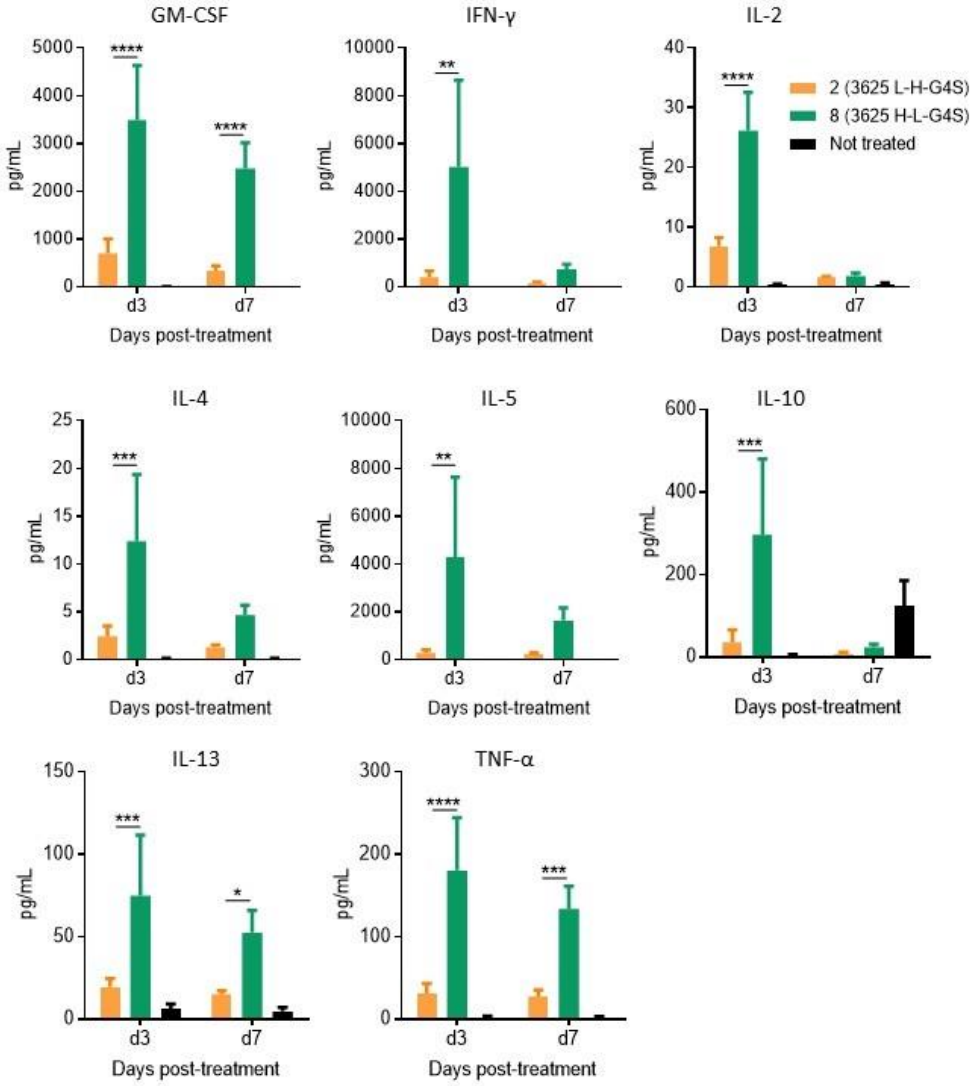

Figure 4.7. The 8-huUCHT1(YT)-TAC-T cells produce more cytokines *in vivo* than the 2-huUCHT1(YT)-TAC-T cells. NRG mice bearing 12-day KMS-11 tumors were treated with 10^6 TAC^+ cryopreserved T cells i.v., n = 4 mice/group. Serums were harvested at indicated time points and analyzed in duplicates by Eve Technologies. Mean and SD are shown. Statistical significance was determined using 2-way ANOVA, followed by Tukey's test.

Discussion

In this set of experiments, we completed humanization of the BCMA-TAC receptor and identified the leading candidate, 2-huUCHT1(YT)-TAC, which included a BCMA-specific scFv TRAC 3625 in the V_L-V_H orientation and a flexible G4S linker between the BCMA-specific scFv and the UCHT1-specific scFv. This construct was more efficacious *in vivo* than the original C11D5.3-based construct and had a more favorable cytokine secretion profile, compared to the second-most efficacious construct, 8-huUCHT1(YT)-TAC.

As noted earlier, TAC is designed with two scFvs, which could potentially influence each other due to fragment mispairing and aggregation[331]. As it is not possible to predict these interactions, empirical assessment of novel scFvs introduced in the TAC framework is necessary. By screening the 24 scFv + linker combinations directly in primary TAC-T cells, we ensured that functional deficiencies stemming from interaction between the two scFvs in the TAC would be accounted for. The screen, however, had several limitations. The first limitation was the absence of virus titration and, as a consequence, mismatched MOIs used for transducing different cultures in the screen. Because of that, transduction measured by the percent of NGFR-positive cells in culture, might be a consequence of different amounts of virus used. Curiously, higher transduction did not always correlate with higher TAC surface expression, with constructs 3, 9, 15, and 21 demonstrating an extreme scenario where T cells were over 40% transduced, but TAC was completely undetected on the surface. Because we measured TAC surface

expression by staining with soluble BCMA, lack of TAC on the surface might represent lack of binding to the antigen. In either case, this would be an undesirable outcome for the new receptors. The second limitation of the screen was lack of adjustment for percent transduction or percent TAC surface expression when setting up the stimulations for the CD69 assessment. However, there was no apparent relationship between TAC surface expression and CD69 activation. For example, among the constructs 4, 5, and 14, which had nearly identical levels of TAC on the surface, only construct 14 triggered CD69 upregulation. Thus, it was reasonable to proceed with the constructs that triggered the highest CD69 upregulation for further functional assessment.

The idea that intrinsic stability of novel scFvs and potential interaction between the BCMA-specific scFv and downstream UCHT1 scFv might affect TAC-T cell functionality is further reinforced by our *in vitro* and *in vivo* studies. BCMA-TAC candidates 8 and 14 were designed with fragments from the scFv TRAC 3625, and construct 8 contained V_H-V_L scFv orientation and a G4S linker, while construct 14 contained V_L-V_H scFv orientation and a helical linker. Both constructs were assessed on two slightly different UCHT1 frameworks – huUCHT1 and huUCHT1(YT). The data with the huUCHT1 framework are limited by the small sample number and use of different donors, compared to the huUCHT1(YT) studies. However, the surface expression trends were similar between the two scaffolds with candidate 8 showing higher BCMA-Fc binding. In the huUCHT1 scaffold, construct 14 elicited more cytokine-producing cells upon *in vitro*

stimulation and induced remissions *in vivo*. Interestingly, this trend was reversed in the huUCHT1(YT) scaffold, where candidate 8 demonstrated improved *in vitro* activation and *in vivo* performance. These results suggest that the most optimal configuration of the 3625 scFv might differ depending on which huUCHT1 scaffold is used.

Interestingly, the TRAC 3625 V_L/V_H fragment pair that ultimately emerged as the winning binder from the 6 candidate pairs, had the highest affinity for BCMA. In the CAR-T cell field, affinity of the antigen-binding scFv is often considered in the context of antigen density. In solid tumor models, target antigens are often expressed at lower levels on healthy tissues and at higher levels on the tumor. In these cases, reduction of the scFv affinity in the CAR antigen-binding domain has been used as a method of increasing CAR-T cell specificity for tumors and decreasing unwanted toxicity[248, 332, 333]. Since BCMA has a very limited expression pattern, having a high-affinity binder might help eliminate BCMA-low myeloma cells without the risk of damaging healthy tissues.

As mentioned earlier, our surface staining for TAC receptor is done with BCMA antigen, so among the variants of the TRAC 3625 fragment pair, lower MFI for the light-heavy orientation, compared to heavy-light orientation, could reflect reduced surface expression or reduced target binding. Similarly, lower MFI for all of the TRAC 3625 variants, compared to C11D5.3, also cannot be attributed to surface expression alone in the current experimental setting. All TAC constructs used in this set of experiments have a c-Myc tag in the extracellular domain.

However, the c-Myc tag is not accessible in the C11D5.3-based receptors. If the difference in MFI among the TRAC 3625 variants is due to differences in surface expression and not affinity, then the data are in line with our conclusions from Chapter 3, where TAC afforded high functionality across a range of receptor levels.

The observation that constructs 2-huUCHT1(YT)-TAC and 8-huUCHT1(YT)-TAC had equivalent *in vivo* efficacy in the KMS-11 model despite markedly different *in vitro* performance prompted further investigations into *in vivo* cytokine secretion profile of each product. Clinical experience with CAR-T cells shows that IFN-γ released by activated T cells triggers IL-6 production by macrophages, which can escalate to systemic CRS in patients[334]. As a consequence, a monoclonal antibody against IL-6 receptor, tocilizumab, is widely used for CRS management in the clinics[335]. Inhibition of TNF-α in a small number of CAR-T cell-treated myeloma patients has also been used to resolve CRS[336]. Preclinical research shows that neutralization of GM-CSF alleviates CRS and neuroinflammation in a CD19 CAR-T cell murine xenograft model[337]. IFN-γ, GM-CSF, TNF-α, and other cytokines were elevated significantly more in the 8-huUCHT1(YT)-TAC-T cell-treated mice, compared to the 2-huUCHT1(YT)-TAC-T cell-treated mice, suggesting that the 8-huUCHT1(YT)-TAC product might be more toxic when taken into the clinics. Since the *in vivo* efficacy was the same between these two types of T cells, we moved forward with the 2-huUCHT1(YT)-TAC candidate as a potentially safer option.

The experiments described in this chapter characterized generation of fully humanized BCMA-specific TAC-T cells with the goal of subsequently taking the top-performing candidate, 2-huUCHT1(YT)-TAC, into clinical testing. However, the value of characterizing novel BCMA-specific scFvs based on the TRAC 3625 antibody extends beyond applications in the TAC-T cell therapy. These new domains could be further applied in the CAR, BiTE, ADC, or monoclonal antibody therapeutic settings or investigated as diagnostic agents for BCMA detection.

Chapter 5

Non-toxic cross-reactivity of the antigen-binding domain supports *in vivo* function of TAC-T cells

Introduction

Prior to gaining access to a set of human BCMA-specific antibody fragments discussed in Chapter 4, we compared two murine BCMA-specific scFvs based on the antibodies C11D5.3[338] and J22.9-xi[339] in the TAC framework.

The C11D5.3 scFv has been included in three BCMA-specific, second-generation CAR-T cell products that have been evaluated in clinical trials[217-219]. These products have been reviewed in Chapter 1, section 3.3. The biggest of the three studies showed evidence of anti-drug antibodies. The likelihood of developing these antibodies increased over time post-treatment, but the researchers found no relationship between the quality or duration of response and the presence of anti-drug antibodies[218]. At the preclinical level, the C11D5.3 scFv has also been tested in a bi-specific CAR construct that included a CD19-specific scFv, FMC63[340]. Although the authors did not specify whether their CAR was able to bind both antigens simultaneously, the bispecific CAR-T cells showed some *in vivo* efficacy against tumor cells expressing either BCMA or CD19[340].

No clinical data with the J22.9-xi scFv in T cell-based therapies have been reported yet, but several preclinical studies with the variants of this scFv incorporated in the CAR constructs have been published. A humanized version of the J22.9-xi scFv with altered post-translational modification sites, J22.9-FSY[341], has been tested in the CD28ζ CAR framework[342]. The researchers observed transient *in vivo* responses in the MM.1S xenograft model with outgrowing tumors

expressing unaltered BCMA levels, suggesting loss of efficacy of the T cell product over time[342]. Another group evaluated the original murine J22.9-xi scFv (referred to as J22.9 in the paper) and their proprietary humanized variant of this scFv in the 4-1BBζ CAR framework[343]. Despite higher *in vivo* T-cell numbers and IFN-γ levels in serum, CAR-T cells carrying the murine J22.9 scFv showed worse survival, which was attributed to higher graft-versus-host toxicity[343]. The authors did not elaborate on the specifics of this toxicity, but suggested that the CAR-T cells with the murine J22.9 scFv proliferated faster and were less likely to persist in the face of repeated stimulation with tumor cells, compared to the CAR-T cells with the humanized J22.9 scFv[343].

The C11D5.3 and the J22.9-xi scFvs and their humanized variants have also been compared in the context of a bi-specific 4-1BBζ CAR targeting BCMA and SLAMF7[344]. Based on the inferior *in vitro* cytotoxicity and proliferation studies, the authors discontinued using the J22.9-xi-containing CAR variants. The authors selected a CAR designed with a humanized anti-SLAMF7 scFv followed by the murine C11D5.3 scFv as the top *in vivo* performer based on its control of the MM.1S tumors engineered to express BCMA, SLAMF7, or both antigens simultaneously[344].

In this chapter, we present our experience with comparing TAC-T cells engineered with the C11D5.3 or the J22.9-xi scFvs in the antigen-binding domain. In the *in vivo* efficacy studies, the J22.9-xi TAC-T cells outperformed the C11D5.3 TAC-T cells. *In vivo* T-cell imaging and histology studies revealed that the J22.9-

xi TAC-T cells proliferated better than the C11D5.3 TAC-T cells. *In vivo* proliferation of J22-TAC-T cells was driven by cross-reactivity to an unknown antigen in mice, but did not lead to any noticeable signs of toxicity.

Results

Based on the TAC scaffold optimization described in Chapter 3, we chose the huUCHT1(YT) backbone for comparing the C11D5.3 and the J22.9-xi scFvs in the antigen-binding domain. For simplicity of reference, the C11D5.3-based TAC is labelled as the C11-TAC and the J22.9-xi-TAC is labelled as the J22-TAC in this chapter. Using the CD8α signal sequence (evaluated in Chapter 3) for both constructs, we observed equivalent surface expression of both TACs in CD4 T cells, with the J22-TAC demonstrating higher expression in CD8 T cells, compared to the C11-TAC (Figure 5.1A). To account for donor-to-donor differences in T cell growth, expansion data were normalized to the expansion of the control cMyc-TAC culture. Prior to the sort based on the transduction marker NGFR, both cultures expanded similarly (Figure 5.1B). Following the sort, the J22-TAC-T cells expanded more than the C11-TAC-T cells (Figure 5.1B). This expansion was not related to differences in the CD4 and CD8 frequencies because the CD4/CD8 ratios were the same across different TAC constructs.

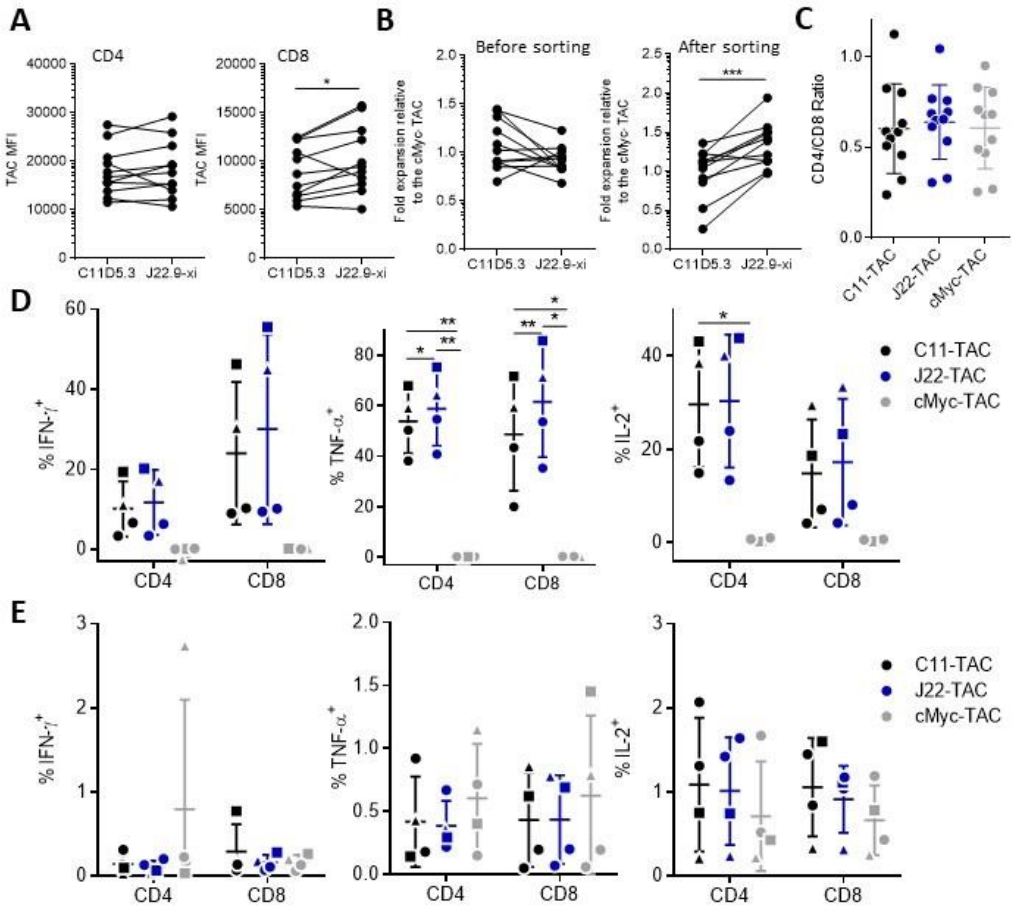

Figure 5.1. J22-TAC-T cells show several improved *in vitro* characteristics, compared to C11-TAC-T cells. (A) Median fluorescence intensity (MFI) of receptor surface expression on transduced cells. Cells were gated on live > singlets > CD4/CD8 > NGFR$^+$. (B) T cell fold expansion before and after NGFR-sorting, normalized to the expansion of the cMyc-TAC. (C) CD4/CD8 ratios at the end of the manufacturing period. (D,E) Cytokine expression. T cells were stimulated with KMS-11 (D) targets at a 2:1 effector:target ratio or not stimulated (E) for 4 hours in the presence of monensin and brefeldin A, stained for intracellular cytokine expression, and assayed by flow cytometry. Cells were gated on live > singlets > CD4/CD8. Statistical significance was determined using paired t-test (A,B) or repeated measures ANOVA, followed by Tukey's test (C-E). Lines show mean and SD and each donor is marked by a different symbol (D,E). Data are representative of 6 (A-C) or 3 (D,E) different donors.

To determine whether the C11D5.3 or the J22.9-xi scFv rendered TAC-T cells more functional, we compared cytokine production, cytotoxicity, and

proliferation responses. Although there were no differences in IFN-γ and IL-2 production upon stimulation, activated J22-TAC-T cells produced more TNF-α, compared to C11-TAC-T cells (Figure 5.1D), with neither culture showing evidence of baseline activation (Figure 5.1E).

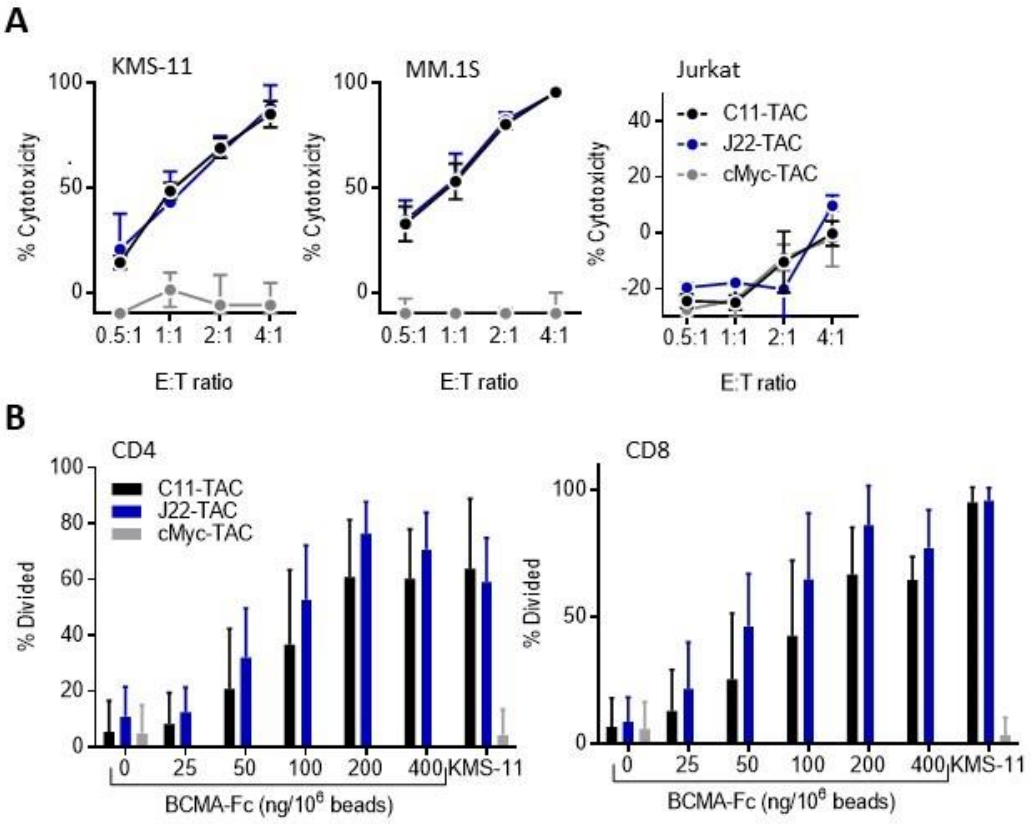

Figure 5.2. C11- and J22-TAC-T cells are equally efficacious at killing tumor targets and proliferating *in vitro*. (A) T cells were incubated with firefly luciferase-expressing BCMA-positive KMS-11 and MM.1S targets or BCMA-negative Jurkat targets for 8 hours at indicated effector:target ratios. Luminescence was read with an open filter upon addition of 0.15 mg/mL D-luciferin substrate and converted to % cytotoxicity. (B) Proliferation analysis. T cells were labelled with CellTrace Violet dye, stimulated with polystyrene protein G beads coated with indicated concentrations of BCMA-Fc at an effector:target ratio 1:1 or KMS-11 tumor targets at an effector:target ratio 2:1 for 4 days and assayed by flow cytometry. Samples were gated as singlets > live > $CD138^-$ > CD4/CD8 > $NGFR^+$. Data are representative of 3 donors. Statistical significance was determined with

ANOVA for non-stimulated and KMS-11-stimulated samples and a t-test for the remaining samples.

This functional difference observed in a 4-hour cytokine production assay, did not carry forward in longer-term assessments of cytotoxicity and proliferation (Figure 5.2), where the C11- and the J22-TAC-T cells proliferated and killed tumor targets equally well. Although there was a trend for higher proliferation of the J22-TAC-T cells in some of the bead-stimulated samples (Figure 5.2B), it was not statistically significant.

Besides TNF-α production upon stimulation, there were no *in vitro* functional differences between the C11- and the J22-TAC-T cells, so we asked whether their efficacy *in vivo* would also be similar. At a higher T-cell dose of 2 x 10^6 TAC-positive T cells per mouse, both types of T cells were able to induce lasting anti-tumor responses (Figure 5.3A, left panel). However, when the T cell dose was titrated down to 0.5 x 10^6 TAC-positive T cells per mouse, there was a trend for better tumor control with the J22-TAC-T cells, compared to the C11-TAC-T cells (Figure 5.3A, right panel). To determine, which T cell product retained its efficacy longer, we rechallenged surviving, tumor-free mice from the 2 x 10^6 TAC-positive T cell dose group with a new injection of tumor cells (Figure 5.3B). Although the sample sizes were small, mice that had received the J22-TAC-T cell treatment were more resistant to the new KMS-11 tumor, compared to mice that had received the C11-TAC-T cell treatment.

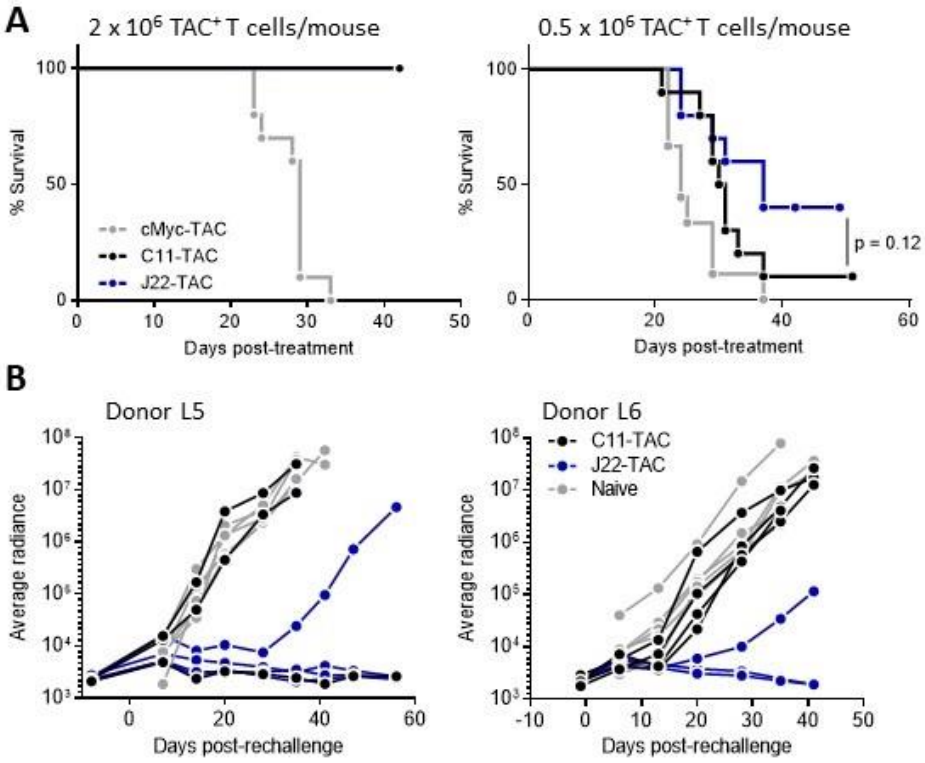

Figure 5.3. J22-TAC-T cells outperform C11-TAC-T cells *in vivo*. (A) KMS-11 tumor-bearing NRG mice were treated with 2 x 10^6 or 0.5 x 10^6 of TAC^+ cryopreserved T cells i.v. on day 12 post-tumor injection. Survival data are shown. Statistical significance was determined using log-rank (Mantel-Cox) test. Data are representative of 2 healthy donors, n = 9-10 mice per group. (B) Surviving, tumor-free mice from the 2 x 10^6 TAC^+ T cells/mouse group were rechallenged with 10^6 luciferase-expressing KMS-11 tumor cells i.v. on days 51 (left panel) and 43 (right panel) post-treatment, n = 3-5 mice per group. Tumor burden was tracked via bioluminescence imaging after i.p. D-luciferin injection.

The *in vivo* efficacy studies suggested that the J22-TAC-T cell product was more potent. In the CAR-T cell field, *in vivo* proliferation and persistence of T cells have been linked to better therapeutic outcomes[242, 345-347]. Thus, we designed imaging and histology studies to assess the *in vivo* kinetics of our engineered TAC-T cell products. At the time of the imaging-based T cell tracking experiments, the C11-TAC construct with the CD8α signal sequence was not yet available, so we

used the C11-TAC construct with the IgK signal sequence, which has lower surface expression. Since our subsequent comparison of these two C11-TACs (described in Chapter 3) showed no difference in *in vivo* efficacy, we deemed this substitution acceptable. The C11-TAC construct with the CD8α signal sequence was available at the time of histological assessment of *in vivo* T cell proliferation, so that comparison of the C11- and the J22-TAC-T cells was performed using TAC constructs with similar surface expression levels.

To track T cells and tumor cells in the same mice, we optimized a dual imaging system, using the enhanced firefly luciferase (effLuc)[256] for labelling T cells and a conjugate of the NanoLuc luciferase to the enhanced green fluorescent protein (eGFP), GpNluc[257], for labelling tumor cells. Due to different substrates used by these two luciferases, the luminescence signals were distinctly tumor- or T cell-specific. The C11-TAC-T cells demonstrated the same kinetics as the control cMyc-TAC-T cells and did not show proliferation *in vivo* (black and grey lines; Figure 5.4A). On the contrary, the J22-TAC-T cells rapidly expanded post-infusion, although this expansion was independent of the presence of the tumor (dark and light blue lines; Figure 5.4A). Despite differences in T cell expansion, both types of TAC-T cells produced equivalent survival outcomes (Figure 5.4B).

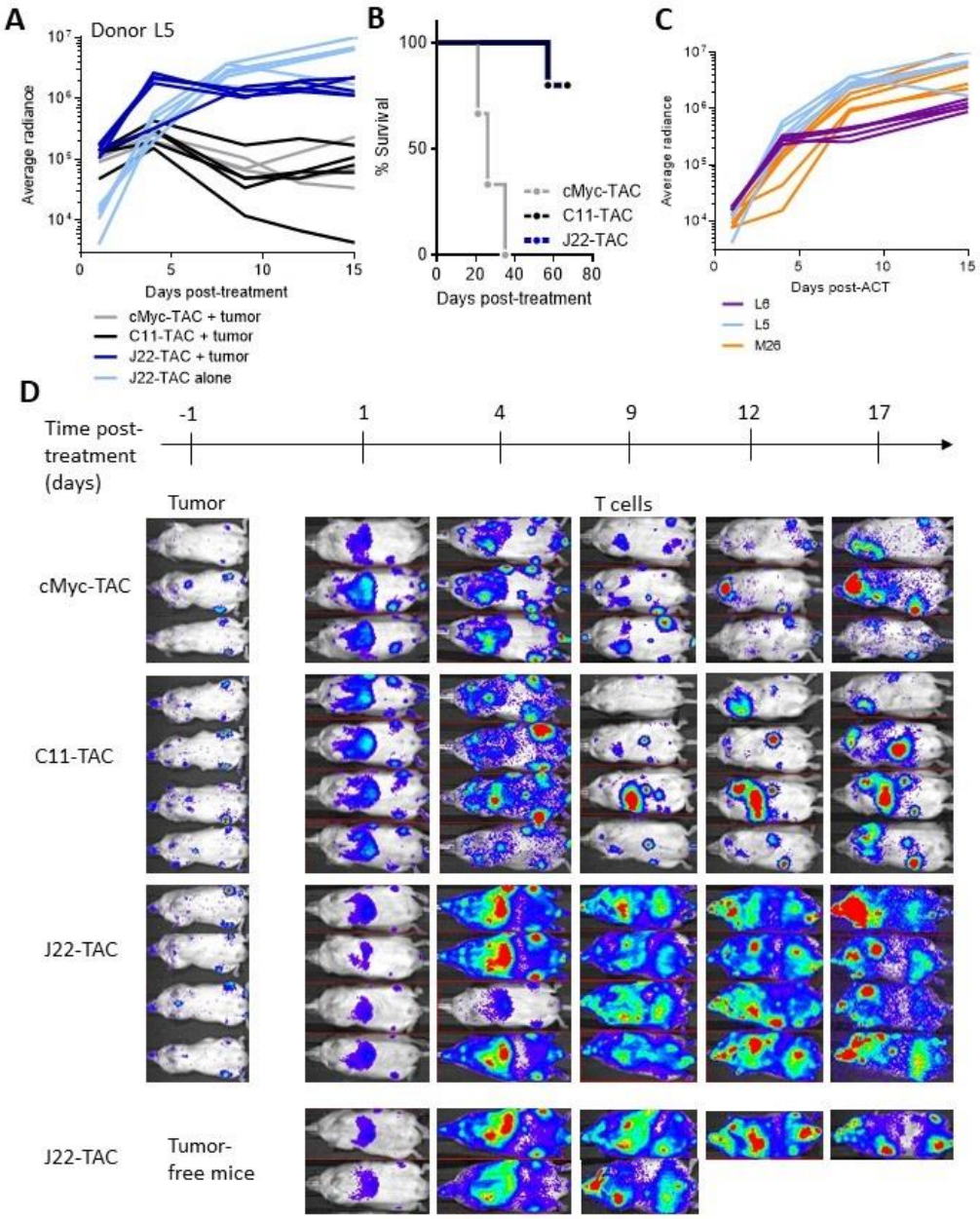

Figure 5.4. *In vivo* kinetics of the C11- and the J22-TAC-T cells. (A) KMS-11 tumor-bearing or tumor-free NRG mice were treated with 4 x 10^6 of TAC^+ cryopreserved T cells i.v. on day 12 post-tumor injection. T cell load was tracked via bioluminescence imaging after i.p. D-luciferin injection. (B) Survival data for mice in A. (C) Tumor-free NRG mice received 4 x 10^6 of TAC^+ cryopreserved T cells i.v. and were monitored as in A. The T cell curves for donor L5 are identical between A and B and are included in both images for comparison. (D) Mice were treated and T cell load was monitored as in A. Tumor burden was tracked via

bioluminescent imaging after i.v. injection of furimazine. Ventral images are shown.

Experiments with two additional donors in tumor-free mice confirmed that the J22-TAC-T cells were likely cross-reacting with a murine antigen *in vivo* (Figure 5.4C). A limitation of the multi-donor T cell tracking experiment was lack of control T cells for each donor, and future experiments will include the proper controls. A closer look at the T cell distribution (Figure 5.4D) suggested that the early J22-TAC-T cell expansion was concentrated in the middle section of the mouse in tumor-bearing and tumor-free mice and was not aligned with the pre-treatment location of the tumor. Baseline tumor signal localized to the femurs and, in some cases, to the sternum. While some T cell signal in the first week post-infusion was found in the femurs, there was a lot of signal in the lung/liver area and some signal in the neck area. Even in the mice that had baseline tumor signal in the sternum, the T cell expansion area was substantially larger than the sternum and covered a big section in the middle of the body.

We wanted to follow the imaging assessment of *in vivo* T cell distribution with a histological analysis. As a pilot study for testing the histological stains, we ran a small-scale experiment with a limited number of tissues. We chose to look at femur because this was the site where tumor cells localized based on the imaging data. We also looked at spleen as an organ through which T cells circulating in blood would pass and liver as an organ localized in the middle of the mouse and potentially the sight that showed high T cell signal in the imaging experiments. The tissues were stained for the expression of human CD3 to identify T cells and Ki67

to identify proliferating cells. The software used for signal quantification was unable to identify some actively proliferating T cells due to a dim CD3 signal. For this reason, the percentage of $CD3^{-}Ki67^{+}$ cells detected in the mice that did not receive tumor or T cells (included as controls for each tissue and each time point) was treated as the true frequency of $CD3^{-}Ki67^{+}$ cells and subtracted from the $CD3^{-}Ki67^{+}$ data for the groups that received T cells. The remaining values were treated as the $CD3^{+}Ki67^{+}$ cells that had been missed due to software limitations.

Histological analysis confirmed imaging data and established clear *in vivo* proliferative superiority of the J22-TAC-T cells over the C11-TAC-T cells (Figure 5.5). In spleens and bone marrow, J22-TAC-T cell infiltration peaked around day 3 and started subsiding by day 7 (Figure 5.5A). In the spleen, the T cells were mostly found in the perivascular areas, whereas in the bone marrow, they were scattered (noted by the blinded pathologist; Figure 5.5C). In contrast, we observed continued expansion of the J22-TAC-T cells in the liver at day 7. The C11- and the cMyc-TAC-T cells were rarely found in the liver (Figure 5.5A,C) and were likely just passing through this tissue. The J22-TAC-T cells presented as small perivascular aggregates in some portal tracts in the liver and were more prevalent in the samples collected at a later time point (noted by the blinded pathologist; Figure 5.5A,C).

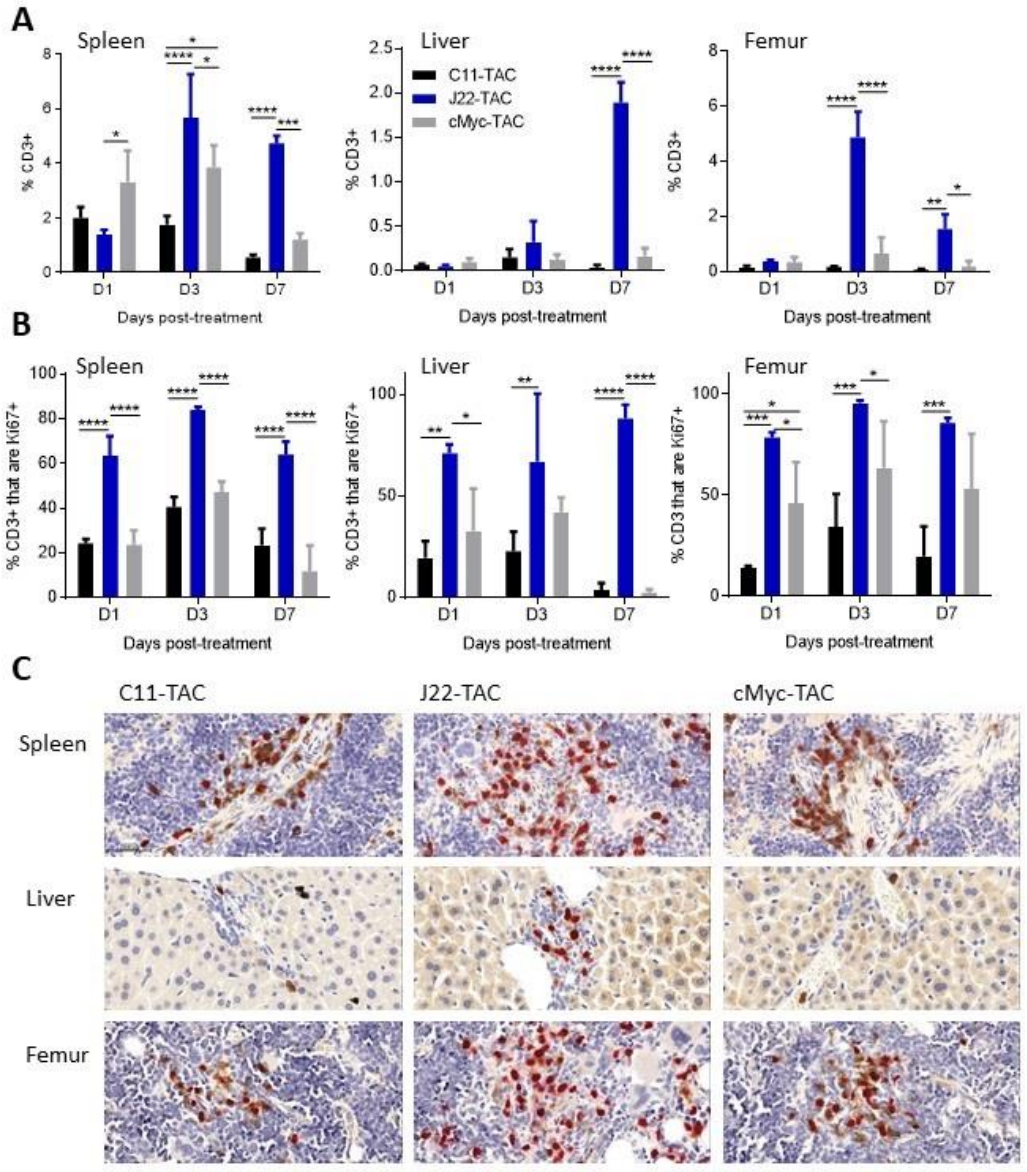

Figure 5.5. J22-TAC-T cells demonstrate robust *in vivo* proliferation. KMS-11 tumor-bearing NRG mice were treated with 4 x 10^6 of TAC^+ cryopreserved T cells i.v. on day 12 post-tumor injection, n = 3 mice per group. Spleens, livers, and femurs were harvested on days 1, 3, and 7 post-treatment. Tissues were fixed, femurs were decalcified, and tissue sections were stained with antibodies targeting human CD3 and Ki67. Images were scanned with the Aperio system at a 40x magnification. (A, B) $CD3^+$ and $Ki67^+$ cells were counted using HALO software v3.2.1851.299 after drawing annotations around each tissue piece and excluding regions of folded tissue. Multiplex IHC v2.1.1 module was used to develop a cellular detection algorithm for each tissue, which was then used across all slides to reduce inter-slide variability. Quantification data of T cell infiltration (A) and T

cell proliferation (B) were analyzed using Prism v.8. Mean and SD are shown. Statistical significance was determined with 2-way ANOVA, followed by Tukey's test. (C) Representative images of the T-cell infiltrate of tissues harvested on day 3 post-treatment. Stains show nuclei (blue), human CD3 (brown), and Ki67 (magenta).

Although the total number of C11-TAC-T cells in the collected tissues did not increase over the time of the experiment (Figure 5.4A), the proliferating fraction of T cells grew by 67% in the spleen and by 140% in the bone marrow between days 1 and 3 post-treatment (Figure 5.4B) and then contracted by day 7. Control cMyc-TAC-T cells had a similar increase in proliferation in the spleen between days 1 and 3, but retained fairly constant levels of proliferation in the bone marrow (Figure 5.4B). These observations suggest that the response of the C11-TAC-T cells in the bone marrow was likely driven by the antigen, but any cell gains from proliferation were probably offset by the activation-induced cell death. The J22-TAC-T cells were significantly more proliferative than the C11- and the cMyc-TAC-T cells (Figure 5.5B), starting from the first measurement time point. The average proportions of proliferating J22-TAC-T cells were higher in the bone marrow, compared to spleen and liver. Moreover, the J22-TAC-T cells remained highly proliferative at the last time point measured.

Considering the sizeable *in vivo* proliferative response of the J22-TAC-T cells, we were surprised by the visible absence of toxicity signs, based on the overall appearance and behavior of mice. We also evaluated weight and core body temperature of the J22-TAC-treated mice and observed no difference, when compared to control mock-treated mice (Figure 5.6).

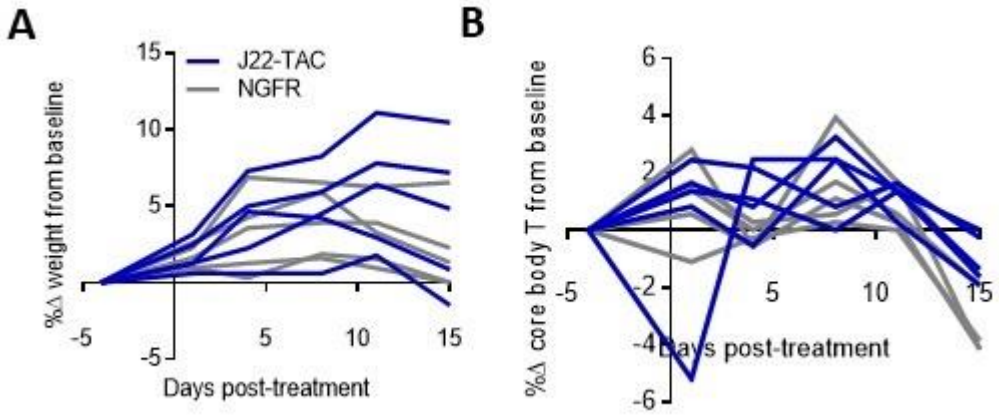

Figure 5.6. J22-TAC-T cell-treated mice do not show signs of toxicity. KMS-11 tumor-bearing NRG mice were treated with 4 x 10^6 of TAC^+ cryopreserved T cells i.v. on day 12 post-tumor injection, n = 5 mice per group. Weights *(A)* and core body temperatures *(B)* were monitored and compared to baseline readings before treatment.

Discussion

In Chapters 3 and 4, we described the process of optimizing fully human BCMA-specific TAC constructs that would form the basis for downstream clinical studies. The murine scFvs used in this chapter, are less attractive for clinical therapeutic applications due to the potential of human anti-mouse responses. These scFvs, however, provide an interesting system for studying broader questions of the impacts of the antigen-binding domains on engineered T cell function beyond the intended target antigen recognition.

At the manufacturing level, both the C11- and the J22-TAC constructs were expressed well on the T cell surface, although the J22-based receptors displayed slightly better expression on CD8 T cells. Interestingly, the J22-TAC-T cell cultures expanded better than the C11-TAC-T cell cultures. Tonic receptor activation or CD4/CD8 distribution could not explain this differential expansion because there was no difference in baseline cytokine production, proliferation, or CD4/CD8 ratios between the C11- and the J22-TAC-T cell cultures. Differences in TCR signaling are known to impact the effector and memory pathways[348]. It is possible that the interactions of the J22-TAC with TCR affect the overall effector and memory cell distribution in the growing culture, promoting a higher proportion of effector cells. A more effector-like phenotype of the J22-TAC-T cells would explain higher proportion of cells secreting TNF-α upon stimulation. The starting point for testing this hypothesis would be to assess the effector/memory state of the J22- and the C11-TAC-T cell cultures at the end of the manufacturing period.

Even if the J22-TAC-T cell culture had a higher fraction of effector cells, it still did not proliferate *in vitro* in the absence of stimulation, similarly to the C11-TAC-T cell culture. Thus, the robust *in vivo* proliferative response of the J22-TAC-T cells in the absence of tumor would still require a stimulus. It is notable that the group evaluating 4-1BBζ CAR-T cells carrying the same murine J22.9-based scFv also observed "faster" *in vivo* expansion, compared to the analogous CAR-T cells with a humanized J22.9 scFv, but they did not investigate why it was faster[343].

Another group testing CD28ζ CAR-T cells carrying the J22.9-FSY scFv quantified T cell load in blood and bone marrow by flow cytometry on days 6 and 13 post-infusion[342]. In these experiments, the J22.9-FSY-CAR-T cell load in blood increased from day 6 to 13 and was substantially higher than the control CAR-T cell load in blood on day 13. The bone marrow J22.9-FSY-CAR-T cell numbers decreased from day 6 to 13 and did not differ from the numbers of control CAR-T cells measured in bone marrow at either of the time points. Although there was no proliferation-specific stain in their panel, the authors interpreted the increase in the J22.9-FSY-CAR-T cell numbers in blood as evidence of antigen-driven expansion. The experiments were performed in the MM.1S xenograft model and the authors detected $CD138^+$ MM.1S cells in the bone marrow by flow cytometry. The observation that the J22.9-FSY-CAR-T cells expanded in blood, but not the bone marrow, suggests that maybe the expansion was independent from the tumor. Additional studies with tumor-free mice with proliferation-specific markers would need to be done to clarify this. Hematoxylin and eosin stains of lung, liver, and

colon 6 days post-treatment did not show any suspicious infiltrates and serum chemistry analysis on days 1 and 3 did not indicate evidence of organ damage. Overall, the observations in the J22.9-FSY-CAR-T cell paper[342] do not contradict our experience. If the J22.9-FSY-CAR-T cell expansion is proven to be tumor-independent, the observations of non-specific, J22.9 scFv-driven T cell expansion in the absence of overt toxicity would directly align with our results.

In our experience, the cross-reactivity of the J22.9-xi scFv to an unknown murine antigen seems to support *in vivo* expansion and potentially persistence of the functional J22-TAC-T cells. A higher number of the J22-TAC-T cells in the system, compared to the C11-TAC-T cells, would explain why the J22-TAC-T cell-treated mice demonstrated stronger anti-tumor responses. The observation that the C11-TAC-T cells were still efficacious seemingly in the absence of *in vivo* expansion suggests that the treatment dose was high enough to be effective against the initial tumor. The idea that receptor cross-reactivity in the absence of toxicity might prolong anti-tumor efficacy is attractive because the field of T cell engineering is very limited by the ability to find tumor-specific targets. Of course, the nature of this cross-reactivity needs to be carefully examined for each receptor with such potential to evaluate if the accompanying toxicities are truly absent and if not, then to what extent.

Finally, our previous experience with a cross-reactive antigen-binding domain in a different tumor model indicates that TAC-T cells are less likely to be toxic than second-generation CAR-T cells[255]. These observations warrant further

studies into whether the J22.9-xi domain could be more toxic when used on a different receptor scaffold, which is investigated in Chapter 6.

Chapter 6

Evaluation of the effects of a cross-reactive antigen-binding domain on the efficacy of second-generation CAR-T cells

Introduction

As discussed in Chapter 1, section 3.3.4, most CAR-T cells constructs tested in the clinics are second-generation designs with a CD28 or a 4-1BB co-stimulatory domain in the intracellular part of the receptor[214]. Although both of these domains serve the purpose of co-stimulation, the functional differences observed between the CD28ζ and the 4-1BBζ CAR-engineered T cells have inspired investigations into the underlying mechanisms of these differences.

In preclinical studies, the CD28ζ CAR-T cells mount a faster *in vivo* response and lead to better anti-tumor efficacy at limiting doses, when compared to the 4-1BBζ CAR-T cells[349]. The CD28ζ CAR-T cells have also been characterized as less persistent *in vivo* than the 4-1BBζ CAR-T cells[350]. The reduced persistence has been linked to a more differentiated effector memory phenotype and glycolytic metabolic profile of the CD28ζ CAR-T cells, compared to the central memory phenotype, oxidative metabolism, and mitochondrial biogenesis attributed to the 4-1BBζ CAR-T cells[350]. The CD28 co-stimulatory domain has also been implicated in exacerbation of exhaustion due to tonic CAR signaling, compared to the 4-1BB co-stimulatory domain[238]. Ramello and colleagues provided immunoproteomic evidence for this tonic signaling and showed baseline phosphorylation of the ζ domain of the CAR and association of the CAR construct with a separate, phosphorylated ζ chain[351].

Gene expression analysis reveals that antigen stimulation leads to stronger upregulation of effector genes in the CD28ζ CAR-T cells, while the 4-1BBζ CAR-T cells are more likely to upregulate genes involved in T cell quiescence and memory[352]. The CD28ζ CAR-T cells also have lower baseline levels of anti-apoptotic proteins Bcl-1 and Bcl-X_L, and this difference in the pro-survival program between the CD28ζ CAR-T cells and the 4-1BBζ CAR-T cells further intensifies post-stimulation[352].

Phosphoproteomic studies[353] echo the observations of a more rapid response by the CD28ζ CAR-T cells that was detected in the *in vivo* analysis mentioned above. Salter and colleagues argue that the more effector-like phenotype of the CD28ζ CAR-T cells is driven by the faster and stronger phosphorylation of the same signaling intermediates that the 4-1BBζ CAR construct activates (e.g. ZAP-70, CD28, PLC-γ, SLP-76, LSP-1, TRAF-2, and Bcl-10)[353]. In this set of experiments, faster activation of the CD28ζ CAR-T cells was associated with more cells producing IFN-γ, TNF-α, and IL-2 *in vitro*, and inferior *in vivo* performance, compared to the 4-1BBζ CAR-T cells.

Results of the clinical studies where each receptor was tested individually align with the preclinical observations of a faster response by the CD28ζ CAR-T cells. The CD28ζ CAR-T cells reach peak *in vivo* proliferation earlier than the 4-1BBζ CAR-T cells, but do not persist for as long as the 4-1BBζ CAR-T cells[210, 211, 354, 355]. A small-scale study in which the patients were infused with a 1:1 mixture of the CD28ζ and the 4-1BBζ CAR-T cells showed peak expansion of the CD28ζ

CAR-T cells on day 9 and peak expansion of the 4-1BBζ CAR-T cells on day 13 post-infusion[356]. Another study aimed at comparing the CD28ζ and the 4-1BBζ CAR-T cells showed higher levels of treatment-induced toxicities in the CD28ζ CAR-T cell-treated group, although the number of patients in each treatment group was very low[357].

Our group has previously described a xenograft model of off-target CAR-T cell-mediated toxicity[260]. Our observations of the J22.9-xi scFv recognizing an unknown antigen in the NRG mice (described in Chapter 5) suggested that we might have found another model to study the cross-reactivity of engineered T cells. Considering that the second-generation CAR-T cells are actively used and investigated in the clinics, we decided to characterize the functionality of the J22.9-xi CD28ζ and 4-1BBζ CAR-T cells *in vitro* and *in vivo*. We found that despite phenotypic evidence of exhaustion, the CD28ζ CAR-T cells were equally or more efficacious than the equivalent 4-1BBζ CAR-T cells *in vitro* and *in vivo*. Exhaustion did not impair *in vivo* proliferation or persistence of the CD28ζ CAR-T cells. The CD28ζ CAR-T cells also proliferated as well in tumor-free mice as they did in tumor-bearing mice. Interestingly, the 4-1BBζ CAR-T cells did not show proliferation in tumor-free or tumor-bearing mice beyond what we would expect from a xenoreactive response, although they still led to tumor-clearance and resistance to rechallenge.

Results

Our earlier experience with CAR- and TAC-T cells carrying a cross-reactive antigen-binding domain indicates that CAR-T cells are more likely to be toxic in murine models[255]. Considering the cross-reactivity of the J22.9-xi scFv in our xenograft model, we reasoned that by incorporating it into CAR constructs that lack the sophisticated autoregulation systems of the TCR, we might push the T cell response to become toxic and provide an additional model for understanding toxicities related to cross-reactive antigen binding domains.

We created CD28ζ and the 4-1BBζ CAR constructs with the J22.9-xi scFv in the antigen-binding domain. The CD28ζ CARs were expressed at significantly higher levels in the CD4 T cells and a similar trend was observed in the CD8 T cells (Figure 6.1A). Expansion kinetics varied from donor to donor, and although it seemed that the CD28ζ CAR-T cells were more proliferative earlier in the culture period and the 4-1BBζ CAR-T cells were more proliferative later, the differences were not statistically significant (Figure 6.1B). There was also a trend for the skewing of the CD4/CD8 ratio towards a higher proportion of CD4 T cells in the CD28ζ CAR-T cell culture, but this trend was not significant (Figure 6.1C).

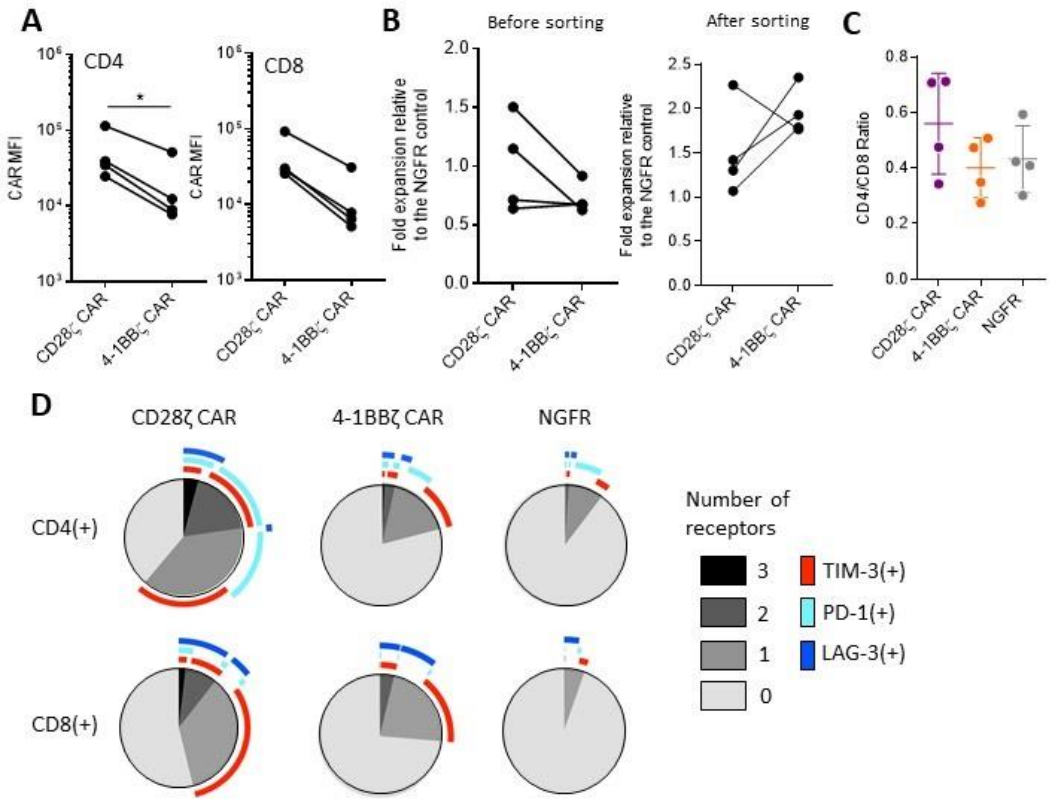

Figure 6.1. J22-CD28ζ CAR-T cells are more exhausted at baseline than J22-4-1BBζ CAR-T cells. (A) Median fluorescence intensity (MFI) of receptor surface expression on transduced cells. Cells were gated on live > singlets > CD4/CD8 > NGFR$^+$. (B) T cell fold expansion before and after NGFR-sorting, normalized to the expansion of the NGFR control-transduced cells. (C) CD4/CD8 ratios at the end of the manufacturing period. Statistical significance was determined with a paired t-test (A,B) or repeated measures ANOVA followed by Tukey's test (C). (D) T cell cultures were stained for PD-1, LAG-3, and TIM-3 surface expression at the end of the 14-day culture period. Plots were gated on live > singlets > CD4/CD8 > NGFR$^+$. Representative images from one donor are shown using a multiparametric SPICE analysis. Data are representative of 3 different donors.

As noted earlier, the expression of checkpoint receptors due to tonic signaling by CARs has been linked to poor performance *in vivo*. Thus, we assessed expression of checkpoint receptors at the end of the manufacturing period in our CAR-T cell cultures (Figure 6.1D). Both types of CAR-T cells were phenotypically more exhausted, compared to control transduced T cells (NGFR). The CD28ζ CAR-

T cells were substantially more exhausted than the 4-1BBζ CAR-T cells with more than half of all CD4 and almost half of all CD8 T cells expressing at least 1 checkpoint receptor. TIM-3 was the most commonly upregulated checkpoint receptor in CD4 and CD8 T cells in both types of CAR-T cells. PD-1 was more commonly elevated on CD4 T cells, whereas LAG-3 was more commonly elevated on CD8 T cells. Moreover, the CD4 T cells in the CD28ζ CAR-T culture had a higher proportion of cells expressing all 3 checkpoint receptors and a noticeable PD-1^{+}TIM-3^{+} population that was substantially larger that the equivalent population in the 4-1BBζ CAR-T culture.

Based on the studies described in literature, the more exhausted phenotype of the CD28ζ CAR-T cells would predict inferior functionality, compared to the 4-1BBζ CAR-T cells[238]. However, this was not the case in our experiments. *In vitro* stimulation with KMS-11 and MM.1S tumor targets revealed very similar ability of the two types of CAR-T cells to produce IFN-γ, TNF-α, and IL-2 (Figure 6.2A,B). The elevated checkpoint receptors on the CD28ζ CAR-T cells suggested underlying tonic signaling[298], so we expected to see background activation in this culture. There was some baseline cytokine production in the CD28ζ and the 4-1BBζ CAR-T cell cultures, which was similar between the two types of CAR-T cells (Figure 6.2C).

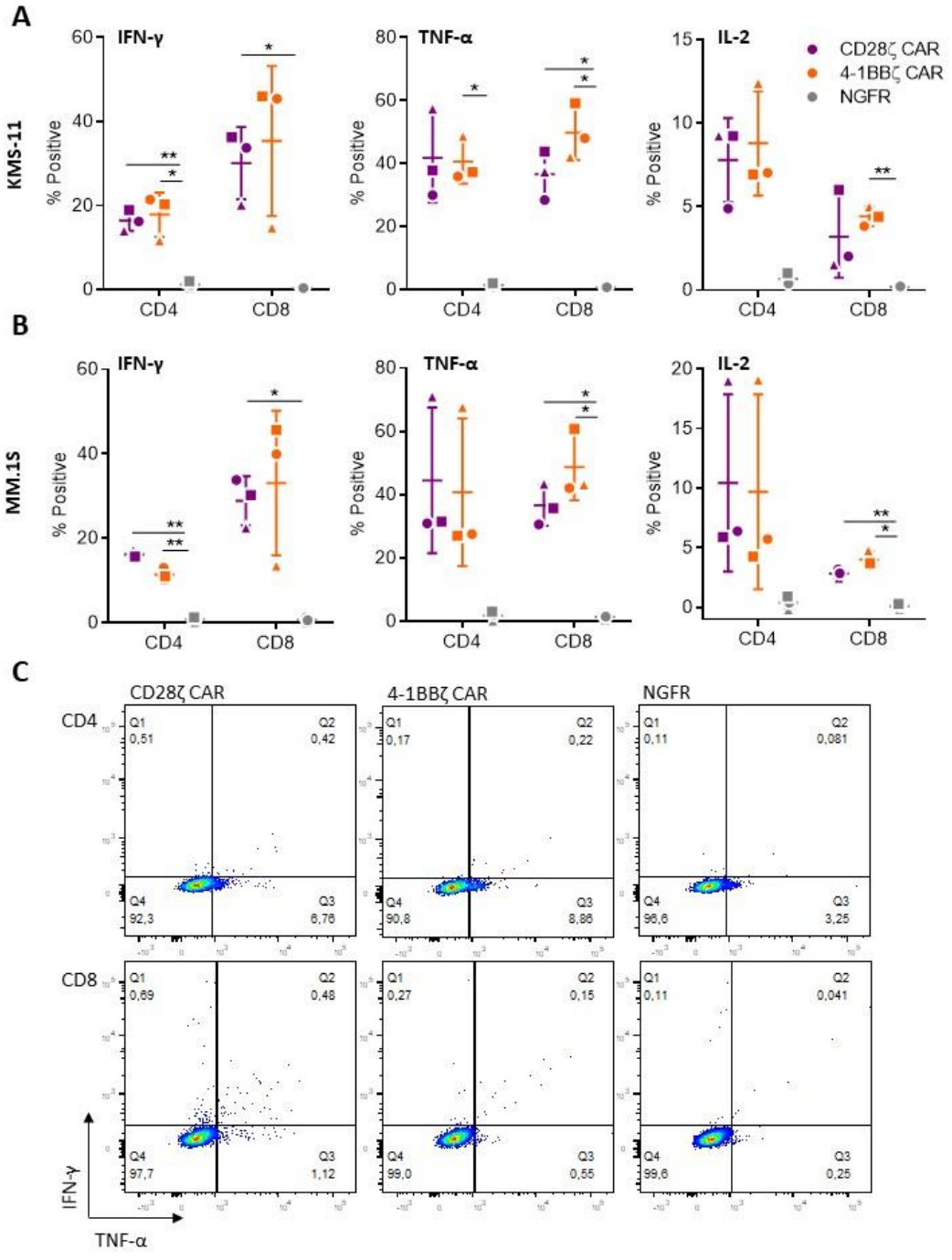

Figure 6.2. J22-CD28ζ and J22-4-1BBζ CAR-T cells have equivalent cytokine production abilities. T cells were stimulated with KMS-11 (A) or MM.1S (B) targets at a 2:1 effector:target ratio or not stimulated (C) for 4 hours in the presence of monensin and brefeldin A, stained for intracellular cytokine expression, and assayed by flow cytometry. Cells were gated on live > singlets > CD4/CD8. (C)

Representative plots of the non-stimulated samples. Statistical significance was determined using repeated measures ANOVA, followed by Tukey's test. Data are representative of 3 different donors with each donor marked by a different symbol.

The CD28ζ CAR-T cells were significantly more cytotoxic towards BCMA-positive tumor cells (Figure 6.3, left and middle panels). Cytotoxicity was in response to BCMA expression on myeloma cells (KMS-11 and MM.1S), and no differences in baseline cytotoxicity were observed against BCMA-negative Jurkat cells (Figure 6.3, right panel). In the proliferation analysis, both types of CAR-T cells proliferated equally well in response to BCMA-positive tumor targets (Figure 6.4A). Moreover, proliferating CD4 and CD8 T cells in the J22-CD28ζ and the J22-4-1BBζ CAR-T cell cultures survived equally well, as evidenced by the cell counts at the end of the proliferation assay (Figure 6.4B).

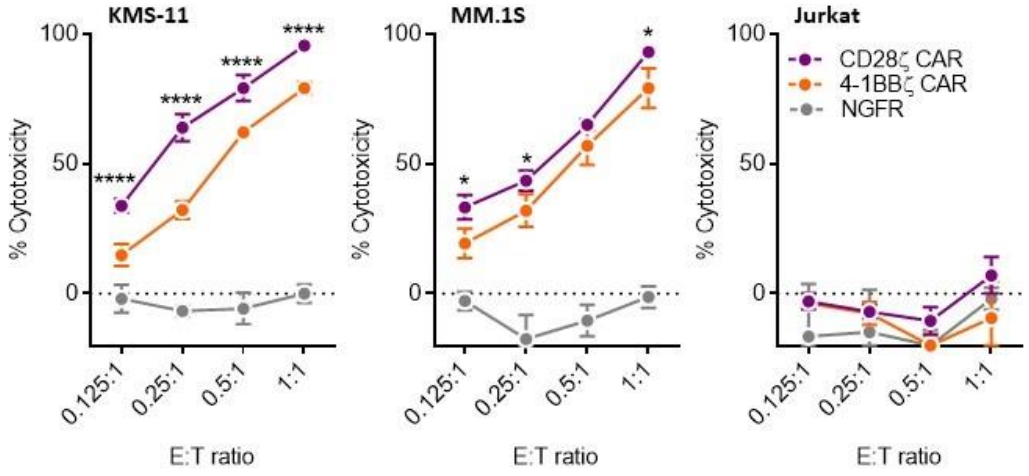

Figure 6.3. J22-CD28ζ CAR-T cells are more cytotoxic than J22-4-1BBζ CAR-T cells. T cells were incubated with firefly luciferase-expressing BCMA-positive KMS-11 and MM.1S targets or BCMA-negative Jurkat targets for 9 hours at indicated effector:target ratios. Luminescence was read with an open filter upon addition of 0.15 mg/mL D-luciferin substrate and converted to % cytotoxicity.

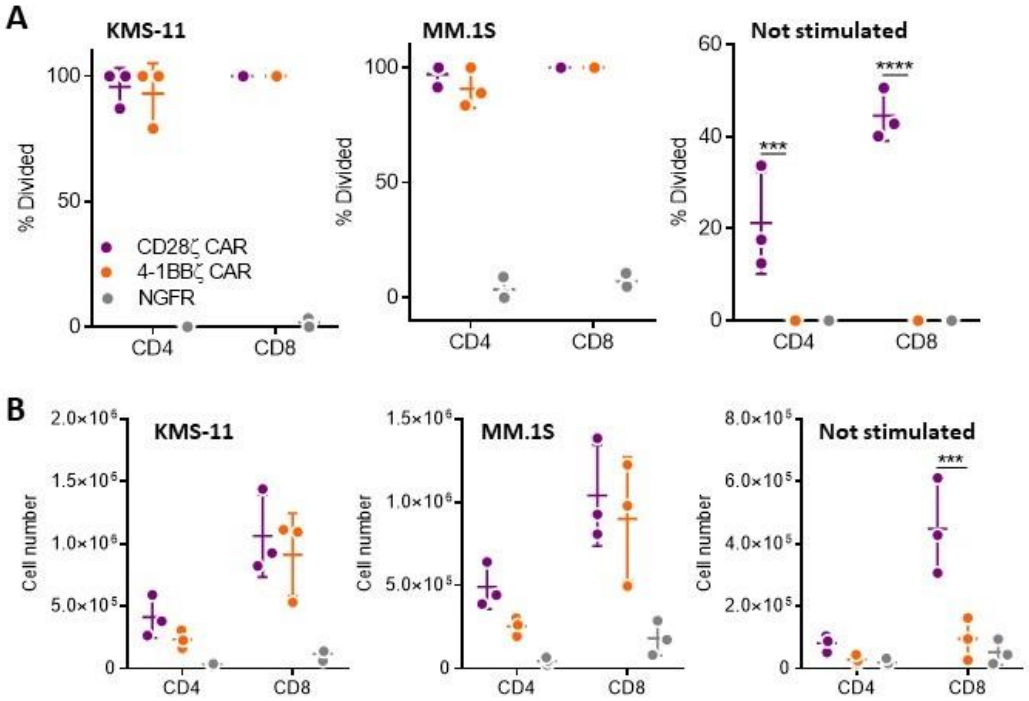

Figure 6.4. J22-CD28ζ and J22-4-1BBζ CAR-T cells show equivalent antigen-driven proliferation despite higher baseline activation of J22-CD28ζ CAR-T cells. T cells were labelled with CellTrace Violet dye, stimulated with KMS-11 or MM.1S tumor targets at an effector:target ratio 2:1 for 4 days and assayed by flow cytometry. Samples were gated as singlets > live > $CD138^-$ > CD4/CD8 > $NGFR^+$. Percent divided (A) and total cell numbers at the end of the assay (B) are shown. Data are representative of 3 donors. Statistical significance was determined with ANOVA followed by Tukey's test.

Among the three *in vitro* functional assays (cytokine production, cytotoxicity, and proliferation), baseline activation of the CD28ζ CAR-T cell culture was the most evident in the proliferation assay. Both CD4 and CD8 CD28ζ CAR-T cells proliferated significantly in the absence of antigen stimulation, whereas the 4-1BBζ CAR-T cells did not proliferate in the absence of stimulation (Figure 6.4A, right panel). The CD8 CD28ζ CAR-T cells significantly outnumbered

the CD8 4-1BBζ CAR-T cells at the end of the assay in the absence of antigen stimulation (Figure 6.4B, right panel).

Our *in vitro* functional data indicated that tonic activation did not impair antigen-driven functionality of the CD28ζ CAR-engineered T cells, but we wanted to see if this would still be the case *in vivo*. To assess effectiveness and durability of anti-tumor responses, we treated mice bearing established, disseminated tumors with a single dose of CAR-T cells and then rechallenged mice in remission with a new dose of tumor 2 months after the original treatment. Based on the tumor-tracking studies in the KMS-11 and MM.1S xenograft tumor models, CD28ζ CAR-T cells exhibited excellent tumor control in 100% of the mice (Figure 6.5A,B). 4-1BBζ CAR-T cells had similar tumor control in the KMS-11 model, although 1 mouse had a delayed response to the treatment and another mouse failed to resist tumor rechallenge (Figure 6.5A). In the MM.1S model, 4-1BBζ CAR-T cell-treated mice had inferior response to treatment, compared to the CD28ζ CAR-T cell-treated mice, although 1 mouse seemed to have a low tumor burden at the time of rechallenge, which grew, but did not impair survival upon rechallenge (Figure 6.5B,C). Upon rechallenge, all of the CD28ζ CAR-T cell-treated and most of the 4-1BBζ CAR-T cell-treated mice still had effective tumor control, but suffered from exacerbation of the GVHD (symptoms included poor body condition, hunched posture, pale skin, and low activity) and had to be euthanized shortly after rechallenge (Figure 6.5C).

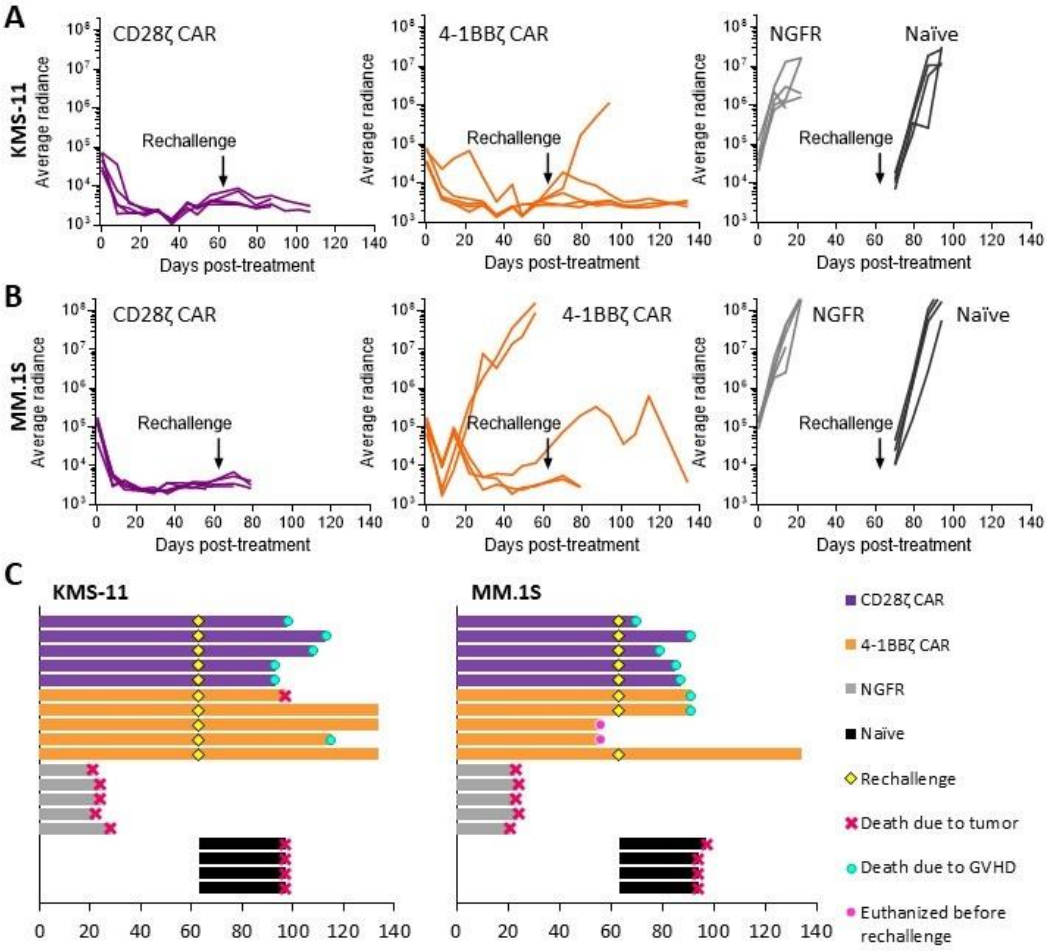

Figure 6.5. Comparison of *in vivo* efficacy of the J22-CD28ζ and J22-4-1BBζ CAR-T cells. NRG mice carrying luciferase-expressing KMS-11 (A) or MM.1S (B) tumors were treated with 2 x 10^6 (A) or 4 x 10^6 (B) of CAR^+ cryopreserved T cells i.v. on day 12 post-tumor injection. Surviving, tumor-free mice were rechallenged with 1 x 10^6 KMS-11 (A) or MM.1S (B) tumor cells i.v. 63 days post-treatment. Tumor signal was monitored by imaging mice after i.p. injection of D-luciferin, 150 mg/kg. Dorsal and ventral average (p/s/cm²/sr) signals were added for each mouse to calculate total tumor burden. N = 5 mice per group (C) Survival data for the mice in (A) and (B).

We also conducted bioluminescence experiments tracking T cell burden in tumor-free and tumor-bearing mice and *in vitro* proliferation studies to further characterize potential toxicities. NGFR-transduced T cells were used as a control and showed xenoreactivity-driven T-cell expansion in tumor-bearing and tumor-

free mice (Figure 6.6). Despite expressing high levels of checkpoint receptors, the CD28ζ CAR-T cells had a very strong proliferative response *in vivo* immediately after infusion and continued to expand for the two months the experiment was monitored (Figure 6.6). The kinetics of the CD28ζ CAR-T cell proliferation were the same, irrespective of the tumor presence. The 4-1BBζ CAR-T cells did not proliferate in the KMS-11 model until approximately 20 days post-infusion (Figure 6.6A). In the MM.1S model, there was a brief expansion of the 4-1BBζ CAR-T cells immediately post-infusion, which quickly subsided and was then followed by a slower expansion phase, similar to that observed in the KMS-11 model (Figure 6.6B). In the tumor-free mice, the 4-1BBζ CAR-T cells did not expand over the course of the follow-up (Figure 6.6C).

Survival monitoring of the mice bearing luciferase-expressing T cells showed that 4/5 of the CD28ζ CAR-T cell-treated mice in the KMS-11 group succumbed to GVHD, while the fifth mouse exhibited GVHD symptoms that had not reached endpoint at the end of the experiment (Figure 6.7, left panel). In the 4-1BBζ CAR-T cell-treated group of the KMS-11 arm of the study, 1 mouse died from tumor burden, 1 mouse died from GVHD, and two surviving mice were showing GVHD symptoms at the end of the study (Figure 6.7, left panel). In the MM.1S arm of the study, the CD28ζ CAR-T cells were more efficacious than the 4-1BBζ CAR-T cells, all of which died from tumor progression (Figure 6.7, right panel). While all of the CD28ζ CAR-T cell-treated mice in the MM.1S arm were alive at the end of the study, all of them were starting to exhibit GVHD symptoms.

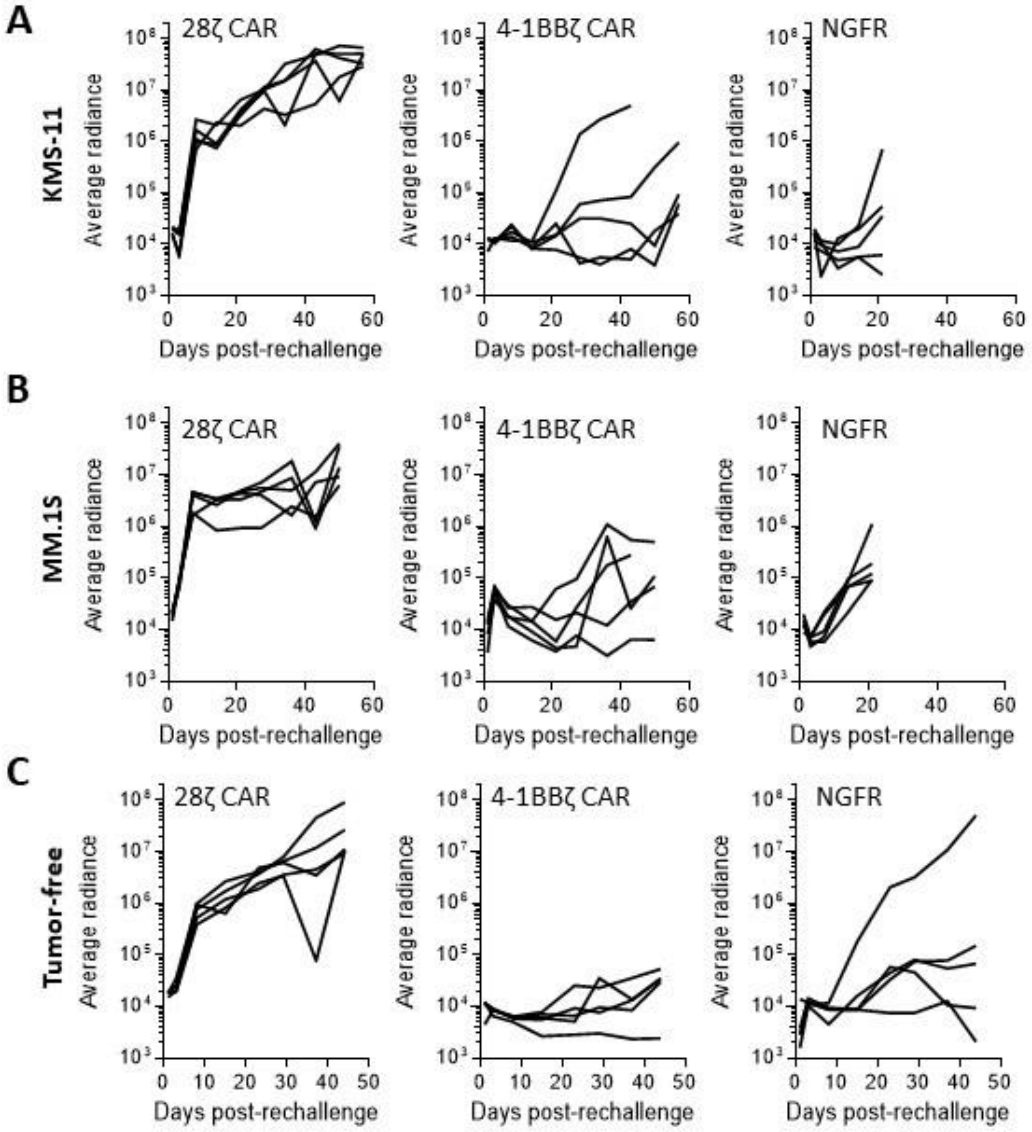

Figure 6.6. *In vivo* proliferation of the J22-CD28ζ and the J22-4-1BBζ CAR-T cells. NRG mice carrying KMS-11 (A) or MM.1S (B) tumors or tumor-free mice (C) were treated with 2 x 10^6 of luciferase-expressing CAR^+ cryopreserved T cells i.v. on day 12 post-tumor injection. T cell signal was monitored by imaging mice after i.p. injection of D-luciferin, 150 mg/kg. Dorsal and ventral average (p/s/cm²/sr) signals were added for each mouse to calculate total T cell burden. N = 5 mice per group.

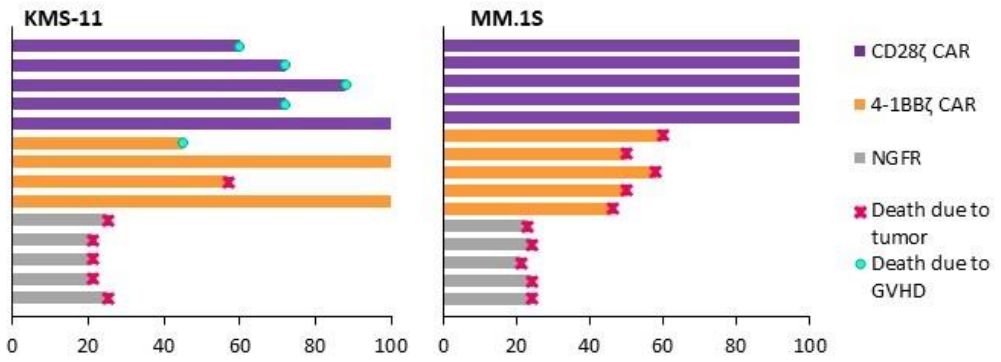

Figure 6.7. Survival data for mice treated with the J22-CD28ζ and the J22-4-1BBζ CAR-T cells. Mice from the experiment described in Figure 6.6 were monitored for survival. N = 4-5 mice per group.

The rapid expansion of the CD28ζ CAR-T cells in tumor-free and tumor-bearing mice was consistent with our observation in Chapter 5 where TAC-T cells carrying the J22.9-xi scFv responded to an unknown antigen leading to proliferation in tumor-bearing and tumor-free mice. In an effort to identify the tissue carrying the unknown cross-reactive antigen, we checked the ability of different mouse tissues to stimulate proliferation of the CD28ζ and the 4-1BBζ CAR-T cells carrying the J22.9-xi scFv in the antigen-binding domain (Figure 6.8A). The mice had been perfused with saline prior to tissue collection to eliminate murine blood cells from the tissues. Compared to the non-stimulated sample, the CD28ζ CAR-T cells seemed to have enhanced proliferation when stimulated with murine blood, although this enhancement did not reach the level of proliferation observed in response to KMS-11 and MM.1S cells. Spleen (with and without red blood cells) and lung cell samples led to the same amount of the CD28ζ CAR-T cell proliferation as observed at baseline. Murine cells from other tissues seemed to

diminish baseline proliferation of the CD28ζ CAR-T cells. The 4-1BBζ CAR-T cells did not proliferate in response to any of the murine cells tested (Figure 6.8A), which was consistent with the *in vivo* T cell tracking data (Figure 6.6).

Although BCMA is regarded as a B cell-specific molecule[124], it can also be expressed by plasmacytoid dendritic cells[358]. We would not expect B cells to be present in our immunodeficient mice, but to control for other potential sources of murine BCMA in the *in vivo* system, we checked whether murine BCMA could stimulate proliferation of the J22-CD28ζ CAR-T cells (Figure 6.8B). We used beads coated with murine or human BCMA-Fc as stimulation targets to ensure that only receptor-antigen interactions were present in the system. Considering that the CD28ζ CAR-T cells proliferate in the absence of stimulation, we included J22-TAC-T cells as a control group that is known to have no baseline proliferation and proliferate in response to beads coated with human BCMA-Fc. Stimulation with murine BCMA only slightly enhanced proliferation of the TAC and CD28ζ CAR-T cells, which was not comparable to proliferation triggered by human BCMA. Considering the magnitude of *in vivo* proliferation in the absence of BCMA-positive tumors, murine BCMA potentially present in mice is unlikely to be the target of cross-reactivity.

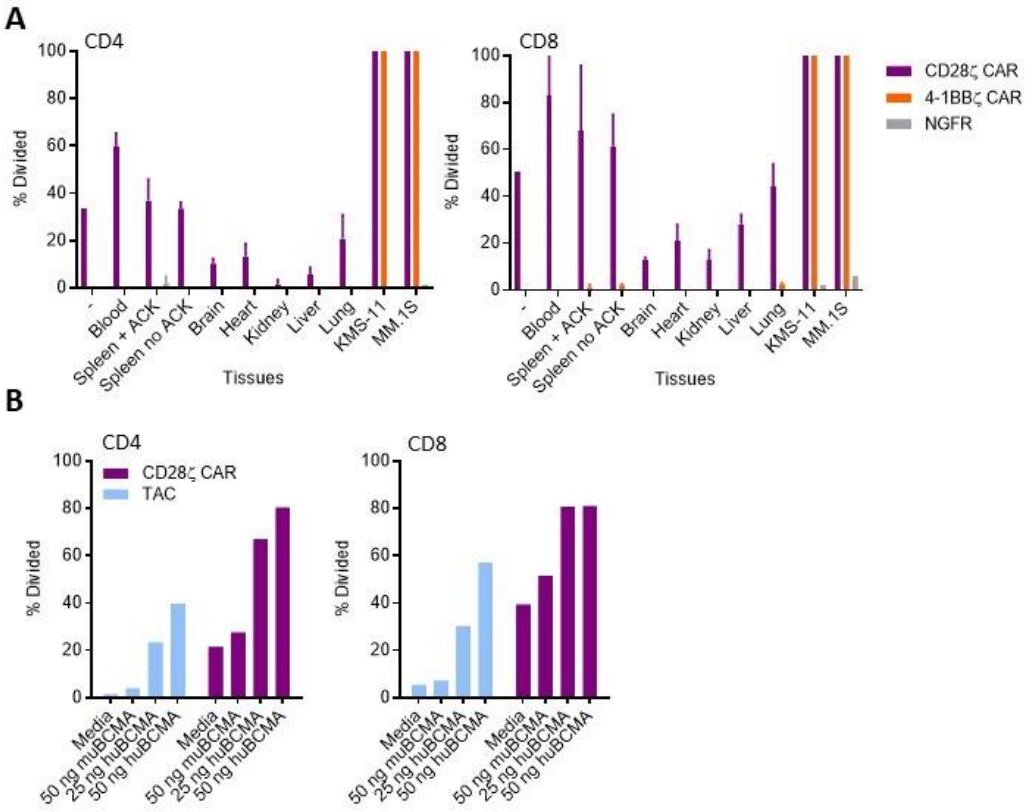

Figure 6.8. Antigen-independent proliferation of T cells engineered with the J22.9-xi scFv-containing receptors. (A) 3 naïve NRG mice were perfused and indicated tissues were collected and processed in a single-cell suspension. T cells were labelled with CellTrace Violet dye, stimulated with mouse cells or KMS-11 and MM.1S tumor targets at an effector:target ratio 1:1 for 4 days and assayed by flow cytometry. Samples were gated as singlets > live > $CD138^-$ > CD4/CD8 > $NGFR^+$. Mean and SD of percent divided are shown. (B) T cells were stimulated with protein G beads coated with the indicated amounts of human or murine BCMA-Fc (ng per 10^6 beads) at a 1:1 effector:target ratio. T cells were labeled and analyzed as in (A). Data are representative of 1 donor.

Discussion

The choice of the co-stimulatory domain for a CAR construct is important because it can influence the differentiation state of the resulting T cell culture, affect the activation threshold necessary for the activation of CAR-T cells, impact their functionality post-activation, and ultimately determine the overall efficacy of the engineered T cell product[359].

The post-manufacturing features of our J22 CAR-T cell cultures are in line with literature reports. The CD28ζ CAR-T cells showed a trend for a bias towards CD4 T cells, which likely stems from tonic signaling by the CAR. CD28 co-stimulation is not very effective at facilitating long-term proliferation and survival of CD8 T cells[360], whereas 4-1BB co-stimulation is more efficient at expanding CD8 T cells[361]. We also observed higher receptor levels on the CD28ζ CAR-T cells, compared to the 4-1BBζ CAR-T cells. Although we did not check the copy number of the transgene in our CAR-T cell cultures, it is possible that the higher receptor levels in the CD28ζ CAR-T cell culture were a result of the elevated proliferation rate early post-activation, since the lentiviral transduction depends on the proliferative state of T cells[362].

Several groups have noted tonic activation of the CD28ζ and the 4-1BBζ CAR-T cells typically characterized by the expression of exhaustion markers PD-1, TIM-3, and LAG-3[238, 298, 299]. Based on the phenotypic analysis of expression of

checkpoint receptors, we also saw that our CAR-T cell cultures, particularly the CD28ζ CAR-T cells, were exhausted.

Curiously, despite phenotypic signs of exhaustion, the CD28ζ CAR-T cells were not functionally impaired. They were as efficient at producing cytokines and more cytotoxic *in vitro*, compared to the 4-1BBζ CAR-T cells. Higher *in vitro* cytotoxicity suggests that the CD28ζ CAR-T cells were more effector-like, as reported by other groups[350, 352]. Although only a small fraction of the CD28ζ CAR-T cells produced cytokines in the absence of antigen stimulation, a fairly large proportion of the CD28ζ CAR-T cells proliferated in the absence of stimulation, providing evidence that a large fraction of these T cells were manifesting tonic signaling. Tonic signaling and the associated checkpoint receptors did not impede *in vivo* proliferation or efficacy of the CD28ζ CAR-T cell product. However, we do not know if the CD28ζ CAR-T cells that proliferated and carried out *in vivo* anti-tumor response were the same cells that were phenotypically exhausted or a smaller proportion of cells that did not express checkpoint receptors and likely retained less differentiated phenotype. To answer this question in the future, we will flow-sort exhausted and non-exhausted T cells and repeat the functional studies. Since TIM-3 was elevated in the majority of the CD28ζ CAR-T cells that expressed one or more checkpoint receptor, it would be a good candidate for the sorting marker.

In vitro, there was a substantial difference between the percentage of CD28ζ CAR-T cells that proliferated in the presence and the absence of antigen. *In vivo*, the T cell proliferation kinetics for this CAR-T cell product were virtually

indistinguishable, suggesting that the cross-reactivity of the J22.9-xi scFv provided a proliferation boost to the CD28ζ CAR-T cells. It is interesting that the 4-1BBζ CAR-T cells had a very different *in vivo* proliferative response, despite carrying the same antigen-binding domain. A model of tonic 4-1BBζ CAR-T cell signaling has revealed that chronic stimulation through the 4-1BBζ CAR exacerbated by high receptor levels can lead to high rates of apoptosis and impair 4-1BBζ CAR-T cell proliferation[299]. It is possible that tonic stimulation due to the J22.9-xi scFv cross-reactivity created a similar scenario in our model, and bioluminescence imaging showed lack of expansion due to high rates of *in vivo* apoptosis of the 4-1BBζ CAR-T cell that offset proliferation. Isolating CD28ζ and 4-1BBζ CAR-T cells post-treatment, followed by intracellular staining for cleaved caspase-3 (marker of apoptosis) and Ki67 (marker of proliferation) should give us a better idea of the rates of *in vivo* proliferation/apoptosis between the two J22 CAR-T cell cultures.

Stronger *in vivo* proliferation of the CD28ζ, compared to the 4-1BBζ CAR-T cells, suggests that there were more functional T cells present at the moment of rechallenge in the CD28ζ CAR-T cell group. This would explain why the mice in the CD28ζ CAR-T cell-treated cohort experienced faster and more severe GVHD following rechallenge. Similarly, in the study where the KMS-11 tumor-bearing mice were followed without rechallenge, a higher proportion of the CD28ζ CAR-T cell-treated mice succumbed to GVHD, which likely indicates that there were more active T cells present in these mice. In our experience, the MM.1S model is harder to treat, so the fact that the CD28ζ CAR T cell-triggered GVHD was less severe in

the MM.1S model suggests that the anti-tumor response might have reduced the number of active T cell in the MM.1S tumor-bearing mice, compared to the KMS-11 tumor-bearing mice.

In our *in vivo* T cell proliferation and anti-tumor efficacy studies, neither tonic signaling in the CD28ζ CAR-T cell product nor cross-reactivity of the antigen-binding domain impaired T cell performance. In fact, the CD28ζ CAR-T cells were more potent than the 4-1BBζ CAR-T cells *in vivo*, in the absence of obvious early post-treatment toxicities that might stem from a cross-reactive antigen-binding domain. This suggests that non-toxic cross-reactivity might be advantageous in supporting engineered T cell expansion and persistence, increasing the durability of anti-tumor response.

The question of off-target toxicity is important, particularly as the field expands to include novel targets and binders. Our *in vitro* proliferation analysis did not point to any specific organs as the targets for the J22.9-xi scFv, but suggested that blood cells might be involved in supporting proliferation of the CD28ζ CAR-T cells. To ensure that the vital organs are not impacted by the J22.9-xi scFv cross-reactivity, we are testing serum of the CD28ζ and 4-1BBζ CAR-treated mice for markers of organ damage and conducting a full-body necropsy, accompanied by the CD3 and Ki67 staining. We also need to repeat stimulation with murine blood cells as targets and engineered T cells from a different donor as effectors. If murine blood cells enhance proliferation of the J22.9-xi-CD28ζ CAR-T cells, then we can

try sorting blood cells into different lineages to further narrow down the target of the cross-reactivity.

Chapter 7

Discussion

The experimental work described in this thesis encompasses two main directions: 1) optimization of a fully human BCMA-specific TAC receptor for subsequent clinical testing against multiple myeloma and 2) assessment of a cross-reactive antigen-binding domain in the context of different synthetic receptor frameworks used in T cell engineering. Thus, the implications of our work discussed in this chapter are organized according to the two directions of the research findings.

1. Optimization of a fully human BCMA-specific TAC receptor

1.1. Summary of findings

The TAC was designed to function as an accessory receptor that engages with the TCR-CD3 complex and allows the T cells to respond to a target of choice through the natural T cell activation pathways. Thus, the CD3 recruitment domain is key to the functionality of TAC. Our original design featured a murine UCHT1 scFv as the CD3-binding domain of TAC, which was chosen based on superior performance, compared to other CD3ε-binding scFvs[255]. Since the goal of the TAC platform is generation of clinically relevant therapeutic products, and immune response to synthetic receptors with murine components has been documented in literature[326, 327], we wanted to develop a completely humanized TAC.

In Chapter 3, we evaluated two humanized variants of the UCHT1 scFv, both of which bound CD3ε stronger than the original murine UCHT1. We ultimately chose the huUCHT1(YT) variant based on its favorable *in vitro* and *in*

vivo profile. In the process of UCHT1 optimization, we discovered that the CD8α signal sequence led to higher TAC surface expression than the IgK signal sequence. Higher TAC surface expression resulted in stronger binding to BCMA-positive targets and faster maturation of the immunological synapse but did not alter long-term *in vitro* or *in vivo* functional performance of TAC-T cells.

In Chapter 4, we compared several humanized BCMA-specific scFvs in the antigen-binding domain of TAC and chose a variant of the TRAC 3625 scFv that had the V_L-V_H orientation and a G4S linker between the BCMA-specific scFv and the CD3ε-specific scFv. TAC-T cells carrying the fully humanized TAC receptors with the TRAC 3625 antigen-binding domain showed excellent *in vivo* efficacy against disseminated MM xenografts and a favorable cytokine secretion profile.

1.2. Implications for the TAC platform

The work described in Chapter 3 serves as the basis for our future modifications to the TAC-T cell platform and broadens our understanding of how receptor expression levels impact performance of TAC-T cells. A fully humanized TAC scaffold can now be applied in constructs targeting other molecules beyond BCMA and other tumor types beyond MM. The solid tumor field, particularly, has not yet seen much success with engineered T cell therapies and represents a large unmet need, where the optimized TAC scaffold can potentially provide therapeutic benefit. Indeed, the outcomes of these experiments informed the design of two TAC

T cell products that are currently in clinical trials for $CD19^+$ and $HER2^+$ malignancies (NCT03880279 and NCT04727151).

The work described in Chapter 4 brings us closer to testing BCMA-TAC-T cells clinically. As such, it is important to consider the assays and models that might aid in further evaluation of the behaviour of the clinical-grade TAC-T cell products and the factors that may affect their performance in humans. For instance, in the clinical trials with CAR-T cells, some patients will receive T-cell products that do not meet all release criteria on compassionate grounds and some patients will not receive the treatment due to manufacturing challenges[210, 211, 218, 354, 363]. Thus, optimizing the manufacturing process is key to successful clinical translation. One strategy for ensuring successful manufacturing of the engineered T cell products has been to select patients who meet defined absolute lymphocyte count or CD3 count (in blood) criteria[364]. MM patients are often lymphopenic[365], and drugs such as daratumumab and bortezomib used in the common treatment regimes can further contribute to lymphopenia[366, 367]. Thus, at the clinical level, strategic timing of the apheresis for the TAC-T cell manufacturing with respect to the chemotherapy schedule might aid downstream manufacturing. Ideally, blood would be collected from patients when they are first diagnosed with MM but this may be impractical. In partnership with the Canadian Cancer Trials Group and Hôpital Maissoneuve Rosemont, we are developing a clinical trial for BCMA-TAC-T cells manufactured from G-CSF-mobilized peripheral blood products that were collected prior to first

transplant. These products are readily available and contain T cells that were collected prior to multiple lines of chemotherapies and daratumumab.

Unfortunately, pre-existing blood products will not be available for all patients and timing of the apheresis to collect T cells for engineering might not always be ideal due to the urgent need for MM control. Therefore, understanding the functionality of BCMA-TAC-T cell products generated from lymphocytes that had been exposed to different types of chemotherapeutic agents could help pre-emptively identify functional limitations and devise strategies for compensating for these deficiencies. MM patient-derived cells used in the experiments in Chapter 3 had been collected after the diagnosis and prior to the start of chemotherapy, so they would be relatively unaltered, compared to the cells that had been harvested after several lines of therapy. Despite the "chemotherapy-naïve" state of these T cells, we observed a number of functional defects, including reduced expansion during manufacturing and higher dependence on receptor density for cytokine production. With regard to common chemotherapies in MM, bortezomib can change the frequencies of CD4 T cell sub-populations and promote survival of T_{regs}[368, 369], which would be undesirable in the TAC-T cell product. Daratumumab eliminates CD38-positive T_{regs}, but also decreases the numbers of naïve CD8 T cells, skewing the CD8 T cell phenotype towards effector memory[99]. As a consequence, a more differentiated starting T cell population could yield an engineered TAC-T cell product with reduced proliferation potential, compared to a less differentiated T cell product[370]. However, not all chemotherapy drugs are

detrimental to the performance of engineered T cells. Lenalidomide improves anti-MM responses in non-engineered T cells in patients[371] and augments CAR-T cell functionality in preclinical models[372, 373]. Studies into the effects of different chemotherapeutic agents alone or in combination will help guide the manufacturing strategy for the clinical BCMA-TAC-T cells to maximize the therapeutic benefit.

In addition to chemotherapy-driven changes to the numbers and functionality of patients' immune cells, there will be inherent donor-dependent differences between TAC-T cells manufactured from different patients. In our preclinical experiences with healthy and patient donor-derived T cells, there is a lot of variability in functional responses between T cells from different donors. In the work described in this thesis, we routinely used cells derived from at least three donors, but larger-scale studies of donor-dependent attributes are needed. RNA sequencing and proteomic approaches can help correlate protein expression patterns with functional performance and map out molecular signatures of donors that have stronger anti-MM responses and would be expected to benefit the most from the TAC-T cell therapy; such an approach has recently identified desirable donor attributes for CD19-CAR T cells[374].

In the CAR-T cell field, stem cell memory T cell (T_{scm}) populations in the engineered products have been implicated in early post-infusion proliferation and long-term persistence, mediating clinical efficacy[375, 376]. T_{scm} cells are metabolically quiescent, strongly favor fatty acid oxidation over glycolysis for fuel, and rely on glutathione for antioxidant activity that inhibits terminal differentiation[377]. At

present, we do not routinely assess the differentiation state of TAC-T cell cultures and have virtually no understanding of metabolic changes that follow TAC receptor-driven activation. The optimized BCMA-TAC construct represents a clinically relevant TAC receptor model system, where the metabolic studies could be conducted. Enhanced understanding of the TAC-T cell metabolism can then inform the manufacturing strategies for TAC-T cell products.

1.3. Broader implications for the engineered T cell field

The engineered T cell field has grown exponentially over the past few years, with multiple academic and industry groups working across the entire spectrum of T cell engineering, from construct design, to manufacturing innovation, to the development of tools and assays for functional assessments. The BCMA-TAC-T cell is entering a crowded space where many BCMA-specific products are demonstrating robust clinical activity. However, all of the BCMA-specific engineered T cell therapies for which the clinical data are available have been designed on the CAR scaffolds. The clinical results obtained with BCMA-TAC-T cells will provide important safety and efficacy data for the TCR-centric synthetic receptors and will help inform the design and manufacturing of the next-generation receptors for MM.

At the preclinical level, the work described in Chapter 4 describes a functional screening strategy that can be adapted to selection of different synthetic receptors aimed at modulating T cell functions. Importantly, while other groups

have used Jurkat or Jurkat-derived cell lines for screening CAR constructs[378, 379], we performed our screen in primary human T cells, thus generating results that are readily applicable to clinical development. We used upregulation of CD69 as the readout for T cell activation, but other functional parameters (e.g. cytokine production or proliferation) can be used to select T cell constructs with desired characteristics. For example, a group conducting a CAR screen in a murine reporter cell line has relied on IL-2 expression as an indicator of the CAR activity[380]. Another group stimulated their CAR-T cell library with antigen-positive target cells and relied on stimulation-driven CAR-T cell proliferation to identify the library clones that were enriched after activation[381]. One or both of these functional selection steps can be incorporated in our TAC-T cell screening system in future studies.

2. Assessment of a cross-reactive antigen-binding domain

2.1. Summary of findings

The antigen-binding domain is an important part of any synthetic receptor as it determines the specificity and functionality of engineered cells. In the course of comparing different BCMA-specific scFvs, we observed that the J22.9-xi scFv triggered antigen-independent *in vivo* proliferation of TAC- and CAR-T cells incorporating this scFv.

In Chapter 5, we compared the J22.9-xi scFv with the C11D5.3 scFv on the TAC scaffold. Despite equivalent *in vitro* proliferation, J22-TAC-T cells were

significantly more proliferative *in vivo* than the C11-TAC-T cells. Enhanced *in vivo* expansion of the J22-TAC-T cells was associated with more potent efficacy and improved resistance to tumor rechallenge. However, *in vivo* T cell tracking studies revealed that the J22-TAC-T cells also proliferated in tumor-free NRG mice, suggesting cross-reactivity of the J22-TAC receptor.

To assess how cross-reactivity of the J22.9-xi scFv would impact performance of T cells engineered with a different type of synthetic receptor, we created CD28ζ and 4-1BBζ CAR constructs carrying the J22.9-xi scFv (Chapter 6). Surprisingly, despite phenotypic evidence of exhaustion (measured by the expression of checkpoint receptors) and functional evidence of substantial tonic signaling, the CD28ζ CAR-T cells proliferated more robustly and killed tumors *in vivo* more efficiently than the 4-1BBζ CAR-T cells. Despite evidence of cross-reactivity of the J22.9-xi scFv in the CAR framework, the CAR-treated mice did not exhibit overt signs of toxicity. Studies are ongoing to assess markers of toxicity in blood and potential tissue damage in tumor-free mice injected with the J22-CD28ζ- and the J22-4-1BBζ-CAR-T cells.

2.2. Implications for the synthetic receptor screening platforms

A common workflow for designing synthetic receptors with new specificities includes screening of an scFv library against a target of interest, incorporation of the top scFv candidates in the synthetic receptor framework, and functional characterization of T cells. The focus is typically on selection of a high-

affinity binder that recognizes the target of interest and triggers T cell activation *in vitro* and *in vivo*. While this workflow is effective at determining whether the newly designed receptor works, it does not always provide a sufficient assessment of the specificity of the new receptor. Our observation of the cross-reactivity of the J22.9-xi scFv in mice does not guarantee that the same cross-reactivity will be in effect in humans. It does, however, highlight the benefit of adding negative selection steps at the stage of scFv selection or an analysis of trafficking of the newly engineered T cells for identification of potential future toxicities.

The J22.9-xi antibody was extensively evaluated for its ability to bind BCMA and BCMA-positive cells, but the only negative control binding test was done with the Jurkat cell line, which showed no binding[382]. Additional validation steps designed to test binding to multiple antigen-negative cells, serum proteins, or tissue arrays might have identified cross-reactivity[383]. The cross-reactivity analysis is particularly important if the antibody is intended to be used for redirecting engineered T cells (as opposed to monoclonal antibody alone) because the T cells will proliferate *in vivo* upon stimulation and can survive for years post-infusion[384], potentially causing long-term toxicities.

Since mice treated with J22.9-xi-based receptors (TAC and CAR) did not show overt signs of toxicity (changes in body condition, behavior, weight, or core body temperature), we would not have suspected cross-reactivity of the J22-engineered T cells if we had not looked at their *in vivo* proliferation. Tracking of engineered T cells in tumor-free mice is not a common piece of analysis for the

evaluation of novel synthetic receptors. Our experience suggests that such studies should be done more often as a part of the safety assessment and to correctly interpret *in vivo* expansion data, which may, or may not, be driven by tumor-associated antigen.

To date, we have not yet identified the source of the cross-reactive antigen that the J22.9-xi scFv recognizes in mice. It is possible that the cross-reactivity does not result in damage of specific organ(s), but instead, manifests in a systemic inflammatory response. The NRG mouse model we have used does not allow us to assess multi-faceted immune responses as we only inject engineered human T cells. However, NRG mice have been successfully humanized using cord blood stem cells that gave rise to a multi-lineage immune repertoire upon engraftment[385]. A humanized NRG mouse model would not be useful for assessing anti-tumor efficacy because the donor-derived immune system would mount an anti-tumor response and facilitate rejection. Nevertheless, such a system could help evaluate systemic immune reactions initiated by cross-reactive engineered T cells, if the engineered T cells were created from the same donor that was used for humanization. Unfortunately, the issue of finding an *in vivo* model system suitable for simultaneous evaluation of anti-tumor efficacy and immune-mediated toxicity is a common challenge in the field of immunotherapeutics. For now, we will have to continue working within the limitations of each *in vivo* model and use combinations of models for answering different questions.

2.3. Comparison of the second-generation CAR-T cells engineered with the J22.9-xi antigen-binding domain

When the studies highlighting tonic signaling in the CD28ζ CAR-T cells and superior *in vivo* persistence of the 4-1BBζ CAR-T cells were first published[211, 238, 298, 350, 354], many research groups started favoring the 4-1BBζ scaffold. Consequently, the majority of the second-generation CAR-T cells currently evaluated in clinical trials are designed with the 4-1BBζ backbone[214]. Yet two of the five CAR-T cell products that have received regulatory approval are based on the CD28ζ scaffold and continue to show durable long-term efficacy[386, 387]. Our results described in Chapter 6 demonstrated that despite tonic signaling, the CD28ζ CAR-T cells induced lasting complete responses and provided resistance to tumor rechallenge *in vivo*. The anti-tumor response of the CD28ζ CAR-T was associated with superior *in vivo* proliferation, when compared to the 4-1BBζ CAR-T cells. Our data showed that the CD28ζ CAR-T cells are capable of lasting *in vivo* persistence, when the stimulus is continuously present. In our studies, the continuous stimulus was a cross-reactive antigen of unknown source – whether tumor-associated antigen can serve as this stimulus for the CD28ζ CAR-T cells, remains to be fully understood. Nevertheless, it is too early to draw definitive conclusions about which second-generation CAR backbone is superior. Clinical efficacy of engineered T cells depends on a complex, multi-faceted response and as the field is still uncovering the factors impacting this response, there is still room for both the CD28ζ and the 4-1BBζ CAR-T cells to make an impact.

3. Concluding remarks

The field of engineered T cell therapies has seen incredible growth and development over the past few years. As a consequence, patients with previously incurable blood cancers, including multiple myeloma, now have a hope for achieving deep remissions and long progression-free survival. The early successes of the T cell therapies are encouraging, but there is still a lot of work to be done in understanding the mechanisms underlying efficacy and toxicity of engineered T cells in order to set up the most optimal engineering and manufacturing strategies. Our lab has developed a novel T cell receptor, TAC, and the work on optimization of the BCMA-specific TAC receptor described in this thesis will serve as a preclinical basis for testing TAC-engineered T cells in clinical trials. Additionally, our work on evaluating different BCMA-specific antigen-binding domains advances our understanding of the impact of these domains on the functionality of synthetic receptors and will inform design of future constructs.

Chapter 8

References

1. Lightman SM, Utley A, Lee KP. Survival of Long-Lived Plasma Cells (LLPC): Piecing Together the Puzzle. *Front Immunol*. 2019;10:965. doi:10.3389/fimmu.2019.00965

2. Amanna IJ, Carlson NE, Slifka MK. Duration of humoral immunity to common viral and vaccine antigens. *N Engl J Med*. Nov 2007;357(19):1903-15. doi:10.1056/NEJMoa066092

3. Manz RA, Thiel A, Radbruch A. Lifetime of plasma cells in the bone marrow. *Nature*. Jul 1997;388(6638):133-4. doi:10.1038/40540

4. Slifka MK, Antia R, Whitmire JK, Ahmed R. Humoral immunity due to long-lived plasma cells. *Immunity*. Mar 1998;8(3):363-72. doi:10.1016/s1074-7613(00)80541-5

5. Manz RA, Löhning M, Cassese G, Thiel A, Radbruch A. Survival of long-lived plasma cells is independent of antigen. *Int Immunol*. Nov 1998;10(11):1703-11. doi:10.1093/intimm/10.11.1703

6. Minges Wols HA, Underhill GH, Kansas GS, Witte PL. The role of bone marrow-derived stromal cells in the maintenance of plasma cell longevity. *J Immunol*. Oct 2002;169(8):4213-21. doi:10.4049/jimmunol.169.8.4213

7. Nguyen DC, Garimalla S, Xiao H, et al. Factors of the bone marrow microniche that support human plasma cell survival and immunoglobulin secretion. *Nat Commun*. 09 2018;9(1):3698. doi:10.1038/s41467-018-05853-7

8. Hargreaves DC, Hyman PL, Lu TT, et al. A coordinated change in chemokine responsiveness guides plasma cell movements. *J Exp Med*. Jul 2001;194(1):45-56. doi:10.1084/jem.194.1.45

9. Cornelis R, Hahne S, Taddeo A, et al. Stromal Cell-Contact Dependent PI3K and APRIL Induced NF-κB Signaling Prevent Mitochondrial- and ER Stress Induced Death of Memory Plasma Cells. *Cell Rep*. Aug 2020;32(5):107982. doi:10.1016/j.celrep.2020.107982

10. Jourdan M, Cren M, Robert N, et al. IL-6 supports the generation of human long-lived plasma cells in combination with either APRIL or stromal cell-soluble factors. *Leukemia*. Aug 2014;28(8):1647-56. doi:10.1038/leu.2014.61

11. Rodríguez-Bayona B, Ramos-Amaya A, López-Blanco R, Campos-Caro A, Brieva JA. STAT-3 activation by differential cytokines is critical for human in vivo-generated plasma cell survival and Ig secretion. *J Immunol*. Nov 2013;191(10):4996-5004. doi:10.4049/jimmunol.1301559

12. Matthes T, Dunand-Sauthier I, Santiago-Raber ML, et al. Production of the plasma-cell survival factor a proliferation-inducing ligand (APRIL) peaks in

myeloid precursor cells from human bone marrow. *Blood*. Aug 2011;118(7):1838-44. doi:10.1182/blood-2011-01-332940

13. Belnoue E, Pihlgren M, McGaha TL, et al. APRIL is critical for plasmablast survival in the bone marrow and poorly expressed by early-life bone marrow stromal cells. *Blood*. Mar 2008;111(5):2755-64. doi:10.1182/blood-2007-09-110858
14. Chu VT, Berek C. Immunization induces activation of bone marrow eosinophils required for plasma cell survival. *Eur J Immunol*. Jan 2012;42(1):130-7. doi:10.1002/eji.201141953
15. O'Connor BP, Raman VS, Erickson LD, et al. BCMA is essential for the survival of long-lived bone marrow plasma cells. *J Exp Med*. Jan 2004;199(1):91-8. doi:10.1084/jem.20031330
16. Peperzak V, Vikström I, Walker J, et al. Mcl-1 is essential for the survival of plasma cells. *Nat Immunol*. Mar 2013;14(3):290-7. doi:10.1038/ni.2527
17. Rennert P, Schneider P, Cachero TG, et al. A soluble form of B cell maturation antigen, a receptor for the tumor necrosis factor family member APRIL, inhibits tumor cell growth. *J Exp Med*. Dec 2000;192(11):1677-84. doi:10.1084/jem.192.11.1677
18. Zhang Y, Li J, Zhang YM, Zhang XM, Tao J. Effect of TACI signaling on humoral immunity and autoimmune diseases. *J Immunol Res*. 2015;2015:247426. doi:10.1155/2015/247426
19. Glatman Zaretsky A, Konradt C, Dépis F, et al. T Regulatory Cells Support Plasma Cell Populations in the Bone Marrow. *Cell Rep*. 02 2017;18(8):1906-1916. doi:10.1016/j.celrep.2017.01.067
20. Wright JH. A CASE OF MULTIPLE MYELOMA. *J Boston Soc Med Sci*. Apr 1900;4(8):195-204.5.
21. Landgren O, Kyle RA, Pfeiffer RM, et al. Monoclonal gammopathy of undetermined significance (MGUS) consistently precedes multiple myeloma: a prospective study. *Blood*. May 2009;113(22):5412-7. doi:10.1182/blood-2008-12-194241
22. Rajkumar SV, Dimopoulos MA, Palumbo A, et al. International Myeloma Working Group updated criteria for the diagnosis of multiple myeloma. *Lancet Oncol*. Nov 2014;15(12):e538-48. doi:10.1016/S1470-2045(14)70442-5
23. Kyle RA, Remstein ED, Therneau TM, et al. Clinical course and prognosis of smoldering (asymptomatic) multiple myeloma. *N Engl J Med*. Jun 2007;356(25):2582-90. doi:10.1056/NEJMoa070389
24. van Nieuwenhuijzen N, Spaan I, Raymakers R, Peperzak V. From MGUS to Multiple Myeloma, a Paradigm for Clonal Evolution of Premalignant Cells.

Cancer Res. 05 2018;78(10):2449-2456. doi:10.1158/0008-5472.CAN-17-3115

25. Smadja NV, Fruchart C, Isnard F, et al. Chromosomal analysis in multiple myeloma: cytogenetic evidence of two different diseases. *Leukemia*. Jun 1998;12(6):960-9. doi:10.1038/sj.leu.2401041

26. Fonseca R, Debes-Marun CS, Picken EB, et al. The recurrent IgH translocations are highly associated with nonhyperdiploid variant multiple myeloma. *Blood*. Oct 2003;102(7):2562-7. doi:10.1182/blood-2003-02-0493

27. Bergsagel PL, Kuehl WM, Zhan F, Sawyer J, Barlogie B, Shaughnessy J. Cyclin D dysregulation: an early and unifying pathogenic event in multiple myeloma. *Blood*. Jul 2005;106(1):296-303. doi:10.1182/blood-2005-01-0034

28. Vermeulen K, Van Bockstaele DR, Berneman ZN. The cell cycle: a review of regulation, deregulation and therapeutic targets in cancer. *Cell Prolif*. Jun 2003;36(3):131-49. doi:10.1046/j.1365-2184.2003.00266.x

29. Pawlyn C, Morgan GJ. Evolutionary biology of high-risk multiple myeloma. *Nat Rev Cancer*. 08 2017;17(9):543-556. doi:10.1038/nrc.2017.63

30. Walker BA, Wardell CP, Chiecchio L, et al. Aberrant global methylation patterns affect the molecular pathogenesis and prognosis of multiple myeloma. *Blood*. Jan 2011;117(2):553-62. doi:10.1182/blood-2010-04-279539

31. Heuck CJ, Mehta J, Bhagat T, et al. Myeloma is characterized by stage-specific alterations in DNA methylation that occur early during myelomagenesis. *J Immunol*. Mar 2013;190(6):2966-75. doi:10.4049/jimmunol.1202493

32. Agirre X, Castellano G, Pascual M, et al. Whole-epigenome analysis in multiple myeloma reveals DNA hypermethylation of B cell-specific enhancers. *Genome Res*. Apr 2015;25(4):478-87. doi:10.1101/gr.180240.114

33. Ria R, Todoerti K, Berardi S, et al. Gene expression profiling of bone marrow endothelial cells in patients with multiple myeloma. *Clin Cancer Res*. Sep 2009;15(17):5369-78. doi:10.1158/1078-0432.CCR-09-0040

34. Rajkumar SV, Mesa RA, Fonseca R, et al. Bone marrow angiogenesis in 400 patients with monoclonal gammopathy of undetermined significance, multiple myeloma, and primary amyloidosis. *Clin Cancer Res*. Jul 2002;8(7):2210-6.

35. Glavey SV, Naba A, Manier S, et al. Proteomic characterization of human multiple myeloma bone marrow extracellular matrix. *Leukemia*. 11 2017;31(11):2426-2434. doi:10.1038/leu.2017.102

36. Roccaro AM, Sacco A, Maiso P, et al. BM mesenchymal stromal cell-derived exosomes facilitate multiple myeloma progression. *J Clin Invest*. Apr 2013;123(4):1542-55. doi:10.1172/JCI66517

37. De Veirman K, Wang J, Xu S, et al. Induction of miR-146a by multiple myeloma cells in mesenchymal stromal cells stimulates their pro-tumoral activity. *Cancer Lett*. 07 2016;377(1):17-24. doi:10.1016/j.canlet.2016.04.024

38. Moloudizargari M, Abdollahi M, Asghari MH, Zimta AA, Neagoe IB, Nabavi SM. The emerging role of exosomes in multiple myeloma. *Blood Rev*. 11 2019;38:100595. doi:10.1016/j.blre.2019.100595

39. Rajkumar SV. Updated Diagnostic Criteria and Staging System for Multiple Myeloma. *Am Soc Clin Oncol Educ Book*. 2016;35:e418-23. doi:10.1200/EDBK_159009

40. Kraj M, Kruk B, Lech-Marańda E, Warzocha K, Prochorec-Sobieszek M. High incidence of intact or fragmented immunoglobulin in urine of patients with multiple myeloma. *Leuk Lymphoma*. 2015;56(12):3348-56. doi:10.3109/10428194.2015.1037753

41. Michallet M, Chapuis-Cellier C, Dejoie T, et al. Heavy+light chain monitoring correlates with clinical outcome in multiple myeloma patients. *Leukemia*. 02 2018;32(2):376-382. doi:10.1038/leu.2017.209

42. Magrangeas F, Cormier ML, Descamps G, et al. Light-chain only multiple myeloma is due to the absence of functional (productive) rearrangement of the IgH gene at the DNA level. *Blood*. May 2004;103(10):3869-75. doi:10.1182/blood-2003-07-2501

43. Beguin Y. Erythropoiesis and erythropoietin in multiple myeloma. *Leuk Lymphoma*. Aug 1995;18(5-6):413-21. doi:10.3109/10428199509059639

44. Silvestris F, Cafforio P, Tucci M, Dammacco F. Negative regulation of erythroblast maturation by Fas-L(+)/TRAIL(+) highly malignant plasma cells: a major pathogenetic mechanism of anemia in multiple myeloma. *Blood*. Feb 2002;99(4):1305-13. doi:10.1182/blood.v99.4.1305

45. Marino S, Roodman GD. Multiple Myeloma and Bone: The Fatal Interaction. *Cold Spring Harb Perspect Med*. 08 2018;8(8)doi:10.1101/cshperspect.a031286

46. Morris EV, Edwards CM. Bone marrow adiposity and multiple myeloma. *Bone*. 01 2019;118:42-46. doi:10.1016/j.bone.2018.03.011

47. Bhutani M, Foureau DM, Atrash S, Voorhees PM, Usmani SZ. Extramedullary multiple myeloma. *Leukemia*. 01 2020;34(1):1-20. doi:10.1038/s41375-019-0660-0

48. Mina R, D'Agostino M, Cerrato C, Gay F, Palumbo A. Plasma cell leukemia: update on biology and therapy. *Leuk Lymphoma*. 07 2017;58(7):1538-1547. doi:10.1080/10428194.2016.1250263

49. Oriol A. Multiple myeloma with extramedullary disease. *Adv Ther*. Nov 2011;28 Suppl 7:1-6. doi:10.1007/s12325-011-0079-0

50. Kyle RA, Therneau TM, Rajkumar SV, et al. Prevalence of monoclonal gammopathy of undetermined significance. *N Engl J Med*. Mar 2006;354(13):1362-9. doi:10.1056/NEJMoa054494

51. Landgren O, Katzmann JA, Hsing AW, et al. Prevalence of monoclonal gammopathy of undetermined significance among men in Ghana. *Mayo Clin Proc*. Dec 2007;82(12):1468-73. doi:10.1016/S0025-6196(11)61089-6

52. Kyle RA, Therneau TM, Rajkumar SV, et al. A long-term study of prognosis in monoclonal gammopathy of undetermined significance. *N Engl J Med*. Feb 2002;346(8):564-9. doi:10.1056/NEJMoa01133202

53. Ravindran A, Bartley AC, Holton SJ, et al. Prevalence, incidence and survival of smoldering multiple myeloma in the United States. *Blood Cancer J*. 10 2016;6(10):e486. doi:10.1038/bcj.2016.100

54. Kristinsson SY, Holmberg E, Blimark C. Treatment for high-risk smoldering myeloma. *N Engl J Med*. 10 2013;369(18):1762-3. doi:10.1056/NEJMc1310911

55. Estimated number of new cases in 2020, both sexes, all ages. International Agency for Research on Cancer. https://gco.iarc.fr/today/online-analysis-table?v=2020&mode=cancer&mode_population=continents&population=900&populations=900&key=asr&sex=0&cancer=39&type=0&statistic=5&prevalence=0&population_group=0&ages_group%5B%5D=0&ages_group%5B%5D=17&group_cancer=1&include_nmsc=1&include_nmsc_other=1

56. Henley SJ, Ward EM, Scott S, et al. Annual report to the nation on the status of cancer, part I: National cancer statistics. *Cancer*. May 2020;126(10):2225-2249. doi:10.1002/cncr.32802

57. Myeloma. Recent Trends in SEER Age-Adjusted Incidence Rates in 2000-2017. https://seer.cancer.gov/explorer/application.html?site=89&data_type=1&graph_type=2&compareBy=sex&chk_sex_1=1&race=1&age_range=1&stage=101&rate_type=2&advopt_precision=1&advopt_display=2

58. Kazandjian D. Multiple myeloma epidemiology and survival: A unique malignancy. *Semin Oncol*. Dec 2016;43(6):676-681. doi:10.1053/j.seminoncol.2016.11.004

59. Brenner DR, Weir HK, Demers AA, et al. Projected estimates of cancer in Canada in 2020. *CMAJ*. 03 2020;192(9):E199-E205. doi:10.1503/cmaj.191292

60. Canadian Cancer Statistics Advisory Committee . Canadian cancer statistics 2019 . Toronto : Canadian Cancer Society. www.cancer.ca/~/media/cancer.ca/CW/publications/Canadian%20Cancer%20Statistics/Canadian-Cancer-Statistics-2019-EN.pdf

61. Statistics Canada Catalogue no. 91-520-X. Population Projections for Canada (2018 to 2068), Provinces and Territories (2018 to 2043). https://www150.statcan.gc.ca/n1/en/pub/91-520-x/91-520-x2019001-eng.pdf?st=HNKDS1g

62. Kyle RA, Rajkumar SV. Multiple myeloma. *Blood*. Mar 2008;111(6):2962-72. doi:10.1182/blood-2007-10-078022

63. Ribatti D. A historical perspective on milestones in multiple myeloma research. *Eur J Haematol*. Mar 2018;100(3):221-228. doi:10.1111/ejh.13003

64. Alexanian R, Bergsagel DE, Migliore PJ, Vaughn WK, Howe CD. Melphalan therapy for plasma cell myeloma. Blood. 1968;31(1):1-10. *Blood*. 08 2016;128(6):741. doi:10.1182/blood-2016-06-724054

65. Esma F, Salvini M, Troia R, Boccadoro M, Larocca A, Pautasso C. Melphalan hydrochloride for the treatment of multiple myeloma. *Expert Opin Pharmacother*. Aug 2017;18(11):1127-1136. doi:10.1080/14656566.2017.1349102

66. Alexanian R, Haut A, Khan AU, et al. Treatment for multiple myeloma. Combination chemotherapy with different melphalan dose regimens. *JAMA*. Jun 1969;208(9):1680-5. doi:10.1001/jama.208.9.1680

67. Attal M, Harousseau JL, Stoppa AM, et al. A prospective, randomized trial of autologous bone marrow transplantation and chemotherapy in multiple myeloma. Intergroupe Français du Myélome. *N Engl J Med*. Jul 1996;335(2):91-7. doi:10.1056/NEJM199607113350204

68. Child JA, Morgan GJ, Davies FE, et al. High-dose chemotherapy with hematopoietic stem-cell rescue for multiple myeloma. *N Engl J Med*. May 2003;348(19):1875-83. doi:10.1056/NEJMoa022340

69. Alyea E, Weller E, Schlossman R, et al. Outcome after autologous and allogeneic stem cell transplantation for patients with multiple myeloma:

impact of graft-versus-myeloma effect. *Bone Marrow Transplant*. Dec 2003;32(12):1145-51. doi:10.1038/sj.bmt.1704289

70. Rueff J, Medinger M, Heim D, Passweg J, Stern M. Lymphocyte subset recovery and outcome after autologous hematopoietic stem cell transplantation for plasma cell myeloma. *Biol Blood Marrow Transplant*. Jun 2014;20(6):896-9. doi:10.1016/j.bbmt.2014.03.007

71. Porrata LF. Autologous Graft-versus-Tumor Effect: Reality or Fiction? *Adv Hematol*. 2016;2016:5385972. doi:10.1155/2016/5385972

72. Porrata LF, Gertz MA, Geyer SM, et al. The dose of infused lymphocytes in the autograft directly correlates with clinical outcome after autologous peripheral blood hematopoietic stem cell transplantation in multiple myeloma. *Leukemia*. Jun 2004;18(6):1085-92. doi:10.1038/sj.leu.2403341

73. Hiwase DK, Hiwase S, Bailey M, Bollard G, Schwarer AP. Higher infused lymphocyte dose predicts higher lymphocyte recovery, which in turn, predicts superior overall survival following autologous hematopoietic stem cell transplantation for multiple myeloma. *Biol Blood Marrow Transplant*. Jan 2008;14(1):116-24. doi:10.1016/j.bbmt.2007.08.051

74. Schmidmaier R, Oversohl N, Schnabel B, Straka C, Emmerich B. Helper T cells (CD3 + /CD4 +) within the autologous peripheral blood stem cell graft positively correlate with event free survival of multiple myeloma patients. *Exp Oncol*. Sep 2008;30(3):240-3.

75. Hiwase DK, Hiwase S, Bailey M, Bollard G, Schwarer AP. The role of stem cell mobilization regimen on lymphocyte collection yield in patients with multiple myeloma. *Cytotherapy*. 2008;10(5):507-17. doi:10.1080/14653240802165665

76. Gaugler B, Arbez J, Legouill S, et al. Characterization of peripheral blood stem cell grafts mobilized by granulocyte colony-stimulating factor and plerixafor compared with granulocyte colony-stimulating factor alone. *Cytotherapy*. Jul 2013;15(7):861-8. doi:10.1016/j.jcyt.2013.03.013

77. Vuckovic S, Minnie SA, Smith D, et al. Bone marrow transplantation generates T cell-dependent control of myeloma in mice. *J Clin Invest*. 01 2019;129(1):106-121. doi:10.1172/JCI98888

78. D'Amato RJ, Loughnan MS, Flynn E, Folkman J. Thalidomide is an inhibitor of angiogenesis. *Proc Natl Acad Sci U S A*. Apr 1994;91(9):4082-5. doi:10.1073/pnas.91.9.4082

79. Singhal S, Mehta J, Desikan R, et al. Antitumor activity of thalidomide in refractory multiple myeloma. *N Engl J Med*. Nov 1999;341(21):1565-71. doi:10.1056/NEJM199911183412102

80. Kumar S, Rajkumar SV. Thalidomide and dexamethasone: therapy for multiple myeloma. *Expert Rev Anticancer Ther*. Oct 2005;5(5):759-66. doi:10.1586/14737140.5.5.759

81. Landgren O, Iskander K. Modern multiple myeloma therapy: deep, sustained treatment response and good clinical outcomes. *J Intern Med*. 04 2017;281(4):365-382. doi:10.1111/joim.12590

82. Fink EC, Ebert BL. The novel mechanism of lenalidomide activity. *Blood*. Nov 2015;126(21):2366-9. doi:10.1182/blood-2015-07-567958

83. LeBlanc R, Hideshima T, Catley LP, et al. Immunomodulatory drug costimulates T cells via the B7-CD28 pathway. *Blood*. Mar 2004;103(5):1787-90. doi:10.1182/blood-2003-02-0361

84. Görgün G, Calabrese E, Soydan E, et al. Immunomodulatory effects of lenalidomide and pomalidomide on interaction of tumor and bone marrow accessory cells in multiple myeloma. *Blood*. Oct 2010;116(17):3227-37. doi:10.1182/blood-2010-04-279893

85. Chanan-Khan AA, Swaika A, Paulus A, et al. Pomalidomide: the new immunomodulatory agent for the treatment of multiple myeloma. *Blood Cancer J*. Sep 2013;3:e143. doi:10.1038/bcj.2013.38

86. Chen D, Frezza M, Schmitt S, Kanwar J, Dou QP. Bortezomib as the first proteasome inhibitor anticancer drug: current status and future perspectives. *Curr Cancer Drug Targets*. Mar 2011;11(3):239-53. doi:10.2174/156800911794519752

87. Scalzulli E, Grammatico S, Vozella F, Petrucci MT. Proteasome inhibitors for the treatment of multiple myeloma. *Expert Opin Pharmacother*. 03 2018;19(4):375-386. doi:10.1080/14656566.2018.1441287

88. Grosicki S, Bednarczyk M, Janikowska G. Heat shock proteins as a new, promising target of multiple myeloma therapy. *Expert Rev Hematol*. 02 2020;13(2):117-126. doi:10.1080/17474086.2020.1711730

89. Cengiz Seval G, Beksac M. A comparative safety review of histone deacetylase inhibitors for the treatment of myeloma. *Expert Opin Drug Saf*. 07 2019;18(7):563-571. doi:10.1080/14740338.2019.1615051

90. Touzeau C, Maciag P, Amiot M, Moreau P. Targeting Bcl-2 for the treatment of multiple myeloma. *Leukemia*. 09 2018;32(9):1899-1907. doi:10.1038/s41375-018-0223-9

91. Theodoropoulos N, Lancman G, Chari A. Targeting Nuclear Export Proteins in Multiple Myeloma Therapy. *Target Oncol*. Dec 2020;15(6):697-708. doi:10.1007/s11523-020-00758-2

92. Wudhikarn K, Wills B, Lesokhin AM. Monoclonal antibodies in multiple myeloma: Current and emerging targets and mechanisms of action. *Best*

Pract Res Clin Haematol. 03 2020;33(1):101143. doi:10.1016/j.beha.2020.101143

93. McMillan A, Warcel D, Popat R. Antibody-drug conjugates for multiple myeloma. *Expert Opin Biol Ther*. Aug 2020:1-13. doi:10.1080/14712598.2020.1802422

94. Horenstein AL, Bracci C, Morandi F, Malavasi F. CD38 in Adenosinergic Pathways and Metabolic Re-programming in Human Multiple Myeloma Cells: In-tandem Insights From Basic Science to Therapy. *Front Immunol*. 2019;10:760. doi:10.3389/fimmu.2019.00760

95. Nooka AK, Kaufman JL, Hofmeister CC, et al. Daratumumab in multiple myeloma. *Cancer*. 07 2019;125(14):2364-2382. doi:10.1002/cncr.32065

96. Richter J, Sanchez L, Thibaud S. Therapeutic potential of isatuximab in the treatment of multiple myeloma: Evidence to date. *Semin Oncol*. 2020 Apr - Jun 2020;47(2-3):155-164. doi:10.1053/j.seminoncol.2020.04.004

97. Abramson HN. Monoclonal Antibodies for the Treatment of Multiple Myeloma: An Update. *Int J Mol Sci*. Dec 2018;19(12)doi:10.3390/ijms19123924

98. Usmani SZ, Weiss BM, Plesner T, et al. Clinical efficacy of daratumumab monotherapy in patients with heavily pretreated relapsed or refractory multiple myeloma. *Blood*. 07 2016;128(1):37-44. doi:10.1182/blood-2016-03-705210

99. Krejcik J, Casneuf T, Nijhof IS, et al. Daratumumab depletes CD38+ immune regulatory cells, promotes T-cell expansion, and skews T-cell repertoire in multiple myeloma. *Blood*. 07 2016;128(3):384-94. doi:10.1182/blood-2015-12-687749

100. Lee JK, Mathew SO, Vaidya SV, Kumaresan PR, Mathew PA. CS1 (CRACC, CD319) induces proliferation and autocrine cytokine expression on human B lymphocytes. *J Immunol*. Oct 2007;179(7):4672-8. doi:10.4049/jimmunol.179.7.4672

101. Tai YT, Dillon M, Song W, et al. Anti-CS1 humanized monoclonal antibody HuLuc63 inhibits myeloma cell adhesion and induces antibody-dependent cellular cytotoxicity in the bone marrow milieu. *Blood*. Aug 2008;112(4):1329-37. doi:10.1182/blood-2007-08-107292

102. Trudel S, Moreau P, Touzeau C. Update on elotuzumab for the treatment of relapsed/refractory multiple myeloma: patients' selection and perspective. *Onco Targets Ther*. 2019;12:5813-5822. doi:10.2147/OTT.S174640

103. Zonder JA, Mohrbacher AF, Singhal S, et al. A phase 1, multicenter, open-label, dose escalation study of elotuzumab in patients with advanced

multiple myeloma. *Blood*. Jul 2012;120(3):552-9. doi:10.1182/blood-2011-06-360552

104. Lonial S, Vij R, Harousseau JL, et al. Elotuzumab in combination with lenalidomide and low-dose dexamethasone in relapsed or refractory multiple myeloma. *J Clin Oncol*. Jun 2012;30(16):1953-9. doi:10.1200/JCO.2011.37.2649
105. Bensinger W, Maziarz RT, Jagannath S, et al. A phase 1 study of lucatumumab, a fully human anti-CD40 antagonist monoclonal antibody administered intravenously to patients with relapsed or refractory multiple myeloma. *Br J Haematol*. Oct 2012;159(1):58-66. doi:10.1111/j.1365-2141.2012.09251.x
106. Hussein M, Berenson JR, Niesvizky R, et al. A phase I multidose study of dacetuzumab (SGN-40; humanized anti-CD40 monoclonal antibody) in patients with multiple myeloma. *Haematologica*. May 2010;95(5):845-8. doi:10.3324/haematol.2009.008003
107. Wichert S, Juliusson G, Johansson Å, et al. A single-arm, open-label, phase 2 clinical trial evaluating disease response following treatment with BI-505, a human anti-intercellular adhesion molecule-1 monoclonal antibody, in patients with smoldering multiple myeloma. *PLoS One*. 2017;12(2):e0171205. doi:10.1371/journal.pone.0171205
108. Kaufman JL, Niesvizky R, Stadtmauer EA, et al. Phase I, multicentre, dose-escalation trial of monotherapy with milatuzumab (humanized anti-CD74 monoclonal antibody) in relapsed or refractory multiple myeloma. *Br J Haematol*. Nov 2013;163(4):478-86. doi:10.1111/bjh.12565
109. Moreau P, Cavallo F, Leleu X, et al. Phase I study of the anti insulin-like growth factor 1 receptor (IGF-1R) monoclonal antibody, AVE1642, as single agent and in combination with bortezomib in patients with relapsed multiple myeloma. *Leukemia*. May 2011;25(5):872-4. doi:10.1038/leu.2011.4
110. Trudel S, Bergsagel PL, Singhal S, et al. A Phase I Study of the Safety and Pharmacokinetics of Escalating Doses of MFGR1877S, a Fibroblast Growth Factor Receptor 3 (FGFR3) Antibody, in Patients with Relapsed or Refractory t(4;14)-Positive Multiple Myeloma. *Blood*. 2012;120(21):4029-4029. doi:10.1182/blood.V120.21.4029.4029
111. Somlo G, Lashkari A, Bellamy W, et al. Phase II randomized trial of bevacizumab versus bevacizumab and thalidomide for relapsed/refractory multiple myeloma: a California Cancer Consortium trial. *Br J Haematol*. Aug 2011;154(4):533-5. doi:10.1111/j.1365-2141.2011.08623.x
112. White D, Kassim A, Bhaskar B, Yi J, Wamstad K, Paton VE. Results from AMBER, a randomized phase 2 study of bevacizumab and bortezomib

versus bortezomib in relapsed or refractory multiple myeloma. *Cancer*. Jan 2013;119(2):339-47. doi:10.1002/cncr.27745

113. Srkalovic G, Hussein MA, Hoering A, et al. A phase II trial of BAY 43-9006 (sorafenib) (NSC-724772) in patients with relapsing and resistant multiple myeloma: SWOG S0434. *Cancer Med*. Oct 2014;3(5):1275-83. doi:10.1002/cam4.276

114. Kovacs MJ, Reece DE, Marcellus D, et al. A phase II study of ZD6474 (Zactima, a selective inhibitor of VEGFR and EGFR tyrosine kinase in patients with relapsed multiple myeloma--NCIC CTG IND.145. *Invest New Drugs*. Nov 2006;24(6):529-35. doi:10.1007/s10637-006-9022-7

115. Gadó K, Domján G, Hegyesi H, Falus A. Role of INTERLEUKIN-6 in the pathogenesis of multiple myeloma. *Cell Biol Int*. 2000;24(4):195-209. doi:10.1006/cbir.2000.0497

116. Voorhees PM, Chen Q, Small GW, et al. Targeted inhibition of interleukin-6 with CNTO 328 sensitizes pre-clinical models of multiple myeloma to dexamethasone-mediated cell death. *Br J Haematol*. May 2009;145(4):481-90. doi:10.1111/j.1365-2141.2009.07647.x

117. Voorhees PM, Manges RF, Sonneveld P, et al. A phase 2 multicentre study of siltuximab, an anti-interleukin-6 monoclonal antibody, in patients with relapsed or refractory multiple myeloma. *Br J Haematol*. May 2013;161(3):357-66. doi:10.1111/bjh.12266

118. Raje NS, Moreau P, Terpos E, et al. Phase 2 study of tabalumab, a human anti-B-cell activating factor antibody, with bortezomib and dexamethasone in patients with previously treated multiple myeloma. *Br J Haematol*. Mar 2017;176(5):783-795. doi:10.1111/bjh.14483

119. Bensinger W, Raptis A, Berenson JR, et al. Safety and tolerability of BION-1301 in adults with relapsed or refractory multiple myeloma. *Journal of Clinical Oncology*. 2019;37(15_suppl):8012-8012. doi:10.1200/JCO.2019.37.15_suppl.8012

120. Raje N, Terpos E, Willenbacher W, et al. Denosumab versus zoledronic acid in bone disease treatment of newly diagnosed multiple myeloma: an international, double-blind, double-dummy, randomised, controlled, phase 3 study. *Lancet Oncol*. 03 2018;19(3):370-381. doi:10.1016/S1470-2045(18)30072-X

121. Singh S, Hassan D, Aldawsari HM, Molugulu N, Shukla R, Kesharwani P. Immune checkpoint inhibitors: a promising anticancer therapy. *Drug Discov Today*. 01 2020;25(1):223-229. doi:10.1016/j.drudis.2019.11.003

122. Mateos MV, Blacklock H, Schjesvold F, et al. Pembrolizumab plus pomalidomide and dexamethasone for patients with relapsed or refractory multiple myeloma (KEYNOTE-183): a randomised, open-label, phase 3

trial. *Lancet Haematol*. Sep 2019;6(9):e459-e469. doi:10.1016/S2352-3026(19)30110-3

123. Usmani SZ, Schjesvold F, Oriol A, et al. Pembrolizumab plus lenalidomide and dexamethasone for patients with treatment-naive multiple myeloma (KEYNOTE-185): a randomised, open-label, phase 3 trial. *Lancet Haematol*. Sep 2019;6(9):e448-e458. doi:10.1016/S2352-3026(19)30109-7

124. Carpenter RO, Evbuomwan MO, Pittaluga S, et al. B-cell maturation antigen is a promising target for adoptive T-cell therapy of multiple myeloma. *Clin Cancer Res*. Apr 2013;19(8):2048-60. doi:10.1158/1078-0432.CCR-12-2422

125. Khattar P, Pichardo J, Jungbluth A, et al. B- Cell Maturation Antigen Is Exclusively Expressed in a Wide Range of B-Cell and Plasma Cell Neoplasm and in a Potential Therapeutic Target for Bcma Directed Therapies. *Blood*. 2017;130(Supplement 1):2755-2755. doi:10.1182/blood.V130.Suppl_1.2755.2755

126. Lonial S, Lee HC, Badros A, et al. Belantamab mafodotin for relapsed or refractory multiple myeloma (DREAMM-2): a two-arm, randomised, open-label, phase 2 study. *Lancet Oncol*. 02 2020;21(2):207-221. doi:10.1016/S1470-2045(19)30788-0

127. Popat R, Nooka A, Stockerl-Goldstein K, et al. DREAMM-6: Safety, Tolerability and Clinical Activity of Belantamab Mafodotin (Belamaf) in Combination with Bortezomib/Dexamethasone (BorDex) in Relapsed/Refractory Multiple Myeloma (RRMM). *Blood*. 2020;136(Supplement 1):19-20. doi:10.1182/blood-2020-139332

128. Trudel S, McCurdy A, Sutherland HJ, et al. Part 1 Results of a Dose Finding Study of Belantamab Mafodotin (GSK2857916) in Combination with Pomalidomide (POM) and Dexamethazone (DEX) for the Treatment of Relapsed/Refractory Multiple Myeloma (RRMM). presented at: American Society of Hematology Annual Meeting; 2020; https://ash.confex.com/ash/2020/webprogram/Paper134836.html

129. Lee HC, Raje NS, Landgren O, et al. Phase 1 study of the anti-BCMA antibody-drug conjugate AMG 224 in patients with relapsed/refractory multiple myeloma. *Leukemia*. 01 2021;35(1):255-258. doi:10.1038/s41375-020-0834-9

130. Kumar SK, Migkou M, Bhutani M, et al. Phase 1, First-in-Human Study of MEDI2228, a BCMA-Targeted ADC in Patients with Relapsed/Refractory Multiple Myeloma. *Blood*. 2020;136(Supplement 1):26-27. doi:10.1182/blood-2020-136375

131. Jagannath S, Heffner LT, Ailawadhi S, et al. Indatuximab Ravtansine (BT062) Monotherapy in Patients With Relapsed and/or Refractory

Multiple Myeloma. *Clin Lymphoma Myeloma Leuk*. 06 2019;19(6):372-380. doi:10.1016/j.clml.2019.02.006

132. Vij R, Nath R, Afar DEH, et al. First-in-Human Phase I Study of ABBV-838, an Antibody-Drug Conjugate Targeting SLAMF7/CS1 in Patients with Relapsed and Refractory Multiple Myeloma. *Clin Cancer Res*. 05 2020;26(10):2308-2317. doi:10.1158/1078-0432.CCR-19-1431
133. Stewart AK, Krishnan AY, Singhal S, et al. Phase I study of the anti-FcRH5 antibody-drug conjugate DFRF4539A in relapsed or refractory multiple myeloma. *Blood Cancer J*. 02 2019;9(2):17. doi:10.1038/s41408-019-0178-8
134. Ailawadhi S, Kelly KR, Vescio RA, et al. A Phase I Study to Assess the Safety and Pharmacokinetics of Single-agent Lorvotuzumab Mertansine (IMGN901) in Patients with Relapsed and/or Refractory CD-56-positive Multiple Myeloma. *Clin Lymphoma Myeloma Leuk*. 01 2019;19(1):29-34. doi:10.1016/j.clml.2018.08.018
135. Berdeja JG, Hernandez-Ilizaliturri F, Chanan-Khan A, et al. Phase I Study of Lorvotuzumab Mertansine (LM, IMGN901) in Combination with Lenalidomide (Len) and Dexamethasone (Dex) in Patients with CD56-Positive Relapsed or Relapsed/Refractory Multiple Myeloma (MM). *Blood*. 2012;120(21):728-728. doi:10.1182/blood.V120.21.728.728
136. Vafa O, Trinklein ND. Perspective: Designing T-Cell Engagers With Better Therapeutic Windows. *Front Oncol*. 2020;10:446. doi:10.3389/fonc.2020.00446
137. Burt R, Warcel D, Fielding AK. Blinatumomab, a bispecific B-cell and T-cell engaging antibody, in the treatment of B-cell malignancies. *Hum Vaccin Immunother*. 2019;15(3):594-602. doi:10.1080/21645515.2018.1540828
138. Topp MS, Duell J, Zugmaier G, et al. Anti-B-Cell Maturation Antigen BiTE Molecule AMG 420 Induces Responses in Multiple Myeloma. *J Clin Oncol*. 03 2020;38(8):775-783. doi:10.1200/JCO.19.02657
139. Goldstein RL, Goyos A, Li CM, et al. AMG 701 induces cytotoxicity of multiple myeloma cells and depletes plasma cells in cynomolgus monkeys. *Blood Adv*. Sep 2020;4(17):4180-4194. doi:10.1182/bloodadvances.2020002565
140. Harrison SJ, Minnema MC, Lee HC, et al. A Phase 1 First in Human (FIH) Study of AMG 701, an Anti-B-Cell Maturation Antigen (BCMA) Half-Life Extended (HLE) BiTE® (bispecific T-cell engager) Molecule, in Relapsed/Refractory (RR) Multiple Myeloma (MM). *Blood*. 2020;136(Supplement 1):28-29. doi:10.1182/blood-2020-134063
141. Garfall AL, Usmani SZ, Mateos M-V, et al. Updated Phase 1 Results of Teclistamab, a B-Cell Maturation Antigen (BCMA) x CD3 Bispecific

Antibody, in Relapsed and/or Refractory Multiple Myeloma (RRMM). *Blood*. 2020;136(Supplement 1):27-27. doi:10.1182/blood-2020-138831

142. Madduri D, Rosko A, Brayer J, et al. REGN5458, a BCMA x CD3 Bispecific Monoclonal Antibody, Induces Deep and Durable Responses in Patients with Relapsed/Refractory Multiple Myeloma (RRMM). *Blood*. 2020;136(Supplement 1):41-42. doi:10.1182/blood-2020-139192
143. Rodriguez C, D'Souza A, Shah N, et al. Initial Results of a Phase I Study of TNB-383B, a BCMA x CD3 Bispecific T-Cell Redirecting Antibody, in Relapsed/Refractory Multiple Myeloma. *Blood*. 2020;136(Supplement 1):43-44. doi:10.1182/blood-2020-139893
144. Polson AG, Zheng B, Elkins K, et al. Expression pattern of the human FcRH/IRTA receptors in normal tissue and in B-chronic lymphocytic leukemia. *Int Immunol*. Sep 2006;18(9):1363-73. doi:10.1093/intimm/dxl069
145. Li J, Stagg NJ, Johnston J, et al. Membrane-Proximal Epitope Facilitates Efficient T Cell Synapse Formation by Anti-FcRH5/CD3 and Is a Requirement for Myeloma Cell Killing. *Cancer Cell*. 03 2017;31(3):383-395. doi:10.1016/j.ccell.2017.02.001
146. Cohen AD, Harrison SJ, Krishnan A, et al. Initial Clinical Activity and Safety of BFCR4350A, a FcRH5/CD3 T-Cell-Engaging Bispecific Antibody, in Relapsed/Refractory Multiple Myeloma. *Blood*. 2020;136(Supplement 1):42-43. doi:10.1182/blood-2020-136985
147. Atamaniuk J, Gleiss A, Porpaczy E, et al. Overexpression of G protein-coupled receptor 5D in the bone marrow is associated with poor prognosis in patients with multiple myeloma. *Eur J Clin Invest*. Sep 2012;42(9):953-60. doi:10.1111/j.1365-2362.2012.02679.x
148. Kodama T, Kochi Y, Nakai W, et al. Anti-GPRC5D/CD3 Bispecific T-Cell-Redirecting Antibody for the Treatment of Multiple Myeloma. *Mol Cancer Ther*. 09 2019;18(9):1555-1564. doi:10.1158/1535-7163.MCT-18-1216
149. Chari A, Berdeja JG, Oriol A, et al. A Phase 1, First-in-Human Study of Talquetamab, a G Protein-Coupled Receptor Family C Group 5 Member D (GPRC5D) x CD3 Bispecific Antibody, in Patients with Relapsed and/or Refractory Multiple Myeloma (RRMM). *Blood*. 2020;136(Supplement 1):40-41. doi:10.1182/blood-2020-133873
150. Trudel S, Lendvai N, Popat R, et al. Antibody-drug conjugate, GSK2857916, in relapsed/refractory multiple myeloma: an update on safety and efficacy from dose expansion phase I study. *Blood Cancer J*. 03 2019;9(4):37. doi:10.1038/s41408-019-0196-6

151. Caraccio C, Krishna S, Phillips DJ, Schürch CM. Bispecific Antibodies for Multiple Myeloma: A Review of Targets, Drugs, Clinical Trials, and Future Directions. *Front Immunol*. 2020;11:501. doi:10.3389/fimmu.2020.00501

152. Zuo P. Capturing the Magic Bullet: Pharmacokinetic Principles and Modeling of Antibody-Drug Conjugates. *AAPS J*. 08 2020;22(5):105. doi:10.1208/s12248-020-00475-8

153. Slaney CY, Wang P, Darcy PK, Kershaw MH. CARs versus BiTEs: A Comparison between T Cell-Redirection Strategies for Cancer Treatment. *Cancer Discov*. 08 2018;8(8):924-934. doi:10.1158/2159-8290.CD-18-0297

154. Cohen AD, Raje N, Fowler JA, Mezzi K, Scott EC, Dhodapkar MV. How to Train Your T Cells: Overcoming Immune Dysfunction in Multiple Myeloma. *Clin Cancer Res*. 04 2020;26(7):1541-1554. doi:10.1158/1078-0432.CCR-19-2111

155. Jenkins M, Canfield R, Robbins M, Ritchie DS, Trapani J, Neeson P. Targeting Mechanisms for Natural Killer Cell Dysfunction in Patients with Multiple Myeloma. *Blood*. 2015;126(23):4237-4237. doi:10.1182/blood.V126.23.4237.4237

156. Besson L, Charrier E, Karlin L, et al. One-Year Follow-Up of Natural Killer Cell Activity in Multiple Myeloma Patients Treated With Adjuvant Lenalidomide Therapy. *Front Immunol*. 2018;9:704. doi:10.3389/fimmu.2018.00704

157. Vairy S, Garcia JL, Teira P, Bittencourt H. CTL019 (tisagenlecleucel): CAR-T therapy for relapsed and refractory B-cell acute lymphoblastic leukemia. *Drug Des Devel Ther*. 2018;12:3885-3898. doi:10.2147/DDDT.S138765

158. van den Berg JH, Heemskerk B, van Rooij N, et al. Tumor infiltrating lymphocytes (TIL) therapy in metastatic melanoma: boosting of neoantigen-specific T cell reactivity and long-term follow-up. *J Immunother Cancer*. Aug 2020;8(2)doi:10.1136/jitc-2020-000848

159. Jafarzadeh L, Masoumi E, Fallah-Mehrjardi K, Mirzaei HR, Hadjati J. Prolonged Persistence of Chimeric Antigen Receptor (CAR) T Cell in Adoptive Cancer Immunotherapy: Challenges and Ways Forward. *Front Immunol*. 2020;11:702. doi:10.3389/fimmu.2020.00702

160. Bernard A, Lamy And L, Alberti I. The two-signal model of T-cell activation after 30 years. *Transplantation*. Jan 2002;73(1 Suppl):S31-5. doi:10.1097/00007890-200201151-00011

161. Hwang JR, Byeon Y, Kim D, Park SG. Recent insights of T cell receptor-mediated signaling pathways for T cell activation and development. *Exp Mol Med*. 05 2020;52(5):750-761. doi:10.1038/s12276-020-0435-8

162. Baniyash M. TCR zeta-chain downregulation: curtailing an excessive inflammatory immune response. *Nat Rev Immunol*. Sep 2004;4(9):675-87. doi:10.1038/nri1434

163. Smith-Garvin JE, Koretzky GA, Jordan MS. T cell activation. *Annu Rev Immunol*. 2009;27:591-619. doi:10.1146/annurev.immunol.021908.132706

164. Love PE, Hayes SM. ITAM-mediated signaling by the T-cell antigen receptor. *Cold Spring Harb Perspect Biol*. Jun 2010;2(6):a002485. doi:10.1101/cshperspect.a002485

165. Rossy J, Williamson DJ, Gaus K. How does the kinase Lck phosphorylate the T cell receptor? Spatial organization as a regulatory mechanism. *Front Immunol*. 2012;3:167. doi:10.3389/fimmu.2012.00167

166. Li Y, Yin Y, Mariuzza RA. Structural and biophysical insights into the role of CD4 and CD8 in T cell activation. *Front Immunol*. 2013;4:206. doi:10.3389/fimmu.2013.00206

167. McNeill L, Salmond RJ, Cooper JC, et al. The differential regulation of Lck kinase phosphorylation sites by CD45 is critical for T cell receptor signaling responses. *Immunity*. Sep 2007;27(3):425-37. doi:10.1016/j.immuni.2007.07.015

168. Lo WL, Shah NH, Ahsan N, et al. Lck promotes Zap70-dependent LAT phosphorylation by bridging Zap70 to LAT. *Nat Immunol*. 07 2018;19(7):733-741. doi:10.1038/s41590-018-0131-1

169. Neumeister EN, Zhu Y, Richard S, Terhorst C, Chan AC, Shaw AS. Binding of ZAP-70 to phosphorylated T-cell receptor zeta and eta enhances its autophosphorylation and generates specific binding sites for SH2 domain-containing proteins. *Mol Cell Biol*. Jun 1995;15(6):3171-8. doi:10.1128/mcb.15.6.3171

170. Bubeck Wardenburg J, Fu C, Jackman JK, et al. Phosphorylation of SLP-76 by the ZAP-70 protein-tyrosine kinase is required for T-cell receptor function. *J Biol Chem*. Aug 1996;271(33):19641-4. doi:10.1074/jbc.271.33.19641

171. Huse M. The T-cell-receptor signaling network. *J Cell Sci*. May 2009;122(Pt 9):1269-73. doi:10.1242/jcs.042762

172. Menk AV, Scharping NE, Moreci RS, et al. Early TCR Signaling Induces Rapid Aerobic Glycolysis Enabling Distinct Acute T Cell Effector Functions. *Cell Rep*. Feb 2018;22(6):1509-1521. doi:10.1016/j.celrep.2018.01.040

173. Conley JM, Gallagher MP, Berg LJ. T Cells and Gene Regulation: The Switching On and Turning Up of Genes after T Cell Receptor Stimulation in CD8 T Cells. *Front Immunol*. 2016;7:76. doi:10.3389/fimmu.2016.00076

174. Dustin ML. The immunological synapse. *Cancer Immunol Res*. Nov 2014;2(11):1023-33. doi:10.1158/2326-6066.CIR-14-0161

175. Fooksman DR, Vardhana S, Vasiliver-Shamis G, et al. Functional anatomy of T cell activation and synapse formation. *Annu Rev Immunol*. 2010;28:79-105. doi:10.1146/annurev-immunol-030409-101308

176. Calvo V, Izquierdo M. Imaging Polarized Secretory Traffic at the Immune Synapse in Living T Lymphocytes. *Front Immunol*. 2018;9:684. doi:10.3389/fimmu.2018.00684

177. Saito T. Mechanisms of T-lymphocyte signaling and activation. Oncohema Key. https://oncohemakey.com/mechanisms-of-t-lymphocyte-signaling-and-activation-2/

178. Chen L, Flies DB. Molecular mechanisms of T cell co-stimulation and co-inhibition. *Nat Rev Immunol*. Apr 2013;13(4):227-42. doi:10.1038/nri3405

179. Liechtenstein T, Dufait I, Lanna A, Breckpot K, Escors D. MODULATING CO-STIMULATION DURING ANTIGEN PRESENTATION TO ENHANCE CANCER IMMUNOTHERAPY. *Immunol Endocr Metab Agents Med Chem*. Sep 2012;12(3):224-235. doi:10.2174/187152212802001875

180. Esensten JH, Helou YA, Chopra G, Weiss A, Bluestone JA. CD28 Costimulation: From Mechanism to Therapy. *Immunity*. 05 2016;44(5):973-88. doi:10.1016/j.immuni.2016.04.020

181. Wikenheiser DJ, Stumhofer JS. ICOS Co-Stimulation: Friend or Foe? *Front Immunol*. 2016;7:304. doi:10.3389/fimmu.2016.00304

182. Watts TH. TNF/TNFR FAMILY MEMBERS IN COSTIMULATION OF T CELL RESPONSES. *Annual Review of Immunology*. 2005;23(1):23-68. doi:10.1146/annurev.immunol.23.021704.115839

183. Zapata JM, Perez-Chacon G, Carr-Baena P, et al. CD137 (4-1BB) Signalosome: Complexity Is a Matter of TRAFs. *Front Immunol*. 2018;9:2618. doi:10.3389/fimmu.2018.02618

184. Jensen SM, Maston LD, Gough MJ, et al. Signaling through OX40 enhances antitumor immunity. *Semin Oncol*. Oct 2010;37(5):524-32. doi:10.1053/j.seminoncol.2010.09.013

185. Denoeud J, Moser M. Role of CD27/CD70 pathway of activation in immunity and tolerance. *J Leukoc Biol*. Feb 2011;89(2):195-203. doi:10.1189/jlb.0610351

186. Tian J, Zhang B, Rui K, Wang S. The Role of GITR/GITRL Interaction in Autoimmune Diseases. *Front Immunol*. 2020;11:588682. doi:10.3389/fimmu.2020.588682

187. van der Weyden CA, Pileri SA, Feldman AL, Whisstock J, Prince HM. Understanding CD30 biology and therapeutic targeting: a historical perspective providing insight into future directions. *Blood Cancer J*. 09 2017;7(9):e603. doi:10.1038/bcj.2017.85

188. Cai G, Freeman GJ. The CD160, BTLA, LIGHT/HVEM pathway: a bidirectional switch regulating T-cell activation. *Immunol Rev*. May 2009;229(1):244-58. doi:10.1111/j.1600-065X.2009.00783.x

189. Leitner J, Grabmeier-Pfistershammer K, Steinberger P. Receptors and ligands implicated in human T cell costimulatory processes. *Immunol Lett*. Feb 2010;128(2):89-97. doi:10.1016/j.imlet.2009.11.009

190. Rohaan MW, van den Berg JH, Kvistborg P, Haanen JBAG. Adoptive transfer of tumor-infiltrating lymphocytes in melanoma: a viable treatment option. *J Immunother Cancer*. 10 2018;6(1):102. doi:10.1186/s40425-018-0391-1

191. Robertson J, Salm M, Dangl M. Adoptive cell therapy with tumour-infiltrating lymphocytes: the emerging importance of clonal neoantigen targets for next-generation products in non-small cell lung cancer. *Immuno-Oncology Technology*. 2019/10/01/ 2019;3:1-7. doi:https://doi.org/10.1016/j.iotech.2019.09.003

192. Geukes Foppen MH, Donia M, Svane IM, Haanen JB. Tumor-infiltrating lymphocytes for the treatment of metastatic cancer. *Mol Oncol*. Dec 2015;9(10):1918-35. doi:10.1016/j.molonc.2015.10.018

193. Noonan KA, Huff CA, Davis J, et al. Adoptive transfer of activated marrow-infiltrating lymphocytes induces measurable antitumor immunity in the bone marrow in multiple myeloma. *Sci Transl Med*. May 2015;7(288):288ra78. doi:10.1126/scitranslmed.aaa7014

194. Johnson LA, Morgan RA, Dudley ME, et al. Gene therapy with human and mouse T-cell receptors mediates cancer regression and targets normal tissues expressing cognate antigen. *Blood*. Jul 2009;114(3):535-46. doi:10.1182/blood-2009-03-211714

195. Simpson AJ, Caballero OL, Jungbluth A, Chen YT, Old LJ. Cancer/testis antigens, gametogenesis and cancer. *Nat Rev Cancer*. Aug 2005;5(8):615-25. doi:10.1038/nrc1669

196. Rapoport AP, Stadtmauer EA, Binder-Scholl GK, et al. NY-ESO-1-specific TCR-engineered T cells mediate sustained antigen-specific antitumor effects in myeloma. *Nat Med*. Aug 2015;21(8):914-921. doi:10.1038/nm.3910

197. Rapoport A, Hoffman JE, Kaufman JL, et al. Open-label pilot study of genetically engineered NY-ESO-1–specific t cells (GSK3377794) alone or in combination with pembrolizumab in relapsed/refractory multiple

myeloma. *Journal of Clinical Oncology*. 2020;38(15_suppl):TPS8555-TPS8555. doi:10.1200/JCO.2020.38.15_suppl.TPS8555

198. Cameron BJ, Gerry AB, Dukes J, et al. Identification of a Titin-derived HLA-A1-presented peptide as a cross-reactive target for engineered MAGE A3-directed T cells. *Sci Transl Med*. Aug 2013;5(197):197ra103. doi:10.1126/scitranslmed.3006034

199. Linette GP, Stadtmauer EA, Maus MV, et al. Cardiovascular toxicity and titin cross-reactivity of affinity-enhanced T cells in myeloma and melanoma. *Blood*. Aug 2013;122(6):863-71. doi:10.1182/blood-2013-03-490565

200. Garrido F, Aptsiauri N, Doorduijn EM, Garcia Lora AM, van Hall T. The urgent need to recover MHC class I in cancers for effective immunotherapy. *Curr Opin Immunol*. Apr 2016;39:44-51. doi:10.1016/j.coi.2015.12.007

201. June CH, O'Connor RS, Kawalekar OU, Ghassemi S, Milone MC. CAR T cell immunotherapy for human cancer. *Science*. 03 2018;359(6382):1361-1365. doi:10.1126/science.aar6711

202. Guedan S, Calderon H, Posey AD, Maus MV. Engineering and Design of Chimeric Antigen Receptors. *Mol Ther Methods Clin Dev*. Mar 2019;12:145-156. doi:10.1016/j.omtm.2018.12.009

203. Guest RD, Hawkins RE, Kirillova N, et al. The role of extracellular spacer regions in the optimal design of chimeric immune receptors: evaluation of four different scFvs and antigens. *J Immunother*. 2005 May-Jun 2005;28(3):203-11. doi:10.1097/01.cji.0000161397.96582.59

204. Hudecek M, Lupo-Stanghellini MT, Kosasih PL, et al. Receptor affinity and extracellular domain modifications affect tumor recognition by ROR1-specific chimeric antigen receptor T cells. *Clin Cancer Res*. Jun 2013;19(12):3153-64. doi:10.1158/1078-0432.CCR-13-0330

205. Hombach A, Hombach AA, Abken H. Adoptive immunotherapy with genetically engineered T cells: modification of the IgG1 Fc 'spacer' domain in the extracellular moiety of chimeric antigen receptors avoids 'off-target' activation and unintended initiation of an innate immune response. *Gene Ther*. Oct 2010;17(10):1206-13. doi:10.1038/gt.2010.91

206. Eshhar Z, Waks T, Gross G, Schindler DG. Specific activation and targeting of cytotoxic lymphocytes through chimeric single chains consisting of antibody-binding domains and the gamma or zeta subunits of the immunoglobulin and T-cell receptors. *Proc Natl Acad Sci U S A*. Jan 1993;90(2):720-4. doi:10.1073/pnas.90.2.720

207. Brocker T, Karjalainen K. Signals through T cell receptor-zeta chain alone are insufficient to prime resting T lymphocytes. *J Exp Med*. May 1995;181(5):1653-9. doi:10.1084/jem.181.5.1653

208. Gong MC, Latouche JB, Krause A, Heston WD, Bander NH, Sadelain M. Cancer patient T cells genetically targeted to prostate-specific membrane antigen specifically lyse prostate cancer cells and release cytokines in response to prostate-specific membrane antigen. *Neoplasia*. Jun 1999;1(2):123-7. doi:10.1038/sj.neo.7900018

209. Brocker T. Chimeric Fv-zeta or Fv-epsilon receptors are not sufficient to induce activation or cytokine production in peripheral T cells. *Blood*. Sep 2000;96(5):1999-2001.

210. Schuster SJ, Bishop MR, Tam CS, et al. Tisagenlecleucel in Adult Relapsed or Refractory Diffuse Large B-Cell Lymphoma. *N Engl J Med*. 01 2019;380(1):45-56. doi:10.1056/NEJMoa1804980

211. Maude SL, Laetsch TW, Buechner J, et al. Tisagenlecleucel in Children and Young Adults with B-Cell Lymphoblastic Leukemia. *N Engl J Med*. 02 2018;378(5):439-448. doi:10.1056/NEJMoa1709866

212. Locke FL, Ghobadi A, Jacobson CA, et al. Long-term safety and activity of axicabtagene ciloleucel in refractory large B-cell lymphoma (ZUMA-1): a single-arm, multicentre, phase 1-2 trial. *Lancet Oncol*. 01 2019;20(1):31-42. doi:10.1016/S1470-2045(18)30864-7

213. Jayaraman J, Mellody MP, Hou AJ, et al. CAR-T design: Elements and their synergistic function. *EBioMedicine*. Aug 2020;58:102931. doi:10.1016/j.ebiom.2020.102931

214. MacKay M, Afshinnekoo E, Rub J, et al. The therapeutic landscape for cells engineered with chimeric antigen receptors. *Nat Biotechnol*. 02 2020;38(2):233-244. doi:10.1038/s41587-019-0329-2

215. Pettitt D, Arshad Z, Smith J, Stanic T, Holländer G, Brindley D. CAR-T Cells: A Systematic Review and Mixed Methods Analysis of the Clinical Trial Landscape. *Mol Ther*. 02 2018;26(2):342-353. doi:10.1016/j.ymthe.2017.10.019

216. Bagley SJ, O'Rourke DM. Clinical investigation of CAR T cells for solid tumors: Lessons learned and future directions. *Pharmacol Ther*. 01 2020;205:107419. doi:10.1016/j.pharmthera.2019.107419

217. Brudno JN, Maric I, Hartman SD, et al. T Cells Genetically Modified to Express an Anti-B-Cell Maturation Antigen Chimeric Antigen Receptor Cause Remissions of Poor-Prognosis Relapsed Multiple Myeloma. *J Clin Oncol*. 08 2018;36(22):2267-2280. doi:10.1200/JCO.2018.77.8084

218. Munshi NC, Anderson LD, Shah N, et al. Idecabtagene Vicleucel in Relapsed and Refractory Multiple Myeloma. *N Engl J Med*. 02 2021;384(8):705-716. doi:10.1056/NEJMoa2024850

219. Alsina M, Shah N, Raje NS, et al. Updated Results from the Phase I CRB-402 Study of Anti-Bcma CAR-T Cell Therapy bb21217 in Patients with Relapsed and Refractory Multiple Myeloma: Correlation of Expansion and Duration of Response with T Cell Phenotypes. *Blood*. 2020;136(Supplement 1):25-26. doi:10.1182/blood-2020-140410

220. Cohen AD, Garfall AL, Stadtmauer EA, et al. B cell maturation antigen-specific CAR T cells are clinically active in multiple myeloma. *J Clin Invest*. 03 2019;129(6):2210-2221. doi:10.1172/JCI126397

221. Mailankody S, Jakubowiak AJ, Htut M, et al. Orvacabtagene autoleucel (orva-cel), a B-cell maturation antigen (BCMA)-directed CAR T cell therapy for patients (pts) with relapsed/refractory multiple myeloma (RRMM): update of the phase 1/2 EVOLVE study (NCT03430011). *Journal of Clinical Oncology*. 2020;38(15_suppl):8504-8504. doi:10.1200/JCO.2020.38.15_suppl.8504

222. Zhao WH, Liu J, Wang BY, et al. A phase 1, open-label study of LCAR-B38M, a chimeric antigen receptor T cell therapy directed against B cell maturation antigen, in patients with relapsed or refractory multiple myeloma. *J Hematol Oncol*. 12 2018;11(1):141. doi:10.1186/s13045-018-0681-6

223. Xu J, Chen LJ, Yang SS, et al. Exploratory trial of a biepitopic CAR T-targeting B cell maturation antigen in relapsed/refractory multiple myeloma. *Proc Natl Acad Sci U S A*. May 2019;116(19):9543-9551. doi:10.1073/pnas.1819745116

224. Madduri D, Berdeja JG, Usmani SZ, et al. CARTITUDE-1: Phase 1b/2 Study of Ciltacabtagene Autoleucel, a B-Cell Maturation Antigen-Directed Chimeric Antigen Receptor T Cell Therapy, in Relapsed/Refractory Multiple Myeloma. *Blood*. 2020;136(Supplement 1):22-25. doi:10.1182/blood-2020-136307

225. Mikkilineni L, Manasanch EE, Vanasse D, et al. Deep and Durable Remissions of Relapsed Multiple Myeloma on a First-in-Humans Clinical Trial of T Cells Expressing an Anti-B-Cell Maturation Antigen (BCMA) Chimeric Antigen Receptor (CAR) with a Fully-Human Heavy-Chain-Only Antigen Recognition Domain. *Blood*. 2020;136(Supplement 1):50-51. doi:10.1182/blood-2020-138839

226. Kumar SK, Baz RC, Orlowski RZ, et al. Results from Lummicar-2: A Phase 1b/2 Study of Fully Human B-Cell Maturation Antigen-Specific CAR T Cells (CT053) in Patients with Relapsed and/or Refractory Multiple Myeloma. *Blood*. 2020;136(Supplement 1):28-29. doi:10.1182/blood-2020-139802

227. Costello CL, Cohen AD, Patel KK, et al. Phase 1/2 Study of the Safety and Response of P-BCMA-101 CAR-T Cells in Patients with Relapsed/Refractory (r/r) Multiple Myeloma (MM) (PRIME) with Novel Therapeutic Strategies. *Blood*. 2020;136(Supplement 1):29-30. doi:10.1182/blood-2020-142695

228. Frigault MJ, Bishop MR, O'Donnell EK, et al. Phase 1 Study of CART-Ddbcma, a CAR-T Therapy Utilizing a Novel Synthetic Binding Domain for the Treatment of Subjects with Relapsed and Refractory Multiple Myeloma. *Blood*. 2020;136(Supplement 1):2-2. doi:10.1182/blood-2020-142931

229. Mailankody S, Matous JV, Liedtke M, et al. Universal: An Allogeneic First-in-Human Study of the Anti-Bcma ALLO-715 and the Anti-CD52 ALLO-647 in Relapsed/Refractory Multiple Myeloma. *Blood*. 2020;136(Supplement 1):24-25. doi:10.1182/blood-2020-140641

230. Mikkilineni L, Kochenderfer JN. Chimeric antigen receptor T-cell therapies for multiple myeloma. *Blood*. 12 2017;130(24):2594-2602. doi:10.1182/blood-2017-06-793869

231. Garfall AL, Stadtmauer EA, Hwang WT, et al. Anti-CD19 CAR T cells with high-dose melphalan and autologous stem cell transplantation for refractory multiple myeloma. *JCI Insight*. 02 2019;4(4)doi:10.1172/jci.insight.127684

232. Gagelmann N, Riecken K, Wolschke C, et al. Development of CAR-T cell therapies for multiple myeloma. *Leukemia*. 09 2020;34(9):2317-2332. doi:10.1038/s41375-020-0930-x

233. Majzner RG, Mackall CL. Tumor Antigen Escape from CAR T-cell Therapy. *Cancer Discov*. 10 2018;8(10):1219-1226. doi:10.1158/2159-8290.CD-18-0442

234. Orlando EJ, Han X, Tribouley C, et al. Genetic mechanisms of target antigen loss in CAR19 therapy of acute lymphoblastic leukemia. *Nat Med*. 10 2018;24(10):1504-1506. doi:10.1038/s41591-018-0146-z

235. Fry TJ, Shah NN, Orentas RJ, et al. CD22-targeted CAR T cells induce remission in B-ALL that is naive or resistant to CD19-targeted CAR immunotherapy. *Nat Med*. Jan 2018;24(1):20-28. doi:10.1038/nm.4441

236. Finney OC, Brakke HM, Rawlings-Rhea S, et al. CD19 CAR T cell product and disease attributes predict leukemia remission durability. *J Clin Invest*. 05 2019;129(5):2123-2132. doi:10.1172/JCI125423

237. Gardner RA, Finney O, Annesley C, et al. Intent-to-treat leukemia remission by CD19 CAR T cells of defined formulation and dose in children and young adults. *Blood*. 06 2017;129(25):3322-3331. doi:10.1182/blood-2017-02-769208

238. Long AH, Haso WM, Shern JF, et al. 4-1BB costimulation ameliorates T cell exhaustion induced by tonic signaling of chimeric antigen receptors. *Nat Med*. Jun 2015;21(6):581-90. doi:10.1038/nm.3838

239. Samur MK, Fulciniti M, Aktas-Samur A, et al. Biallelic Loss of BCMA Triggers Resistance to Anti-BCMA CAR T Cell Therapy in Multiple Myeloma. *Blood*. 2020;136(Supplement 1):14-14. doi:10.1182/blood-2020-139040

240. Laurent SA, Hoffmann FS, Kuhn PH, et al. γ-Secretase directly sheds the survival receptor BCMA from plasma cells. *Nat Commun*. Jun 2015;6:7333. doi:10.1038/ncomms8333

241. Pont MJ, Hill T, Cole GO, et al. γ-Secretase inhibition increases efficacy of BCMA-specific chimeric antigen receptor T cells in multiple myeloma. *Blood*. 11 2019;134(19):1585-1597. doi:10.1182/blood.2019000050

242. Raje N, Berdeja J, Lin Y, et al. Anti-BCMA CAR T-Cell Therapy bb2121 in Relapsed or Refractory Multiple Myeloma. *N Engl J Med*. 05 2019;380(18):1726-1737. doi:10.1056/NEJMoa1817226

243. Ali SA, Shi V, Maric I, et al. T cells expressing an anti-B-cell maturation antigen chimeric antigen receptor cause remissions of multiple myeloma. *Blood*. 09 2016;128(13):1688-700. doi:10.1182/blood-2016-04-711903

244. Cohen AD, Garfall AL, Dogan A, et al. Serial treatment of relapsed/refractory multiple myeloma with different BCMA-targeting therapies. *Blood Adv*. 08 2019;3(16):2487-2490. doi:10.1182/bloodadvances.2019000466

245. Morgan RA, Yang JC, Kitano M, Dudley ME, Laurencot CM, Rosenberg SA. Case report of a serious adverse event following the administration of T cells transduced with a chimeric antigen receptor recognizing ERBB2. *Mol Ther*. Apr 2010;18(4):843-51. doi:10.1038/mt.2010.24

246. Lamers CH, Sleijfer S, van Steenbergen S, et al. Treatment of metastatic renal cell carcinoma with CAIX CAR-engineered T cells: clinical evaluation and management of on-target toxicity. *Mol Ther*. Apr 2013;21(4):904-12. doi:10.1038/mt.2013.17

247. Laetsch TW, Myers GD, Baruchel A, et al. Patient-reported quality of life after tisagenlecleucel infusion in children and young adults with relapsed or refractory B-cell acute lymphoblastic leukaemia: a global, single-arm, phase 2 trial. *Lancet Oncol*. 12 2019;20(12):1710-1718. doi:10.1016/S1470-2045(19)30493-0

248. Liu X, Jiang S, Fang C, et al. Affinity-Tuned ErbB2 or EGFR Chimeric Antigen Receptor T Cells Exhibit an Increased Therapeutic Index against Tumors in Mice. *Cancer Res*. Sep 2015;75(17):3596-607. doi:10.1158/0008-5472.CAN-15-0159

249. Santomasso B, Bachier C, Westin J, Rezvani K, Shpall EJ. The Other Side of CAR T-Cell Therapy: Cytokine Release Syndrome, Neurologic Toxicity, and Financial Burden. *American Society of Clinical Oncology Educational Book*. 2019;(39):433-444. doi:10.1200/edbk_238691

250. Lee DW, Gardner R, Porter DL, et al. Current concepts in the diagnosis and management of cytokine release syndrome. *Blood*. Jul 2014;124(2):188-95. doi:10.1182/blood-2014-05-552729

251. Lee DW, Santomasso BD, Locke FL, et al. ASTCT Consensus Grading for Cytokine Release Syndrome and Neurologic Toxicity Associated with Immune Effector Cells. *Biol Blood Marrow Transplant*. 04 2019;25(4):625-638. doi:10.1016/j.bbmt.2018.12.758

252. Xu Y, Yang Z, Horan LH, et al. A novel antibody-TCR (AbTCR) platform combines Fab-based antigen recognition with gamma/delta-TCR signaling to facilitate T-cell cytotoxicity with low cytokine release. *Cell Discov*. 2018;4:62. doi:10.1038/s41421-018-0066-6

253. Ying ZT, Long L, Liu H, et al. ET190L1-ARTEMIS T cell therapy to induce complete remission of relapsed and refractory (r/r) B-cell lymphoma with no cytokine release syndrome in the first-in-human clinical study. *Journal of Clinical Oncology*. 2018;36(15_suppl):3049-3049. doi:10.1200/JCO.2018.36.15_suppl.3049

254. Baeuerle PA, Ding J, Patel E, et al. Synthetic TRuC receptors engaging the complete T cell receptor for potent anti-tumor response. *Nat Commun*. 05 2019;10(1):2087. doi:10.1038/s41467-019-10097-0

255. Helsen CW, Hammill JA, Lau VWC, et al. The chimeric TAC receptor co-opts the T cell receptor yielding robust anti-tumor activity without toxicity. *Nat Commun*. Aug 2018;9(1):3049. doi:10.1038/s41467-018-05395-y

256. Rabinovich BA, Ye Y, Etto T, et al. Visualizing fewer than 10 mouse T cells with an enhanced firefly luciferase in immunocompetent mouse models of cancer. *Proc Natl Acad Sci U S A*. Sep 2008;105(38):14342-6. doi:10.1073/pnas.0804105105

257. Schaub FX, Reza MS, Flaveny CA, et al. Fluorophore-NanoLuc BRET Reporters Enable Sensitive In Vivo Optical Imaging and Flow Cytometry for Monitoring Tumorigenesis. *Cancer Res*. Dec 2015;75(23):5023-33. doi:10.1158/0008-5472.CAN-14-3538

258. Helsen CW, Bramson J, Dvorkin-Gheva A, Denisova GF, Bezverbnaya K, Mwawasi KA, inventors; T Cell-Antigen Coupler with Y182T Mutation and Methods and Uses Thereof (PCT/CA2018/051290). patent application PCT/CA2018/051290. 2019.

259. Whitlow M, Bell BA, Feng SL, et al. An improved linker for single-chain Fv with reduced aggregation and enhanced proteolytic stability. *Protein Eng*. Nov 1993;6(8):989-95.

260. Hammill JA, Kwiecien JM, Dvorkin-Gheva A, et al. A Cross-Reactive Small Protein Binding Domain Provides a Model to Study Off-Tumor CAR-T Cell Toxicity. *Mol Ther Oncolytics*. Jun 2020;17:278-292. doi:10.1016/j.omto.2020.04.001

261. Hammill JA, VanSeggelen H, Helsen CW, et al. Designed ankyrin repeat proteins are effective targeting elements for chimeric antigen receptors. *J Immunother Cancer*. 2015;3:55. doi:10.1186/s40425-015-0099-4

262. Kozakov D, Hall DR, Xia B, et al. The ClusPro web server for protein-protein docking. *Nat Protoc*. Feb 2017;12(2):255-278. doi:10.1038/nprot.2016.169

263. Sobolev V, Sorokine A, Prilusky J, Abola EE, Edelman M. Automated analysis of interatomic contacts in proteins. *Bioinformatics*. Apr 1999;15(4):327-32. doi:10.1093/bioinformatics/15.4.327

264. Monaco G, Chen H, Poidinger M, Chen J, de Magalhães JP, Larbi A. flowAI: automatic and interactive anomaly discerning tools for flow cytometry data. *Bioinformatics*. 08 2016;32(16):2473-80. doi:10.1093/bioinformatics/btw191

265. Van Gassen S, Callebaut B, Van Helden MJ, et al. FlowSOM: Using self-organizing maps for visualization and interpretation of cytometry data. *Cytometry A*. Jul 2015;87(7):636-45. doi:10.1002/cyto.a.22625

266. Weber LM, Nowicka M, Soneson C, Robinson MD. diffcyt: Differential discovery in high-dimensional cytometry via high-resolution clustering. *Commun Biol*. 2019;2:183. doi:10.1038/s42003-019-0415-5

267. Amir e-A, Davis KL, Tadmor MD, et al. viSNE enables visualization of high dimensional single-cell data and reveals phenotypic heterogeneity of leukemia. *Nat Biotechnol*. Jun 2013;31(6):545-52. doi:10.1038/nbt.2594

268. *CATALYST: Cytometry dATa anALYSis Tools. R Package Version 1.14.0*. 2020.

269. Bertolet G, Liu D. The Planar Lipid Bilayer System Serves as a Reductionist Approach for Studying NK Cell Immunological Synapses and Their Functions. *Methods Mol Biol*. 2016;1441:151-65. doi:10.1007/978-1-4939-3684-7_13

270. Schindelin J, Arganda-Carreras I, Frise E, et al. Fiji: an open-source platform for biological-image analysis. *Nat Methods*. Jun 2012;9(7):676-82. doi:10.1038/nmeth.2019

271. Holstein SA, McCarthy PL. Immunomodulatory Drugs in Multiple Myeloma: Mechanisms of Action and Clinical Experience. *Drugs*. Apr 2017;77(5):505-520. doi:10.1007/s40265-017-0689-1

272. Asatsuma-Okumura T, Ito T, Handa H. Molecular mechanisms of cereblon-based drugs. *Pharmacol Ther*. Oct 2019;202:132-139. doi:10.1016/j.pharmthera.2019.06.004

273. Kunacheewa C, Orlowski RZ. New Drugs in Multiple Myeloma. *Annu Rev Med*. 01 2019;70:521-547. doi:10.1146/annurev-med-112017-091045

274. Ghobrial I, Cruz CH, Garfall A, et al. Immunotherapy in Multiple Myeloma: Accelerating on the Path to the Patient. *Clin Lymphoma Myeloma Leuk*. Jun 2019;19(6):332-344. doi:10.1016/j.clml.2019.02.004

275. Kriegsmann K, Kriegsmann M, Cremer M, et al. Cell-based immunotherapy approaches for multiple myeloma. *Br J Cancer*. 01 2019;120(1):38-44. doi:10.1038/s41416-018-0346-9

276. Yu B, Liu D. Antibody-drug conjugates in clinical trials for lymphoid malignancies and multiple myeloma. *J Hematol Oncol*. Sep 2019;12(1):94. doi:10.1186/s13045-019-0786-6

277. Iftikhar A, Hassan H, Iftikhar N, et al. Investigational Monoclonal Antibodies in the Treatment of Multiple Myeloma: A Systematic Review of Agents under Clinical Development. *Antibodies (Basel)*. May 2019;8(2)doi:10.3390/antib8020034

278. Smith EL, Harrington K, Staehr M, et al. GPRC5D is a target for the immunotherapy of multiple myeloma with rationally designed CAR T cells. *Sci Transl Med*. 03 2019;11(485)doi:10.1126/scitranslmed.aau7746

279. Hatzoglou A, Roussel J, Bourgeade MF, et al. TNF receptor family member BCMA (B cell maturation) associates with TNF receptor-associated factor (TRAF) 1, TRAF2, and TRAF3 and activates NF-kappa B, elk-1, c-Jun N-terminal kinase, and p38 mitogen-activated protein kinase. *J Immunol*. Aug 2000;165(3):1322-30. doi:10.4049/jimmunol.165.3.1322

280. Novak AJ, Darce JR, Arendt BK, et al. Expression of BCMA, TACI, and BAFF-R in multiple myeloma: a mechanism for growth and survival. *Blood*. Jan 2004;103(2):689-94. doi:10.1182/blood-2003-06-2043

281. Topp MS, Duell J, Zugmaier G, et al. Evaluation of AMG 420, an anti-BCMA bispecific T-cell engaged (BiTE) immunotherapy, in R/R multiple myeloma (MM) patients: Updated results of a first in-human (FIH) phase I dose escalation study. presented at: ASCO Annual Meeting; 2019;

282. Cohen AD, Melenhorst JJ, Garfall AL, et al. Predictors of T Cell Expansion and Clinical Responses Following B-Cell Maturation Antigen-Specific Chimeric Antigen Receptor T Cell Therapy (CART-BCMA) for

Relapsed/Refractory Multiple Myeloma (MM). *Blood*. 2018;132(Supplement 1):1974-1974. doi:10.1182/blood-2018-99-119665

283. Berdeja JG, Alsina M, Shah ND, et al. Updated Results from an Ongoing Phase 1 Clinical Study of bb21217 Anti-Bcma CAR T Cell Therapy. *Blood*. 2019;134(Supplement_1):927-927. doi:10.1182/blood-2019-126660

284. Costello CL, Gregory TK, Ali SA, et al. Phase 2 Study of the Response and Safety of P-Bcma-101 CAR-T Cells in Patients with Relapsed/Refractory (r/r) Multiple Myeloma (MM) (PRIME). *Blood*. 2019;134(Supplement_1):3184-3184. doi:10.1182/blood-2019-129562

285. Madduri D, Usmani SZ, Jagannath S, et al. Results from CARTITUDE-1: A Phase 1b/2 Study of JNJ-4528, a CAR-T Cell Therapy Directed Against B-Cell Maturation Antigen (BCMA), in Patients with Relapsed and/or Refractory Multiple Myeloma (R/R MM). *Blood*. 2019;134(Supplement_1):577-577. doi:10.1182/blood-2019-121731

286. Mailankody S, Htut M, Lee KP, et al. JCARH125, Anti-BCMA CAR T-cell Therapy for Relapsed/Refractory Multiple Myeloma: Initial Proof of Concept Results from a Phase 1/2 Multicenter Study (EVOLVE). *Blood*. 2018;132(Supplement 1):957-957. doi:10.1182/blood-2018-99-113548

287. Han L, Gao Q, Zhou K, et al. The phase I clinical study of CART targeting BCMA with humanized alpaca-derived single-domain antibody as antigen recognition domain. *Journal of Clinical Oncology*. 2019;37(15_suppl):2535-2535. doi:10.1200/JCO.2019.37.15_suppl.2535

288. Khalaf WS, Garg M, Mohamed YS, Stover CM, Browning MJ. Generation of Cytotoxic T Cells With Potential for Adoptive Tumor Immunotherapy of Multiple Myeloma. *Front Immunol*. 2019;10:1792. doi:10.3389/fimmu.2019.01792

289. Stadtmauer EA, Faitg TH, Lowther DE, et al. Long-term safety and activity of NY-ESO-1 SPEAR T cells after autologous stem cell transplant for myeloma. *Blood Adv*. Jul 2019;3(13):2022-2034. doi:10.1182/bloodadvances.2019000194

290. Jahn L, Hombrink P, Hagedoorn RS, et al. TCR-based therapy for multiple myeloma and other B-cell malignancies targeting intracellular transcription factor BOB1. *Blood*. 03 2017;129(10):1284-1295. doi:10.1182/blood-2016-09-737536

291. Raje NS, Berdeja JG, Lin Y, et al. bb2121 anti-BCMA CAR T-cell therapy in patients with relapsed/refractory multiple myeloma: Updated results from a multicenter phase I study. J Clin Oncol; 2018:Abstract 8007.

292. Ramos CA, Savoldo B, Torrano V, et al. Clinical responses with T lymphocytes targeting malignancy-associated κ light chains. *J Clin Invest*. 07 2016;126(7):2588-96. doi:10.1172/JCI86000

293. Fischer J, Paret C, El Malki K, et al. CD19 Isoforms Enabling Resistance to CART-19 Immunotherapy Are Expressed in B-ALL Patients at Initial Diagnosis. *J Immunother*. 06 2017;40(5):187-195. doi:10.1097/CJI.0000000000000169

294. Sotillo E, Barrett DM, Black KL, et al. Convergence of Acquired Mutations and Alternative Splicing of CD19 Enables Resistance to CART-19 Immunotherapy. *Cancer Discov*. Dec 2015;5(12):1282-95. doi:10.1158/2159-8290.CD-15-1020

295. Shalaby MR, Shepard HM, Presta L, et al. Development of humanized bispecific antibodies reactive with cytotoxic lymphocytes and tumor cells overexpressing the HER2 protooncogene. *J Exp Med*. Jan 1992;175(1):217-25. doi:10.1084/jem.175.1.217

296. Zhu Z, Carter P. Identification of heavy chain residues in a humanized anti-CD3 antibody important for efficient antigen binding and T cell activation. *J Immunol*. Aug 1995;155(4):1903-10.

297. Helsen CW, Bramson J, Dvorkin-Gheva A, Denisova GF, Bezverbnaya K, Mwawasi KA, inventors; T Cell-Antigen Coupler with Y182T Mutation and Methods and Uses Thereof (WO2019071358). patent application PCT/CA2018/051290. 2019.

298. Frigault MJ, Lee J, Basil MC, et al. Identification of chimeric antigen receptors that mediate constitutive or inducible proliferation of T cells. *Cancer Immunol Res*. Apr 2015;3(4):356-67. doi:10.1158/2326-6066.CIR-14-0186

299. Gomes-Silva D, Mukherjee M, Srinivasan M, et al. Tonic 4-1BB Costimulation in Chimeric Antigen Receptors Impedes T Cell Survival and Is Vector-Dependent. *Cell Rep*. Oct 2017;21(1):17-26. doi:10.1016/j.celrep.2017.09.015

300. Sakemura R, Terakura S, Watanabe K, et al. A Tet-On Inducible System for Controlling CD19-Chimeric Antigen Receptor Expression upon Drug Administration. *Cancer Immunol Res*. 08 2016;4(8):658-68. doi:10.1158/2326-6066.CIR-16-0043

301. Ritter AT, Asano Y, Stinchcombe JC, et al. Actin depletion initiates events leading to granule secretion at the immunological synapse. *Immunity*. May 2015;42(5):864-76. doi:10.1016/j.immuni.2015.04.013

302. Monks CR, Freiberg BA, Kupfer H, Sciaky N, Kupfer A. Three-dimensional segregation of supramolecular activation clusters in T cells. *Nature*. Sep 1998;395(6697):82-6. doi:10.1038/25764

303. Ashouri JF, Weiss A. Endogenous Nur77 Is a Specific Indicator of Antigen Receptor Signaling in Human T and B Cells. *J Immunol*. 01 2017;198(2):657-668. doi:10.4049/jimmunol.1601301

304. Smith KA. Interleukin-2: inception, impact, and implications. *Science*. May 1988;240(4856):1169-76. doi:10.1126/science.3131876

305. Walter P, Johnson AE. Signal sequence recognition and protein targeting to the endoplasmic reticulum membrane. *Annu Rev Cell Biol*. 1994;10:87-119. doi:10.1146/annurev.cb.10.110194.000511

306. Owji H, Nezafat N, Negahdaripour M, Hajiebrahimi A, Ghasemi Y. A comprehensive review of signal peptides: Structure, roles, and applications. *Eur J Cell Biol*. Aug 2018;97(6):422-441. doi:10.1016/j.ejcb.2018.06.003

307. Eyquem J, Mansilla-Soto J, Giavridis T, et al. Targeting a CAR to the TRAC locus with CRISPR/Cas9 enhances tumour rejection. *Nature*. 03 2017;543(7643):113-117. doi:10.1038/nature21405

308. Roybal KT, Rupp LJ, Morsut L, et al. Precision Tumor Recognition by T Cells With Combinatorial Antigen-Sensing Circuits. *Cell*. Feb 2016;164(4):770-9. doi:10.1016/j.cell.2016.01.011

309. Tsun A, Qureshi I, Stinchcombe JC, et al. Centrosome docking at the immunological synapse is controlled by Lck signaling. *J Cell Biol*. Feb 2011;192(4):663-74. doi:10.1083/jcb.201008140

310. Labrecque N, Whitfield LS, Obst R, Waltzinger C, Benoist C, Mathis D. How much TCR does a T cell need? *Immunity*. Jul 2001;15(1):71-82. doi:10.1016/s1074-7613(01)00170-4

311. Perez OD, Mitchell D, Jager GC, et al. Leukocyte functional antigen 1 lowers T cell activation thresholds and signaling through cytohesin-1 and Jun-activating binding protein 1. *Nat Immunol*. Nov 2003;4(11):1083-92. doi:10.1038/ni984

312. Fuller MJ, Zajac AJ. Ablation of CD8 and CD4 T cell responses by high viral loads. *J Immunol*. Jan 2003;170(1):477-86. doi:10.4049/jimmunol.170.1.477

313. Itoh Y, Germain RN. Single cell analysis reveals regulated hierarchical T cell antigen receptor signaling thresholds and intraclonal heterogeneity for individual cytokine responses of CD4+ T cells. *J Exp Med*. Aug 1997;186(5):757-66. doi:10.1084/jem.186.5.757

314. Brown RD, Pope B, Yuen E, Gibson J, Joshua DE. The expression of T cell related costimulatory molecules in multiple myeloma. *Leuk Lymphoma*. Oct 1998;31(3-4):379-84. doi:10.3109/10428199809059231

315. Mozaffari F, Hansson L, Kiaii S, et al. Signalling molecules and cytokine production in T cells of multiple myeloma-increased abnormalities with advancing stage. *Br J Haematol*. Feb 2004;124(3):315-24. doi:10.1046/j.1365-2141.2003.04789.x

316. Bianchi A, Mariani S, Beggiato E, et al. Distribution of T-cell signalling molecules in human myeloma. *Br J Haematol*. Jun 1997;97(4):815-20. doi:10.1046/j.1365-2141.1997.1482961.x

317. Bezverbnaya K, Mathews A, Sidhu J, Helsen CW, Bramson JL. Tumor-targeting domains for chimeric antigen receptor T cells. *Immunotherapy*. 01 2017;9(1):33-46. doi:10.2217/imt-2016-0103

318. Ahmad ZA, Yeap SK, Ali AM, Ho WY, Alitheen NB, Hamid M. scFv antibody: principles and clinical application. *Clin Dev Immunol*. 2012;2012:980250. doi:10.1155/2012/980250

319. Tiller KE, Tessier PM. Advances in Antibody Design. *Annu Rev Biomed Eng*. 2015;17:191-216. doi:10.1146/annurev-bioeng-071114-040733

320. Kang TH, Seong BL. Solubility, Stability, and Avidity of Recombinant Antibody Fragments Expressed in Microorganisms. *Front Microbiol*. 2020;11:1927. doi:10.3389/fmicb.2020.01927

321. Gil D, Schrum AG. Strategies to stabilize compact folding and minimize aggregation of antibody-based fragments. *Adv Biosci Biotechnol*. Apr 2013;4(4a):73-84. doi:10.4236/abb.2013.44A011

322. Chen X, Zaro JL, Shen WC. Fusion protein linkers: property, design and functionality. *Adv Drug Deliv Rev*. Oct 2013;65(10):1357-69. doi:10.1016/j.addr.2012.09.039

323. Gu X, Jia X, Feng J, et al. Molecular modeling and affinity determination of scFv antibody: proper linker peptide enhances its activity. *Ann Biomed Eng*. Feb 2010;38(2):537-49. doi:10.1007/s10439-009-9810-2

324. Shen Z, Yan H, Zhang Y, Mernaugh RL, Zeng X. Engineering peptide linkers for scFv immunosensors. *Anal Chem*. Mar 2008;80(6):1910-7. doi:10.1021/ac7018624

325. Nie Y, Lu W, Chen D, et al. Mechanisms underlying CD19-positive ALL relapse after anti-CD19 CAR T cell therapy and associated strategies. *Biomark Res*. 2020;8:18. doi:10.1186/s40364-020-00197-1

326. Turtle CJ, Hanafi LA, Berger C, et al. CD19 CAR-T cells of defined CD4+:CD8+ composition in adult B cell ALL patients. *J Clin Invest*. 06 2016;126(6):2123-38. doi:10.1172/JCI85309

327. Maus MV, Haas AR, Beatty GL, et al. T cells expressing chimeric antigen receptors can cause anaphylaxis in humans. *Cancer Immunol Res*. Jul 2013;1(1):26-31. doi:10.1158/2326-6066.CIR-13-0006

328. Kuroda D, Shirai H, Jacobson MP, Nakamura H. Computer-aided antibody design. *Protein Eng Des Sel*. Oct 2012;25(10):507-21. doi:10.1093/protein/gzs024

329. Simms PE, Ellis TM. Utility of flow cytometric detection of CD69 expression as a rapid method for determining poly- and oligoclonal lymphocyte activation. *Clin Diagn Lab Immunol*. May 1996;3(3):301-4.

330. Otsuki T, Yamada O, Yata K, et al. Expression and production of interleukin 10 in human myeloma cell lines. *Br J Haematol*. Dec 2000;111(3):835-42.

331. Husain B, Ellerman D. Expanding the Boundaries of Biotherapeutics with Bispecific Antibodies. *BioDrugs*. Oct 2018;32(5):441-464. doi:10.1007/s40259-018-0299-9

332. Park S, Shevlin E, Vedvyas Y, et al. Micromolar affinity CAR T cells to ICAM-1 achieves rapid tumor elimination while avoiding systemic toxicity. *Sci Rep*. 10 2017;7(1):14366. doi:10.1038/s41598-017-14749-3

333. Richman SA, Nunez-Cruz S, Moghimi B, et al. High-Affinity GD2-Specific CAR T Cells Induce Fatal Encephalitis in a Preclinical Neuroblastoma Model. *Cancer Immunol Res*. 01 2018;6(1):36-46. doi:10.1158/2326-6066.CIR-17-0211

334. Shimabukuro-Vornhagen A, Gödel P, Subklewe M, et al. Cytokine release syndrome. *J Immunother Cancer*. 06 2018;6(1):56. doi:10.1186/s40425-018-0343-9

335. Si S, Teachey DT. Spotlight on Tocilizumab in the Treatment of CAR-T-Cell-Induced Cytokine Release Syndrome: Clinical Evidence to Date. *Ther Clin Risk Manag*. 2020;16:705-714. doi:10.2147/TCRM.S223468

336. Zhang L, Wang S, Xu J, et al. Etanercept as a new therapeutic option for cytokine release syndrome following chimeric antigen receptor T cell therapy. *Exp Hematol Oncol*. Feb 2021;10(1):16. doi:10.1186/s40164-021-00209-2

337. Sterner RM, Sakemura R, Cox MJ, et al. GM-CSF inhibition reduces cytokine release syndrome and neuroinflammation but enhances CAR-T cell function in xenografts. *Blood*. 02 2019;133(7):697-709. doi:10.1182/blood-2018-10-881722

338. Kalled SL, Hsu Y-M, inventors; Anti-BCMA antibodies. United States of America patent application US20120082661A1. 2012.

339. Lipp M, Oden F, Hopken U, et al, inventors; An antibody that binds CD269 (BCMA) suitable for use in the treatment of plasma cell diseases such as multiple myeloma and autoimmune diseases. patent application WO2014068079A1. 2014.

340. Kang L, Zhang J, Li M, et al. Characterization of novel dual tandem CD19/BCMA chimeric antigen receptor T cells to potentially treat multiple myeloma. *Biomark Res*. 2020;8:14. doi:10.1186/s40364-020-00192-6

341. Oden F, Marino S, Daumke O, inventors; Humanized antibodies against CD269 (BCMA). patent application US2019/0112382A1. 2019.

342. Bluhm J, Kieback E, Marino SF, et al. CAR T Cells with Enhanced Sensitivity to B Cell Maturation Antigen for the Targeting of B Cell Non-Hodgkin's Lymphoma and Multiple Myeloma. *Mol Ther*. 08 2018;26(8):1906-1920. doi:10.1016/j.ymthe.2018.06.012

343. Perez-Amill L, Suñe G, Antoñana-Vildosola A, et al. Preclinical development of a humanized chimeric antigen receptor against B cell maturation antigen for multiple myeloma. *Haematologica*. 01 2021;106(1):173-184. doi:10.3324/haematol.2019.228577

344. Zah E, Nam E, Bhuvan V, et al. Systematically optimized BCMA/CS1 bispecific CAR-T cells robustly control heterogeneous multiple myeloma. *Nat Commun*. 05 2020;11(1):2283. doi:10.1038/s41467-020-16160-5

345. Porter DL, Hwang WT, Frey NV, et al. Chimeric antigen receptor T cells persist and induce sustained remissions in relapsed refractory chronic lymphocytic leukemia. *Sci Transl Med*. Sep 2015;7(303):303ra139. doi:10.1126/scitranslmed.aac5415

346. Lee DW, Kochenderfer JN, Stetler-Stevenson M, et al. T cells expressing CD19 chimeric antigen receptors for acute lymphoblastic leukaemia in children and young adults: a phase 1 dose-escalation trial. *Lancet*. Feb 2015;385(9967):517-528. doi:10.1016/S0140-6736(14)61403-3

347. Fraietta JA, Lacey SF, Orlando EJ, et al. Determinants of response and resistance to CD19 chimeric antigen receptor (CAR) T cell therapy of chronic lymphocytic leukemia. *Nat Med*. 05 2018;24(5):563-571. doi:10.1038/s41591-018-0010-1

348. Teixeiro E, Daniels MA, Hamilton SE, et al. Different T cell receptor signals determine CD8+ memory versus effector development. *Science*. Jan 2009;323(5913):502-5. doi:10.1126/science.1163612

349. Zhao Z, Condomines M, van der Stegen SJC, et al. Structural Design of Engineered Costimulation Determines Tumor Rejection Kinetics and Persistence of CAR T Cells. *Cancer Cell*. Oct 2015;28(4):415-428. doi:10.1016/j.ccell.2015.09.004

350. Kawalekar OU, O'Connor RS, Fraietta JA, et al. Distinct Signaling of Coreceptors Regulates Specific Metabolism Pathways and Impacts Memory Development in CAR T Cells. *Immunity*. Feb 2016;44(2):380-90. doi:10.1016/j.immuni.2016.01.021

351. Ramello MC, Benzaïd I, Kuenzi BM, et al. An immunoproteomic approach to characterize the CAR interactome and signalosome. *Sci Signal*. 02 2019;12(568)doi:10.1126/scisignal.aap9777

352. Li G, Boucher JC, Kotani H, et al. 4-1BB enhancement of CAR T function requires NF-κB and TRAFs. *JCI Insight*. 09 2018;3(18)doi:10.1172/jci.insight.121322

353. Salter AI, Ivey RG, Kennedy JJ, et al. Phosphoproteomic analysis of chimeric antigen receptor signaling reveals kinetic and quantitative differences that affect cell function. *Sci Signal*. 08 2018;11(544)doi:10.1126/scisignal.aat6753

354. Neelapu SS, Locke FL, Bartlett NL, et al. Axicabtagene Ciloleucel CAR T-Cell Therapy in Refractory Large B-Cell Lymphoma. *N Engl J Med*. 12 2017;377(26):2531-2544. doi:10.1056/NEJMoa1707447

355. Park JH, Rivière I, Gonen M, et al. Long-Term Follow-up of CD19 CAR Therapy in Acute Lymphoblastic Leukemia. *N Engl J Med*. 02 2018;378(5):449-459. doi:10.1056/NEJMoa1709919

356. Cheng Z, Wei R, Ma Q, et al. In Vivo Expansion and Antitumor Activity of Coinfused CD28- and 4-1BB-Engineered CAR-T Cells in Patients with B Cell Leukemia. *Mol Ther*. 04 2018;26(4):976-985. doi:10.1016/j.ymthe.2018.01.022

357. Ying Z, He T, Wang X, et al. Parallel Comparison of 4-1BB or CD28 Co-stimulated CD19-Targeted CAR-T Cells for B Cell Non-Hodgkin's Lymphoma. *Mol Ther Oncolytics*. Dec 2019;15:60-68. doi:10.1016/j.omto.2019.08.002

358. Schuh E, Musumeci A, Thaler FS, et al. Human Plasmacytoid Dendritic Cells Display and Shed B Cell Maturation Antigen upon TLR Engagement. *J Immunol*. 04 2017;198(8):3081-3088. doi:10.4049/jimmunol.1601746

359. Weinkove R, George P, Dasyam N, McLellan AD. Selecting costimulatory domains for chimeric antigen receptors: functional and clinical considerations. *Clin Transl Immunology*. 2019;8(5):e1049. doi:10.1002/cti2.1049

360. Laux I, Khoshnan A, Tindell C, et al. Response differences between human CD4(+) and CD8(+) T-cells during CD28 costimulation: implications for immune cell-based therapies and studies related to the expansion of double-positive T-cells during aging. *Clin Immunol*. Sep 2000;96(3):187-97. doi:10.1006/clim.2000.4902

361. Zhang H, Snyder KM, Suhoski MM, et al. 4-1BB is superior to CD28 costimulation for generating CD8+ cytotoxic lymphocytes for adoptive immunotherapy. *J Immunol*. Oct 2007;179(7):4910-8. doi:10.4049/jimmunol.179.7.4910

362. Verhoeyen E, Costa C, Cosset FL. Lentiviral vector gene transfer into human T cells. *Methods Mol Biol*. 2009;506:97-114. doi:10.1007/978-1-59745-409-4_8

363. Abramson JS, Palomba ML, Gordon LI, et al. Lisocabtagene maraleucel for patients with relapsed or refractory large B-cell lymphomas (TRANSCEND NHL 001): a multicentre seamless design study. *Lancet*. 09 2020;396(10254):839-852. doi:10.1016/S0140-6736(20)31366-0

364. Shah NN, Fry TJ. Mechanisms of resistance to CAR T cell therapy. *Nat Rev Clin Oncol*. 06 2019;16(6):372-385. doi:10.1038/s41571-019-0184-6

365. Shi L, Qin X, Wang H, et al. Elevated neutrophil-to-lymphocyte ratio and monocyte-to-lymphocyte ratio and decreased platelet-to-lymphocyte ratio are associated with poor prognosis in multiple myeloma. *Oncotarget*. Mar 2017;8(12):18792-18801. doi:10.18632/oncotarget.13320

366. Cottini F, Williams N, Bumma N, et al. Daratumumab-induced lymphopenia predicts adverse events and outcomes in patients with myeloma. *Journal of Clinical Oncology*. 2020;38(15_suppl):e20534-e20534. doi:10.1200/JCO.2020.38.15_suppl.e20534

367. Jung SH, Bae SY, Ahn JS, et al. Lymphocytopenia is associated with an increased risk of severe infections in patients with multiple myeloma treated with bortezomib-based regimens. *Int J Hematol*. Mar 2013;97(3):382-7. doi:10.1007/s12185-013-1270-7

368. Blanco B, Pérez-Simón JA, Sánchez-Abarca LI, et al. Bortezomib induces selective depletion of alloreactive T lymphocytes and decreases the production of Th1 cytokines. *Blood*. May 2006;107(9):3575-83. doi:10.1182/blood-2005-05-2118

369. Blanco B, Pérez-Simón JA, Sánchez-Abarca LI, et al. Treatment with bortezomib of human CD4+ T cells preserves natural regulatory T cells and allows the emergence of a distinct suppressor T-cell population. *Haematologica*. Jul 2009;94(7):975-83. doi:10.3324/haematol.2008.005017

370. Stock S, Schmitt M, Sellner L. Optimizing Manufacturing Protocols of Chimeric Antigen Receptor T Cells for Improved Anticancer Immunotherapy. *Int J Mol Sci*. Dec 2019;20(24)doi:10.3390/ijms20246223

371. Krämer I, Engelhardt M, Fichtner S, et al. Lenalidomide enhances myeloma-specific T-cell responses in vivo and in vitro. *Oncoimmunology*. May 2016;5(5):e1139662. doi:10.1080/2162402X.2016.1139662

372. Otáhal P, Průková D, Král V, et al. Lenalidomide enhances antitumor functions of chimeric antigen receptor modified T cells. *Oncoimmunology*. Apr 2016;5(4):e1115940. doi:10.1080/2162402X.2015.1115940

373. Works M, Soni N, Hauskins C, et al. Anti-B-cell Maturation Antigen Chimeric Antigen Receptor T cell Function against Multiple Myeloma Is Enhanced in the Presence of Lenalidomide. *Mol Cancer Ther*. 12 2019;18(12):2246-2257. doi:10.1158/1535-7163.MCT-18-1146

374. Chen GM, Chen C, Das RK, et al. Integrative bulk and single-cell profiling of pre-manufacture T-cell populations reveals factors mediating long-term persistence of CAR T-cell therapy. *Cancer Discov*. Apr 2021;doi:10.1158/2159-8290.CD-20-1677

375. Biasco L, Izotova N, Rivat C, et al. Clonal expansion of T memory stem cells determines early anti-leukemic responses and long-term CAR T cell persistence in patients. *Nature Cancer*. 2021/05/24 2021;doi:10.1038/s43018-021-00207-7

376. Xu Y, Zhang M, Ramos CA, et al. Closely related T-memory stem cells correlate with in vivo expansion of CAR.CD19-T cells and are preserved by IL-7 and IL-15. *Blood*. Jun 2014;123(24):3750-9. doi:10.1182/blood-2014-01-552174

377. Pilipow K, Scamardella E, Puccio S, et al. Antioxidant metabolism regulates CD8+ T memory stem cell formation and antitumor immunity. *JCI Insight*. 09 2018;3(18)doi:10.1172/jci.insight.122299

378. Rydzek J, Nerreter T, Peng H, et al. Chimeric Antigen Receptor Library Screening Using a Novel NF-κB/NFAT Reporter Cell Platform. *Mol Ther*. 02 2019;27(2):287-299. doi:10.1016/j.ymthe.2018.11.015

379. Bloemberg D, Nguyen T, MacLean S, et al. A High-Throughput Method for Characterizing Novel Chimeric Antigen Receptors in Jurkat Cells. *Mol Ther Methods Clin Dev*. Mar 2020;16:238-254. doi:10.1016/j.omtm.2020.01.012

380. Di Roberto RB, Castellanos-Rueda R, Frey S, et al. A Functional Screening Strategy for Engineering Chimeric Antigen Receptors with Reduced On-Target, Off-Tumor Activation. *Mol Ther*. 12 2020;28(12):2564-2576. doi:10.1016/j.ymthe.2020.08.003

381. Ochi T, Maruta M, Tanimoto K, et al. A single-chain antibody generation system yielding CAR-T cells with superior antitumor function. *Commun Biol*. Mar 2021;4(1):273. doi:10.1038/s42003-021-01791-1

382. Oden F, Marino SF, Brand J, et al. Potent anti-tumor response by targeting B cell maturation antigen (BCMA) in a mouse model of multiple myeloma. *Mol Oncol*. Aug 2015;9(7):1348-58. doi:10.1016/j.molonc.2015.03.010

383. Leach MW, Halpern WG, Johnson CW, et al. Use of tissue cross-reactivity studies in the development of antibody-based biopharmaceuticals: history, experience, methodology, and future directions. *Toxicol Pathol*. Dec 2010;38(7):1138-66. doi:10.1177/0192623310382559

384. Melenhorst JJ, Chen GM, Wang M, et al. Decade-long remissions of leukemia sustained by the persistence of activated CD4⁺ CAR T-cells. *bioRxiv*. 2021:2021.05.07.443194. doi:10.1101/2021.05.07.443194

385. Pearson T, Shultz LD, Miller D, et al. Non-obese diabetic-recombination activating gene-1 (NOD-Rag1 null) interleukin (IL)-2 receptor common gamma chain (IL2r gamma null) null mice: a radioresistant model for human lymphohaematopoietic engraftment. *Clin Exp Immunol*. Nov 2008;154(2):270-84. doi:10.1111/j.1365-2249.2008.03753.x

386. Jacobson C, Locke FL, Ghobadi A, et al. Long-Term Survival and Gradual Recovery of B Cells in Patients with Refractory Large B Cell Lymphoma Treated with Axicabtagene Ciloleucel (Axi-Cel). *Blood*. 2020;136(Supplement 1):40-42. doi:10.1182/blood-2020-134362

387. Wang M, Munoz J, Goy AH, et al. One-Year Follow-up of ZUMA-2, the Multicenter, Registrational Study of KTE-X19 in Patients with Relapsed/Refractory Mantle Cell Lymphoma. *Blood*. 2020;136(Supplement 1):20-22. doi:10.1182/blood-2020-136382

Appendix

Special Report

Immunotherapy

Tumor-targeting domains for chimeric antigen receptor T cells

Immunotherapy with chimeric antigen receptor (CAR) T cells has been advancing steadily in clinical trials. Since the ability of engineered T cells to recognize intended tumor-associated targets is crucial for the therapeutic success, antigen-binding domains play an important role in shaping T-cell responses. Single-chain antibody and T-cell receptor fragments, natural ligands, repeat proteins, combinations of the above and universal tag-specific domains have all been used in the antigen-binding moiety of chimeric receptors. Here we outline the advantages and disadvantages of different domains, discuss the concepts of affinity and specificity, and highlight the recent progress of each targeting strategy.

Ksenia Bezverbnaya[1], Ashish Mathews[1], Jesse Sidhu[1], Christopher W Helsen[1] & Jonathan L Bramson*[,1]

[1]Department of Pathology & Molecular Medicine, McMaster University, Hamilton, Canada

*Author for correspondence: bramsonj@mcmaster.ca

First draft submitted: 25 August 2016; Accepted for publication: 11 November 2016; Published online: 21 December 2016

Keywords: adoptive cell therapy • antigen recognition • CAR • engineered T cells • immunotherapy

Engineered T-cell therapy has demonstrated impressive clinical results in the treatment of blood cancers [1–6]. This approach relies upon genetic modification of a patient's T cells to directly recognize a tumor-associated antigen and elicit specific killing responses. Among the recombinant receptors designed for retargeting T cells, chimeric antigen receptors (CARs) have made the greatest clinical progress.

CARs consist of an antigen-binding domain, a hinge region, transmembrane and intracellular signaling domains (Figure 1). This article focuses on the antigen-binding moiety; extensive information regarding the other receptor components can be found in earlier reviews [7,8]. The availability of suitable antigen-binding domains is important for the success of engineered T-cell therapy, as it influences possible target choices. Specificity for the marker of interest and sufficient affinity for triggering downstream signaling and T-cell activation are desirable when designing these domains. To limit immunologic response against the CAR and avoid off- or on-target off-tumor toxicities [9,10], careful consideration and detailed preclinical evaluation are needed during selection of potential binding candidates. Here, we review protein structures currently used for antigen recognition by CARs, highlight advantages and disadvantages of different approaches (Table 1), and discuss the concepts of affinity and specificity as they apply to receptor design.

Antigen-binding domains described in literature

Single-chain variable fragments (scFv)

Most CARs, including those that have progressed farthest in clinical studies (Table 1), utilize single-chain variable fragments (scFvs) for antigen recognition. A typical scFv is composed of variable fragments from heavy (V_H) and light (V_L) chains joined via a synthetic linker, mimicking their spatial arrangement in an intact antibody molecule (Figure 1). The availability of high-diversity scFv libraries, the ability of scFvs to target

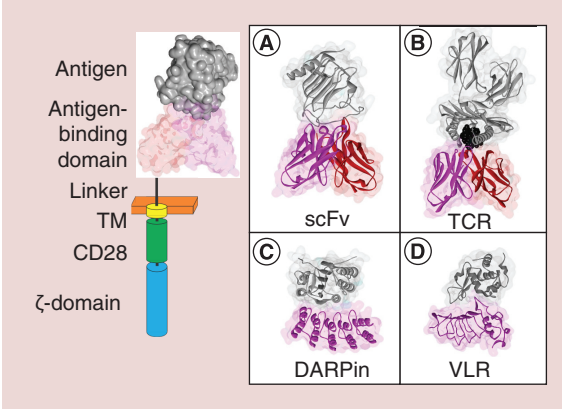

Figure 1. Overview of a chimeric antigen receptor with different antigen-binding domains. A common second-generation CAR contains a transmembrane domain (yellow), a CD28 co-stimulation domain (green) and an activating ζ-domain (blue). This receptor is connected to the potential antigen-binding domain via a short linker. Here, the CAR is shown embedded in the plasma membrane (orange) and interacting with a target antigen (gray). Models in **A–D** were taken from the PDB, and their respective PDB codes are given in curly brackets. (A) scFv chA21 {3h3b} (pink and red) interacting with $p185^{HER2/Neu}$ (gray) [117]. (B) A part of the αβ TCR {5C07} (pink and red) domain interacting with MHC class I (gray) presenting a peptide antigen (black) [118]. (C) DARPin C7_16 {4jb8} (pink) interacting with caspase 7 (gray) [119]. (D) VLR {g3b} (pink) in complex with lysozyme (gray) [120].
CAR: Chimeric antigen receptor; CD: Cluster of differentiation; DARPin: Designed ankyrin-repeat protein; MHC: Major histocompatibility complex; PDB: Protein Data Bank; scFv: Single-chain variable fragment; TCR: T-cell receptor; TM: Transmembrane domain; VLR: Variable lymphocyte receptor.

proteins, carbohydrates and glycolipids and the wealth of data available regarding scFv generation and clinical performance, make this technology particularly attractive for CAR T-cell applications.

Targets amenable to scFv recognition

Since scFvs are derived from antibodies, they can bind peptides, carbohydrates and glycolipids (Table 1). Single chain-based CARs can successfully differentiate between different glycoforms of mucin 1 antigen and elicit tumor-specific T-cell responses *in vivo* [11,12]. Disialoganglioside GD2, expressed on neural and epithelial tumors, is another common nonpeptide antigen targeted with scFv-based CARs. Currently, six anti-GD2 Phase I trials with scFv-targeted CAR T or natural killer cells are registered with the National Institutes of Health (NCT02107963, NCT01953900, NCT02439788, NCT01822652, NCT02765243 and NCT02761915).

To expand the pool of antigens for scFv-based CAR recognition, several groups have generated single chains against human leukocyte antigen (HLA)-peptide complexes [13–16]. These TCR-like CARs allow for recognition of intracellular protein targets. However, clinical experience with TCR-engineered T cells suggests that receptors with TCR-like specificity can exhibit off-target toxicities if a similar peptide epitope is expressed on healthy tissues. Two different affinity-modified TCRs against MAGE-A3 have led to cardiac toxicity due to the presence of a similar peptide epitope in titin [17] and neurologic toxicity due to recognition of several MAGE-A protein family members unexpectedly expressed in neurons [18]. These outcomes emphasize the need for extensive preclinical characterization of potential epitope targets for high-affinity ligand-binding domains that react to HLA–peptide complexes. In addition to the antigen expression pattern analyses in tissue arrays, new computational strategies for characterizing the suitability of peptide–HLA pairs for engineered T-cell therapies [19,20] can provide useful *in silico* assessment for choosing target antigens.

Design & generation of scFvs

Some scFvs are created from a known antibody clone, while others are selected from synthetic libraries. Among the screening methods, phage display has gained the most popularity due to the availability of libraries with large diversity and the suitability of phage libraries for high-throughput screening [21,22]. Different scFv display strategies have been reviewed in [23]. In recent years, a novel CARbody approach was introduced, where the scFv library was directly cloned into a CAR framework, expressed in primary T cells, and selected based on T-cell activation against cell surface-expressed target [24]. This strategy could streamline the process of scFv selection by shifting the focus on scFvs, which promote desired T-cell characteristics. However, the diversity of the CARbody library was estimated at low 10^5 [24], which is several orders of magnitude lower than the typical phage display libraries, which often contain over 10^{10} different variants [25,26]. Thus, the CARbody strategy is likely most useful following an initial screen with phage display.

B cells produced naturally in the body undergo selection based on affinity rather than stability of their B-cell receptors. When joining V_H and V_L segments, optimization of biophysical properties is required to minimize aggregation and maximize conformational stability, while preserving affinity for the desired antigen [27]. Factors influencing proper folding and aggregation of individual variable fragments and whole scFvs, as well as complementarity determining region loop grafting between different frameworks and screening for stabilizing mutations as ways of domain optimization, have been reviewed previously by [28].

Table 1. Antigen-binding domains of chimeric antigen receptors.

Types of antigen-binding domains		Advantages	Disadvantages	Examples of target antigens	Disease	Stage of development	Ref.
Monovalent	Single-chain antibody variable fragments	– HLA-independent – Peptide, carbohydrate and glycolipid antigens – Diverse libraries available – Clinically proven effectiveness	– Limited to cell surface-expressed antigens (unless the scFv has been selected against HLA–peptide complex) – Optimization required to improve stability and minimize misfolding and aggregation	CD19	AML, ALL, CLL, lymphomas (HL and NHL)	Phase II	[83–85]
				HER2 (ErbB2)	Breast, ovarian, lung, gastric, colorectal and pancreatic cancers, glioblastoma	Phase I/II	[80,86,87]
				MUC1	Breast, non-small-cell lung, gastric, colorectal, hepatocellular and pancreatic cancers, T-cell leukemia, glioma	Phase I/II	[11,88]
				EpCAM	Hepatocellular and gastric cancers	Phase I/II	[89]
				CD20	ALL, CLL, NHL	Phase II	[90]
				CD22	ALL, NHL	Phase I/II	[91]
				CD30	Lymphomas (HL and NHL)	Phase I/II	[92]
				CD33	AML	Phase I/II	[93]
				BCMA	MM	Phase I	[4]
				VEGFR2	Melanoma	Phase I/II	[94]
				CD138	MM	Phase I/II	[95]
				GD2	Neuroblastoma, sarcoma	Phase I	[96,97]
				CD123	AML	Phase I	[98]
				CD171	Neuroblastoma	Phase I	[99]
				GPC3	Hepatocellular and lung squamous cell carcinomas	Phase I/II	[100]
				Mesothelin	Mesothelioma, breast, lung and pancreatic cancers	Phase I	[101]
				CEA	Breast, lung, gastric, colorectal and pancreatic cancers	Phase I	[102]
				κ-light chain	CLL, BCL, MM	Phase I	[103]

ALL: Acute lymphoblastic leukemia; AML: Acute myeloid leukemia; BCL: B-cell lymphoma; CLL: Chronic lymphocytic leukemia; DARPin: Designed ankyrin-repeat protein; FITC: Fluorescein; HCV: Hepatitis C virus; HL: Hodgkin lymphoma; HIV: Human immunodeficiency virus; HLA: Human leukocyte antigen; JMML: Juvenile myelomonocytic leukemia; MDS: Myelodysplastic syndrome; MM: Multiple myeloma; NHL: Non-Hodgkin lymphoma; NSCLC: Non-small-cell lung cancer; PNE: Peptide neo-epitope; SCC: Squamous cell carcinoma; scFv: Single-chain variable fragment; TCR: T-cell receptor; VLR: Variable lymphocyte receptor.

Table 1. Antigen-binding domains of chimeric antigen receptors (cont.).

Types of antigen-binding domains	Advantages	Disadvantages	Examples of target antigens	Disease	Stage of development	Ref.
			PSCA	Gastric, pancreatic, bladder and prostate cancer	Phase I	[104,105]
			HCV/E2 glycoprotein	HCV	*In vitro*	[106]
			Lewis Y	AML, MM, SCC, lung, colorectal and ovarian cancer	Phase I	[107]
			ROR1	ALL, CLL, MCL, NSCLC, breast cancer	Phase I	[108]
Natural ligand	– HLA-independent – Evolutionarily selected affinity and specificity of the receptor–ligand pair	– Limited to cell surface-expressed antigens – Availability of known natural ligands significantly restricts target repertoire	NKG2D ligands	AML, MDS, MM, glioma, melanoma, breast, lung, hepatocellular, kidney, colon, prostate and ovarian cancers	Phase I	[33,34,109]
			GMR	JMML	*In vitro*	[110]
			ErbB dimers	Various carcinomas	*In vivo*	[111]
			IL13Rα	Glioblastoma	Phase I	[38]
			CD70	Renal cell carcinoma, glioblastoma, lymphomas (HL and NHL), MM	Phase I	[112]
			gp120	HIV	Phase II	[113]
			IL11Rα	Osteosarcoma, breast, gastric, colon and prostate cancer	*In vivo*	[114]
			FSHR	Ovarian cancer	*In vivo*	[35]
Repeat protein	– HLA-independent – Diverse libraries available – Each unit folds rapidly and independently – Modular structure facilitates protein design	– Limited to cell surface-expressed antigens	HER2	Breast cancer	*In vivo*	DARPin [40]
			Murine BCR (proof-of-concept), CD5	Leukemia	*In vitro*	VLR [41]

ALL: Acute lymphoblastic leukemia; AML: Acute myeloid leukemia; BCL: B-cell lymphoma; CLL: Chronic lymphocytic leukemia; DARPin: Designed ankyrin-repeat protein; FITC: Fluorescein; HCV: Hepatitis C virus; HL: Hodgkin lymphoma; HIV: Human immunodeficiency virus; HLA: Human leukocyte antigen; JMML: Juvenile myelomonocytic leukemia; MDS: Myelodysplastic syndrome; MM: Multiple myeloma; NHL: Non-Hodgkin lymphoma; NSCLC: Non-small-cell lung cancer; PNE: Peptide neo-epitope; SCC: Squamous cell carcinoma; scFv: Single-chain variable fragment; TCR: T-cell receptor; VLR: Variable lymphocyte receptor.

Table 1. Antigen-binding domains of chimeric antigen receptors (cont.).

Types of antigen-binding domains	Advantages	Disadvantages	Examples of target antigens	Disease	Stage of development	Ref.
TCR variable fragments	– Recognize both intracellular and cell surface-expressed antigens	– HLA-dependent – Only peptide antigens – Optimization required to maximize thermodynamic stability	SIYRYYGL peptide in the context of H2-K^b	Proof-of-concept, murine B16 melanoma	*In vivo*	[47]
Multivalent	– Reduces potential antigen escape by targeting multiple tumor-cell populations – Can combine targeting of intracellular and cell surface-expressed antigens	– Optimization required to maximize thermodynamic stability and prevent mispairing (in the case of scFv's) – Potentially higher risk of off-target activity	CD19, HER2	Proof-of-concept	*In vivo*	[49]
			CD19, CD20	B-cell leukemias and lymphomas	*In vivo*	[50]
			HER2, IL13Rα	Glioblastoma	*In vivo*	[51]
			gp120 (different epitopes)	HIV	*In vitro*	[115]
Universal switchable	– Target multiple antigens simultaneously – Custom changes to the repertoire of targets throughout the treatment course – Modulation of T cell activity via dosing of the soluble switch	– Dependent on bioavailability and biodistribution of soluble switches and engineered T cells	Mesothelin, FRα, EpCAM	Multiple	*In vivo*	Avidin–biotin [52]
			CD20, HER2	Multiple	*In vivo*	CD16-Fc [53]
			CD19, CD20	Multiple	*In vivo*	PNE and anti-PNE scFv [116]
			EGFR, HER2, CD20, PR1	Multiple	*In vivo*	FITC and anti-FITC scFv [13,56]

ALL: Acute lymphoblastic leukemia; AML: Acute myeloid leukemia; BCL: B-cell lymphoma; CLL: Chronic lymphocytic leukemia; DARPin: Designed ankyrin-repeat protein; FITC: Fluorescein; HCV: Hepatitis C virus; HL: Hodgkin lymphoma; HIV: Human immunodeficiency virus; HLA: Human leukocyte antigen; JMML: Juvenile myelomonocytic leukemia; MDS: Myelodysplastic syndrome; MM: Multiple myeloma; NHL: Non-Hodgkin lymphoma; NSCLC: Non-small-cell lung cancer; PNE: Peptide neo-epitope; SCC: Squamous cell carcinoma; scFv: Single-chain variable fragment; TCR: T-cell receptor; VLR: Variable lymphocyte receptor.

In addition to amino acid composition and configuration (V_H-V_L vs V_L-V_H) of variable fragments, the linker also influences thermodynamic stability of single chains [29]. For instance, Whitlow *et al.* developed an 18 amino acid Gly and Ser-rich linker, which increased proteolytic stability and reduced propensity of scFvs to aggregate [30].

The origin of scFv should also be taken into consideration. While murine scFvs are currently quite common, they are susceptible to immune-mediated rejection, which can result in a range of outcomes from reduced persistence of CAR T cells [31] to anaphylaxis [32]. Humanization of scFvs and the use of scFv libraries derived from human B cells can help overcome these pitfalls [31].

Natural ligands & ligand-binding domains

Natural ligands and ligand-binding domains found in the human body are poorly immunogenic due to T-cell tolerance and, thus, should offer an advantage over synthetic ligand-binding domains. However, the pool of known binding candidates is small, limited by antigen expression patterns, availability of a known ligand on tumor cells and the specificity of receptor–ligand interaction. NKG2D, expressed on the surface of natural killer cells, is an example of a receptor that can be used for redirecting CAR T cells. Zhang *et al.* demonstrated the ability of NKG2D-targeted CAR T cells to respond to tumors expressing NKG2D ligands [33]. VanSeggelen *et al.* observed that NKG2D-targeted CARs can produce lethal toxicity *in vivo* [34]. Here, expression of NKG2D ligands on tumor cells was insufficient to predict response of engineered T cells to healthy tissues, which expressed low ligand levels.

FSH has been used to redirect CARs to ovarian cancer cells, which express high levels of FSH receptor. Peptides derived from FSH were introduced as the CAR antigen-binding domain [35]. Monitoring of tissue pathology and organ biochemistry in ovarian cancer murine models did not reveal harmful effects of using an FSH-targeted CAR [36], supporting further evaluation of this natural ligand for targeting tumors.

A similar approach has been employed for targeting glioblastoma multiforme with IL-13, where the cytokine was linked directly to a CAR yielding a structure known as a zetakine [37]. The IL-13 zetakine consists of an extracellular IL-13 E13Y mutein attached to a CD3-ζ chain. The use of mutated IL-13 is crucial, as it preferentially binds IL13Rα2, expression of which is restricted to gliomas. This strategy can minimize on-target off-tumor toxicity, as supported by the first-in-human IL-13 zetakine trial [38].

Repeat proteins

One of the most attractive features of scFvs is their ability to bind a broad diversity of potential targets. Immunoglobulin-based single chains, however, are not the only class of protein domains capable of recognizing a wide array of antigens. Repeat proteins are common in nature and have advanced to clinical evaluations as an alternative to antibodies (NCT02462486, NCT02194426).

Modular structure, compact size, ability to fold quickly and high thermodynamic stability make designed ankyrin-repeat proteins (DARPins) highly suitable for biomedical engineering applications [39]. A DARPin against HER2 has been used successfully in a CAR framework (Figure 1) to elicit tumor-specific killing and cytokine production from engineered T cells [40]. Similar to scFvs, DARPins can target a wide variety of antigens and provide HLA-independent recognition at the cost of being limited to cell surface-expressed targets only. High thermodynamic stability and modular structure make DARPins particularly interesting for the creation of multispecific receptors. DARPin consensus framework is based on naturally occurring scaffolds, and limited clinical experience does not suggest high immunogenicity [39]. However, further studies with this class of proteins are required to understand the immunogenicity of DARPin CARs.

Variable lymphocyte receptors (VLRs) obtained from sea lamprey are being investigated for the use in CARs. As members of the family of leucine-rich repeat proteins, VLRs exhibit a high degree of specificity and avidity and serve a function similar to antibodies in mammals. VLRs specific against murine B-cell leukemia have been cloned into CAR receptors, and have shown high levels of activation and specific killing [41]. Additionally, other repeat proteins have the potential to serve as ligand-binding domains in the future. Modifications and redesign of VLRs have resulted in the development of 'repebodies', which show high thermodynamic and pH stability [42] and have already been used to bind therapeutically relevant targets, such as VEGF [43].

TCR variable fragments

TCR variable fragments can be directly linked together in a single chain (Figure 1) to confer TCR-liked specificity to a CAR and allow for recognition of intracellular proteins. Although the principle of TCR variable fragments is analogous to scFv production, the progress of single-chain TCR applications has been lagging due to poor expression in conventional display platforms, low stability and a tendency to aggregate [44–46]. Fusion of variable fragments from high-affinity TCR-α and -β chains successfully directed CAR T cells against

melanoma [47]. A TCR-based CAR offers opportunities for targeting intracellular proteins, however, from the engineering point of view, it faces nontrivial optimization challenges. Thus, when designing a V_{α}-V_{β} single chain, researchers will most likely have to improve thermodynamic stability of the structure, while maintaining antigen specificity [48]. Additionally, since intracellular protein antigens are targeted as peptides presented in the context of HLA on the cell surface, design of CARs with TCR-like specificity will have to account for multiple HLA–peptide combinations observed among patients and the propensity of tumors to downregulate HLA processing and presentation.

Multivalent domains

Engineered T cells directed against a single target exert selective pressure on the tumor and can promote selection of epitope- and/or antigen-loss variants. Multispecific receptors reduce the risk of tumor escape by targeting several populations in a heterogeneous malignant mass. In a proof-of-concept study, Grada *et al.* engineered a bi-specific tandem CAR containing scFvs against CD19 and HER2 joined via a flexible linker [49]. The tandem CAR prolonged survival of cancer-bearing mice and demonstrated *in vitro* antitumor activity in an antigen-loss model. Similarly, to address the problem of antigen escape in CD19-positive cancers, a bispecific tandem scFv CAR redirected against CD19 and CD20 was developed [50]. Both the CD19/HER2 and the CD19/CD20 models use two single chains linked in a sequence. In a different approach, a tandem CAR with an scFv against HER2 and a natural ligand for IL13Rα, showed augmented effectiveness in a glioblastoma model [51]. Whether multivalent CARs are engineered using two single chains, a single chain and a natural ligand, or an alternative combination of monovalent structures described earlier, they will require significant optimization to facilitate proper folding of each domain and minimize mispairing of individual components (in the case of scFvs) and steric hindrance.

Universal switchable domains

To retain flexibility in the choice of targets, several groups have been pursuing the strategy of universal chimeric receptors. The idea behind this approach is to generate a CAR specific for a known tag, redirected to the tumor via administration of labeled soluble mediators, which simultaneously recognize tumor antigens and bind the universal antigen-recognition domain of the receptor. Candidate-binding partners include biotin–avidin [52], Fc receptor CD16 and antibodies [53], peptide neo-epitopes (PNE) and corresponding anti-PNE scFv [54], and fluorescein and anti-fluorescein scFv [55,56]. The universal receptor approach can potentially allow for targeting multiple antigens simultaneously, change the repertoire of targets throughout the course of the treatment, and modulate T-cell activity by dosing the switch molecules. However, the strategy relies on a two-component system and will depend on the bioavailability and biodistribution of both soluble switches and chimeric receptor-bearing T cells. Universal switchable CARs are yet to be tested in humans (Table 1), so it remains to be determined whether their nonfixed specificity and modular design translate into improved antitumor efficacy.

Characteristics of the binding interaction

Receptor affinity, T-cell avidity & target antigen density

The activity of a given CAR construct is ultimately defined by its ability to bind target antigen. When designing CARs, the main goal is to generate engineered T cells with maximum antitumor efficacy and minimum off-tumor toxicity.

The molecular term 'affinity' is commonly used in literature and refers to the strength of association between a receptor and its ligand [57]. Most of our understanding about the relationship between receptor affinity and T-cell functionality comes from experiments with TCRs. Since CARs and TCRs are structured differently [8], the activation thresholds will likely vary, but the factors influencing these thresholds are relevant for both types of receptors. In-depth studies of TCRs that defined their characteristics influencing efficacy of T-cell responses have led to the term 'functional avidity' [58,59]. Functional avidity refers to the concentration of antigen (peptide–HLA complexes) required for activating a T cell and is influenced by many factors, including: TCR affinity, expression levels of TCRs and cell-adhesion molecules participating in immunological synapse, and distribution of signal transduction proteins [60]. This definition is distinct from the classic use of the term 'avidity', which describes avidity as a sum of individual affinities of a multivalent molecule [61]. Given that the activity of CAR T cells is defined by more than mere receptor binding, the concept of functional avidity is more pertinent to the discussion of CARs. While affinity of the antigen-binding domain will often correlate with functional avidity, it is not the sole predictor of a T-cell response.

High-avidity cytotoxic T lymphocytes can elicit a response against cells expressing low levels of target antigen, while low-avidity cytotoxic T lymphocytes require high antigen density to become effective. High-avidity T cells also show enhanced antitumor efficacy, which, unfortunately, correlates with increased

incidence of autoimmune sequelae [62]. These data highlight the potential drawbacks of high avidity-engineered CAR T cells, especially those with TCR-like specificity. Currently, the overwhelming majority of CARs use antibody-derived single-chain fragments in the antigen-binding domain (discussed earlier). Naturally occurring antibodies typically display affinities in the low nanomolar to high picomolar range [63], which are significantly higher than those of TCRs (typically in the micromolar range) [64]. Further experimentation is required to determine whether the application of lower affinity, TCR-based antigen-binding domains will yield CAR T cells that have lower propensity for autoimmune responses, compared with CAR T cells employing high-affinity scFvs.

As stated above, functional avidity can impact the T cells' ability to differentiate between tumor cells with abnormally high antigen expression and normal tissues with low to medium antigen expression. HER2 is expressed at low to medium levels on a variety of epithelial cells [65], overexpressed in approximately 30% of breast cancer tumors and associated with especially aggressive disease and, consequently, poor prognosis [66]. Based on the clinical successes of targeting HER2-expressing tumors with a monoclonal antibody Herceptin® (Trastuzumab), a HER2-specific CAR was engineered, but caused fatal toxicities when administered at high doses [67]. The unexpected pulmonary complications were likely a consequence of engineered T cells responding to low levels of HER2 expressed in the lung tissue. This raises the issue that relevant tumor targets such as HER2 or EGFR are often expressed at low levels on healthy cells and, thus, may not be suitable for CAR T-cell therapy. Consequently, it is reasonable to assume that CAR T cells with high functional avidity will be unable to discriminate between healthy tissues that express low levels of antigen and cancerous tissue expressing high levels of the desired target [68] [69]. This important safety concern has led to the concept of 'affinity tuning' [68], where CAR T cells were developed that could distinguish between cells expressing different antigen densities by employing scFvs with reduced binding affinity for the target. In both cases, CARs with lower receptor affinity also showed lower functional avidity, which manifested in none or reduced efficacy of CAR T cells against cells expressing low levels of antigen [68] [69]. Interestingly, cells expressing high levels of antigen were equally susceptible to T cells engineered to be either high or low avidity. This suggests that an increase in CAR receptor affinity is not necessarily associated with enhanced tumor efficacy, but may cause a loss in cell target specificity [70]. These findings support the concept of enhancing tumor specificity by developing T cells with low functional avidity that are no longer reactive to low antigen densities and, therefore, highly specific for the desired tumor cells.

Receptor specificity

At the molecular level, T-cell specificity refers to its ability to distinguish between different potential ligands. The importance of target selection has been highlighted recently in reports of studies with affinity-matured TCRs. Although CARs are structurally distinct from TCRs, the principles of protein–protein interactions governing antigen binding apply to both receptors. An affinity-matured TCR for myeloma- and melanoma-associated MAGE-A3 peptide (EVDPIGHLY) caused rapid and lethal cardiogenic shock in humans [17]. The toxicity was attributed to cross-reactivity of the receptor with a similar peptide found in the smooth muscle protein titin (ESDPIVAQY) [71]. In a second study, T cells were engineered with a distinct anti-MAGE-A3 TCR recognizing epitopes in MAGE-A3/A9/A12 [18]. In five out of nine patients, treatment caused adverse neurologic effects leading to fatal toxicity in two cases. In-depth analysis of brain tissue revealed that MAGE-A12 was unexpectedly expressed in the brain, likely causing the observed toxicities [18].

The studies described above highlight the two challenges in the field of T-cell therapy. First, predicting off-target effects in humans [17,71] is extremely difficult and poses a major hurdle to preclinical characterization of chimeric receptors. As proposed by [64], low-affinity TCRs may have been evolutionarily selected to reduce the risk of cross-reactivity. In a CAR framework, high-affinity single-chain TCR fragment has demonstrated reduced specificity [47], but it is unclear whether other ligand-binding domains, such as single-chain antibody fragments, will follow the same principles. The second challenge is on-target off-tumor toxicity, as was observed in the second MAGE trial [18]. Rather than cross-reactivity, unexpected expression of the target antigen in vital tissues can cause severe complications. It is very challenging to determine the expression of any given antigen in all human tissues, especially since commonly used preclinical xenograft models cannot predict such outcomes. Syngeneic mouse models have been described for such self-antigens as CD19 [72], EGFRvIII [73] and CEA [74] and can be used to gain valuable biological and mechanistic understanding and address potential toxicities of CAR T-cell treatments in immunocompetent mice. To predict potential on-target off-tumor toxicities, this approach relies heavily on conserved gene expression among multiple tissues. While some genes have a high level of tissue-specific expression conservation [75], others diverge in their expression

patterns between mice and humans [76]. Thus, predictive value of syngeneic self-antigen models is limited and can hinder the wide acceptance of such toxicity investigations.

A common assumption is that the higher the affinity between the two molecules, the more optimal the 'molecular interface fit' and the more unique the 'interaction interface' [77]. In an ideal case, this would lead to a high level of specificity between the two molecules [77]. However, it cannot be ruled out that secondary interactions also gain an increase in affinity alongside the primary interaction and, ultimately, lower the molecule's specificity. This phenomenon was observed in high-affinity TCRs that gained the ability to cross-react and activate cells against peptides that were similar to the main target peptide [17,71,78,79]. As discussed previously, all of the currently studied options for antigen-binding domains have features that influence affinity and specificity, but further investigations are required to determine how affinity of ligand-binding domains and density of chimeric receptors on T cells and antigens on tumors ultimately impact the ability of CAR T cells to discriminate specific tumor targets from cross-reactive and/or lowly-expressed targets on healthy tissues.

Functional avidity of engineered T cells and specificity of chimeric receptors influence the binding interaction between a T cell and its target, but represent only some of the variables underlying potential toxicities of CAR T-cell therapies. For example, when a target antigen has a broad expression pattern, as in the case of HER2, different combinations of intracellular signaling domains and alternative dosing strategies can contribute to markedly distinct clinical outcomes [67,80]. While in the first trial [67] CAR T-cell treatment was lethal in one patient, the second trial showed no evidence of toxicity [80]. Besides a different HER2-specific scFv, the second trial employed three orders of magnitude lower dosing strategy and a second-generation CAR scaffold [80], compared with a third-generation CAR from the first trial [67]. Variations in trial design complicate assessment of the specific role of antigen-binding domains on differential clinical outcomes. Given the modular nature of CARs and the multistep process of adoptive cell transfer treatments, it is worth considering antigen-binding domains in the context of alternative receptor configurations and treatment strategies, which have been reviewed elsewhere [9,10,81,82].

Conclusion

Engineered CAR T cells have proven highly potent in a clinical setting. Their rapid and powerful responses can be both therapeutic and toxic. The antigen-binding domain plays a major role in redirecting T cells against tumors and needs to be chosen carefully. Ideally, the antigen-binding domain should display high specificity for its intended target, bind with sufficient strength to trigger cytotoxic T-cell responses, and exhibit high folding and thermodynamic stability. If the target antigen is expressed on the cell surface, scFv, natural ligand and repeat proteins are suitable candidate ligand-binding domains. Intracellular antigens are best targeted with TCR variable fragments or TCR-mimetic scFvs. Theoretically, it should also be possible to design repeat protein domains with HLA-peptide specificity, but none have been reported in literature. Regardless of the category, the ligand-binding domain should be thermodynamically stable to avoid misfolding, aggregation and other biochemical pitfalls preventing proper surface expression of the receptor. Generally, high-affinity antigen-binding domains are favored in literature. However, high affinity does not guarantee ligand specificity and can, in fact, increase the chances of engineered T cells recognizing structurally similar, but unrelated markers or mounting responses against healthy tissues expressing low levels of the intended target [17,18,78]. Since the consequences of off- or on-target off-tumor T-cell activation are potentially lethal, receptor specificity should be evaluated extensively during the stages of receptor design and preclinical testing.

Future perspective

Prediction of tissues, besides the targeted tumor, which will trigger activation of engineered T cells remains the biggest challenge in the field. We expect future studies introducing novel chimeric receptors to focus on minimizing off- and on-target off-tumor toxicities by fine-tuning receptor design and incorporating safety switches into the constructs. Common selection of candidates for an antigen-binding domain involves one or more affinity-based library screening steps. Negative selection should not be overlooked during this process, as it can help eliminate binders with unexpected off-tumor specificities.

Since tumor and healthy cells share expression of many markers, future research in the field of antigen-binding domains will likely include novel recognition modalities outside of the scFv family, for example, repeat proteins and nanobodies, and diversify into targeting unique tumor-associated mutations as well as nonpeptide antigens. Size, biophysical stability, diversity, potential affinity for targets and ability to be expressed in standard display platforms (prokaryotic, eukaryotic or viral) are important characteristics, which will facilitate development of the novel groups of binders.

Finally, we expect to see the growth of the multivalent receptor field, aimed at reaching multiple cancerous populations, because monospecific CAR T-cell therapies are prone to tumor escape via antigen loss or modification. Since addition of several domains can potentially complicate optimization process by interfering with receptor folding and expression, it will be useful to explore combinations that are less prone to mispairing (for example, a natural ligand and an scFv or a repeat protein and an scFv, as opposed to scFv–scFv).

Financial & competing interests disclosure

All authors work in the Bramson lab at McMaster University. The Bramson lab gratefully acknowledges funding from the following sources: Terry Fox Foundation, Samuel Family Foundation, Canadian Breast Cancer Foundation, Juravinski Cancer Centre Foundation, Owen and Marta Boris Foundation, Canadian Institutes for Health Research, BioCanRx and Triumvira Immunologics, Inc. The authors have no other relevant affiliations or financial involvement with any organization or entity with a financial interest in or financial conflict with the subject matter or materials discussed in the manuscript apart from those disclosed. No writing assistance was utilized in the production of this manuscript.

Executive summary

- Chimeric antigen receptor (CAR) technology shows excellent promise in clinical trials.
- Antigen-binding domains of chimeric receptors influence target choice, timing and location of activation of engineered T cells.

Antigen-binding domains described in literature

- Among antigen-binding domains, single-chain variable fragment technology is the most studied and advanced clinically, despite common requirement for nontrivial optimization.
- While providing an opportunity to capitalize on endogenous binder pairs, natural ligands should be evaluated carefully for suitability for T-cell redirection due to commonly wide target expression patterns.
- Repeat protein-based antigen-binding domains are new in the field and offer favorable biophysical properties for receptor design.
- T-cell receptor variable fragment strategy allows for targeting both intracellular and cell-surface antigens, but its technological progress is lagging due to protein optimization challenges.
- Multivalent receptors are designed to overcome antigen escape problem by combining domains with different antigen specificities.
- Universal switchable CARs offer continuous flexibility in target choice, but rely on bioavailability and biodistribution of soluble switch molecules.

Characteristics of the binding interaction

- Along with expression levels and cellular distribution of the activating receptor and other molecules participating in immunological synapse, receptor affinity is one of the components influencing functional avidity of CAR T cells.
- Specificity of the receptor reflects its ability to differentiate between several targets.
- Increase in affinity does not guarantee higher specificity.

Conclusion

- Monovalent, multivalent or universal antigen-binding domains have to exhibit specificity for their target, biophysical stability and affinity sufficient for triggering downstream-activating signals.
- On-target off-tumor and off-target toxicities remain the biggest concerns in the field of chimeric receptor design.

References

Papers of special note have been highlighted as: • of interest.

1 Morris EC, Stauss HJ. Optimizing T cell receptor gene therapy for hematologic malignancies. *Blood* 127(26), 3305–3311 (2016).

2 Maus MV, June CH. Making better chimeric antigen receptors for adoptive T-cell therapy. *Clin. Cancer Res.* 22(8), 1875–1884 (2016).

3 Almåsbak H, Aarvak T, Vemuri MC. CAR T cell therapy: a game changer in cancer treatment. *J. Immunol. Res.* 2016, 5474602 (2016).

4 Ali SA, Shi V, Maric I *et al.* T cells expressing an anti-B-cell-maturation-antigen chimeric antigen receptor cause remissions of multiple myeloma. *Blood* 128(13), 1688–1700 (2016).

5 Dai H, Wang Y, Lu X, Han W. Chimeric antigen receptors modified T-cells for cancer therapy. *J. Natl Cancer Inst.* 108(7), 1–15 (2016).

6 Newick K, Moon E, Albelda SM. Chimeric antigen receptor T-cell therapy for solid tumors. *Mol. Ther. Oncolytics.* 3, 16006 (2016).

7 Sadelain M, Brentjens R, Rivière I. The basic principles of chimeric antigen receptor design. *Cancer Discov.* 3(4), 388–398 (2013).

8 Harris DT, Kranz DM. Adoptive T cell therapies: a comparison of T cell receptors and chimeric antigen receptors. *Trends Pharmacol. Sci.* 37(3), 220–230 (2016).

9 Bonifant CL, Jackson HJ, Brentjens RJ, Curran KJ. Toxicity and management in CAR T-cell therapy. *Mol. Ther. Oncolytics* 3, 16011 (2016).

10 Brudno JN, Kochenderfer JN. Toxicities of chimeric antigen receptor T cells: recognition and management. *Blood* 127(26), 3321–3330 (2016).

11 Posey AD, Schwab RD, Boesteanu AC *et al.* Engineered CAR T cells targeting the cancer-associated Tn-glycoform of the membrane mucin MUC1 control adenocarcinoma. *Immunity* 44(6), 1444–1454 (2016).

12 Wilkie S, Picco G, Foster J *et al.* Retargeting of human T cells to tumor-associated MUC1: the evolution of a chimeric antigen receptor. *J. Immunol.* 180(7), 4901–4909 (2008).

13 Ma Q, Garber HR, Lu S *et al.* A novel TCR-like CAR with specificity for PR1/HLA-A2 effectively targets myeloid leukemia *in vitro* when expressed in human adult peripheral blood and cord blood T cells. *Cytotherapy* 18, 985–994 (2016).

14 Schuberth PC, Jakka G, Jensen SM *et al.* Effector memory and central memory NY-ESO-1-specific re-directed T cells for treatment of multiple myeloma. *Gene Ther.* 20(4), 386–395 (2012).

15 Zhang G, Wang L, Cui H *et al.* Anti-melanoma activity of T cells redirected with a TCR-like chimeric antigen receptor. *Sci. Rep.* 4, 3571 (2014).

16 Zhao Q, Ahmed M, Tassev DV *et al.* Affinity maturation of T-cell receptor-like antibodies for Wilms tumor 1 peptide greatly enhances therapeutic potential. *Leukemia* 29(11), 2238–2247 (2015).

17 Linette GP, Stadtmauer EA, Maus MV *et al.* Cardiovascular toxicity and titin cross-reactivity of affinity-enhanced T cells in myeloma and melanoma. *Blood.* 122(6), 863–871 (2013).

18 Morgan RA, Chinnasamy N, Abate-Daga D *et al.* Cancer regression and neurological toxicity following anti-MAGE-A3 TCR gene therapy. *J. Immunother.* 36(2), 133–151 (2013).

• **Work highlighting the on-target off-tumor risks of high-affinity T-cell receptors (TCRs).**

19 Dhanik A, Kirshner JR, MacDonald D *et al. In-silico* discovery of cancer-specific peptide-HLA complexes for targeted therapy. *BMC Bioinformatics* 17(1), 286 (2016).

20 Haase K, Raffegerst S, Schendel DJ, Frishman D. Expitope: a web server for epitope expression. *Bioinformatics* 31(11), 1854–1856 (2015).

21 Hu D, Hu S, Wan W *et al.* Effective optimization of antibody affinity by phage display integrated with high-throughput DNA synthesis and sequencing technologies. *PLoS ONE* 10(6), e0129125 (2015).

22 Pansri P, Jaruseranee N, Rangnoi K, Kristensen P, Yamabhai M. A compact phage display human scFv library for selection of antibodies to a wide variety of antigens. *BMC Biotechnol.* 9(1), 6 (2009).

23 Farajnia S, Ahmadzadeh V, Tanomand A, Veisi K, Khosroshahi SA, Rahbarnia L. Development trends for generation of single-chain antibody fragments. *Immunopharmacol. Immunotoxicol.* 36(365), 297–308 (2014).

24 Alonso-Camino V, Sanchez-Martin D, Compte M *et al.* CARbodies: human antibodies against cell surface tumor antigens selected from repertoires displayed on T cell chimeric antigen receptors. *Mol. Ther. Nucleic Acids* 2, e93 (2013).

25 Sblattero D, Bradbury A. Exploiting recombination in single bacteria to make large phage antibody libraries. *Nat. Biotechnol.* 18, 75–80 (2000).

26 Vaughan TJ, Williams AJ, Pritchard K *et al.* Human antibodies with sub-nanomolar affinities isolated from a large non-immunized phage display library. *Nat. Biotechnol.* 14(3), 309–314 (1996).

27 Glockshuber R, Schmidt T, Plückthun A. The disulfide bonds in antibody variable domains: effects on stability, folding *in vitro*, and functional expression in *Escherichia coli*. *Biochemistry* 31(5), 1270–1279 (1992).

• **An in-depth study of the influence of disulfide bonds on the stability of antibodies and antibody-derived fragments.**

28 Perchiacca JM, Tessier PM. Engineering aggregation-resistant antibodies. *Annu. Rev. Chem. Biomol. Eng.* 3, 263–286 (2012).

29 Worn A, Pluckthun A. Stability engineering of antibody single-chain Fv fragments. *J. Mol.* 305, 989–1010 (2001).

30 Whitlow M, Bell BA, Feng SL *et al.* An improved linker for single-chain Fv with reduced aggregation and enhanced proteolytic stability. *Protein Eng.* 6(8), 989–995 (1993).

31 Maude SL, Barrett DM, Ambrose DE *et al.* Efficacy and safety of humanized chimeric antigen receptor (CAR)-modified T cells targeting CD19 in children with relapsed/refractory ALL. *Blood* 126(23), 683 (2015).

32 Maus MV, Haas AR, Beatty GL *et al.* T cells expressing chimeric antigen receptors can cause anaphylaxis in humans. *Cancer Immunol. Res.* 1, 26–32 (2013).

33 Zhang T, Lemoi BA, Sentman CL. Chimeric NK-receptor-bearing T cells mediate antitumor immunotherapy. *Blood* 106(5), 1544–1551 (2005).

34 VanSeggelen H, Hammill JA, Dvorkin-Gheva A *et al.* T cells engineered with chimeric antigen receptors targeting NKG2D ligands display lethal toxicity in mice. *Mol. Ther.* 23(10), 1600–1610 (2015).

• **Experimental evidence that a natural ligand with broad expression patterns of receptors can lead to *in vivo* chimeric antigen receptor T-cell toxicity.**

35 Urbanska K, Stashwick C, Poussin M, Powell DJJ. Follicle-stimulating hormone receptor as a target in the redirected T-cell therapy for cancer. *Cancer Immunol. Res.* 3(10), 1130–1137 (2015).

36 Perales-Puchalt A, Svoronos N, Rutkowski MR *et al.* Follicle-stimulating hormone receptor is expressed by most ovarian cancer subtypes and is a safe and effective immunotherapeutic target. *Clin. Cancer Res.*pii: clincanres.0492.2016 (2016) (Epub ahead of print).

37 Kahlon KS, Kahlon KS, Brown C *et al.* Specific recognition and killing of glioblastoma multiforme by 13-zetakine redirected cytolytic T cells. *Cancer Res.* 64(24), 9160–9166 (2004).

38 Brown CE, Badie B, Barish ME *et al.* Bioactivity and safety of IL13Ralpha2-redirected chimeric antigen receptor $CD8^+$ T cells in patients with recurrent glioblastoma. *Clin. Cancer Res.* 21(18), 4062–4072 (2015).

39 Plückthun A. Designed ankyrin repeat proteins (DARPins): binding proteins for research, diagnostics, and therapy. *Annu. Rev. Pharmacol. Toxicol.* 55, 489–511 (2015).

40 Hammill JA, Vanseggelen H, Helsen CW *et al.* Designed ankyrin repeat proteins are effective targeting elements for chimeric antigen receptors. *J. Immunother. Cancer* 3, 55 (2015).

41 Moot R, Raikar S, Fleischer LC *et al.* Expanding the ligand binding repertoire of chimeric antigen receptors using lamprey variable lymphocyte receptors. *Blood* 126(23), 3244 (2015).

42 Lee S-C, Park K, Han J *et al.* Design of a binding scaffold based on variable lymphocyte receptors of jawless vertebrates by module engineering. *Proc. Natl Acad. Sci. USA* 109(9), 3299–3304 (2012).

43 Hwang DE, Ryou JH, Oh JR, Han JW, Park TK, Kim H-S. Anti-human VEGF repebody effectively suppresses choroidal neovascularization and vascular leakage. *PLoS ONE* 11(3), e0152522 (2016).

44 Maynard J, Adams EJ, Krogsgaard M, Petersson K, Liu CW, Garcia KC. High-level bacterial secretion of single-chain αβ T-cell receptors. *J. Immunol. Methods* 306(1–2), 51–67 (2005).

45 Kieke M, Shusta E, Boder E, Teyton L, Wittrup K, Kranz D. Selection of functional T cell receptor mutants from a yeast surface-display library. *Proc. Natl Acad. Sci. USA* 96(10), 5651–5656 (1999).

46 Pecorari F, Tissot AC, Plückthun A. Folding, heterodimeric association and specific peptide recognition of a murine alphabeta T-cell receptor expressed in *Escherichia coli*. *J. Mol. Biol.* 285, 1831–1843 (1999).

47 Stone JD, Harris DT, Soto CM *et al.* A novel T cell receptor single-chain signaling complex mediates antigen-specific T cell activity and tumor control. *Cancer Immunol. Immunother.* 63(11), 1163–1176 (2014).

48 Richman SA, Aggen DH, Dossett ML *et al.* Structural features of T cell receptor variable regions that enhance domain stability and enable expression as single-chain ValphaVbeta fragments. *Mol. Immunol.* 46(5), 902–916 (2009).

49 Grada Z, Hegde M, Byrd T *et al.* TanCAR: a novel bispecific chimeric antigen receptor for cancer immunotherapy. *Mol. Ther. Nucleic Acids.* 2, e105 (2013).

50 Zah E, Lin M-Y, Silva-Benedict A, Jensen MC, Chen YY. T cells expressing CD19/CD20 bi-specific chimeric antigen receptors prevent antigen escape by malignant B cells. *Cancer Immunol. Res.* 4(6), 498–508 (2016).

• **A demonstration of how targeting of multiple tumor-associated antigens can help overcome tumor antigen escape.**

51 Hegde M, Mukherjee M, Grada Z *et al.* Tandem CAR T cells targeting HER2 and IL13Rα2 mitigate tumor antigen escape. *J. Clin. Invest.* 126(8), 3036–3052 (2016).

52 Urbanska K, Lanitis E, Poussin M *et al.* A universal strategy for adoptive immunotherapy of cancer through use of a novel T-cell antigen receptor. *Cancer Res.* 72(7), 1844–1852 (2012).

53 Kudo K, Imai C, Lorenzini P *et al.* T lymphocytes expressing a CD16 signaling receptor exert antibody-dependent cancer cell killing. *Cancer Res.* 74(1), 93–102 (2014).

54 Rodgers DT, Mazagova M, Hampton EN *et al.* Switch-mediated activation and retargeting of CAR-T cells for B-cell malignancies. *Proc. Natl Acad. Sci. USA* 113(4), E459–E468 (2016).

55 Ma JSY, Kim JY, Kazane SA *et al.* Versatile strategy for controlling the specificity and activity of engineered T cells. *Proc. Natl Acad. Sci. USA* 113(4), E450–E458 (2016).

56 Tamada K, Geng D, Sakoda Y *et al.* Redirecting gene-modified T cells toward various cancer types using tagged antibodies. *Clin. Cancer Res.* 18(23), 6436–6445 (2012).

57 Kuo SC, Lauffenburger D A. Relationship between receptor/ligand binding affinity and adhesion strength. *Biophys. J.* 65(5), 2191–2200 (1993).

58 Alexander-Miller MA, Leggatt GR, Berzofsky JA. Selective expansion of high- or low-avidity cytotoxic T lymphocytes and efficacy for adoptive immunotherapy. *Proc. Natl Acad. Sci. USA* 93(9), 4102–4107 (1996).

59 Zeh HJ 3rd, Perry-lalley D, Dudley ME *et al.* High avidity CTLs for two self-antigens demonstrate superior *in vitro* and *in vivo* antitumor efficacy. *J Immunol J. Immunol.* 162(19), 989–994 (2016).

60 Viganò S, Utzschneider DT, Perreau M, Pantaleo G, Zehn D, Harari A. Functional avidity: a measure to predict the efficacy of effector T cells? *Clin. Dev. Immunol.* 2012, 153863 (2012).

61 Rudnick SI, Adams GP. Affinity and avidity in antibody-based tumor targeting. *Cancer Biother. Radiopharm.* 24(2), 155–161 (2009).

62 Zhong S, Malecek K, Johnson LA *et al.* T-cell receptor affinity and avidity defines antitumor response and autoimmunity in T-cell immunotherapy. *Proc. Natl Acad. Sci. USA* 110(17), 6973–6978 (2013).

63 Poulsen TR, Jensen A, Haurum JS *et al.* Limits for antibody affinity maturation and repertoire diversification in hypervaccinated humans. *J. Immunol.* 187, 4229–4235 (2011).

64 Chervin AS, Stone JD, Holler PD *et al.* The impact of TCR-binding properties and antigen presentation format on T cell responsiveness. *J. Immunol.* 183(2), 1166–1178 (2009).

• **A good explanation of how TCR affinity affects specificity.**

65 Press MF, Cordon-Cardo C, Slamon DJ. Expression of the HER-2/neu proto-oncogene in normal human adult and fetal tissues. *Oncogene* 5(7), 953–962 (1990).

66 Slamon DJ, Clark GM, Wong SG, Levin WJ, Ullrich A, McGuire WL. Human breast cancer: correlation of relapse and survival with amplification of the HER-2/neu oncogene. *Science* 235(4785), 177–182 (1987).

67 Morgan RA, Yang JC, Kitano M, Dudley ME, Laurencot CM, Rosenberg SA. Case report of a serious adverse event following the administration of T cells transduced with a chimeric antigen receptor recognizing ERBB2. *Mol. Ther.* 18(4), 843–851 (2010).

68 Liu X, Jiang S, Fang C *et al.* Affinity-tuned ErbB2 or EGFR chimeric antigen receptor T cells exhibit an increased therapeutic index against tumors in mice. *Cancer Res.* 75(17), 3596–3607 (2015).

- **The concept of 'affinity tuning' illustrated in the example of an anti-ErbB2 chimeric antigen receptor.**

69 Caruso HG, Hurton LV, Najjar A *et al.* Tuning sensitivity of CAR to EGFR density limits recognition of normal tissue while maintaining potent antitumor activity. *Cancer Res.* 75(17), 3505–3518 (2015).

70 Chmielewski M, Hombach A, Heuser C, Adams GP, Abken H. T cell activation by antibody-like immunoreceptors: increase in affinity of the single-chain fragment domain above threshold does not increase T cell activation against antigen-positive target cells but decreases selectivity. *J. Immunol.* 173(12), 7647–7653 (2004).

71 Cameron BJ, Gerry AB, Dukes J *et al.* Identification of a titin-derived HLA-A1-presented peptide as a cross-reactive target for engineered MAGE A3-directed T cells. *Sci. Transl. Med.* 5(197), 197ra103 (2013).

- **Work showcasing off-target effects of high-affinity TCRs.**

72 Kochenderfer JN, Yu Z, Frasheri D *et al.* Adoptive transfer of syngeneic T cells transduced with a chimeric antigen receptor that recognizes murine CD19 can eradicate lymphoma and normal B cells. *Blood* 116(19), 3875–3886 (2010).

73 Sampson JH, Choi BD, Sanchez-Perez L *et al.* EGFRvIII mCAR-modified T-cell therapy cures mice with established intracerebral glioma and generates host immunity against tumor-antigen loss. *Clin. Cancer Res.* 20(4), 972–984 (2014).

74 Chmielewski M, Hahn O, Rappl G *et al.* T cells that target carcinoembryonic antigen eradicate orthotopic pancreatic carcinomas without inducing autoimmune colitis in mice. *Gastroenterology* 143(4), 1095–1107 (2012).

75 Zheng-Bradley X, Rung J, Parkinson H, Brazma A. Large scale comparison of global gene expression patterns in human and mouse. *Genome Biol.* 11(12), R124 (2010).

76 Miller JA, Horvath S, Geschwind DH. Divergence of human and mouse brain transcriptome highlights Alzheimer disease pathways. *Proc. Natl Acad. Sci. USA* 107(28), 12698–12703 (2010).

77 Eaton BE, Gold L, Zichi DA. Let's get specific: the relationship between specificity and affinity. *Chem. Biol.* 2(10), 633–638 (1995).

78 Stone JD, Chervin AS, Kranz DM. T-cell receptor binding affinities and kinetics: impact on T-cell activity and specificity. *Immunology* 126, 165–176 (2009).

79 Campochiaro PA, Channa R, Berger BB *et al.* Treatment of diabetic macular edema with a designed ankyrin repeat protein that binds vascular endothelial growth factor: a Phase I/II study. *Am. J. Ophthalmol.* 155(4), 697–704.e2 (2013).

80 Ahmed N, Brawley VS, Hedge M *et al.* Human epidermal growth factor receptor 2 (HER2)-specific chimeric antigen receptor-modified T cells for the immunotherapy of HER2-positive sarcoma. *J. Clin. Oncol.* 33(15), 1688–1696 (2015).

81 Ruella M, June CH. Chimeric antigen receptor T cells for B cell neoplasms: choose the right CAR for you. *Curr. Hematol. Malig. Rep.* 11(5), 368–384 (2016).

82 Kalaitsidou M, Kueberuwa G, Schutt A, Gilham DE. CAR T-cell therapy: toxicity and the relevance of preclinical models. *Immunotherapy* 7(5), 487–497 (2015).

83 Grupp SA, Maude SL, Shaw PA *et al.* Durable remissions in children with relapsed/refractory ALL treated with T cells engineered with a CD19-targeted chimeric antigen receptor (CTL019). Presented at: *57th American Society of Hematology Annual Meeting*. Orlando, FL, USA, 5–8 December 2015 (Abstract 681).

84 Kochenderfer JN, Dudley ME, Kassim SH *et al.* Chemotherapy-refractory diffuse large B-cell lymphoma and indolent B-cell malignancies can be effectively treated with autologous T cells expressing an anti-CD19 chimeric antigen receptor. *J. Clin. Oncol.* 33(6), 540–549 (2015).

85 Porter DL, Hwang W-T, Frey NV *et al.* Chimeric antigen receptor T cells persist and induce sustained remissions in relapsed refractory chronic lymphocytic leukemia. *Sci. Transl. Med.* 7(303), 303ra139 (2015).

86 Ahmed N, Salsman VS, Kew Y *et al.* HER2-specific T cells target primary glioblastoma stem cells and induce regression of autologous experimental tumors. *Clin. Cancer Res.* 16(2), 474–485 (2010).

87 Morgan RA, Yang JC, Kitano M, Dudley ME, Laurencot CM, Rosenberg SA. Case report of a serious adverse event following the administration of T cells transduced with a chimeric antigen receptor recognizing ERBB2. *Mol. Ther.* 18(4), 843–851 (2010).

88 You F, Jiang L, Zhang B *et al.* Phase 1 clinical trial demonstrated that MUC1 positive metastatic seminal vesicle cancer can be effectively eradicated by modified Anti-MUC1 chimeric antigen receptor transduced T cells. *Sci. China Life Sci.* 59(4), 386–397 (2016).

89 Deng Z, Wu Y, Ma W, Zhang S, Zhang Y-Q. Adoptive T-cell therapy of prostate cancer targeting the cancer stem cell antigen EpCAM. *BMC Immunol.* 16, 1 (2015).

90 Zhang W, Wang Y, Guo Y, Dai H, Yang Q, Zhang Y. Treatment of CD20-directed chimeric antigen receptor-modified T cells in patients with relapsed or refractory B-cell Non-Hodgkin lymphoma: an early Phase IIa trial report. *Signal Transduct. Target. Ther.* 1, 16002 (2016).

91 Haso W, Lee DW, Shah NN *et al.* Anti-CD22-chimeric antigen receptors targeting B-cell precursor acute lymphoblastic leukemia. *Blood* 121(7), 1165–1171 (2013).

92 Hombach AA, Gorgens A, Chmielewski M *et al.* Superior therapeutic index in lymphoma therapy: CD30(+) CD34(+) hematopoietic stem cells resist a chimeric antigen receptor (CAR) T cell attack. *Mol. Ther.* 24(8), 1423–1434 (2016).

93 Wang Q, Wang Y, Lv H *et al.* Treatment of CD33-directed chimeric antigen receptor-modified T cells in one patient with relapsed and refractory acute myeloid leukemia. *Mol. Ther.* 23(1), 184–191 (2015).

94 Chinnasamy D, Yu Z, Theoret MR *et al.* Gene therapy using genetically modified lymphocytes targeting VEGFR-2 inhibits the growth of vascularized syngenic tumors in mice. *J. Clin. Invest.* 120(11), 3953–3968 (2010).

95 Bo G, Xia CM, Wang HQ *et al.* CD138-directed adoptive immunotherapy of chimeric antigen receptor (CAR)-modified T cells for multiple myeloma. *J. Cell. Immunother.* 2, 28–35 (2015).

96 Louis CU, Savoldo B, Dotti G *et al.* Antitumor activity and long-term fate of chimeric antigen receptor – positive T cells in patients with neuroblastoma. *Blood.* 118(23), 6050–6056 (2011).

97 Prapa M, Caldrer S, Spano C *et al.* A novel anti-GD2/4–1BB chimeric antigen receptor triggers neuroblastoma cell killing. *Oncotarget* 6(28), 24884–24894 (2015).

98 Mardiros A, Dos Santos C, McDonald T *et al.* T cells expressing CD123-specific chimeric antigen receptors exhibit specific cytolytic effector functions and antitumor effects against human acute myeloid leukemia. *Blood* 122(18), 3138–3148 (2013).

99 Künkele A, Taraseviciute A, Finn LS *et al.* Preclinical assessment of CD171-directed CAR T cell adoptive therapy for childhood neuroblastoma: CE7 epitope target safety and product manufacturing feasibility. *Clin. Cancer Res.*doi:10.1158/1078-0432.CCR-16-0354 (2016) (Epub ahead of print).

100 Gao H, Li K, Tu H *et al.* Development of T cells redirected to glypican-3 for the treatment of hepatocellular carcinoma. *Clin. Cancer Res.* 20(24), 6418–6428 (2014).

101 Beatty GL, Haas AR, Maus MV *et al.* Mesothelin-specific chimeric antigen receptor mRNA-engineered T cells induce anti-tumor activity in solid malignancies. *Cancer Immunol Res.* 2(2), 112–120 (2014).

102 Katz SC, Burga RA, McCormack E *et al.* Phase I hepatic immunotherapy for metastases study of intra-arterial chimeric antigen receptor-modified T-cell therapy for CEA+ liver metastases. *Clin. Cancer Res.* 21(14), 3149–3159 (2015).

103 Vera J, Savoldo B, Vigouroux S *et al.* T lymphocytes redirected against the κ light chain of human immunoglobulin efficiently kill mature B lymphocyte-derived malignant cells. *Blood* 108(12), 3890–3897 (2006).

104 Abate-Daga D, Lagisetty KH, Tran E *et al.* A novel chimeric antigen receptor against prostate stem cell antigen mediates tumor destruction in a humanized mouse model of pancreatic cancer. *Hum. Gene Ther.* 25(12), 1003–1012 (2014).

105 Slawin KM, Mahendravada A, Shinners N *et al.* Inducible MyD88/CD40 to allow rimiducid-dependent activation for control of proliferation and survival of chimeric antigen receptor (CAR) T cells targeting prostate stem cell antigen (PSCA). *ASCO Meet. Abstr.* 34(Suppl. 2), 206 (2016).

106 Sautto G A, Wisskirchen K, Clementi N *et al.* Chimeric antigen receptor (CAR)-engineered T cells redirected against hepatitis C virus (HCV) E2 glycoprotein. *Gut* 65(3), 512–523 (2016).

107 Ritchie DS, Neeson PJ, Khot A *et al.* Persistence and efficacy of second generation CAR T cell against the LeY antigen in acute myeloid leukemia. *Mol. Ther.* 21(11), 2122–2129 (2013).

108 Hudecek M, Schmitt TM, Baskar S *et al.* The B-cell tumor-associated antigen ROR1 can be targeted with T cells modified to express a ROR1-specific chimeric antigen receptor. *Blood* 116(22), 4532–4541 (2010).

109 Spear P, Barber A, Rynda-Apple A, Sentman CL. NKG2D CAR T-cell therapy inhibits the growth of NKG2D ligand heterogeneous tumors. *Immunol. Cell Biol.* 91(6), 435–440 (2013).

110 Nakazawa Y, Matsuda K, Kurata T *et al.* Anti-proliferative effects of T cells expressing a ligand-based chimeric antigen receptor against CD116 on CD34(+) cells of juvenile myelomonocytic leukemia. *J. Hematol. Oncol.* 9(1), 27 (2016).

111 Davies DM, Foster J, Van Der Stegen SJC *et al.* Flexible targeting of ErbB dimers that drive tumorigenesis by using genetically engineered T cells. *Mol. Med.* 18, 565–576 (2012).

112 Shaffer DR, Savoldo B, Yi Z *et al.* T cells redirected against CD70 for the immunotherapy of CD70-positive malignancies. *Blood* 117(16), 4304–4314 (2011).

113 Scholler J, Brady TL, Binder-Scholl G *et al.* Decade-long safety and function of retroviral-modified chimeric antigen receptor T cells. *Sci. Transl. Med.* 4(132), 132ra53 (2012).

114 Huang G, Yu L, Cooper LJN, Hollomon M, Huls H, Kleinerman ES. Genetically modified T cells targeting interleukin-11 receptor α-chain kill human osteosarcoma cells and induce the regression of established osteosarcoma lung metastases. *Cancer Res.* 72(1), 271–281 (2012).

115 Liu L, Patel B, Ghanem MH *et al.* Novel CD4-based bispecific chimeric antigen receptor designed for enhanced anti-HIV potency and absence of HIV entry receptor activity. *J. Virol.* 89(13), 6685–6694 (2015).

116 Rodgers DT, Mazagova M, Hampton EN *et al.* Switch-mediated activation and retargeting of CAR-T cells for B-cell malignancies. *Proc. Natl Acad. Sci. USA* 113(4), E459–E468 (2016).

117 Zhou H, Zha Z, Liu Y *et al.* Structural insights into the down-regulation of overexpressed p185 her2/neu protein of transformed cells by the antibody chA21. *J. Biol. Chem.* 286(36), 31676–31683 (2011).

118 Cole DK, Bulek AM, Dolton G *et al.* Hotspot autoimmune T-cell receptor binding to pathogen and insulin peptide cross-reactivity. *J. Clin. Invest.* 6, 2191–2204 (2016).

119 Seeger MA, Zbinden R, Flutsch A *et al.* Design, construction, and characterization of a second-generation DARPin library with reduced hydrophobicity. *Protein Sci.* 22(9), 1239–1257 (2013).

120 Velikovsky CA, Deng L, Tasumi S *et al.* Structure of a lamprey variable lymphocyte receptor in complex with a protein antigen. *Nat. Struct. Mol. Biol.* 16(7), 725–730 (2009).